



# Design, synthesis and biological evaluation of new polymer-drug conjugates based on polyglutamic acid and 5-Fluorouracil for the treatment of advanced colorectal cancer

Helena Plà Solans

**ADVERTIMENT.** La consulta d'aquesta tesi queda condicionada a l'acceptació de les següents condicions d'ús: La difusió d'aquesta tesi per mitjà del servei TDX ([www.tdx.cat](http://www.tdx.cat)) i a través del Dipòsit Digital de la UB ([diposit.ub.edu](http://diposit.ub.edu)) ha estat autoritzada pels titulars dels drets de propietat intel·lectual únicament per a usos privats emmarcats en activitats d'investigació i docència. No s'autoritza la seva reproducció amb finalitats de lucre ni la seva difusió i posada a disposició des d'un lloc aliè al servei TDX ni al Dipòsit Digital de la UB. No s'autoritza la presentació del seu contingut en una finestra o marc aliè a TDX o al Dipòsit Digital de la UB (framing). Aquesta reserva de drets afecta tant al resum de presentació de la tesi com als seus continguts. En la utilització o cita de parts de la tesi és obligat indicar el nom de la persona autora.

**ADVERTENCIA.** La consulta de esta tesis queda condicionada a la aceptación de las siguientes condiciones de uso: La difusión de esta tesis por medio del servicio TDR ([www.tdx.cat](http://www.tdx.cat)) y a través del Repositorio Digital de la UB ([diposit.ub.edu](http://diposit.ub.edu)) ha sido autorizada por los titulares de los derechos de propiedad intelectual únicamente para usos privados enmarcados en actividades de investigación y docencia. No se autoriza su reproducción con finalidades de lucro ni su difusión y puesta a disposición desde un sitio ajeno al servicio TDR o al Repositorio Digital de la UB. No se autoriza la presentación de su contenido en una ventana o marco ajeno a TDR o al Repositorio Digital de la UB (framing). Esta reserva de derechos afecta tanto al resumen de presentación de la tesis como a sus contenidos. En la utilización o cita de partes de la tesis es obligado indicar el nombre de la persona autora.

**WARNING.** On having consulted this thesis you're accepting the following use conditions: Spreading this thesis by the TDX ([www.tdx.cat](http://www.tdx.cat)) service and by the UB Digital Repository ([diposit.ub.edu](http://diposit.ub.edu)) has been authorized by the titular of the intellectual property rights only for private uses placed in investigation and teaching activities. Reproduction with lucrative aims is not authorized nor its spreading and availability from a site foreign to the TDX service or to the UB Digital Repository. Introducing its content in a window or frame foreign to the TDX service or to the UB Digital Repository is not authorized (framing). Those rights affect to the presentation summary of the thesis as well as to its contents. In the using or citation of parts of the thesis it's obliged to indicate the name of the author.



**DESIGN, SYNTHESIS AND BIOLOGICAL EVALUATION OF NEW  
POLYMER-DRUG CONJUGATES BASED ON POLYGLUTAMIC ACID  
AND 5-FLUOROURACIL FOR THE TREATMENT OF ADVANCED  
COLORECTAL CANCER**

Memoria presentada por:

**Helena Plà Solans**

Para optar al título de Doctor por la Universidad de Barcelona.  
Programa de doctorado: BIOMEDICINA

Director:

Director/Tutor:

Director:

Dr. Ibane Abasolo

Dr. Simó Schwartz

Dr. Míriam Royo

Barcelona, Septiembre 2014

---

# ABBREVIATIONS

---

$\delta$	Chemical shift
$\lambda$	Wavelength
Abs	Absorbance
ACN	Acetonitrile
Ala (A)	L-alanine
Amberlite	Exchange resin Amberlite IR120 hydrogen form
anh.	Anhydrous
Arg (R)	L-arginine
BSA	Bovine serum albumin
Boc	<i>tert</i> -butoxycarbonyl
CDCl <sub>3</sub>	Deuterated chloroform
CF	6-carboxyfluorescein
CI	Combination index
CHCl <sub>3</sub>	Chloroform
CH <sub>2</sub> THF	5,10-methylene tetrahydrofolate
<sup>13</sup> C-NMR	Carbon nuclear magnetic resonance
CRC	Colorectal cancer
CPT	Camptothecin
d	Doublet ( <sup>1</sup> H-NMR)
D	Dose
DCC	Dicyclohexylcarbodiimide
DCM	Dichloromethane
ddH <sub>2</sub> O	Double distilled water
DDS	Drug delivery system
DIC	<i>N,N'</i> -Diisopropylcarbodiimide
DIEA	Diisopropyl ethyl amide
DLS	Dynamic light scattering
Dm	Median-effect dose
DMAP	4-( <i>N,N</i> -dimethylamino)pyridine
DMF	<i>N,N</i> -Dimethylformamide
DMSO	Dimethyl sulfoxide

DPD	Dihydropyrimidine dehydrogenase
DMSO-d <sub>6</sub>	Deuterated dimethyl sulfoxide
DSC	n,n'-disuccinimidyl carbonate
D <sub>2</sub> O	Deuterated water
dUMP	Deoxyuridine monophosphate
dUTMP	Deoxythymidine monophosphate
dUTP	Deoxyuridine triphosphate
dTMP	Deoxythymidine monophosphate
ECM	Extracellular matrix
ED	Effect dose
EDC·HCl	1-Ethyl-3-(3-dimethylaminopropyl)carbodiimide chlorhydrate
EGFR	Epidermal growth factor receptor
EPR	Enhanced permeability and retention
eq	Equivalent(s)
ESI <sub>found</sub>	Electrospray ionization peak
EtOAc	Ethyl acetate
fa	Fraction affected
FA	Folinic acid
FD	Free drug
FdUMP	Fluorodeoxyuridine monophosphate
FdUTP	Fluorodeoxyuridine triphosphate
Fmoc	Fluorenylmethoxycarbonyl chloride
5-FU	5-Fluorouracil
FUDP	Fluorouridine diphosphate
FUMP	Fluorouridine monophosphate
FUTP	Fluorouridine triphosphate
fu	Fraction unaffected
Gly (G)	Glycine
h	Hour(s)
Ile (I)	L-isoleucine
KCN	Potassium cyanide
Leu (L)	L-leucine
LMWD	Low molecular weight drugs
LV	Leucovorin
HCl	Hydrochloric acid



<sup>1</sup> H-NMR	Proton nuclear magnetic resonance
HOBt	1-Hydroxybenzotriazole
HPLC	High performance liquid chromatography
IC <sub>50</sub>	50% inhibitory concentration
i.v.	Intravenous administration
J	Coupling constant ( <sup>1</sup> H-NMR)
m	Multiplet ( <sup>1</sup> H-NMR)
MeOH	Methanol
min	Minute(s)
mol	Moles
MTD	Maximum tolerated dose
MTT	3-(4,5-Dimethylthiazol-2-yl)-2,5-diphenyltetrazolium bromide
MTX	Methotrexate
Mw	Molecular weight
Mw <sub>calc</sub>	Molecular weight calculated
m/z	Mass/charge relation
NaOH	Sodium hydroxide
nm	Nanometre(s)
NMR	Nuclear magnetic resonance
N <sub>2</sub>	Nitrogen
PBS	Phosphate buffered saline
PDC	Polymer drug conjugate
PDI	Polydispersion index
PEG	Poly(ethylene glycol)
PGA	Poly(glutamic acid)
PPC	Polymer protein conjugate
ppm	Parts per million
Pro (P)	L-Proline
PRPP	Phosphoribosyl pyrophosphate
OPRT	Orotate phosphoribosyltransferase
RES	Reticuloendothelial system
RI	Refractive index
rt	Room temperature
s	Singlet ( <sup>1</sup> H-NMR)
SD	Standard deviation

sec	Second(s)
SEC	Size exclusion chromatography
SEM	Scanning electron microscopy
SEM	Standard error of the mean
Ser (S)	L-Serine
SMANCS	Styrene-co-maleic anhydride-neocarzinostatin
t	Triplet ( <sup>1</sup> H-NMR)
TDL	Total drug loading
TFA	Trifluoroacetic acid
THF	Tetrahydrofuran
TLC	Thin layer chromatography
TIS	Triisopropylsilane
TK	Tymidine kinase (TK) enzyme
Trp (W)	L-Tryptophane
TS	Thymidylate synthase
UDG	Uracil-DNA glycosylase
UK	Uridine kinase
UP	Uridine phosphorylase
UV	Ultraviolet
Val (V)	L-Valine

---

# INDEX

---

<b>1. GENERAL INTRODUCTION .....</b>	<b>1</b>
<b>1.1 Colorectal Cancer .....</b>	<b>1</b>
1.1.1 Current treatment of CRC .....	3
1.1.1.1 Cytotoxic treatment .....	3
1.1.1.2 Antiangiogenic treatment .....	8
1.1.1.3 New strategies combining different therapies.....	9
<b>1.2 Nanomedicine .....</b>	<b>10</b>
1.2.1 Polymer therapeutics.....	12
<b>1.3 Polymer conjugates.....</b>	<b>14</b>
1.3.1 Polymer-drug conjugates.....	15
1.3.1.1 Polymer-drug conjugates structure .....	15
1.3.1.2 Polymer-drug conjugates based on biodegradable polymers.....	16
1.3.1.3 Biodegradable Polymer-drug conjugates based on PGA.....	17
1.3.2 Polymer-drug conjugates for anticancer therapy.....	18
1.3.2.1 Passive targeting: Enhanced Permeability Retention Effect .....	19
1.3.2.2 Active targeting .....	20
1.3.2.3 Cellular drug delivery of polymer-drug conjugates in tumors .....	25
1.3.3 Polymer-drug conjugates for combination therapy.....	26
1.3.4 Polymer-drug conjugates for treating other diseases .....	28
1.3.5 Current state of polymer-drug conjugates .....	29
<b>2. OBJECTIVES .....</b>	<b>31</b>
<b>3. MATERIALS AND METHODS .....</b>	<b>33</b>
<b>3.1 General Instruments .....</b>	<b>33</b>
<b>3.2 Materials.....</b>	<b>34</b>
3.2.1 Solvents.....	34
3.2.2 Chemical reagents.....	34
3.2.3 Buffers.....	35
<b>3.3 Methods.....</b>	<b>36</b>
3.3.1 General methodology for Solid Phase Peptide Synthesis (SPPS) .....	36
<b>3.4 Purification.....</b>	<b>38</b>
<b>3.5 Characterization .....</b>	<b>39</b>
<b>3.6 Stability and Degradation assays.....</b>	<b>41</b>

3.6.1	pH degradation .....	41
3.6.2	Plasma stability .....	42
3.6.3	Cathepsin B degradation.....	42
3.6.4	Incubation of products with MMPs .....	42
<b>3.7</b>	<b>Tissue homogenization and drug quantification.....</b>	<b>43</b>
<b>3.8</b>	<b>Synthesis .....</b>	<b>45</b>
<b>3.9</b>	<b>In vitro validation techniques.....</b>	<b>62</b>
3.9.1	MTT methodology to evaluate the cell viability .....	63
3.9.2	Cell internalization .....	64
<b>3.10</b>	<b>In vivo studies .....</b>	<b>66</b>
3.10.1	Tumor-accumulation and whole-body biodistribution of PGA-5FU-AF750.....	66
3.10.2	Tumor growth inhibition of PGA-5-FU.....	67
<b>4.</b>	<b>RESULTS .....</b>	<b>69</b>
<b>4.1</b>	<b>Polymer-drug conjugates based on Poly-(L-glutamic acid) and 5-Fluorouracil .....</b>	<b>71</b>
4.1.1	Synthesis optimization of PGA-5-FU conjugates.....	72
4.1.1.1	Synthesis of PGA-5-FU conjugate.....	72
4.1.1.2	Synthesis of an AF750 labelled PGA-5-FU conjugate .....	81
4.1.1.3	Synthesis of a carboxyfluorescein labelled PGA-5-FU conjugate .....	83
4.1.2	Physico-chemical characterization of PGA-5-FU conjugates .....	84
4.1.2.1	Determination of PGA-5-FU size by Dynamic Light Scattering (DLS) .....	84
4.1.2.2	Study of the aggregation of PGA-5-FU conjugate in solution measured by DLS.....	85
4.1.2.3	Determination of the Mw and the PI of PGA-5-FU conjugate by SEC-MALS-IR .....	88
4.1.2.4	Stability studies <i>in vitro</i> of PGA-5-FU conjugate .....	89
4.1.3	<i>In vitro</i> cytotoxicity assays in HT-29 and HCT-116 colorectal cancer cell lines .....	92
4.1.4	Cell internalization studies of PGA-5FU-CF conjugate .....	93
4.1.4.1	Confocal fluorescence microscopy studies of PGA-5FU-CF.....	94
4.1.4.2	Flow cytometry studies of PGA-5FU-CF .....	95
4.1.5	5-FU quantification in tissue and plasma: HPLC method development and validation.....	96
4.1.5.1	Method validation: Tissue homogenization.....	96
4.1.5.2	Method Validation: Pre-treatment of tissue homogenates.....	97
4.1.5.3	Method Validation: HPLC .....	97
4.1.6	<i>In vivo</i> studies in xenograft mice models.....	100
4.1.6.1	Tumor-accumulation and whole-body Biodistribution in athymic nude female mice bearing a CRC tumor.....	100
4.1.6.2	Tumor-accumulation and whole-body biodistribution on subcutaneous HCT-116.Fluc2-C9 human CRC tumors growing in athymic nude female mice (BD1).....	100
4.1.6.3	Tumor-accumulation and whole-body biodistribution on subcutaneous HT-29.Fluc-C4 human CRC tumors growing in athymic nude female mice (BD2).....	107
4.1.6.4	Comparison of the BD1 and BD2 experiments.....	113
4.1.6.5	<i>In vivo</i> tumor growth inhibition studies .....	114
4.1.7	Conclusions .....	120

<b>4.2</b>	<b>Polymer-drug conjugates based on Poly-(L-glutamic acid) and 5-Fluorouracil sensitive to Matrix Metalloproteinases .....</b>	<b>121</b>
4.2.1	Synthesis of MMP sensitive peptides .....	121
4.2.1.1	Sequence recognition cleavage assay of the MMP-sensitive peptides synthesized .....	123
4.2.2	Study of the bond nature between the drug and the MMP-sensitive peptide .....	125
4.2.2.1	Methodology for the synthesis of the 5-FU conjugated to the MMP-sensitive peptide containing a carbamate bond.....	125
4.2.2.2	Conjugation of 5-FU to the MMP-sensitive peptide through an ester bond .....	135
4.2.2.3	Stability tests of the unit 5-FU-peptide moiety conjugated through an ester bond.....	136
4.2.3	Synthesis of the PGA-based polymer-drug conjugate sensitive to MMP7: PGA-MMP7pept-5FU .	140
4.2.3.1	Determination of the particle size of PGA-MMP7pept-5FU conjugate [37] .....	142
4.2.3.2	Stability studies <i>in vitro</i> of PGA-MMP7pept-5FU [37] conjugate.....	143
4.2.3.3	Cytotoxicity assays of PGA-MMP7pept-5FU conjugate .....	146
4.2.4	Conclusions .....	149
<b>4.3</b>	<b>Polymer-drug conjugates based on Poly-(L-glutamic acid), 5-Fluorouracil and SN-38 ... ..</b>	<b>151</b>
4.3.1	Synthesis of PGA-SN38.....	152
4.3.1.1	SN-38 derivatization .....	152
4.3.1.2	Conjugation of the SN-38 derivatized to PGA (PGA-SN38) .....	155
4.3.1.3	Cytotoxicity assays of PGA-SN38 [48] <i>in vitro</i> in HT-29 and HCT-116 CRC cell lines .....	158
4.3.2	Design and synthesis of a PGA-5FU-SN38 family with different loadings of 5-FU and SN-38 .....	159
4.3.2.1	Optimization of PGA-5FU-SN38 production.....	159
4.3.2.2	Synergism experiments of 5-FU and SN-38 as single drugs .....	162
4.3.2.3	Design of a small family of PGA-5FU-SN38 conjugates carrying different ratios of drugs .....	162
4.3.3	Conclusions .....	171
<b>5.</b>	<b>DISCUSSION.....</b>	<b>173</b>
<b>6.</b>	<b>GENERAL CONCLUSIONS .....</b>	<b>177</b>
<b>7.</b>	<b>RESUMEN .....</b>	<b>179</b>
	<b>REFERENCES.....</b>	<b>195</b>

---

# 1. General Introduction

---

## 1.1 Colorectal Cancer

Each year colorectal cancer (CRC) is diagnosed in more than 1.2 million people worldwide and the annual mortality in 2012 was over 600.000 deaths<sup>1,2</sup>. The incidence rates of CRC are slightly higher in men than in women worldwide, being the third most prevalent cancer in men (after prostate and lung cancers) and the second in women (after breast cancer).

CRC progresses through a series of clinical and histopathological stages going from single crypt lesions through small benign tumors (adenomatous polyps, adenomas) to malignant cancers (carcinomas) that finally spread through the layers that form the wall of the colon and rectum (Figure 1.1)<sup>3</sup>.

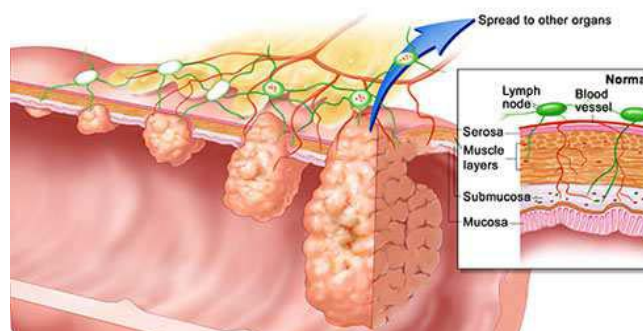


Figure 1. 1 Scheme of the CRC progression through the different stages and the description of the layers on the colon wall (adapted from T.Winslow)<sup>4</sup>.

In the earliest phase (stage 0), adenomas are placed in the inner layer (mucosa) of the colon wall. In the stage I, cancer has a bigger size but it has not spread beyond the mucosal wall of the colon. In the stage II, cancer has grown through the mucosa layer and extends into the muscle layer of the colon wall. In the following stage III, cancer has reached one or more lymph nodes in the area. And finally, in the latest stage IV, cancer spreads to distant organs, such as liver, lungs, or distant lymph nodes. This phase is referred as the metastatic stage, or advanced colorectal cancer.

Cancer stage at diagnosis has a strong influence on the length of survival. The earlier colon and rectum cancer is detected, the higher chances a person has of surviving five years after being diagnosed. Around 40% of the CRC cases are diagnosed at the local stage, where the 5-year survival rate is 90.1%. For those patients with regional spread, the 5-year survival rate is 69.2%. However, 20% of patients are diagnosed of metastatic colorectal cancer (mCRC), in which 5-year survival rates drops to 11.7%<sup>5</sup>. These figures reinforce the need of early diagnosis of CRC as well as more effective treatments for advanced CRC.

Individual's probability to acquire CRC is related to a large variety of factors: genetic predisposition, excessive alcohol consumption, high consumption of red and processed meat, obesity, diabetes and smoking, among others. However, approximately 70% of CRC cases lack clear genetic basis and are generally classified as sporadic<sup>6</sup>. In addition, 35% of CRC risk might be attributable to hereditary factors, but only 3-5% CRC hereditary forms contribute to all CRC. Only 5% of CRC diagnosed as hereditary genetic aberrations are known, the rest are still incompletely understood<sup>5</sup>. The two most common forms of hereditary CRC are hereditary non-polyposis colon cancer (Lynch syndrome) and familial adenomatous *polyposis coli*.

The progression from normal epithelium through adenoma to colorectal carcinoma is characterized by accumulated abnormalities of particular genes. Highly penetrant mutations are described in the molecular basis of CRC. The CRC often develops over more than 10 years, and in the 70% of colorectal adenomas (early stage) mutations in the so called Adenomatous Polyposis Coli gene (APC) are detected, and considered an early event in the multistep process of CRC development<sup>5</sup>. Gene mutations are often accompanied by chromosomal instability. Mutations in mismatch-repair genes cause microsatellite instability in a small percentage of cases which in turns generate successive mutations in additional CRC genes. For instance, the development of carcinoma is promoted by activating mutations of KRAS oncogene and by inactivating mutations of the TP53 tumor-suppressor gene<sup>7</sup>.

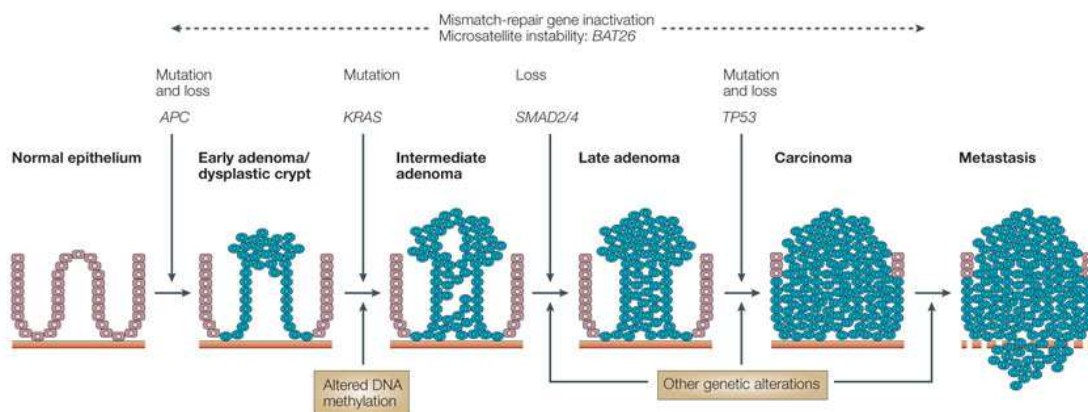


Figure 1. 2 Colorectal adenoma-carcinoma sequence (adapted from Davies et al)<sup>7</sup>.

In addition to this genetic alteration, many genes are upregulated in colon cancer. Particularly, one class of genes often upregulated in colorectal cancer are the matrix metalloproteinases (MMPs). MMPs are not activated by gene mutations but rather their expression is increased either as a direct effect of the activation of an oncogenic pathway, or as an indirect response of the tumor cell<sup>8</sup>. In fact, the MMP family apart from its natural physiologic role has important functions in pathologic conditions, particularly due to an excessive degradation of the ECM within tumor microenvironment. Since the ECM is viewed as a barrier to tumor invasion, an excessive degradation of the ECM produced by a pathologic malfunction of MMPs helps tumor cells to metastasize. Thus, MMP malfunction would allow the tumor cell to invade locally or intravasate to the circulation and then extravasate at a distant site.

### 1.1.1 Current treatment of CRC

Treatment option of CRC depends largely on the stage at time of diagnosis. Since most of the CRC cases are diagnosed when tumor is still localized in the intestinal area (stages 0 to II), surgery is commonly the first-line treatment for colorectal cancer. After the surgery, and in many cases only as an adjuvant therapy, CRC patients are treated with chemotherapy. For those patients with advanced CRC, surgery that includes total mesorectal excision (removal of the rectum together with the mesorectum around it and the surrounding envelope) often provides the best possible patient outcomes and survival<sup>9</sup>, greatly reducing local recurrences without any adjuvant therapy. To follow-up a curative resection of CRC, colonoscopy is recommended every 3–5 years to detect recurrences<sup>9</sup>.

Currently, there are different treatment options for mCRC in combination, or not, with the surgery process. The classical one is chemotherapeutic treatment based on cytotoxic drugs. Radiation therapy has become also an essential therapeutic tool in the treatment of CRC, alone or combined with chemotherapy. Although surgery alone remains the mainstay of CRC treatment of patients diagnosed at an early stage, radiation therapy applied after surgery showed reduction of local relapse to 10% and increases survival to 50-60%. Radiation therapy is also applied as a preoperative adjuvant therapy in patients diagnosed of intermediate stage rectal tumors. Currently, antiangiogenic drugs begin to play an important role as target-specific agents. As the knowledge on the molecular basis of CRC increases day by day, the selection of the most appropriate treatment for each patient is actually a clinical concern.

#### 1.1.1.1 Cytotoxic treatment

Several drugs have been studied during the last decades for the treatment of CRC, but, after 50 years 5-Fluorouracil (5-FU) still remains the essential systemic treatment. Nonetheless, since 1960s different drugs have been approved for the treatment of CRC. Different classes of cytotoxic agents can be distinguished regarding its chemical structure and biological activity. Fluoropyrimidines, camptothecin derivatives and platinate compounds are the most important anticancer drugs for cytotoxic based treatments.

##### 1.1.1.1.1 Cytotoxic treatment: Fluoropyrimidines

Fluoropyrimidines were discovered in the 50s after observing that mice hepatoma cells use fluoropyrimidines for RNA synthesis pyrimidine uracil (one of the four nitrogenous bases found in RNA) faster than normal tissues. Thus, suggesting that uracil metabolism could be a powerful chemotherapeutic target<sup>10</sup>.

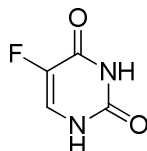


Figure 1.3 Chemical structure of 5-Fluorouracil.



The fluoropyrimidine 5-fluorouracil (5-FU) (Figure 1. 3) is an antimetabolite drug. As an anticancer agent, inhibits essential biosynthetic processes by (i) the inhibition of thymidylate synthase (TS) enzyme necessary for DNA replication or by (ii) the incorporation of its metabolites into macromolecules such as RNA and DNA, thus, inhibiting its normal function. Intracellularly, 5-FU is converted to several active metabolites (Figure 1. 4): fluorodeoxyuridine monophosphate (FdUMP), fluorodeoxyuridine triphosphate (FdUTP) and fluorouridine triphosphate (FUTP). These active metabolites disrupt RNA synthesis and inhibit TS activity.

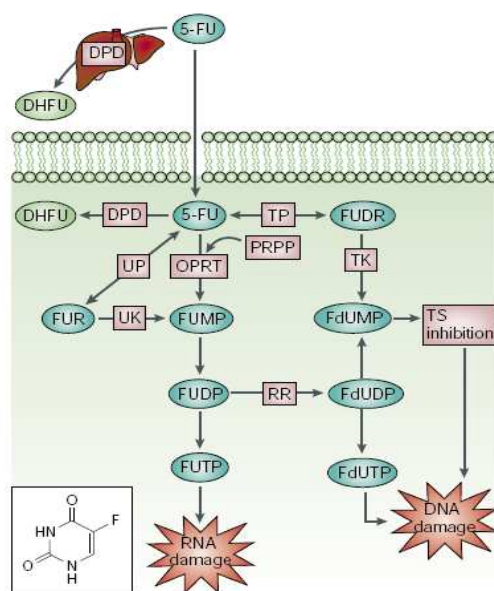


Figure 1. 4 Mechanism of activation of 5-FU (adapted from Longley et al)<sup>11</sup>.

The main mechanism of action of 5-FU requires its conversion to fluorouridine monophosphate (FUMP) directly by orotate phosphoribosyltransferase (OPRT) with phosphoribosyl pyrophosphate (PRPP) as the cofactor or indirectly via fluorouridine (FUR) through the sequential action of uridine phosphorylase (UP) and uridine kinase (UK). FUMP is then phosphorylated to fluorouridine diphosphate (FUDP), which produces RNA damage. In turn, FdUDP can either be phosphorylated or dephosphorylated to generate the active metabolites FdUTP and FdUMP, respectively, finally producing DNA damage. An alternative activation pathway starts with the 5-FU conversion to FUDR catalyzed by TS. Then, FUDR is phosphorylated to FdUMP by thymidine kinase (TK) enzyme, an active metabolite that finally produces DNA damage.

There is a rate-limiting step of 5-FU catabolism related to the dihydropyrimidine dehydrogenase (DPD)-mediated conversion of 5-FU to DHFU, that is an inactive metabolite (Figure 1. 4). The main drawback is that the 80% of the administered drug is normally catabolized primarily by the liver where DPD is abundantly expressed. For this reason, the design of new pro-drugs of 5-FU or the incorporation of 5-FU in new drug delivery systems (DDS) has gained all the attention in the last decades in order to protect the drug from degradation and increase its therapeutic efficacy.

5-FU-based chemotherapy improves overall and disease-free survival of patients with rejected stage III colorectal cancer<sup>12</sup>, and survival of patients with mCRC (stage IV) with 5-FU-based

chemotherapy is only 10–15%<sup>11</sup>. Unfortunately, the efficacy rate of 5-FU as a single agent in patients with mCRC is still low. To overcome this drawback, several strategies have been studied to enhance the anticancer activity of 5-FU. In detail, two different approaches have been explored: (i) the development of 5-FU pro-drugs and (ii) the combination of 5-FU or its pro-drugs with other cytotoxic agents.

### (i) Pro-drugs of 5-FU

Tegafur and Capecitabine (Figure 1. 5) are two pro-drugs of 5-FU approved for the treatment of mCRC.

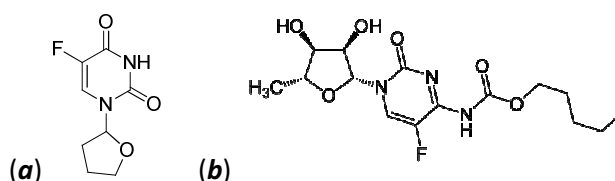


Figure 1. 5 Chemical structure of Tegafur (a) and Capecitabine (b) pro-drugs of 5-FU.

Tegafur (Orzel®) was the first pro-drug synthesized. It evades the erratic intestinal absorption of 5-FU by the co-administration of this oral fluoropyrimidine with an inhibitor of DPD (uracil), thereby allowing for a more uniform absorption and bioavailability. Although its higher oral bioavailability, Tegafur showed CNS toxicity and did not provide an increased survival compared to 5-FU. Its development was discontinued in the United States although it is available in Europe and Asia<sup>3</sup>.

Capecitabine (Xeloda®) is an oral pro-drug of 5-FU absorbed intact through the gastrointestinal mucosa. It undergoes a three-step enzymatic conversion to 5-FU by the action of an esterase, a deaminase and a phosphorylase. The latter enzyme is over-expressed in CRC tumors. This leads to a higher concentration of 5-FU in the tumor compared to normal tissue or plasma<sup>13</sup>. However, even though Capecitabine shows a reduction of some side effects (neutropenia, diarrhea, stomatitis and nausea) compared to 5-FU, some other severe adverse effects (high levels of bilirubin) are observed. Nonetheless, Capecitabine has been approved in more than 50 countries and is currently the only oral 5-FU pro-drug approved in the United States. It is also administered in combination with other drugs (such as Irinotecan or Oxaliplatin).

### (ii) 5-FU in combination with adjuvant drugs

Two different adjuvant drugs have been approved for the administration in combination with 5-FU showing improvements in the final efficacy of the treatment: Leucovorin and Methotrexate. Understanding the mechanism of thymidylate synthase inhibition by 5-Fluorouracil, the purpose of the adjuvant therapy based on Leucovorin (LV) and Methotrexate (MTX) is comprehended.

TS catalyses the conversion of deoxyuridine monophosphate (dUMP) to deoxythymidine monophosphate (dTMP) with 5,10-methylene tetrahydrofolate (CH<sub>2</sub>THF) as methyl donor. The 5-FU active metabolite FdUMP binds to the nucleotide-binding site of TS and forms a stable ternary

complex with TS and CH<sub>2</sub>THF, blocking access of dUMP to the nucleotide-binding site and inhibiting dTMP synthesis. This, results in deoxynucleotide (dNTP) pool imbalances and increased levels of deoxyuridine triphosphate (dUTP), both of which cause DNA damage. The extent of DNA damage caused by dUTP is dependent on the levels of the pyrophosphatase dUTPase and uracil-DNA glycosylase (UDG). dTMP can be recovered from thymidine through the action of TK. dTMP can be salvaged from thymidine through the action of TK, thereby alleviating the effects of TS deficiency. This salvage pathway represents a potential mechanism of resistance to 5-FU<sup>11</sup>.

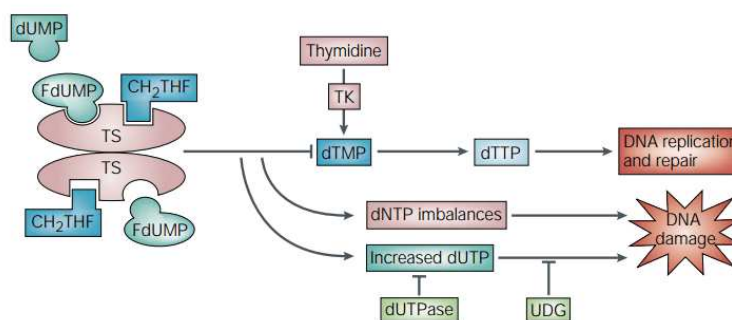


Figure 1. 6 Mechanism of TS inhibition by 5-FU (adapted from Longley et al)<sup>11</sup>.

Leucovorin (LV) (also known as Folinic Acid (FA)) increases the intracellular pool CH<sub>2</sub>THF, thereby enhancing TS inhibition by FdUMP. It is well known that leucovorin increases the activity of 5-FU in the treatment of colorectal cancer by stabilizing the complex of 5-FU and TS<sup>14</sup>. 5-FU and Leucovorin are currently in clinical practice routine, and often administered in combination with other drugs.

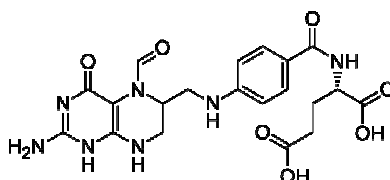


Figure 1. 7 Chemical structure of Leucovorin.

Methotrexate (MTX) is thought to increase 5-FU activation by increasing phosphoribosyl pyrophosphate (PRPP) levels, which is the cofactor required for the conversion of 5-FU to FUMP by orotate phosphoribosyl transferase (OPRT) (Figure 1. 64). Several investigators have found that the antitumor activity of 5-FU was enhanced by pre-treatment with MTX, and this correlated with increased formation of 5-FU ribonucleotides and increased 5-FU incorporation into RNA<sup>15</sup>. Clinically, the combination of MTX and 5-FU was found to be significantly superior to bolus single-agent 5-FU for the treatment of CRC, both in terms of response rate (19% vs. 10%) and overall survival (10.7 months vs. 9.1 months)<sup>16</sup>.

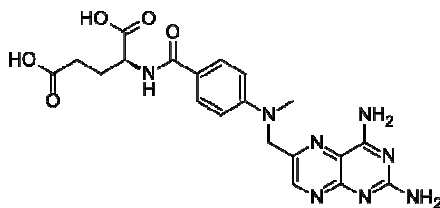


Figure 1. 8 Chemical structure of Methotrexate.

**1.1.1.1.2 Cytotoxic treatment: Camptothecins**

Camptothecins are a large spectrum of anticancer drugs originally isolated from Chinese/Tibetan ornamental tree *Camptotheca acuminata* that specifically target DNA topoisomerase I (Topo I), an enzyme that catalyses the relaxation of negatively super coiled DNA through the formation of stable topoisomerase I-DNA cleavable complexes. The formation of a cleavable drug-Topo I-DNA complex results in lethal double-strand DNA breakage and cell death. Irinotecan (CPT-11) is a semi synthetic analog of camptothecin. Camptothecins cause S-phase-specific cell killing by poisoning Topo I in the cell. It was first discovered and synthesized in Japan in 1983, and it has demonstrated potent antitumor activity against a wide range of tumors<sup>17</sup>.

Currently, a camptothecin (CPT) derivative Irinotecan (CPT-11) is used in the clinics for the treatment of CRC (Figure 1. 10). Irinotecan (CPT-11) is metabolized in the liver by cytochrome P450 (CYP) isoforms, and is transported across cell membranes by members of the ABC-binding cassette transporter family. SN-38, SN-38G, APC and NPC are the four active metabolites of Irinotecan (CPT-11)<sup>14</sup>. It can be converted into SN-38 active metabolite by carboxylesterases (CES) outside or inside the cell. CPT-11 and SN-38 are both substrates of ABC transport proteins.

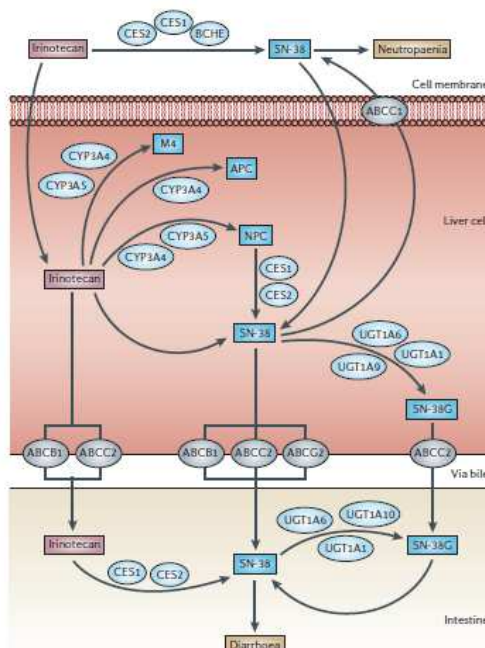


Figure 1. 9 Scheme of metabolism and transport of Irinotecan (adapted from Scripture et al)<sup>14</sup>.

Nonetheless, Irinotecan (CPT-11) has several limitations; the first example is the limited and variable conversion of Irinotecan (CPT-11) to the active metabolite SN-38 by endogenous enzymes. Only 2% to 8% of the total drug is converted to SN-38, depending on the metabolism of the patient<sup>18</sup>. The drug safety profile is an extra limitation that is related to an accumulation of SN-38 in the intestine resulting from bile excretion of Irinotecan (CPT-11) and its metabolites. It is observed in 30 to 40% of treated patients, and is a major limitation because dose has to be reduced for further treatment cycles<sup>19,20</sup>. Another limitation is its low antitumor activity as a single agent. Because all of these limitations, it is suggested that the direct delivery of the active metabolite SN-38 can improve antitumor efficacy while at the same time limiting its gastrointestinal toxicity.

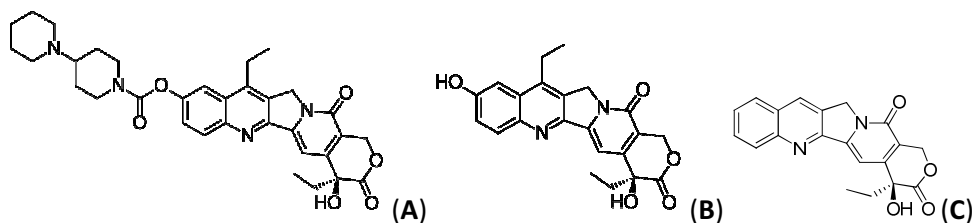


Figure 1. 10 Chemical structure of Irinotecan (CPT-11)(A), SN-38(B) and CPT(C).

In fact, SN-38 shows higher cytotoxicity against tumor cells *in vitro* (100- to 1000-fold more potent than Irinotecan (CPT-11)), although it seems to be less effective *in vivo* when compared to Irinotecan (CPT-11)<sup>21</sup>. However, SN-38 is insoluble in pharmaceutical approved solvent mediums and it cannot be administered directly<sup>22</sup>. For this reason and taking profit of the advantages of new drug delivery systems, SN-38-based delivery systems are nowadays regarded as an instrument to overcome Irinotecan (CPT-11) limitations<sup>23</sup>. In addition, the use of SN-38 might also surpass resistance to CPT-11 in patients.

#### 1.1.1.1.3 Cytotoxic treatment: Platinum based compounds

Platinum based compounds are coordination complexes of platinum used as chemotherapeutic agents. They inhibit DNA repair and/or DNA synthesis in cancer cells by the formation of drug/DNA crosslinks. However, the main dose-limiting side effect of cancer treatment with platinum compounds is neurotoxicity. The most popular platinum based compounds are Cisplatin and Oxaliplatin. The former was the first to be developed in United States in 1978. Oxaliplatin as a single-agent has limited efficacy, but in combination with 5-FU and LV is routine clinically used in patients with mCRC<sup>24</sup>.

#### 1.1.1.1.2 Antiangiogenic treatment

Angiogenesis consists on the formation of new blood vessels from existing ones. The new blood vessels facilitate the delivery of necessary oxygen and nutrients, and the removal of waste products. Angiogenesis is regulated by a tuned balance between factors capable of stimulating and inhibiting blood vessel formation. The endothelial cells of existing blood vessels respond to these angiogenic molecules by undergoing differentiation, migration and proliferation<sup>25</sup>. Angiogenesis is upregulated in many diseases, including cancer. In tumors beyond 2-3 mm, angiogenesis is related

with the tumor growth, invasion and metastasis. Interestingly, the new vessels formed in tumors are irregular, tortuous and with a leaky vascular network, leading a permeable vasculature that also facilitates tumor cell invasion<sup>26</sup>.

Since angiogenesis is a key step in cancer development, the study of antiangiogenic therapies are considered one of the most promising approaches for eradicating cancer. Different anticancer drugs are based on the concept that removal of the angiogenic blood vessels will hamper the supply of nutrients and oxygen to cancer cells. Thus, interrupting the angiogenic process by inhibiting the endogenous angiogenic factors, degradative enzymes or necessary endothelial cell processes will disrupt cancer progression. Whether antiangiogenic compounds are able to effectively inhibit tumor cells proliferation and metastasis formation has become a research subject as target-orientated therapies. Moreover, combination of antiangiogenic and chemotherapeutic drugs are yielding promising results, so far.

Antiangiogenic drugs can be divided into agents targeting tumor epidermal growth factor receptor (EGFR), and those targeting vascular endothelial growth factor (VEGF) or its receptors (VEGFR) that are expressed in endothelial cells and stimulates angiogenesis. These new drugs are currently administered in combination with other cytotoxic agents.

Bevacizumab<sup>27</sup>, Cetuximab<sup>28</sup> and the latest approved Aflibercept<sup>29,30</sup> are nowadays the three more important antiangiogenic drugs. Bevacizumab is a monoclonal antibody directed against VEGF, Cetuximab is a chimeric IgG1 immunoglobulin acting as an EGFR inhibitor, and Aflibercept is a novel human recombinant protein designed to block the angiogenesis network (binding VEGF-A and VEGF-B).

### 1.1.1.3 New strategies combining different therapies

Pharmacodynamic interactions have been used for years for therapeutic benefit in oncology. In this sense, combination chemotherapy looks for synergistic effects of different drugs that can result in increased cytotoxic activity which translates into an improved clinical response. However, because synergistic interactions can also increase adverse effects, is necessary to evaluate their possible limitations.

5-FU can be administered in a wide range of schedule regimens intravenously. Due that administration of 5-FU/LV has shown great advantages in comparison to 5-FU alone, different combinations of 5-FU/LV with Irinotecan and Oxaliplatin has improved the response rates for mCRC<sup>24,31</sup>. Two main chemotherapy regimens are approved for the systemic treatment nowadays: FOLFIRI and FOLFOX. (i) FOLFIRI regimen consists on the combination therapy of 5-FU-Leucovorin-Irinotecan as the first-line treatment for patients with mCRC. It has demonstrated improvements in progression-free and overall survival when this combination therapy is administered vs the 5-FU/LV regimen. In addition, these new therapeutic regimens have considerably improved survival compared with single-agent fluorouracil (median survival >20 months compared with about 11–12 months)<sup>3,9,32</sup>. (ii) FOLFOX regimen consists on the combination therapy of 5-FU-LV-Oxaliplatin in 5-FU-resistant CRC. This combination increases tumor response rates and disease free-survival vs the

5-FU/LV treatment (8.2 vs 7.2 months, respectively)<sup>24</sup>. Several versions of this regimen have been developed from FOLFOX1 to FOLFOX7 to improve the 5-FU related toxicity and patient compliance, but there is no evidence of improvement in terms of efficacy.

Combination of chemotherapeutic regimens with antiangiogenic therapies is nowadays becoming a standard of care for mCRC. Some studies have shown that Bevacizumab is able to prolong median overall survival when administered in combination with Irinotecan as a first line treatment or with FOLFOX after failure of a prior regimen that contains Irinotecan<sup>33</sup>. In patients with untreated mCRC combination of Bevacizumab to FOLFOX or FOLFIRI showed improvements in tumor response rate and progression-free survival among patients with mCRC. On the other hand, the monoclonal antibody Cetuximab produced significant increase in response rate when combined to Irinotecan in Irinotecan-resistant CRC with a 10% of increase<sup>33</sup>. It also shows improvements of efficacy once administered in combination to FOLFOX and FOLFIRI. Further, Aflibercept has recently been approved in combination with FOLFIRI in mCRC resistant to or showing progression after oxaliplatin-containing regimens<sup>30</sup>.

## 1.2 Nanomedicine

Since applied nanotechnology lies in the frontier of different disciplines, from physics to chemistry or biology, many interpretations of the term “Nanomedicine” have appeared. In order to achieve a consensus, the European Science Foundation (ESF) defined Nanomedicine in this way:

*“Nanomedicine uses nano-sized tools for the diagnosis, prevention and treatment of disease to gain increased understanding of the complex underlying patho-physiology of disease. The ultimate goal is improve quality-of-life.”*<sup>34</sup>

Indeed, Nanomedicine is an overall term that includes nanopharmaceuticals, nanoimaging agents and theranostics, also known as patient-centered nanotechnologies<sup>35</sup>. Nanopharmaceuticals can be defined either as DDS or biologically active drug products. In both cases these nanopharmaceuticals are “nanometer size scale complex systems, consisting of at least two components, one of which is the active ingredient”<sup>36</sup>. Nanoimaging agents and monitoring technologies can be used for diagnostic or sensing applications. Moreover, combination of therapeutic and diagnostic capabilities into a single construct has given name to the term theranostics. In all cases, nanointeractions that occur in a subcellular or a cellular nanoscale system, should be taking into account to include active components or complexes in the size range of 1-1000 nm.

First generation Nanomedicines were born during the second half of the 20<sup>th</sup> Century (Figure 1. 11) as a way to improve the therapeutic index of treatments and find alternative therapeutic strategies. At that time, small molecules were thought to be the best approach to cure diseases, so new Nanomedicines were received skeptically, especially due to their size. Indeed, the large majority of clinically used drugs are low-molecular-weight compounds (typically under 500 g·mol<sup>-1</sup>) that exhibit a short half-life in the blood stream and a high overall clearance rate. In addition, they diffuse

rapidly into healthy tissues and are distributed within the body. As a consequence, small amounts of drugs reach the target site, producing side-effects in the patient and reducing the therapeutic index of drugs to a really narrow window. Nanomedicines offer an alternative to new drug design. By developing a drug delivery “vehicle”<sup>34</sup> able to target a bioactive agent more precisely to its desired place of action and/or control drug release to ensure that its optimal concentration is maintained at the therapeutic target over a desired time frame. On the other hand, Nanomedicine has also changed the drug delivery system concept that was seen historically, by offering new approaches to improve the performance of an established drug, rendering better formulations, better route of administration, and/or improved therapeutic indexes.

Liposomes, polymer-drug conjugates, polymer-protein conjugates, block copolymer micelles, nanogels, polymers or dendrimers considered new drugs, nanocrystals, nanoparticles and nanocapsules are the main classes of first generation Nanomedicines. They all have different physicochemical features and are placed in different nanoscale range. Some of them can be defined as particulate delivery systems in which the drugs are physically incorporated into nanoparticles, whereas in some others drugs are linked to the carrier through chemical conjugation.

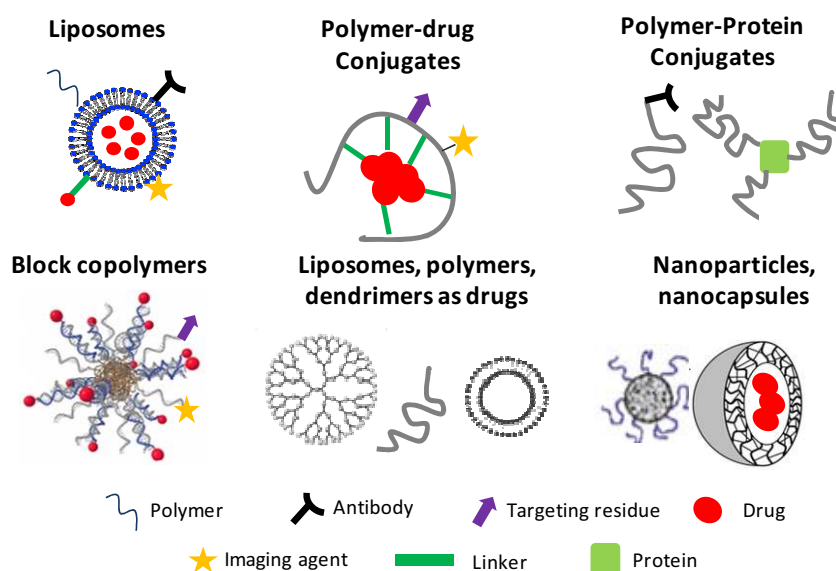


Figure 1.11 Scheme of the main classes of first generation Nanomedicines in clinical trial and routine clinical use (adapted from Duncan et al)<sup>34</sup>.

Over the last 20 years more than 40 Nanomedicines have been approved for routine human use and many more are currently in clinical trial<sup>34</sup>. This research has generated huge knowledge related to toxicity, side-effects, linking chemistry, doses, etc. All this information has a great importance for the next generation Nanomedicines that are under research or clinical development nowadays. This multicomponent second generation Nanomedicines are tailor-made systems that improve the drawbacks of the first generation Nanomedicines in several aspects: structure optimization, definition of product and formulation specifications, development of new characterization methods and improvement of the therapeutic index.



Low molecular weight compounds easily distribute via passive diffusion across cell membranes whereas macromolecular systems cannot pass through the capillary walls of healthy tissues. Internalization of nanomedicines is done mainly by endocytosis following lysosomal delivery or receptor mediated endocytosis (detailed in section 1.3.2.3).

### 1.2.1 Polymer therapeutics

Synthetic polymers have been explored as therapeutics since 1940s. Previously, in 1920s Herman Staudinger was the first to demonstrate the existence of macromolecules and defined them as polymers. Not only did Staudinger give us the concept of covalently linked macromolecules, he also noticed the potential of their use in biomedical applications<sup>37</sup>. At the beginning, polymers were mainly plasma expanders (PVP and dextran) and materials used as wound dressings and antiseptics (PVP-iodine) or also used as coatings. One example is the colloidal iron nanoparticle complexes used to treat anemia since 1930s leading to a safe product for parenteral administration. From the 1960s synthetic polymer-based drugs, polymer-drug conjugates and polymer-peptide conjugates, especially with the polymer poly(ethyleneglycol) (PEG) began to emerge. It was in the 1970s when the interest on the lysosomotropic polymer-drug conjugates, block copolymer micelles, and PEG-protein conjugates began to grow exponentially. Due to this research an increasing number of PEGylated proteins, and more recently aptamers, have appeared as medical products. It was at this time and due to the advances in cell biology and polymer chemistry when the rational design of new anticancer polymer-drug conjugates began, a promising line of research up to now.

In the 1990s the term “polymer therapeutics” was coined by Duncan and Conors<sup>38</sup> when the development of a novel, water-soluble synthetic polymer-based systems made for improved diagnostics and treatment of disease became a step forward in the field of polymer chemistry, biology, physics and medicine. Polymer therapeutics include different subclasses of Nanomedicines: polymeric drugs, polymer-drug conjugates, polymer-protein conjugates and polymeric micelles in which drugs are covalently bound and multicomponent polyplexes<sup>39</sup>. They are defined as new chemical entities (NCEs) rather than conventional drug delivery systems or formulations that simply entrap, solubilize or control drug release without resort to the chemical conjugation<sup>40</sup>.

Modern polymer chemistry produces complicated polymer structures including multivalent polymers, branched polymers, dendrimers, dendronized polymers, block copolymers, graft polymers, stars and peptide derivatives. These new polymeric structures can be produced with a more defined chemical composition, tailored surface multivalency and the capacity to create specific three-dimensional structures. On the other hand, linear and random-coil structure polymers have been used to synthesize polymer therapeutics that has been transferred to the clinical practice. Some examples are PEG, N-(2-hydroxypropyl)methacrylamide (HPMA) as synthetic polymers; dextran, hyaluronic acid, chitosans and dextrin as natural polymers and pseudosynthetic polymers such as the man-made poly(amino acids) poly(L-lysine), poly(glutamic acid) (PGA), poly(malic acid) and poly(aspartamides)<sup>39</sup>. HPMA-doxorubicin conjugates became the first synthetic

polymer-drug conjugates to enter Phase I/II clinical trials in 1994<sup>41</sup> and in the 1980s/90s the first block copolymer micelles entered to Phase I/II clinical trials<sup>42</sup>.

Polymer therapeutics reviewed by Duncan<sup>39</sup> encloses five different types (Figure 1. 12): active polymeric drugs, polymer-drug conjugates, polymer-protein conjugates, polymeric micelles (to which drug is covalently bound) and multi-component polyplexes developed as non-viral vectors for gene interfering ribonucleic acid (siRNA) delivery.

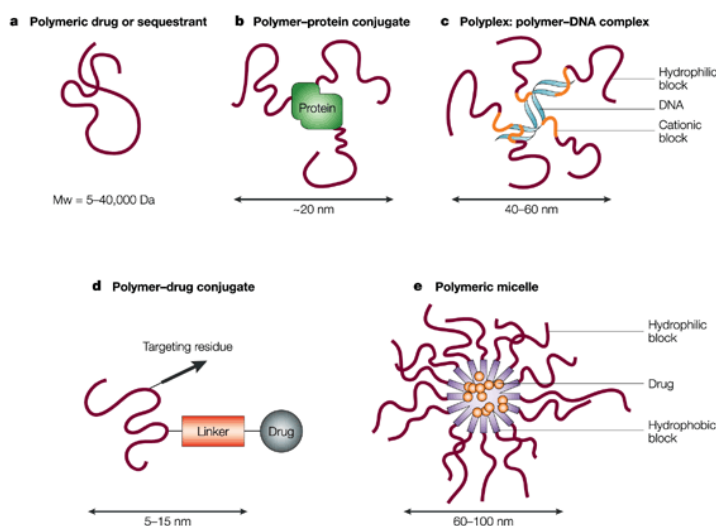


Figure 1. 12 Scheme of the different types of polymer therapeutics (adapted from Duncan et al)<sup>40</sup>.

**Polymer drugs** have a Mw between 5000 and 40000 g/mol are defined as polymers that have an inherent therapeutic activity. The **polymeric micelles** have a nanosize between 10 and 200 nm and are based in amphiphilic block copolymers with a drug covalently linked to the polymer backbone triggering in aqueous solutions at concentrations above the critical micellar concentration colloidal nanoparticles. This group is also known as core-shell structures because in aqueous solution, the hydrophobic segment forms the core (which contains the hydrophobic therapeutic drug) and the hydrophilic block forms the external micelle shell. It provides the necessary interactions with the solvent to make the nanostructure stable in solution. **Polyplexes**<sup>43</sup> are polymer-based non-viral vectors for cytosolic delivery of genes. Polyplexes have a nanosize between 90-160 nm and are formed by polymers capable of interacting with DNA/RNA. The last subclass of polymer therapeutics are **polymer conjugates**, and specially **polymer-drug conjugates** family, detailed in section 1.3.

Polymer therapeutics has been considered the most successful first generation Nanomedicines during the last quarter of the 20<sup>th</sup> century<sup>34</sup> comparing it to liposome and nanoparticles, where the bioactive agent is not covalently attached to the vehicle. Indeed, several candidates have progressed to market (Table 1.1): polymeric drugs, polymeric sequestrants, PEG-conjugates and PEG-aptamer conjugates.

Table 1. 1 Polymer therapeutics in the market and clinical development. (Adapted from Duncan et al<sup>34</sup>).

Polymer Therapeutics	Examples	Composition	Clinical Use	Status		
Polymeric Drugs	Copaxone	Glu, Ala, Tyr copolymer	Multiple Sclerosis	Market		
	Vivagel	Lysine-based dendrimer	Microbiocide	Phase III		
	Hyaluronic acid	Hyalgal, Synvisc	Osteoarthritis	Market		
Polymeric sequestrants	Renagel	Phosphate binding polymer	End Stage Renal Failure	Market		
	Welchol	poly(allylamine hydrochloride)	Reduce LDL/Type II	Market		
Polymer – Protein Conjugates (PPC)	PPC	Zinostatin	Styrene maleic anhydride-neocarzinostatin, (SMANCS)	Hepatocellular	Market	
		SuliXen	Polysialylated insulin	Diabetes	Phase I/II	
	PEGylated proteins	Cimzia	PEG-anti-TNF Fab	Rheumatoid arthritis	Market	
		Mircera	PEG-EPO	Anemia associated with	Market	
		Peg-intron	PEG-Interferon alpha 2b	Chronic hepatitis C	Market	
		Pegasys	PEG-Interferon alpha 2a	Hepatitis C	Market	
		Neulasta	PEG-hrGCSF	Chemotherapy	Market	
		Uricase-PEG 20	PEG-uricase	Hyperuricemia	Market	
		ADI-PEG 20	PEG-arginine deaminase	Cancer-melanoma	Phase II	
	PEGylated-aptamer	Macugen	PEG-aptamer (apataniab)	AMD	Market	
		E10030	PEG-anti-PDGF aptamer	Ophthalmological	Phase II	
		ARC1779	PEG-anti-platelet-binding factor	HIV	Phase II	
	Polymer – Drug Conjugates (PDC)	PDC	CT-2103;	Poly-glutamic acid (PGA)-paclitaxel	Cancer-NSCLC, ovarian,	Phase III
			Prolindac	HPMA-copolymer-DACH palatinat	Cancer-melanoma,	Phase II
			PEG-SN38	Multiarm-PEG-camptothecin	Cancer-various	Phase II
XMT-1001			Polyacetal-camptothecin conjugate	Cancer-various	Phase I	
NKTR-118			PEG-naloxone	Opiod-induced	Phase III	
Block copolymer micelles		SP1049C	Doxorubicin block copolymer micelle	Cancer-various	Phase I/II	
		NK 105	Paclitaxel block copolymer micelle	Cancer-various	Phase II	
		NK-6004	Cisplatin block copolymer micelle	Cancer-various	Phase II	
Self assembled polymer conjugate nanoparticles		IT-101	Polymer-conjugated-cyclodextrin	Cancer-various	Phase II	
	CALAA 01	Polymer-conjugated-cyclodextrin nanoparticle-siRNA	Cancer-various	Phase I		

### 1.3 Polymer conjugates

Polymer conjugates have a nanosize between 2-25 nm and can be defined as polymer-based systems conjugated to a protein or a drug: (i) **polymer-protein conjugates** (PPC) and (ii) **polymer-drug conjugates** (PDC), respectively (see Table 1.1). Both families of polymer conjugates are tailor-made using a tripartite structure: the polymeric backbone, the linker and the bioactive agent<sup>44</sup>.

Moreover, polymer conjugates can bring a targeting moiety or an imaging agent as an additional part of the structure.

Polymer conjugation to proteins reduces immunogenicity, enhances protein stability and prolongs plasma half-life through prevention of renal elimination and avoidance of receptor-mediated protein uptake by cells of the reticuloendothelial system (RES). In consequence, therapies based on polymer therapeutics require less frequent dosing, enhancing patient compliance<sup>45</sup>. During the past 20 years an increasing number of polymer-protein conjugates have entered into routine clinical use in oncology (Table 1.1).

Polymer conjugation to drugs improves the pharmacokinetic profile of the drug and in most cases, enhances the solubility of hydrophobic drugs. Moreover, conjugation of drugs to polymer reduces their toxicity in healthy tissues and enhances the therapeutic activity in the target tissues increasing plasma half-life and optimize volume distribution. In addition, the polymer also protects the drug from degradation and premature interaction with its biological environment and it reduces kidney and liver clearance<sup>46,47</sup>.

Polymer therapeutics are mainly designed for intravenous administration (i.v.). This administration route ensures fast bioavailability of the therapeutic compound and reduces the number of barriers to be crossed. It is therefore the most effective. It enters the bloodstream directly and it is distributed throughout the body within seconds. However, intravenous administration holds many drawbacks for the patient and therefore leads to a lower patient compliance. Several formulations in the market today are designed to be administered subcutaneously (s.c.) and intramuscularly (i.m.). These routes allow slow drug release from the injection sites to the bloodstream and therefore less frequent injections are required. Intraperitoneal (i.p.) administration is also an alternative, being the elimination rates  $i.p. > s.c. > i.m.$ . Nonetheless, oral administration is used and considered the best route in terms of patient compliance. However, orally-administered drugs need to pass several barriers to reach systemic circulation which can decrease drug bioavailability. In contrast, polymer-drug conjugates designed to be administered orally can be used to: (i) protect sensitive drugs from stomach and gut lumen, (ii) enhance absorption in the intestine by increasing water solubility (iii) overcome drug resistance mechanisms and (iv) protect the drug from degradation by liver enzymes<sup>50</sup>.

### 1.3.1 Polymer-drug conjugates

#### 1.3.1.1 Polymer-drug conjugates structure

As mentioned before, the main parts of the polymer conjugates are the polymeric backbone, the linker, the drug and, in some cases, a targeting moiety.

The **polymeric backbone** is defined as the water-soluble carrier and makes the platform capable of solubilizing a hydrophobic drug. It is crucial in order to allow an intravenous administration of the polymer conjugate. The ideal carrier is characterized by its multifunctionality, biocompatibility (non-toxic and non-immunogenic), low polydispersity and biodegradability. In addition, it should be

suitable for repeated administration. Multifunctionality can be found in pendant groups or end groups on the polymer backbone. Therefore, targeting moieties, imaging agents and drugs can be conjugated in a single polymer conjugate.

The **linker** is the molecular part of the polymer conjugate that connects the drug to the polymeric backbone. Much research is being done in order to improve the selective release of the drug attending to linker chemistry. The ideal linker should be stable during transport to the target tissue (i.e. solid tumors), but also able to release the drug at an optimum rate up on arrival<sup>44</sup>. Due to most polymer-drug conjugates are designed for lysosmotropic delivery, two types of linkers have emerged for this delivery pathway: pH labile linkers and peptidyl linkers. The latter, are enzyme susceptible linkers designed to be stable in the bloodstream and other biological fluid but are degraded when exposed to specific lysosomal enzymes. Thus, the aim of the linker goes further than binding the polymer to a bioactive agent: it also become active by triggering drug release under certain conditions. One of the most relevant cases of peptidyl polymer-drug linkers is the HPMA copolymer-Gly-Phe-Leu-Gly-Doxorubicin conjugate<sup>41</sup>. This tetrapeptide linker is stable in circulation but becomes cleaved by the lysosomal thiol-dependant protease Cathepsin B following endocytic uptake of the conjugate<sup>48,49,50</sup>.

In the case of MMP overexpression it is reported the use of sensitive linkers to MMP overexpressed in cancer tissues with the aim of delivering the drug in the cancer tissue by a MMP cleavage<sup>51</sup>. Since this type of linkers is studied in this thesis, a more detailed description is given in section 1.3.4 of this General Introduction. Peptidyl linkers designed for cleavage tumor-associated legumain<sup>52</sup> are a different example of linkers developed for deliver drugs in specific sites. Moreover, both, steric factors (length of the linker) and structural factors (sequence of the amino acids) affect the cleavage of the bioactive agent from the polymer. As mentioned above, the other group of linkers is the acid labile linkers. These linkers should be also stable during blood circulation too at a physiological pH but will be hydrolyzed under the acidic environment of the endocytic pathway (pH=4 -6.5)<sup>49</sup>. Linkers based on cis-aconitryl, acetal or hidrazone moieties undergo pH-dependant hydrolysis following internalization through the endocytic pathway.

### **1.3.1.2 Polymer-drug conjugates based on biodegradable polymers**

Most of the polymer-drug conjugates in clinical development use either PEG or HPMA as carriers. Although their molecular weight can be tailored to maximize the chance of renal elimination (< 40.000 g/mol) and they are well tolerated clinically, these non-biodegradable polymers have the potential to accumulate intracellularly at the lysosomal compartment and therefore can cause "lysosomal storage disease" syndrome<sup>53</sup>. Because of this, if non-biodegradable polymers are used is necessary to carefully consider the administered dose and the frequency of dosing. They are clearly not recommended for long term administrations. For these reasons, during the last decades many efforts have been done to minimize any adverse effects that polymers can cause. In that sense, biodegradable polymers have become a great alternative. They allow utilization of higher molecular weight platforms to optimize pharmacokinetics, and they are essential for treatment of diseases requiring chronic treatments. Polymers that degrade enzymatically or hydrolytically currently in preclinical or clinical development include dextrin<sup>54</sup>, hydroxyethylstarch (HES)<sup>34</sup>, polyglutamic acid

(PGA)<sup>55,56</sup>, polyacetals and polysialic acids. PGA (detailed in section 1.3.2.1) is being increasingly used as a drug carrier; it is degraded by lysosomal Cathepsin B (lysosomal thiol-dependant protease). Other biodegradable polymers are: dextrin (degraded by  $\alpha$ -amilase), hyaluronic acid (degraded by hyaluronidase), HES, the “Fleximer” polyacetal technology and poly(sialic acid)<sup>37</sup>.

### 1.3.1.3 Biodegradable Polymer-drug conjugates based on PGA

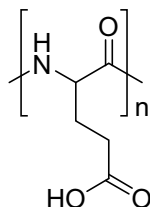


Figure 1. 13 Chemical structure of poly(L-glutamic acid).

PGA is a polypeptide approved by the FDA that is composed of natural L-glutamic acid linked together through amide bonds rather than non-biodegradable C-C backbone. The pendent  $\gamma$ -carboxyl group in each repeating unit of L-glutamic acid is negatively charged at a neutral pH, which renders the polymer water-soluble. Limited aqueous solubility of several anticancer drugs can be solved by conjugating them to PGA, taking also the general advantages of PDC selectivity to cancer tissues. Drug introduction in PGA-polymer-drug conjugates is through the carboxyl groups. Despite drug attachment blocked carboxyl groups, these final conjugates are still negatively charged. Some problems have been discussed regarding the possibility of an electrostatic repulsion in the cellular uptake due to the negatively charged surface of the cells. However, it has been reported that PGA nanoconjugates do not diminish their accumulation in solid tumors<sup>57</sup>. In addition, glutamic acid, the breakdown product of PGA, can enter normal cellular metabolism and it is not excreted by the kidney<sup>55</sup>.

PGA can be produced from bacteria and in a synthetic manner. Nowadays, PGA is the only biodegradable and water-soluble polymer that can be synthesized or purchased with a polydispersity index around 1.2 -1.4.

Multiple proteins and drugs (mostly anticancer drugs) have been conjugated to PGA, and some polymer-drug conjugates have already reached clinical trials. Different classes of anticancer drugs attached to the PGA polymeric chain are reported in the literature: anthracyclines, antimetabolites, DNA-binding drugs, paclitaxel or camptothecin<sup>55</sup>. Among all PGA-based polymer-drug conjugates the most promising one is OPAXIO<sup>®</sup> (Formerly Xyotax, CT-2103 form Cell Therapeutics Inc.)<sup>53</sup>. It is a poly-L-glutamic acid (PGA)-paclitaxel conjugate that contains a covalent conjugation through an ester bound of paclitaxel to  $\gamma$ -acids of poly-L-glutamic acid. This PDC is now in phase III clinical trial as a maintenance therapy in women with advanced ovarian cancer. OPAXIO has also been evaluated in phase II clinical trials for ovarian cancer as a single agent, and for non-small-cell lung cancer in combination with carboplatin<sup>58</sup>. This is also an example of personalized polymer therapeutics because it requires Cathepsin B degradation to release the drug. Oestradiol levels in women seem to correlate with levels of lysosomal Cathepsin B, and therefore, oestradiol levels have been used recently to guide patient selection in clinical trials<sup>59</sup>.

Another example of a promising PDC based on PGA is PGA-CPT (CT-2106). A Poly-L-glutamic-Camptothecin from Cell Therapeutics developed for treating ovarian, lung and advanced colorectal cancers. CT-2106 as a single agent and/or in combination with 5-FU showed significantly enhanced antitumor activity in several relevant animal tumor models<sup>60</sup>. Although the most important PGA based polymer-drug conjugates are those recently explained some other examples are: PGA conjugated with the DNA intercalating agent doxorubicin<sup>61</sup>, PGA conjugated with antimetabolites of uracil and uridine derivatives<sup>62</sup>, PGA-Mitomycin C<sup>63</sup> and PGA-Apaf1 conjugate that inhibits apoptosis<sup>56</sup>, among others.

### 1.3.2 Polymer-drug conjugates for anticancer therapy

Chemotherapeutic treatment has to deliver the largest portion of the administered drug to the target site at the proper time and for as long time as possible to reach efficacy. Because of this, new anticancer drugs must ideally show sustained, controlled and targeted release<sup>25</sup>. Furthermore, the acquisition of multidrug resistance (MDR) by cancer cells has appeared as a new problem in chemotherapy. MDR is mainly attributed to over-expression of the plasma membrane P-glycoprotein (P-gp), which is capable of pumping drugs out from the cell. Other mechanisms of MDR acquisition include enzymatic deactivation, decreased permeability (drugs cannot enter the cell) and alteration of binding-sites and metabolic pathways, among others.

In order to enhance treatment response, two different approaches have been designed to improve therapeutic indexes of chemotherapeutic drugs. The former one consists on the design of new low molecular weight drugs (LMWD) and the search for novel, tumor-specific molecular targets<sup>64</sup>. Even though a targeted low molecular weight anticancer drug would perform better than most current chemotherapeutic agents, there are still high difficulties to overcome. Among them, drawbacks associated with their size and specificity, mostly because strong genomic and proteomic research efforts have not yet provided an optimal target. LMWD are characterized by a high pharmacokinetic volume of distribution which contribute to higher cytotoxicity; LMWD are easily excreted, hence higher concentration is ultimately required producing higher toxicity and limiting in consequence maximal allowable drug dose. In addition, low specificity when administered alone cause damage to healthy tissues because does not greatly differentiate between cancerous and normal cells. For these reasons a second line of research to improve chemotherapeutic treatment for cancer diseases is focused on the development of new DDS for LMWD in order to achieve more specific targeting of the drug in cancerous tissues, thereby improving efficacy and minimizing adverse side effects. Thus, new DDS as cancer treatments are designed to achieve controlled release of the bioactive agent and to improve drug tumor targeting. This second line of research has succeeded during the last two decades since HPMA copolymer-doxorubicin conjugate (PK1)<sup>41</sup> entered in clinical trial in 1994. Some polymer therapeutics have entered in clinical trials or have reached the market as anticancer therapy (summarized in Table 1.1). In that sense, polymer-drug conjugates begin to play an important role in this new area of research and are currently considered the most promising compounds of the next-generation Nanomedicines<sup>37</sup>.

### 1.3.2.1 Passive targeting: Enhanced Permeability Retention Effect

Tumors smaller than  $1\text{-}2\text{ mm}^3$  are not vascularized because oxygen and nutrients can reach the center of the tumor by simple diffusion. However, tumors larger than  $2\text{ mm}^3$ , enter a state of cellular hypoxia that marks the onset of tumoral angiogenesis: the sprouting of new blood vessels from existing vessels. In tumor progression, development of new blood vessels supports tumor growth and allows the dissemination of cancer cells throughout the body, leading to metastasis. However, within a tumor, the vascular network is not a stable system<sup>25</sup>. In this sense tumors offer a great advantage regarding treatment with macromolecular Nanomedicines due to their vascular anatomical-pathophysiological differences with normal tissues<sup>65</sup>. Intratumoral vascular leakage results in an enhanced accumulation of nanomedicines, and by extension PDC, in damaged tissues. A phenomenon known as the Enhanced Permeability Retention Effect (EPR), first described by Maeda in 1986<sup>66</sup>.

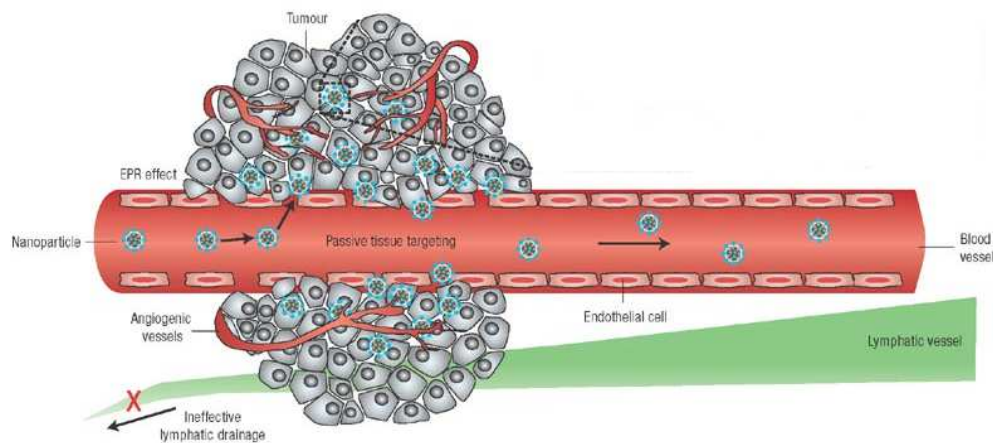


Figure 1. 14 Scheme of the EPR effect (adapted from Peer et al)<sup>67</sup>.

New vessels generated during the angiogenic process in cancer are characterized by two facts that lead to the EPR effect: (i) hiperpermeability (leakiness) of the tumor vasculature, that will ensure a sufficient supply of nutrients to tumor tissues to ensure rapid growth and (ii) lack of an effective lymphatic drainage. Most solid tumors have blood vessels with defective architecture that facilitates the transport of macromolecules into tumor tissues, and its passive accumulation due to the lack of a lymphatic drainage. It is known that molecules larger than 40 kDa selectively extravasate from tumor vessels and accumulate in tumor tissues thanks to the EPR effect. In this way, this unique phenomenon in solid tumors might facilitate targeting of PDC containing LMWD to the tumors.

Most anticancer drugs used in conventional chemotherapy have no tumor selectivity and are randomly distributed along the whole body often resulting in low therapeutic indexes. As they are LMWD, they diffuse into normal tissue through capillarity. Macromolecular systems such as PDC can not pass through normal endothelial cells by diffusion, but they offer a promising system able to control the pharmacokinetics of a given drug allowing its accumulation within the tumor due to the EPR effect. This type of tumor accumulation is known also as passive targeting.



Although EPR effect has been one of the most pursued objectives for new anticancer drug delivery systems, this strategy has still some major difficulties to overcome. Large tumors (>1-2 cm in diameter) might show great vascular heterogeneity, and some areas might not exhibit EPR effect. Also, larger tumors tend to contain more necrotic tissues or highly hypovascular areas (with thus less chance of vascular leakage and EPR, and lower drugs access because of the lack of blood vessels)<sup>68</sup>. Thus, EPR effect is tumor-size dependant. To overcome these problems, recently developed methods to intensify the EPR effect artificially and achieve a more homogenous drug delivery to tumors have been studied. Maeda studied two factors: the bradykin (which facilitates vascular leakage by the use of a peptide that causes dilation of blood vessels causing a lower blood pressure) and applying nitric oxide (NO)-releasing agents (which facilitates vascular blood flow).

### **1.3.2.2 Active targeting**

Understanding disease site microenvironment is crucial to achieve an optimal targeted drug release, called active targeting. In the case of cancer, methods to efficiently increase the delivery of drugs to tumor cells might take advantage of over-expressed cell surface proteins. The lower pH of cancerous tissues is an additional advantage. Conjugated drugs need to be delivered at the target site (intra- or extracellularly), so multiple pathophysiological conditions in the extracellular environment might offer excellent targets.

Different ways of targeting have been studied by using directing moieties attached to the PDC that interact with cell surface receptors or by using sensitive linkers to conjugate the drug to the polymeric backbone. These linkers can be susceptible to an acidic pH, or to a chemical shift or biological element overexpressed at the pathological site. In the polymer therapeutics field, most current linkers are sensitive to enzymes<sup>51,41</sup> or pH dependant<sup>50</sup>.

It is expected that an active targeting strategy will achieve higher and faster intra-tumor drug accumulation and in the case of active targeting with internalizing ligands, increased intracellular drug concentration. However, when active tumor targeting is desired it is necessary to keep in mind that tumors contain genetically unstable cell populations with different cell-surface receptors, and therefore it will be mandatory for oncologists to know if those targets are over-expressed in each cancer patient, searching for a tailor-made personalized treatment.

In the field of PDC, enzymatically-cleavable linkers are commonly used for a selective targeting of PDC. Cathepsins are generally the most important enzymes used to activate the release of a drug (e.g. in the HPMA-Dox PDC it was seen that the GPLG linker was responsible for Cathepsin-B-activated release of Doxorubicin (section 1.3.1.1))<sup>69</sup>. Because we have developed a new PDC designed to achieve an active targeting based on MMPs, the MMP substrates are detailed below.

#### **1.3.2.2.1 Active targeting based on MMP-sensitive delivery**

MMPs are a family of zinc-dependent neutral endopeptidases that are capable of degrading most components of the extracellular matrix (ECM). They play an important role in the physiologic

degradation of ECM: morphogenesis, uterine involution, tissue repair, angiogenesis and wound healing, among others<sup>70</sup>.

In CRC, MMPs contribute to multiple stages of disease progression including growth of the primary adenoma, invasion of CRC cells and cell migration to metastatic sites and metastasis growth.

MMP enzymes have both, a descriptive name and a number, based on the order of discovery. The descriptive name informs about the preferable substrate of the enzymes distinguishing: Collagenase, Stromelysin, Matrilysin and Gelatinase, and there is also a subclass known as membrane-type MMPs, a subset of MMPs that do not belong to the previous groups (see Figure 1.16). So the name classification is due to shared structural motifs among some of them.

In the case of CRC, it has been shown that human colon tumors over-express MMP-1, -2, -3, -7, -8, -9, -10, -11, -12 and -14<sup>73</sup>. The number of different MMPs and the level of expression are increased as the tumors become more advanced (Figure 1. 15) and a correlation between tumor cells ability to invade surrounding tissue and increased MMP expression has been demonstrated<sup>71</sup>. Further, MMP activity has been associated with an enhanced tumor invasion often resulting in a poorer prognosis<sup>72</sup>. In addition to tumor spread, certain MMPs may play a role in tumor vascularization. Experiments performed *in vivo* to inhibit angiogenesis by certain MMP inhibitors showed that MMPs can function in both, modulating angiogenesis and structuring the ECM<sup>75</sup>.

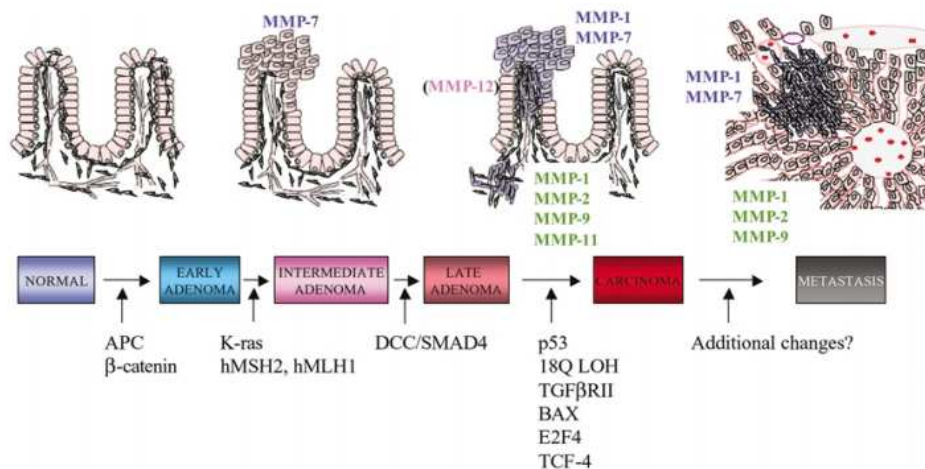


Figure 1. 15 Scheme of MMPs contribution to multiple stages of colon cancer progression. MMPs contribute to all stages of CRC including the growth of the primary adenoma, invasion of the CRC cells, migration of cancer cells to metastatic sites and growth of metastatic focus (adapted from Wagenaar-Miller et al)<sup>74</sup>.

The basic structure of MMPs consists on the following homologous domain: (i) a signal peptide which directs MMPs to the secretory pathway (is usually rich in hydrophobic amino acids and targets the enzymes to the endoplasmatic reticulum for possible excretion from the cell); (ii) a prodomain that confers latency to the enzymes by occupying the active site Zn making the catalytic enzyme inaccessible to substrates; (iii) a Zn containing catalytic site (the propeptide contains a highly conserved PRCGVPD sequence that contains a cysteine residue that interacts with Zn); (iv) a

homeopexin domain which mediates interactions with substrates and confers specificity to the enzymes; and (v) a hinge region which links the catalytic and hemopexin domain<sup>73,74</sup> (Figure 1. 16).

Variations within the residues forming the catalytic domain of the structure play a major role in binding and catalysis. However, discrete MMP substrate binding domains exist in non-catalytic regions that further increase substrate specificity of different MMPs<sup>76</sup>.

Since MMPs are involved not only in malignant processes but also in physiological situations, the activity of MMPs is regulated at several levels to ensure tight control. Enzyme activation and inhibition are the two ways in which MMPs are regulated<sup>74</sup>. MMPs are synthesized by stoma and tumoral cells as zymogens (inactive state). The prodomain of the enzyme must be removed to generate an enzymatically active protein. The removal of the entire pro-domain produces the mature form of the enzyme, but also a portion of the pro-domain can be removed by other MMPs, thus destabilizing the complex. The majority of MMPs are activated extracellularly and only some of them can be activated intracellularly by other proteases<sup>75</sup>.

MMP subclass	MMP designation	Common Name	Domain Structure <sup>8</sup>
<b>Matrilysins</b>	MMP-7	Matrilysin	SP   Pro   Catalytic
	MMP-26		SP   Pro   Catalytic
<b>Collagenases</b>	MMP-1	Interstitial collagenase	SP   Pro   Catalytic   Hinge   Hemopexin-like
	MMP-8	Neutrophil collagenase	SP   Pro   Catalytic   Hinge   Hemopexin-like
<b>Stromelysins</b>	MMP-13	Collagenase-3	SP   Pro   Catalytic   Hinge   Hemopexin-like
	MMP-3	Stromelysin-1	SP   Pro   Catalytic   Hinge   Hemopexin-like
	MMP-10 MMP-11	Stromelysin-2 Stromelysin-3	SP   Pro   Catalytic   Hinge   Hemopexin-like
<b>Gelatinases</b>	MMP-2	Gelatinase A	SP   Pro   F   Catalytic   Hinge   Hemopexin-like
	MMP-9	Gelatinase B	SP   Pro   F   Catalytic   Hinge   Hemopexin-like or C5   Hemopexin-like
<b>Membrane-type MMPs</b>	MMP-14	MT1-MMP	SP   Pro   F   Catalytic   Hinge   Hemopexin-like   TM   Cs
	MMP-15	MT2-MMP	SP   Pro   F   Catalytic   Hinge   Hemopexin-like   TM   Cs
	MMP-16	MT3-MMP	SP   Pro   F   Catalytic   Hinge   Hemopexin-like   TM   Cs
	MMP-24	MT5-MMP	SP   Pro   F   Catalytic   Hinge   Hemopexin-like   TM   Cs
	MMP-17	MT4-MMP	SP   Pro   F   Catalytic   Hinge   Hemopexin-like   TM   Cs
	MMP-25	MT6-MMP	SP   Pro   F   Catalytic   Hinge   Hemopexin-like   TM   Cs
<b>Others</b>	MMP-12	Metalloelastase	SP   Pro   Catalytic   Hinge   Hemopexin-like
	MMP-20	Enamelysin	SP   Pro   Catalytic   Hinge   Hemopexin-like
	MMP-19		SP   Pro   Catalytic   Hinge   Hemopexin-like
	MMP-27		SP   Pro   Catalytic   Hinge   Hemopexin-like
	MMP-28	Epilysin	SP   Pro   F   Catalytic   Hinge   Hemopexin-like
	MMP-23		SP   Pro   F   Catalytic   Cys   IgG-like

Figure 1. 16 Mammalian Matrix Metalloproteinases (MMP) Family (Originally table from Vartak et al)<sup>76</sup>.

In most malignant tumors, stoma fibroblasts are the primary source of MMPs. However, when tumors have been generated, the main sources of MMPs to the peritumoral environment are inflammatory cells. These cells can also produce cytokines, which enhance expression of MMPs by tumor and stomal cells. On the other hand, tumor cells produce factors, which enhance production

of MMPs by fibroblasts. It is therefore likely that MMPs form a network in which a single MMP cleaves certain native or partially degraded matrix components and activates other latent MMPs<sup>75</sup>.

Within the different MMPs that contribute to cancer, **MMP-7** shows unique characteristics that make it distinct to other MMPs in some aspects briefly discussed below.

- The natural substrates of MMP-7 are matrylisins.
- It is the most representative enzyme within the MMP family regarding its level of expression and contribution to metastasis.
- It has been found to be expressed in 90% of colonic adenocarcinomas and also described that MMP-7 has a role in CRC development and progression. Although their levels increased as cancer progresses it is known that MMP-7 plays an important role in early stages of tumorigenesis.
- It is also known that MMP-7 is produced by cells of epithelial origins whereas other MMPs are generated by stromal cells.
- Studies carried out in mice indicated that MMP-7 may serve as suitable target to control disease progression in some patients with risk of developing CRC<sup>77</sup>.

Nevertheless, other MMPs are also key factors on CRC progression: It is also known that levels of **MMP-2/-9** in CRC patients correlate well with metastasis and poor prognosis. Major characteristics are detailed below.

- The main substrates of MMP-2 and MMP-9 are gelatinases.
- Increased plasma MMP-2 expression was observed in lymph node-positive patients with CRC compared to those without lymph node metastasis<sup>78</sup>. However, increased levels of MMP-9 have been attributed to the inflammation typically seen in and around neoplasms a part from its association with CRC progression<sup>70</sup>.

#### **1.3.2.2.1.1 Drug development based on MMPs**

The alteration of MMPs levels is not only attributed to cancer but also to other diseases such as arthritis, inflammatory, cerebrovascular and cardiovascular alterations<sup>79,80</sup>. Different drug development strategies have been designed to take profit from the overexpression of specific MMPs. In the case of cancer, two different approaches are currently being studied. The first one consists on the design of protease inhibitors and the second strategy relays in the conjugation of protease substrates to a bioactive agent to ensure drug release at the target site.

##### **(a) Drug development based on selective MMP inhibitors in cancer therapy**

Inhibition of MMP activity in the extracellular space has been extensively studied as an approach to inhibit growth and invasion of cancer. For this reason many efforts have been done to develop MMP inhibitors (MMPi) with the aim of finding alternatives to conventional cytotoxic treatments.

Many preclinical studies performed with mice showed promising results in terms of tumor regression and prevention of its evolution to metastatic stages. However, Clinical Trials showed unexpected results<sup>81</sup>. The majority of the MMPi tested showed poor oral bioavailability and relevant side-effects such musculoskeletal pain and inflammation. Contrary to what happened in animal models, determining the optimal dose to achieve maximal biological response in humans was difficult. Moreover, all trials were performed in patients with late stage of the disease, while mouse experiments were carried out in animals with early-stage cancer. The efficacy of MMPi in clinical trials was remarkably low<sup>74</sup>.

Currently, the therapeutic role of MMPi in cancer remains uncertain, but the lessons learned from first generation MMPi development will be really important to design next generation MMPi that are under research<sup>82,83</sup>, and also for more specific MMP-activable drugs.

### (b) MMP activable pro-drugs

Many linkers cleavable by MMPs have been studied as substrates for specific MMPs to release a drug. Table 1.2 summarizes some examples of MMP-cleavable pro-drugs, called also MMP-activable pro-drugs that are currently under research.

Table 1. 2 Summary of MMP-activable pro-drugs (ADR: Adriamycin, ALB: albumin, BHQ3: black hole quencher 3, DEX: Dextran) (Adapted from Markovsky et al)<sup>69</sup>.

	MMP	Construct	Drug
<b>Peptide-based Pro-drug</b>	MMP-2/-9/-14	Glu-Pro-Cit-Gly-Hof-Tyr-Leu-X	Dox
	MMP-7	BHQ3-Lys-Arg-Ala-Leu-Gly-Leu-Pro-Gly-X	PH-A
<b>Polymer-based Pro-drug</b>	MMP2/-9	DEX-Gly-Ile-Leu-Gly-Val-Pro-X	Dox
	MMP-2/-9	ALB-Gly-Pro-Leu-Gly-Ile-Ala-Gly-Gln-X	MTX
	MMP-2/-9	DEX-Pro-Val-Gly-Leu-Ile-Gly-X	MTX
	MMP-2	PEG-Pro-Val-Gly-Leu-Ile-Gly-X	ADR <sup>140</sup>

In addition to the MMP-activable prodrugs, the use of peptidyl sequences sensitive to specific MMPs linked to a fluorescent molecule has also been used to develop molecular probes for diagnosis, imaging of MMP activity as well as for activate cell penetrating peptides. In the case of the fluorescent probes, the design of a near IR proteolytic fluorescent probe to determine MMP-2 activity in tumors showed promising results to determine MMP inhibition<sup>84</sup>. On the other hand, MMP-7 served as a target to describe *in vivo* detection and imaging of tumor-associated MMP-7 activity using a fluorophore linked to a MMP-7-cleavable peptide<sup>141</sup> and colorectal adenomas detection<sup>173</sup>; and Cy5.5 was conjugated to a MMP-13 cleavable peptide nanoprobe to detect neoplastic lesions in mice bearing murine squamous cell carcinoma SCC-7 cell tumors<sup>85</sup>.

### 1.3.2.3 Cellular drug delivery of polymer-drug conjugates in tumors

As mentioned previously, low molecular weight compounds easily distribute via passive diffusion across cell membranes whereas PDC or other macromolecular systems cannot pass through the capillary walls of healthy tissues. De Duve was the first who introduced the term “lysosmotropic drug delivery” when he observed that DNA could be used as carrier to deliver drugs by endocytosis<sup>86</sup>.

The endocytic pathway (Figure 1. 17) consists on the internalization of macromolecules present in the extracellular fluid via deformation of the membrane and the consecutive formation of carriers/vesicles inside the cell (endosomes and lysosomes). These vesicles then undergo a complex series of fusion events directing the internalized substances to the appropriate intracellular compartment. We can distinguish receptor-mediated endocytosis (cadherin-mediated, caveolae/lipid raft-mediated, clathrin-mediated), adsorptive endocytosis (caveolae-independent endocytosis) and fluid-phase endocytosis (see Figure 1.17). During endocytosis a significant drop in the pH value takes place from the physiological value (pH= 7.2 –7.4) in the extracellular space to pH 6.5–5.0 in the endosomes and to around pH 4.0 in primary and secondary lysosomes. A great number of lysosomal enzymes become active in this acidic environment, for example, phosphatases, nucleases, proteases, esterases, and lipases.

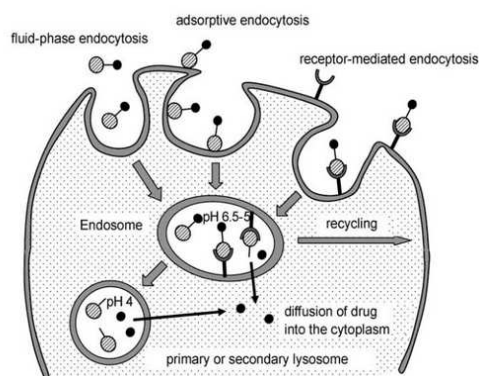


Figure 1. 17 Endocytic pathway for the cellular uptake of macromolecules and nanocarriers for drug delivery (adapted from Haag et al)<sup>87</sup>.

In the case of polymer therapeutics, Duncan distinguished between intracellular and extracellular delivery<sup>39</sup> (see Figure 1.18). In the former one, lysosmotropic and endosmotropic delivery can occur depending on the pH lability of the polymer-drug conjugate linker. The extracellular delivery occurs when the drug is released in the microenvironment of the cell and the drug enters by diffusion.

In addition to the EPR effect, tumor cells show a higher degree of uptake of macromolecules by endocytosis than healthy cells, as a result of the enhanced metabolic activity of cancer cells<sup>87</sup>. Combination of the EPR effect and lysosmotropic drug delivery constitute the basis of new polymer-drug conjugates designed to increase drug specificity and reduce side effects.

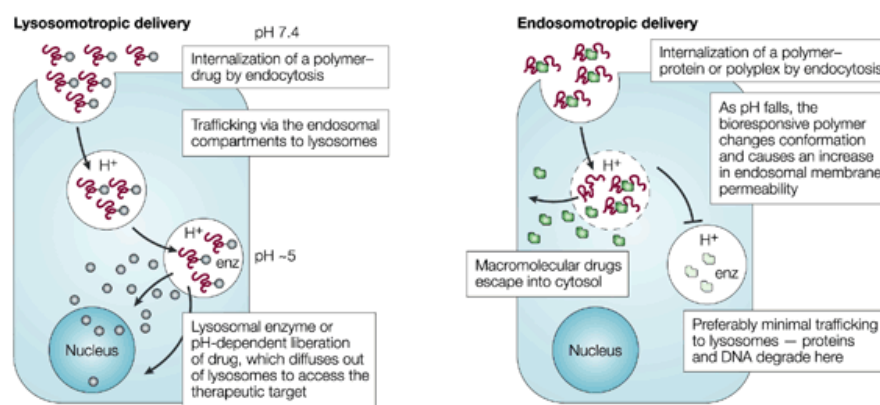


Figure 1.18 Scheme of the two types of intracellular delivery: lysosomotropic and endosomotropic (adapted from Duncan et al)<sup>39</sup>.

### 1.3.3 Polymer-drug conjugates for combination therapy

A deeper knowledge of the molecular mechanisms of many biochemical alterations has allowed the study of combination therapy treatments for many diseases, including malaria, HIV, diabetes and cancer among others. Different approaches have been studied with the aim of obtaining a better long-term prognosis and reduced side effects. The concept “combination therapy” encompasses either the simultaneous administration of two or more bioactive agents or the combination of different types of therapy. In many cases the advantage of using a combination therapy is that the use of two or more agents can modulate different molecular pathways in diseased cells, thus increasing the final efficacy<sup>88</sup>.

It is necessary to mention that although the combination therapy strategy generally looks for an improvement of the therapeutic index, a positive assessment does not always involve the achievement of a better efficacy. In some cases the achievement of comparable efficacy with reduced toxicity is the final objective. In that sense, combination chemotherapeutic treatments can also be used as palliative treatment to reduce symptoms and prolong life expectancy rather than cure the disease, or as an adjuvant pre- or post-surgery (e.g. to reduce tumor mass of advanced cancers)<sup>88</sup>.

Currently, combination therapy in cancer treatment is based on the administration of different small molecule chemotherapeutic drugs, the use of combinations based on endocrine therapy (for those hormone dependant cancers) or use of monoclonal antibodies (antiangiogenic treatment) and the combination of different types of therapies (e.g. chemotherapy + radiotherapy).

The study of DDS for combination therapy in cancer was initiated during the last decade. It was well demonstrated that the administration of drug combination showed better patients outcomes. Moreover, the use of DDS for treating cancer also showed promising results improving the efficacy and specificity of the treatment and reducing side effects. The hybridization of both developments resulted in the development of new DDS carrying a combination of drugs with the aim of ensure

the arrival and release of the different agents at the target site. It was in the field of polymer-drug conjugates where the first designs were investigated.

Four different types of polymer-drug conjugates for combination therapy can be distinguished as it is detailed in Table 1. 3.

Regarding the first type of combinations, it is important to mention that the combination of a PDC and radiotherapy might be synergistic because it enhances the accumulation of the PDC in the targeted tissues. It is known that radiotherapy can impact on tumor vasculature, possibly magnifying the EPR effect that enhances the accumulation of macromolecules. As depicted in Table 1.3, only the first type of combinations has reached clinical trials status. However, promising results are being achieved in preclinical experiments for the rest. One of the most interesting polymer-drug conjugates carrying a combination of drugs is the conjugate HPMA-Dox-AGM<sup>93</sup>. This was the first polymer-drug conjugate designed for a combination therapy by merging chemotherapy and endocrine therapy for treating breast cancer. *In vitro* cell studies determined that PDC containing only Dox or AGM did not show any synergistic effect, whereas the conjugate carrying both drugs was more active.

Table 1. 3 Examples of different types of polymer-based combination and their status (Adapted from Greco et al<sup>88</sup>).

Type	Description	Examples	Status
I	A PDC carrying a single drug is administered in combination of a single drug or a different treatment	PGA-Paclitaxel + Cisplatin <sup>89</sup>	Phase I
		PGA-Paclitaxel + Radiotherapy <sup>90</sup>	Phase III
II	Two PDC carrying a single drug are administered in combination	HPMA-Dox + HPMA-mesochlorin e6 <sup>91</sup>	Preclinical
		PEG-ZnPP + PEG-DAO <sup>92</sup>	Preclinical
III	A single polymeric vehicle carrying 2 or more drugs	HPMA-Dox-AGM <sup>93</sup>	Preclinical
		PEG-NO-EPI <sup>94</sup>	Preclinical
		HPMA-Gem-Dox <sup>88</sup>	Preclinical
IV	A PDC carrying a single drug is administered in combination of a polymer-enzyme conjugate (PDEPT) or a polymer-phospholipase conjugate (PELT).	HPMA-Dox + HPMA-Cathepsin B <sup>95</sup>	Preclinical
		HPMA-Dox + HPMA- $\beta$ -lactamase <sup>96</sup>	Preclinical



The conjugation of two or more drugs in a single polymeric carrier can bring advantages in comparison to the administration of a single drug. Moreover, it can be administered as a single dose, thus enhancing patient compliance. Although advantages can be achieved with these new designs in preclinical experiments, the identification of the optimal drug ratios as well as those drugs that are best delivered together or in a sequential manner is a key aspect that needs previous extensive research before moving to clinical trials.

### 1.3.4 Polymer-drug conjugates for treating other diseases

Polymer-drug conjugates are mainly used as anticancer agents, but during the last decade the field of polymer-drug conjugates has expanded to improve the treatment of other diseases such as diabetes, hypertension, infections, diseases of the digestive tract and rheumatoid arthritis, to mention some. In addition, promising research based on polymer conjugates as tools to promote tissue repair, wound healing, bone resorption and ischemia/reperfusion injuries is undergoing<sup>97</sup>.

Table 1. 4. Examples of PT in the market for treating other diseases than cancer (adapted from Vicent et al)<sup>46</sup>.

Disease	Polymer	Drug
Diabetes	PGA	Phloridzin
Hypertension	SMA	AHPP
HIV	PEG	Saquinavir
	k-carrageenan	Azidovudine
	Dextrin	Azidovudine
Hepatitis	PHEA	Azidovudine
	Dextran	Lamivudine
Fungal infection	PEG	Amphotericin B
	PEG	Amphotericin B
Leishmaniosis	Arabino-galactan	Amphotericin B
	HPMA copolymer	Amphotericin B
	HPMA copolymer	NPC161
Sepsis	PEG	Peptoid 7
Bowel constipation	PEG	Naloxol
Ulcerative colitis	Dextran	Budesonide
Inflammatory bowel	pDMAEMA	Dexamethasone
Rheumatoid arthritis	HPMA copolymer	a-methylpredniolone
	CDP	N-acetyl cysteine
Neuroinflammation	PAMAM	Glucoamine
Wound healing	PAMAM	Glucoamine-6-
	PGA	APAF-1 inhibitors
	Modified Dextran	17 b-oestradiol

### 1.3.5 Current state of polymer-drug conjugates

The second-generation of polymer-drug conjugates is taking benefit of the huge data that clinical trial and preclinical studies of first-generation PDC has generated during the last decades. Moreover, thanks to new biomarkers found in molecular biology, new polymer therapeutic will be able to more appropriately target diseased cells enhancing patient compliance. This opens to personalized therapies anticipating possible drawbacks. One example is found on most polymer anticancer drug conjugates that take profit of passive tumor targeting by EPR effect. A pre-selection of patients whose tumors display functional EPR effect should be a criteria indicating patient suitability for these therapies<sup>37</sup>. Thus, the emergence of improved diagnostic techniques based on imaging techniques or quantification of specific biomarkers should facilitate personalized treatments.

Since HPMA-Doxorubicin (PK1) was the first drug-polymer conjugate to enter human trials in 1994 different PDCs have reach clinical trials and many more are under preclinical validation. PK1 was improved to PK2, which is related to PK1 but incorporates an additional targeting ligand, namely, a galactosamine group that was designed to be taken up by the asialoglycoprotein receptor of liver tumor cells for clinical trials<sup>41</sup>. Nonetheless, the most advanced polymer-drug conjugate is the marketed drug OPAXIO<sup>98</sup> (also known as Xyotax) from Cell Therapeutics (section 1.3.2.1).

At the present moment, due to the molecular complexity of human pathologies, development of new combination therapies has become mandatory in order to achieve synergism between different drugs and therapies and enhance the therapeutic outcomes of the treatments. Currently, many investigations are focused on the design of new PDCs carrying different therapeutic agents or its administration in combination with other single-agents and therapies (section 4.3). In this sense, identifying adequate drug combinations, proportions and kinetic release of the different drugs opens many possibilities in the design of the new generation PDC.



---

## 2. Objectives

---

The main objective of this thesis is the design, synthesis, characterization and biological evaluation of different new polymer-drug conjugates based on PGA to improve the efficacy of current 5-FU treatment for advanced CRC disease.

Because biodegradable polymers have become the most appropriate carriers for the design of drug delivery systems for treating diseases that require chronic parenteral administration, in this project the PGA biodegradable polymer has been chosen as the carrier of the designed polymer-drug conjugates.

Because the chemotherapeutic agent 5-FU is the mainstay of cytotoxic therapy against mCRC, in all PDC designed 5-FU will be conjugated to PGA polymeric backbone. The difference between the set of PGA-5-FU PDC generated will be found on the type of release designed (passive targeting evaluating a new PGA-based PDC using enzymatically-cleavable linkers, particularly MMP-sensitive peptides) and the evaluation of combination therapy between 5-FU and SN-38, conjugated in a single PDC. For this reason, the present work is structured in three main sections in which the therapeutic efficacy of all PDC will be evaluated *in vitro*, and in some cases *in vivo* in mouse animal models.

Thereby, the principal objectives of each section are described separately:

- **Design, synthesis and biological evaluation of the polymer-drug conjugate based on PGA and 5-FU conjugated through an ester bond (PGA-5-FU).**
  - a. Synthesis and physico-chemical characterization of the PGA-5-FU in terms of drug loading, size and stability in different mediums.
  - b. Obtention of fluorescently labeled conjugates for *in vivo* biodistribution and cell internalization studies.
  - c. Evaluation of the *in vitro* cytotoxicity and cell internalization in CRC cell lines.
  - d. *In vivo* validation studies of PGA-5-FU in terms of biodistribution, tumor accumulation and efficacy in athymic nude mice.

- **Design, synthesis and biological evaluation of the polymer-drug conjugate based on PGA and 5-FU sensitive to MMP-7 and MMP-9 (PGA-MMPpept-5FU).**
  - a. Study of the nature of the linkage between 5-FU and the MMP-sensitive peptides in terms of stability and specificity of drug release.
  - b. Design and synthesis of the new MMP-sensitive polymer-drug conjugate based on PGA and 5-FU (PGA-MMPpept-5FU).
  - c. Physico-chemical characterization of the PGA-MMPpept-5FU PDC.
  - d. Evaluation of the *in vitro* cytotoxicity of the PGA-MMPpept-5FU PDC against 5-FU and PGA-5-FU in CRC cell lines overexpressing MMPs.
  
- **Synthesis, characterization, *in vitro* validation of polymer-drug conjugates based on PGA for combination therapy of 5-FU and SN-38 (PGA-5FU-SN38).**
  - a. Set up the synthetic methodology for the conjugation of a 20(S)-O-acylated SN-38 derivative to the PGA carrier (PGA-SN38).
  - b. Design and synthesis of a family of polymer-drug conjugates (PGA-5FU-SN38) for combination therapy
  - c. Evaluation of the *in vitro* cytotoxicity and combination synergism of the PGA-5FU-SN38 family.

*To achieve the proposed objectives, this work has been done in collaboration between the Combinatorial Chemistry Unit at the Barcelona Science Park (UQC-PCB) and the Functional Validation and Preclinical Research (FVPR) area and the Drug Delivery and Targeting Group of CIBBIM-Nanomedicine at the Vall d'Hebron Research Institute.*

---

## 3. Materials and Methods

---

### 3.1 General Instruments

<b>Scales</b>	Mettler Toledo PB3002-S, 2 significant figures. Sartorius, CP224S, 4 significant figures. Mettler Toledo AT261 Detlarange, 5 significant figures.
<b>Centrifuges</b>	Beckman Coulter, Allegra 21R. Centrifuge for 15 and 50 mL tubes. Beckman Coulter, 5415D eppendorf. Centrifuge for 1.5 y 2 mL tubes.
<b>Spectrophotometer</b>	Spectrophotometer UV/Vis Jasco, V630.
<b>Freeze-drier</b>	VirTis Genesis. Christ, Alpha 1-4 LD.
<b>Rotary evaporator</b>	Heidolph Laborota 4001-Efficient
<b>pHmeter</b>	Crisol pH meter GLP21
<b>RMN</b>	Varian Mercury 400 MHz

Instruments for purification and characterization of synthetic compounds are described in sections 3.4 and 3.5. Instruments used in the FVPR Laboratory (CIBBIM-Nanomedicine, VHIR) for *in vitro* and *in vivo* experiments were:

<b>Scales</b>	OHAUS, Adventurer Pro AV 4101 AS (RADWAG) AS 220/C/2 OHAUS Pioneer
<b>Elisa Plate reader (Spectrophotometer)</b>	Biotek, Epoch
<b>Tissue Homogenizer</b>	Fast Prep 24, MP Biomedicals, Lysing Matrix D tubes
<b>Confocal Microscope</b>	FV1000, Olympus
<b>Flow Cyometer</b>	FacsCalibur
<b>Incubator</b>	AutoFlow IR direct heat
<b>Automatic cell counter</b>	Countess, Invitrogen
<b><i>In vivo</i> optical imaging system</b>	IVIS Spectrum, Perkin-Elmer

## 3.2 Materials

### 3.2.1 Solvents

Solvents were used without any pre-treatment application. The most commonly used are summarized in Table 3. 1.

Table 3. 1 Summary of the solvents used.

Abbreviation	Name	Quality	Supplier
ACN	Acetonitrile	HPLC grade	Scharlau
EtAcO	Ethyl Acetate	Synthesis	Scharlau
CDCl <sub>3</sub>	Deuterated chloroform-d	99.8% atom D	Sigma-Aldrich
DCM	Dichloromethane	Synthesis 99.5%	Scharlau
DCM anhydrous	Dichloromethane anhydrous	Synthesis 99.5%	Sigma-Aldrich
DMF	Dimethylformamide	Synthesis 99.5%	Panreac
DMF anhydrous	Dimethylformamide anhydrous	Synthesis 99.5%	Sigma – Aldrich
DMSO	Dymethylsulfoxide	Synthesis 99.5%	Panreac
DMSO-d <sub>6</sub>	Deuterated Dymethylsulfoxide	99.8% atom D	Sigma-Aldrich
D <sub>2</sub> O	Deuterium Oxide	99.8% atom D	Sigma-Aldrich
H <sub>2</sub> O	Water	Milli-Q	Millipore
Hexane	Hexane	Synthesis 95%	Scharlau
MeOH	Methanol	HPLC grade	Panreac
MeOD	Deuterated methanol-d	99.8% atom D	Sigma-Aldrich
THF	Tetrahydrofuran	Synthesis 99.5%	Panreac

### 3.2.2 Chemical reagents

Chemical reagents were obtained from different suppliers. The most commonly used are depicted in Table 3.2.

Table 3. 2 Summary of chemical reagents used.

Abbreviation	Name	Quality	Supplier
5-FU	5-Fluorouracil	Reagent > 99%	Sigma-Aldrich
AF750	Alexa Fluor® 750 Carboxylic Acid, Succinimidyl Ester	-	Invitrogen
CF	5(6)-Carboxyfluoresceine	Reagent > 95%	Sigma-Aldrich
DIC	N,N'-diisopropylcarbodiimide	Reagent > 99%	Fluka
DIEA	N,N-Diisopropylethylamine	Synthesis	Sigma-Aldrich
EDC-HCl	1-Ethyl-3-(3-dimethylaminopropyl)carbodiimide	Reagent > 99%	Iris Biotech GMBH
TEA	Triethylamine	Synthesis	Sigma-Aldrich
HCl	Hydrogen chloride acid	Reagent > 99%	Fluka
HCOOH	Formic acid	Analysis	Merck
HOBt-H <sub>2</sub> O	Hydroxybenzotriazole	Reagent > 99%	Iris Biotech GMBH
MMP-7	Matrix Metalloprotease 7	Recombinant, expressed in E. coli, buffered aqueous solution	Sigma-Aldrich
MMP-9	Matrix Metalloprotease 9	Recombinant, expressed in NSO cells, >95%, buffered aqueous solution	Sigma-Aldrich
NaCl <sub>(s)</sub>	Sodium Chloride	Synthesis	Panreac
NaHCO <sub>3</sub>	Sodium Bicarbonate	Synthesis	Sigma-Aldrich
PBS	Phosphate Buffer Saline		Sigma-Aldrich
PGA	Polyglutamic acid	Reagent > 99%	Polypeptide Solutions, S.L.
Resorcinol	Resorcinol	Reagent > 99%	Sigma-Aldrich
SN-38	7-Ethyl-10-hydroxy-camptothecin	Reagent > 99%	Astatech
TFA	Trifluoroacetic acid	Synthesis	Fluorochem

### 3.2.3 Buffers

- Phosphate Buffer Saline (PBS) at pH 7.4 was prepared by dissolving 1 tablet of PBS (from Sigma-Aldrich) in 200 mL of Milli-Q water, yielding 0.01 M phosphate buffer, 0.0027 M potassium chloride and 0.137 M sodium chloride. Buffers at pH 5.5 and 6.5 were obtained by adding HCl.
- 50 mM ammonium carbonate buffer was prepared by dissolving 79 mg of ammonium bicarbonate (NH<sub>4</sub>HCO<sub>3</sub>) in 20 mL of Milli-Q water.



### 3.3 Methods

#### 3.3.1 General methodology for Solid Phase Peptide Synthesis (SPPS)

SPPS is a synthesis technique based on a sequential addition of  $\alpha$ -amino and side-chain protected amino acid residues to an insoluble polymeric support (resin). The complete process is schematized in Figure 3. 1. The peptide is attached to the resin via a linker through its C-terminal. After removal of the N- $\alpha$ -amino protecting group, the next protected amino acid is added using a coupling reagent. Side-chain protecting groups are chosen to be cleaved simultaneously with the detachment of the peptide from the resin.

SPPS was performed manually using syringes of polypropylene containing a polyethylene porous filter. A polypropylene block Vacman<sup>®</sup> was employed for filtration and washing steps that SPPS requires.

2-Chlorotrytil (IRIS 100-200 mesh, loading 1.60 mmol Cl/g resin) polymeric support was stirred manually with Teflon<sup>®</sup> bars or by an automatic orbital shaker. Excess of reagents, solvents and by-products in solution were removed by vacuum filtration.

#### Preconditioning of the resin:

Before starting the coupling of amino acids, resin was washed abundantly:

5 x 1 min DMF and 5 x 1 min DCM; using 10 mL of solvent per gram of resin.

#### Amino acid coupling conditions:

For each coupling reaction amino acids were used protected with Fmoc group on the  $\alpha$ -amino and were added in excess (5 eq respect resin mmols). DIC and Oxyme were used as coupling agents (3

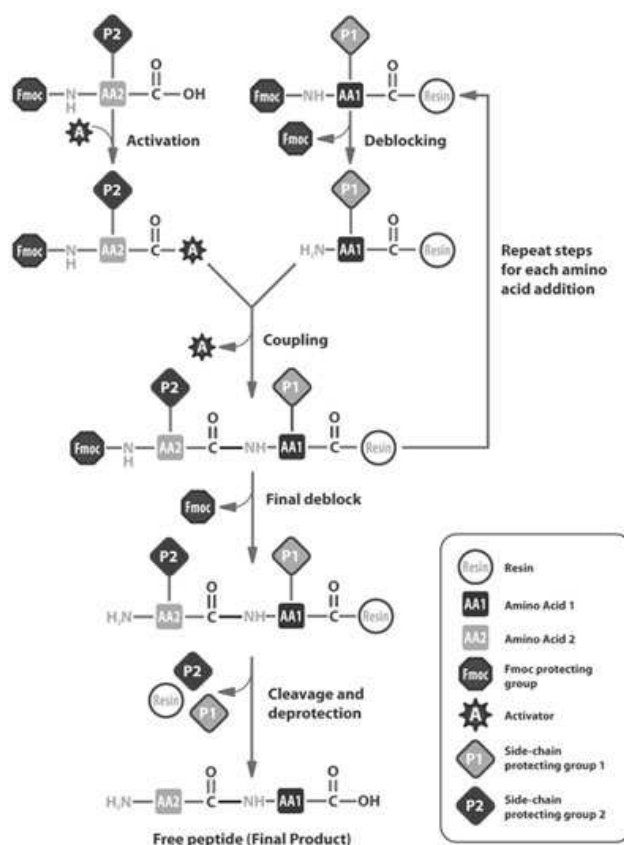


Figure 3. 1 Scheme of the general procedure for SPPS using Fmoc-protected amino acids.

eq respect resin mmols). After each reaction, protection, deprotection and coupling, resin was washed: 5 x 1 min DMF and 5 x 1 min DCM; using 10 mL of solvent per gram of resin.

**Fmoc removal:**

Fmoc group removal from the amino acid anchored in the peptide chain was carried out following these steps:

(i) DMF (5 x 1 min) , (ii) piperidine / DMF (2:8) (1 x 1 min , 2 x 20 min), (iii) DMF (5 x 1 min), ( iv) DCM (5 x 1 min).

**Cleavage of the sequence anchored into the resin:**

Resin was treated with an acidic solution of DCM:TFA (95:5, v/v) at room temperature for 30 min. Resin was then filtered and washed with the same solution collecting the filtered solution. TFA was evaporated and synthesized peptide precipitated in cold diethyl ether. After removal the crude was analyzed by HPLC-MS. Once side chain protected groups were eliminated, the compounds dissolved in H<sub>2</sub>O – ACN were purified by RP-HPLC-semipreparative, when needed.

**Removal of the side chain protecting group:**

Removal was carried out after the cleavage step previously described. Crude was dissolved in a solution of TIS:H<sub>2</sub>O:EDT:TFA (1:2.5:2.5:94, v/v/v/v)for 24 h. Removal of the protecting groups was monitored by HPLC-MS and after complete elimination TFA solution evaporated. Purified by RP-HPLC-semipreparative was required.

All couplings as well as the removal of protecting groups were preceded by a qualitative assay (Kaiser and Chloranil tests) to assess full completion of the reaction.

**3.3.1.1 Kaiser Test**

Kaiser test is also known as Ninhydrin test and is a colorimetric assay to detect primary amines in a polymeric support. The test proceeds by adding 3 drops of Solution A and 1 drops of Solution B into a glass tube containing 0.5 – 2.0 mg of resin previously washed with DCM. The tub was heated at 110°C during 3 min.

Preparation of Solution A: 40 g of phenol were dissolved in absolute EtOH (10 mL) and 65 mg of KCN were dissolved in H<sub>2</sub>O (100 mL); 2 mL of the resulting solution were diluted in freshly distilled pyridine over ninhydrin (100 mL). The two solutions were stirred separately for 45 min with 4 g of Amberlite MB -3 resin, and then filtered and mixed.

Preparation of Solution B: 2.5 g of ninhydrin were dissolved in absolute EtOH (50 mL). The solution was kept in an opaque container to protect it from light exposure.

A yellow color of the resin and the solution indicate the absence of primary amines in the polymeric support (negative test), whereas a blue color of both signifies the presence of primary amines (positive test).

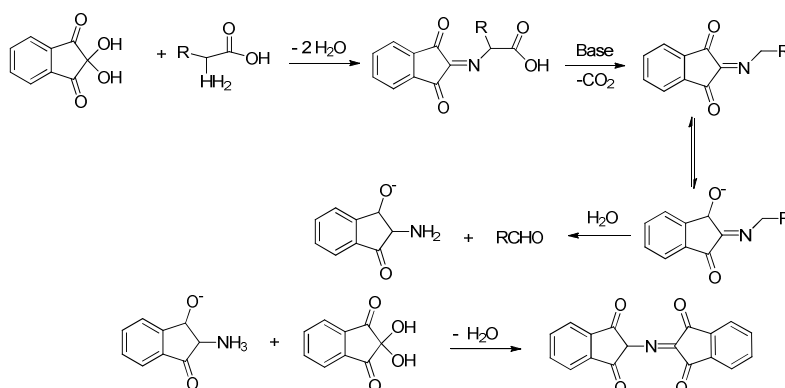


Figure 3. 2 Kaiser test scheme.

### 3.3.1.2 Chloranil test

Chloranil test is a colorimetric assay to detect secondary amines in a polymeric support.

After drying the resin previously washed with DCM, 0.5-2.0 mg of the resin were placed in a glass tube and 5 drops of a saturated solution of chloranil in toluene and 20 drops of acetone were added. The glass tube was stirred 5 min at room temperature. A yellow color resin indicates the absence of secondary amines (negative test) while a blue-green color indicates the presence of secondary amines (positive test).

## 3.4 Purification

### Manual Chromatography

Manual chromatography on reverse-phase C18 for purification was carried out with OASIS HLB<sup>3</sup> 35cc Vac cartridges (10 g sorbent /cartridge - 60 μm particle size) from Waters using H<sub>2</sub>O Milli-Q and ACN as the elution system.

### Flash Chromatography

Flash chromatography on normal phase silica was done automatically with the computer module Teledyne Isco Companion<sup>®</sup> with Photodiode array detector. Pre-packed silica gel columns (Silica-RediSep<sup>®</sup> columns) of different sizes according to the amount of crude to purify were used. Elution systems were: (I) A: DCM and B: DCM:MeOH (80/20, v/v) and (II) A: DCM and B: EtOAc.

### Semipreparative RP-HPLC-MS

*Semipreparative – Reverse Phase- High Performance Liquid Chromatography – Mass Spectrometry*

The columns used depend on the nature of the compounds. Briefly,

XBridge™ Prep C18 (19 x 100 mm, 5 μM OBDTM) from Waters.  
XBridge™ BEH130 Prep C18 (19 x 100 mm, 5 μM OBDTM) from Waters.  
SunFire™ Prep C18 (19 x 100 mm, 5 μM OBDTM) from Waters.

Semipreparative HPLC equipment used for purification of the compounds consisted of a Waters 600 Controller module comprising two pumps, a high pressure mixer, a module 2767 Sample Manager Waters Alliance with an injector, a fraction collector a UV-visible Detector Dual λ Absorbance Detector 2489 and Micromass ZQ mass spectrometer. Compounds were detected by their  $[M + H]^+$ , using adjusted gradients for each case at a flow of 16 or 25 mL/min. Elution systems were: (III) A: H<sub>2</sub>O:HCOOH (99.9:0.1, v/v) and B: ACN:HCOOH (99.9:0.1, v/v), (IV) A: H<sub>2</sub>O:TFA (99.9:0.1, v/v) and B: ACN:TFA (99.9:0.1, v/v) and (V) A: H<sub>2</sub>O and B: ACN. Software employed was Masslynx V4.1.

### Membrane Dialysis Purification

PDC were purified by dialysis of each compound against Milli-Q H<sub>2</sub>O using a semipermeable membrane with a Mw cutoff of 6-8 kDa. Crude was introduced on a previously hydrated and dialyzed for 24h membrane (4 x 5 L). The solution was then lyophilized to yield the purified conjugates. Product entities were confirmed by RP-HPLC.

### Manual SEC

#### *Manual Size Exclusion Chromatography*

PDC bounded to CF or AF750 fluorophores were purified by means of size exclusion chromatography (SEC) using PD10 columns (Sephadex, G-2MM columns, Supelco, GE Healthcare) and H<sub>2</sub>O as elution system. Fractions of 1 mL were collected and lyophilized.

## 3.5 Characterization

### Thin Layer Chromatography (TLC)

TLC was performed on pre-treated plates (silica gel 60ACC, F<sub>254</sub>, Merck). Visualization was performed using ultraviolet light ( $\lambda = 254$  nm).

### Analytic HPLC

#### *Analytic – High Performance Liquid Chromatography*

For 5-FU and SN-38 quantification in PDC, RP-HPLC using ultraviolet detection was performed.

Different columns were used:

SunFire™ C18 (4.6 x 75 mm, 3.5 μm) from Waters.  
XSelect HSS T3 (4.6 x 250 mm, 3.5 μm) from Waters.

Analytical HPLC equipment used for characterization of the compounds consisted of a Waters Alliance 2695 with a dual  $\lambda$  absorbance detector model 2487. Millennium 3.2 Waters software was employed and chromatograms were registered at 214 nm and 254 nm for 5-FU containing compounds and 378 nm for SN-38 containing compounds.

The flow applied was 1 mL/min and the elution system was: (A) H<sub>2</sub>O:TFA (99.9:0.1, v/v) and (B) ACN:TFA (99.9:0.1, v/v) or (A) H<sub>2</sub>O and (B) ACN. Different gradients were adjusted in each case except for 5-FU tissue analysis where an isocratic flow of 0.6 mL/min was used.

## **HPLC-MS**

*High Performance Liquid Chromatography – Mass Spectrometry*

HPLC-MS was used to monitor reactions and determine the purity of the synthesized compounds.

HPLC-MS analysis was performed using a Waters Alliance HT 2795 with a UV-visible photodiode detector model 2996, ELS 2420 detector and a Micromass ZQ mass spectrometer. The software used was MassLynx V4.1.

The column used was XBridge™ C18 (4.6 x 50 mm, 3.5  $\mu$ M). Flow was set at 2 mL/min and the elution system was: (A) H<sub>2</sub>O:HCOOH (99.9:0.1, v/v) and (B) ACN:HCOOH (99.93:0.07, v/v). Different gradients were adjusted for each compound analyzed. The purity of the compounds was determined at 214 and 254 nm wavelength.

## **SEC-MALS-IR**

*Size Exclusion Chromatograph- Multi Angle Light Scattering – Infrared Detector* was used to quantify the Mw of the nanoconjugates synthesized and their polydispersity.

The equipment used consisted on a Waters System 1525 Binary HPLC pump, Injector Waters 717 plus Autosampler and a detector waters 2487 Dual I Absorbance (controlled by a Breeze, Waters). The column used was an Ultrahydrogel 500 (7.8 x 300 mm, 10  $\mu$ m) from Waters and the elution system was 50 mM NaHCO<sub>3</sub> and ACN. Detector was set at 220 nm. An isocratic flow (80 : 20) during 50 min was set at 0.7 mL/min. BSA protein was used for equipment calibration.

## **UV-Spectroscopy**

For SN-38 quantification a spectrophotometer UV/Vis Jasco (Model V630) was used.

1 mL containing solutions of SN-38 product of interest were analyzed at 378 nm wavelength ( $n \geq 3$ ) using a calibration curve in the range of 0-0.1 mg/ml.

## **Nuclear Magnetic Resonance Spectroscopy**

Proton (<sup>1</sup>H) and carbon (<sup>13</sup>C) Nuclear Magnetic Resonance (NMR) analysis were performed at 298 K with a Varian Mercury400 Fourier Transform spectrometer (NMR Unit, Scientific and Technical Services, University of Barcelona). Data was processed using the program MestreNova (Mestrelab Research). The chemical shifts ( $\delta$ ) are expressed in ppm units taking as internal reference

deuterated solvent signal used (CDCl<sub>3</sub> (<sup>1</sup>H NMR δ: 7.26, <sup>13</sup>C NMR δ: 77.0); DMSO-d<sub>6</sub> (<sup>1</sup>H NMR δ: 2.50, <sup>13</sup>C NMR δ: 39.5); MeOD (<sup>1</sup>H NMR δ: 3.31 and 4.84, <sup>13</sup>C NMR δ: 49.1). Chemical shifts are reported as s (singlet), d (doublet), t (triplet), q (quartet) and m (multiplet).

### Mass Spectrometry MALDI-TOF

*Matrix-Assisted Laser Desorption/Ionization – Time of Flight* mass spectrometry of the synthesized peptides was carried out at the Proteomics Platform of PCB by using a MALDI Voyager DE RP time-of-flight spectrometer (Applied Biosystems, Framingham). To prepare ACH (α-cyano-4-hydroxycinnamic acid) matrix, 10.0 μg of ACH were dissolved in 1 mL of H<sub>2</sub>O/ACN (1:1) at 0.1% of TFA. The analysis of the compounds was carried out by mixing 1.0 μL of sample solution at 0.5 mM with 1.0 μL of ACH matrix. To record the mass spectrum, 1.0 μL of the resulting mixture was deposited on a test plate. Analysis was performed using the positive reflex mode laser at different intensities depending on the compound to be analyzed.

### Dynamic Light Scattering (DLS)

DLS measurements of PDC synthesized were performed using a Malvern Zetasizer NanoZS (Malvern Instruments, Malvern, UK) in the Automated Crystallography Platform of the Institute for Research in Biomedicine (IRB, Barcelona). Analysis of the compounds was carried out at room temperature using H<sub>2</sub>O Milli-Q and PBS (pH 7.4) at a concentration of 0.1 mg/mL. Micelle size distribution by volume (%) was measured (diameter, nm) for each PDC (n≥3).

## 3.6 Stability and Degradation assays

### 3.6.1 pH degradation

PDC of PGA (10 mg/mL) were incubated at 37°C in phosphate buffer solution (PBS) at different pH for 7 days. Five μL of the sample were taken at various time points: 0, 10, 20, 30 min and 1, 2, 4, 6, 8 and 24h, and every 24 h after. Samples were frozen in dry ice and stored at -20°C until analyzed. Prior to analysis, 35 μL of PBS pH 5.5 (to avoid the breakdown of the ester bond) were mixed with the aliquots and directly analyzed by RP-HPLC using a SunFire™ C18 (4.6 x 75 mm, 3.5 μm) column with the UV detector settled at λ= 260 nm for PGA-5-FU PDC and λ= 378 nm for PGA-SN38 PDC with a flow rate of 1 mL/min.

Elution system was: (A) H<sub>2</sub>O:TFA (99.9:0.1, v/v) and (B) ACN:TFA (99.9:0.1, v/v). Resorcinol was used as HPLC internal standard; 40 mg were added to the initial PBS pH 7.4 solution, from which the rest of buffer solutions were prepared. The elution was performed using the following gradient: 5→100%B in 7 min. (5-FU (tr) 1.5 min, SN-38 (tr) 4.4 min, resorcinol (tr) 4min). Calibration curves of 5-FU and SN-38, respectively, were performed by triplicate for each concentration point and used to quantify by HPLC total release of 5-FU and SN-38 from the conjugates. Experiments were carried out in triplicate.

### 3.6.2 Plasma stability

Experiments were performed in mice and human plasma following the same procedure. Mouse plasma was obtained from FVPR (CIBBIM-Nanomedicine, VHIR) and were kept frozen at -20°C until needed. Human plasma was purchased from Sigma-Aldrich and also kept at -20°C.

PDC of PGA (10 mg/mL) was incubated at 37°C in plasma for up to 96 h. At scheduled times (0, 5, 10, 15, 20, 30 min and 1, 1.5, 2, 4, 6, 8, 24, 48, 72 and 96 h), aliquots of 5 µL were collected and kept on dry ice. A volume of 35 µL of ACN (containing resorcinol (0.2 mg/mL)) was added to each sample in order to precipitate serum proteins. Following centrifugation (14000 rpm, 5 min) supernatants were analyzed by RP-HPLC as reported above. Triplicate experiments were carried out.

### 3.6.3 Cathepsin B degradation

300 µL of PGA-5-FU and PGA-SN38 PDC (10 mg/mL) were incubated at 37°C with 5 µL of Cahtepsin B (from bovine spleen, Sigma Aldrich; 10 units/mL using PBS 7.4 as a solvent) for seven days.

At scheduled times (0, 30 min and 1, 1.5, 2, 4, 8, 24, 48, 72 and 96 h), aliquots of 5 µL were collected and kept on dry ice. 35 µL of ACN (containing resorcinol (0.2 mg/mL)) were added to each sample. Following centrifugation (14000 rpm, 5 min) supernatants were analyzed by RP-HPLC as reported above.

### 3.6.4 Incubation of products with MMPs

#### 3.6.4.1 Sequence recognition assays

For peptides GPVGLIG, GIVGPLG, AHX-RPLALWRS-AHX and AHX-RSWLPLRA-AHX, (**9-12**), a sequence recognition assay was performed to confirm their sensibility against MMP-9 and MMP-7 enzymes. In detail, 1 mg of peptides [**9-12**] were dissolved in 50 µL of PBS and then 5 µL of MMP-9 (for [**9-10**] peptides) or MMP-7 (for [**11-12**] peptides) were added. The mix was left in a thermomixer at 37°C during 24 h and then analyzed by HPLC-MS.

#### 3.6.4.2 Responsiveness assay against MMPs

For the evaluation of the MMP responsiveness of products 5FU-Ala-MMP9pept [**26**], 5FU-adipic-MMP7pept [**28**] and 5FU-adipic-MMP9pept [**30**] 1 mg of each product was dissolved in 100 µL of H<sub>2</sub>O and 5 µL of MMP-7 or MMP-9 (10 µg/mL) were added. After 24 h samples were collected and mixed with 50 µL of ACN. Following centrifugation (14000 rpm, 5 min) supernatants were analyzed by RP-HPLC-MS to determine the Mw of the cleaved fraction.

### 3.6.4.3 Degradation assay against MMPs

A time course 5-FU release study of products 5FU-Ala-MMP9pept [26] and PGA-MMP7pept-5FU [37] was performed. Briefly, 1 mg of each product was dissolved in 100  $\mu$ L of H<sub>2</sub>O and 5  $\mu$ L of MMP-9 or MMP-7 (10  $\mu$ g/mL), respectively were added. Mix was incubated at 37 °C up to 140 h and at specific scheduled times (0, 5, 15, 30 min, 1, 4, 6, 24, 48, 72 and 140 h) aliquots of 5  $\mu$ L were collected and kept on dry ice. 35  $\mu$ L of ACN were added to each sample. Following centrifugation (14000 rpm, 5 min) supernatants were analyzed by RP-HPLC-UV as reported above.

For product 5FU-Ala-MMP9pept [26], the quantification of the 5-FU-GPVG released by RP-HPLC-UV was performed measuring the % diminution in the area under the peak corresponding to product 5FU-Ala-MMP9pept [26]. For product PGA-MMP7pept-5FU [37], the release caused by MMP-7 was measured by RP-HPLC-UV measuring the area of the 5-FU-RPLA released. Then, it was interpolated in a calibration curve of 5-FU-RPLA. Triplicate experiments were carried out.

## 3.7 Tissue homogenization and drug quantification

Below is detailed the set up protocol for the quantification of 5-FU in different tissue homogenates and in plasma. The method was validated and the following validation parameters were set up: selectivity, linearity, limit of detection (LOD), limit of quantification (LOQ) and recovery. Three different quality control solutions (QC-L, QC-M and QC-H) were added to tissues and plasma to quantify the % of 5-FU recovered at the end of the process.

To proceed with the tissue homogenization using the FastPrep 24 (MP Biomedicals), first the tissue was washed with PBS and dried with a filter paper. Approximately 200 mg of each tissue were placed in bead-containing 2 mL homogenizer tubes (lysing matrix D, MP Biomedicals). Then 100  $\mu$ L of 0.1M HCl and 900  $\mu$ L of PBS were added to each tube as well as a known amount (50  $\mu$ L of a solution 1 mg/mL) of the IS Resorcinol. Tissues were then homogenized using the FastPrep 24 at a speed of 5 m/s for 40 s. This process was repeated 15 times with 5 min intervals for each sample. Tissue samples were cooled on ice after each homogenization turn. Following completion, the tubes were centrifuged at 14,000 rpm for 30 min at 10°C and the supernatant was separated for each tube. Then, 500  $\mu$ L of TCA 5% were added to the supernatant for protein precipitation and the mixed solution centrifuged at 14,000 rpm for 15 min at 10°C. Supernatant (SN1) was kept at -20°C. The solid tissue residue was treated with 500  $\mu$ L of NaOH 0.02 N. The mixture was shaken in a Thermomixer® for 24 h at 37 °C. The mixed solution centrifuged at 14,000 rpm for 15 min at 10°C and the supernatant was separated. Then, 500  $\mu$ L of TCA were added to the supernatant and the mixture was centrifuged at 14,000 rpm for 15 min at 10°C. This supernatant (SN2) was added to the thawed SN1 and the final mixture centrifuged again at 14,000 rpm for 15 min. The supernatant was left at 37°C for 1 h in 1 M NaOH (100  $\mu$ L) in order to release the remaining 5-FU still conjugated to the polymer. Then it was ultrafiltrated to remove the interference components for quantitative determination of 5-FU in tissue samples using 4 mL ultrafiltration cell with a 3 K cutoff membrane (Amicon Ultra Merck). Supernatant was placed in the cell and 3 consecutive centrifugation



processes of 40 min (4,000 rpm, 4°C) were carried out. The 2 mL of filtrate obtained were then lyophilized and reconstituted in 2 mL of PBS at pH 5. Finally, 20 µL of it were analyzed by HPLC (described below) and the rest stored at -20°C.

In the case of plasma, 50 µL of a solution 1 mg/mL of Resorcinol were added to 200 µL of plasma. Proteins were precipitated adding 200 µL TCA 5%. The mixture was centrifuged at 14,000 rpm for 15 min at 10°C. Supernatant was left at 37°C for 1 h in 1 M NaOH (50 µL) in order to release the 5-FU still conjugated to the polymer. The solution was reconstituted to 2 mL with PBS, ultracentrifugated and lyophilized following the methodology explained for tissue samples, and acidified to pH 5 to further quantify by HPLC (described below) the 5-FU content.

HPLC separation of tissue homogenates and plasma was done with a C-18 reverse phase column (XSelect HSS T3 3.5 µm, 4.6 x 250 mm, Waters). A guard column packed with the same material was used to protect the column. 5-FU and Resorcinol were detected at 254 nm wavelength. The elution system was A: H<sub>2</sub>O and B: MeOH and the gradient 0 → 0%B (30 min) → 20%B (32 min) → 80%B (45 min) → 80%B (50 min) → 100%B (56 min). Then it was necessary to equilibrate the column during 25 min with 100%A. Flow rate was 0.6 mL/min.

The injection volume was 20 µL. Retention times: 5-FU (15 min) and Resorcinol (42 min). A calibration curve in the range of 10 to 25000 ng/mL of 5-FU was performed by doing triplicates to quantify the drug content in tissue and plasma samples. Recoveries of 5-FU for each tissue were applied to the results regarding the level of % ID measured.

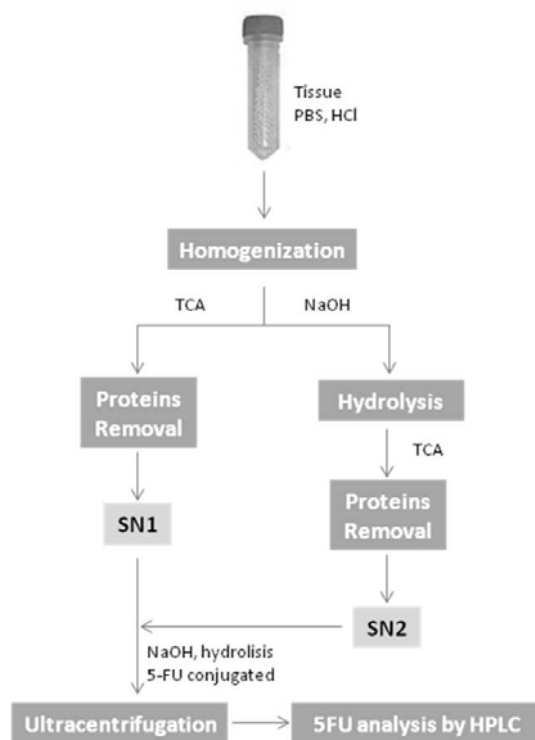


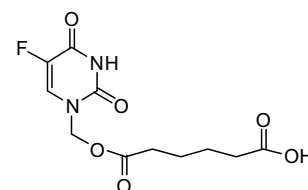
Figure 3. 3. Scheme of the tissue homogenization procedure.

### 3.8 Synthesis

#### 6-((5-fluoro-2,4-dioxo-3,4-dihydropyrimidin-1(2H)-yl)methoxy)-6-

#### oxohexanoic acid (5-FU-adipic, Product 2):

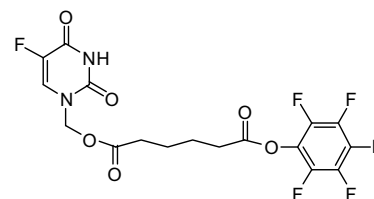
5-FU (100 mg, 0.76 mmol) was mixed with a 37% HCHO solution in water (200  $\mu$ L, 5.56 mmol) and it was left to react 1 h at 55°C under agitation. Then, the solvent was fully evaporated under vacuum until transparent oil was obtained (Product 1). Product 1 was dissolved directly in 10 mL of dry DMF and adipic acid (377.25 mg, 2.5 mmol), DCC (476.14 mg, 2.3 mmol) and DMAP (46.98 mg, 0.3 mmol) were added as a solid. The reaction was left to react overnight at rt. Product formation was confirmed by HPLC-MS and evaporated under vacuum. The dry pellet was purified by semipreparative-HPLC using a XBridge C18 Column, the elution system III and a gradient 5 $\rightarrow$ 50%B in 12 min. 71 mg of product 2 were obtained as a white solid (0.25 mmol, 33% yield). Purity by HPLC-MS: 98.1%.  $Mw_{calc}(C_{11}H_{13}FN_2O_6)=288.23$  g/mol,  $ESI_{found}[M+H]^+=288.93$  g/mol.  $^1H-NMR$  (400 MHz, DMSO-d<sub>6</sub>)  $\delta$ : 8.11 (d, J=8Hz, 1H), 5.55 (s, 2H), 2.35 (t, J=8Hz, 2H), 2.19 (t, J=8Hz, 2H), 1.57-1.44 (m, 4H).  $^{13}C-NMR$  (101 MHz, DMSO-d<sub>6</sub>)  $\delta$ : 174.64, 172.83, 158.34, 149.69, 140.21, 130.15, 71.34, 33.87, 32.26, 24.25, 24.10.



#### (5-fluoro-2,4-dioxo-3,4-dihydropyrimidin-1(2H)-yl)methyl

#### (pentafluorophenyl) adipate, Product 3:

5-FU-adipic 2 (100 mg, 0.34 mmol) was dissolved in 15 mL of DCM and then pentafluorophenol (95 mg, 0.51 mmol), EDC (99.5 mg, 0.51 mmol) and DMAP (2.5 mg, 0.18 mmol) were added as a solid. The reaction mixture was left to react at room temperature under agitation during 2 h. Formation of product 3 was confirmed by HPLC-MS. The crude was washed with saturated NaCl (3 x 20 mL) and saturated NaHCO<sub>3</sub> (3 x 20 mL). The organic phase was evaporated under vacuum. Finally, 168 mg of product 3 were obtained as a white solid (yield=90%). Purity by HPLC-MS: 97.0%.  $Mw_{calc}(C_{17}H_{12}F_6N_2O_6)=454.03$  g/mol,  $ESI_{found}[M+H]^+=454.98$  g/mol.

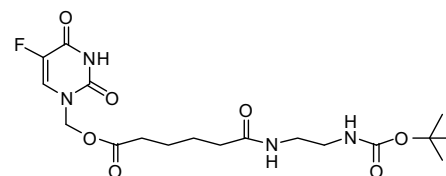


#### (5-fluoro-2,4-dioxo-3,4-dihydropyrimidin-1(2H)-yl)methyl

#### 6-((2-((tert-butoxycarbonyl)amino)ethyl)amino)-6-

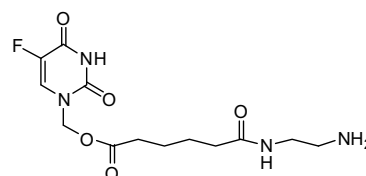
#### oxohexanoate, Product 4:

Product 3 (500 mg, 1.01 mmol) was dissolved in 10 mL of dry DMF. Then, N-Boc-ethylenediamine (22.5  $\mu$ L, 0.9 mmol) dissolved in 1 mL of dry DMF (pH adjusted to pH=7 with acetic acid) was added to product 3 solution. The reaction was left to react overnight at rt and the product formation was confirmed by HPLC-MS. The solvent was evaporated under vacuum and the dry pellet was purified by flash chromatography using a 40 g SiO<sub>2</sub> column, elution system I and a gradient 5 $\rightarrow$ 50%B in 25 min. Finally, 156 mg of 5-FU-adipic product were obtained as a white solid (0.25 mmol, 90% yield). Purity by HPLC-MS: 99.3%. HPLC-MS: 97.0%.  $Mw_{calc}(C_{18}H_{27}FN_4O_7)=430.93$  g/mol,  $ESI_{found}[M+H]^+=431.09$  g/mol.  $^1H-NMR$  (400 MHz,



DMSO-d6)  $\delta$ : 8.11 (d, J=8Hz, 2H), 7.81-7.75 (m, 1H), 6.80-6.73 (m, 1H), 5.55 (s, 2H), 3.04 (q, J=8Hz, 2H), 2.94 (q, J=4Hz, 2H), 2.33 (t, J=4.5Hz, 2H), 2.04 (t, J=4.5Hz, 2H), 1.51-1.37 (m, 4H), 1.37 (s, 9H).  $^{13}\text{C-NMR}$  (101 MHz, DMSO-d6)  $\delta$ : 172.12, 171.54, 157.18, 156.90, 148.87, 140.22, 137.92, 77.28, 70.15, 34.56, 32.49, 27.86, 24.12, 23.37.

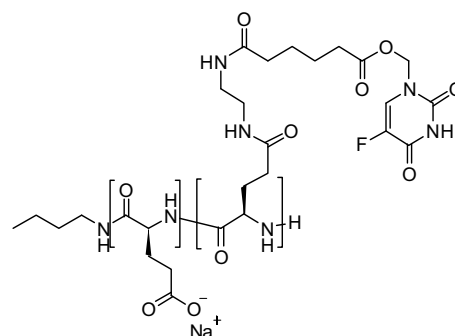
**(5-fluoro-2,4-dioxo-3,4-dihydropyrimidin-1(2H)-yl)methyl 6-((2-aminoethyl)amino)-6-oxohexanoate, Product 5:** Product 4 (138 mg, 0.32 mmol) was dissolved in a solution of DCM:TFA (2:1, v/v) to deprotect the amine group. It was left to react during 1 h at rt under agitation. Complete deprotection was confirmed by HPLC-



MS and the solvent was evaporated under vacuum. After the DCM mixture removal, colorless oil was obtained. Purity by **HPLC-MS**: 99.3%.  $M_{w,calc}(C_{13}H_{19}FN_1O_5)= 329.29$  g/mol,  $ESI_{found}[M+H]^+= 331.13$  g/mol.  $^1\text{H-NMR}$  (400 MHz, DMSO-d6)  $\delta$ : 8.10 (d, J=8Hz, 2H), 7.98 (t, J=4Hz, 2H), 5.54 (s, 2H), 3.24 (q, J=4Hz, 2H), 2.82 (t, J=8Hz, 2H), 2.33 (t, J=4Hz, 2H), 2.07 (t, J=4Hz, 2H), 1.53-1.42 (m, 4H).  $^{13}\text{C-NMR}$  (101 MHz, DMSO-d6)  $\delta$ : 173.03, 157.96, 157.72, 149.74, 130.01, 70.94, 39.13, 36.84, 35.26, 33.01, 24.69, 24.18.

#### PGA-5-FU, Product 6:

The conjugation of product 5 to PGA was carried out in solution. Different coupling conditions were explored. Table 3.3 details the different conditions used in the synthesis of all batches of PGA-5-FU and also the commercial source of PGA (I: Sigma-Aldrich (PI=3.43) and II: Polypeptide Solutions, SL (PI=1.1)), because it was observed that polymer polydispersity affects the conjugation of product 5. All experiments were performed with an estimated TDL of 5-FU of 15%.



For the evaluation of *in vitro* and *in vivo* experiments, different batches were synthesized and mixed in a single final batch of nanoconjugate named PGA-5FU pool.

Table 3.4 details the nine different batches mixed. The coupling conditions were B and the PGA was from Polypeptide Solutions S.L.

Table 3. 3 Summary of the different syntheses batches of PGA-5-FU.

# Batch	Coupling conditions*	PI of PGA	TDL% (mg/mg)	Mass obtained (mg)	Yield%
#1	A	3.43	1.6	28.5	27%
#2	B	3.43	7.63	22.5	27%
#3	B	3.43	10.2	32	22%
#4	B	1.1	3.29	168	25%
#5	B	1.1	7.23	102.1	40%
#6	B	1.1	11.89	103.6	48%
#7	B	1.1	9.06	40.5	37%

\*Coupling conditions (A): 1.5 eq DIC, DMAP (catalytic), DMF and (B): 1.5 eq DIC, 1.5 eq HOBT, pH=8 adjusted with DIEA, DMF.

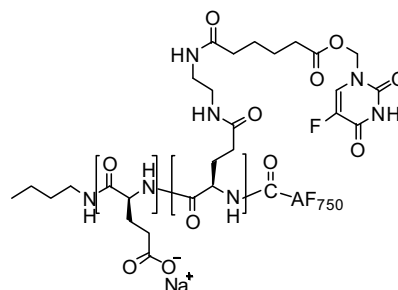
Table 3. 4 Summary of the different batches synthesized for the final batch used for in vitro and in vivo experiments.

# Batch	TDL% (mg/mg)	Mass obtained (mg)	Yield%
#8	12.82	246.9	28%
#9	9.18	250	35%
#10	10.2%	1203	61%
#11	9.51%	245	55%
#12	5.04%	175	66%
#13	1.92%	153.8	20%
#14	6.27%	509.2	42%
#15	5.68%	808.9	58%
#16	8.70%	586.2	68%
<b>PGA-5-FU pool [6]*</b>	7.66%	4175	-

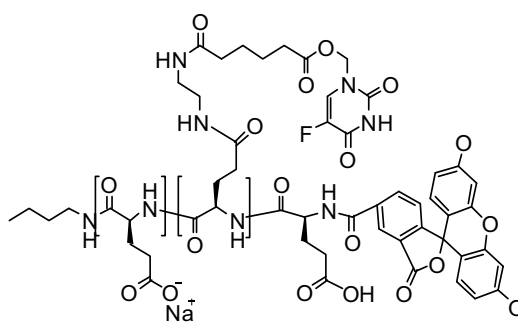
Below is detailed as an example the synthesis of the PGA-5-FU conjugate as a single batch (#10) following the selected reaction conditions.

To a solution of PGA (805.5 mg, 6.24 mmol) in dry DMF (30 mL), DIC (217  $\mu$ L, 1.38 mmol) and 5 min later HOBt (189.1 mg, 1.4 mmol) were added. After 10 min, product **5** (309 mg, 0.93 mmol) was added and the pH of the final mixture adjusted with DIEA to pH= 8. At time 24 h, DIC (217  $\mu$ L, 1.38 mmol) was added again. Reaction was left during 36 h at rt under agitation. DMF was evaporated under vacuum and a white solid obtained. PGA-5-FU was purified by dialysis to remove salt excess and free drug. The crude was dissolved in 3 mL of a NaHCO<sub>3</sub> 0.1M (pH=7 adjusted with acetic acid) solution, introduced in the membrane previously hydrated and dialyzed against MilliQ-H<sub>2</sub>O (3 x5 L) for 24 h. Finally, the product was lyophilized and 1203 mg of a white foamy solid were obtained (yield=61%). Total drug load (TDL) and Free Drug (FD) were measured following the protocol described in section 2.3.1.1.2 by HPLC. TDL was 10.2% and a FD< 0.1%.

**PGA-5FU-AF750, Product 7:** To a solution of PGA-5-FU (364 mg, 2.1 mmol) in dry DMF (15 mL) AF750 fluorophore (0.3 mg, 0.23  $\mu$ mol) was added as a solid. The reaction was left overnight at rt under agitation. DMF was evaporated under vacuum and a white solid obtained. To remove the salt excess and the unreacted AF750 was purified through a PD10 column (1 x5 cm) previously washed and equilibrated with MilliQ-H<sub>2</sub>O as eluent. Then, the crude was dissolved in maximum 2 mL of NaHCO<sub>3</sub> 0.1 M at pH=7 adjusted with acetic acid. 25 fractions of 1 mL each were collected and freeze dried. The amount of AF750 (206.6  $\mu$ g, 0.16  $\mu$ mol) was quantified by UV-spectroscopy.



**PGA-5FU-CF, Product 8:** To a solution of PGA-5-FU (10 mg, 0.06 mmol) in dry DMF (2 mL), DIC (2.5  $\mu$ L, 0.01 mmol) and 5 min later HOBt (189.1 mg, 0.01 mmol) were added. After 10 min, carboxifluoresceine (0.326 mg, 0.78  $\mu$ mol) was also added. The pH of the final mixture was adjusted with DIEA to pH=8. The reaction was left overnight at rt under agitation. DMF was evaporated under vacuum and a white solid obtained. To remove the salt excess and the unreacted carboxifluoresceine it was purified through a PD10 column (1 x5 cm), previously washed and equilibrated with MilliQ-H<sub>2</sub>O as eluent. The crude was dissolved in maximum 2 mL of NaHCO<sub>3</sub> 0.1M at pH=7 adjusted with acetic acid. 25 fractions of 1 mL each were collected and freeze dried. It was confirmed by HPLC the absence of unreactant carboxifluoresceine.



**MMP-9 related peptides: GPVGLIG 9** MMP9-sensitive peptide and **GIVGPLG [10]** Scrambled MMP9-sensitive peptide were synthesized following the solid-phase synthetic route detailed in section 3.3.1. Purification of both was performed by precipitation of the peptide sequences in diethyl ether in cold followed by a centrifugation process. After solvent removal by liophilization a white solid was obtained in both cases. HPLC-MS and MALDI-TOF were performed to evaluate the purity of the compound. Its characterization is summarized in Table 3. 5.

Table 3. 5 MMP-9 sensitive peptide and its corresponding scrambled peptide

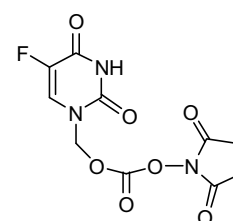
Compound [9-10]	mg product	Mw <sub>calc</sub>	ESI [M+H] <sup>+</sup> HPLC-MS	[M+H] <sup>+</sup> MALDI-TOF	Purity by HPLC-MS
GPVGLIG	305.6	611.73	612.35	612.50	97.3%
GIVGPLG	149.8	611.73	612.53	-	96.8%

**MMP-7 related peptides: RPLALWRS [11]** MMP7-sensitive peptide and **RSWLPLRA [12]** scrambled MMP7-sensitive peptide were synthesized following the solid-phase synthetic route detailed in section 3.3.1. Purification of both was carried out by semipreparative-HPLC using a BEH column, elution system III and a gradient 15→30%B in 7 min. After solvent removal by lyophilisation a slightly yellow sticky solid was obtained in both cases. HPLC-MS and MALDI-TOF were performed to evaluate the purity of the compound. Its characterization is summarized in Table 3. 6:

Table 3. 6 MMP-7 sensitive peptide and its corresponding scrambled peptide.

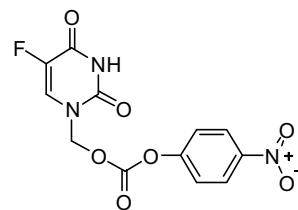
Product [11-12]	mg product	Mw <sub>calc</sub>	ESI [M+3H] <sup>3+</sup> HPLC-MS	[M+H] <sup>+</sup> MALDI-TOF	Purity by HPLC-MS
AHX-RPLALWRS-AHX	139.1	1223.75	409.1	1225.01	97.7%
AHX-RSWLPLRA-AHX	170.1	1223.75	409.3	1224.96	97.8%

**2,5-dioxopyrrolidin-1-yl ((5-fluoro-2,4-dioxo-3,4-dihydropyrimidin-1(2H)-yl)methyl) carbonate, Product 13:** Formaldehyde (350 μL, 9.55 mmol) was added to 5-FU (15.1 mg, 0.12 mmol) and left to react under stirring for 1h at 55°C. The resulted solution was evaporated until water was eliminated (**Product 1**). The obtained colorless oil **1** was dissolved in dry DCM (5 mL) and TEA (160.5 μL, 1.14 mmol) and DSC (295 mg, 1.15 mmol) were added. The reaction mixture was left overnight at rt. The product formation was confirmed by HPLC-MS. Purity by **HPLC-MS**: 41.2% (not purified). Mw<sub>calc</sub>(C<sub>10</sub>H<sub>8</sub>FN<sub>3</sub>O<sub>7</sub>)= 301.03 g/mol, ESI<sub>found</sub>[M+H]<sup>+</sup>= 301.07 g/mol.



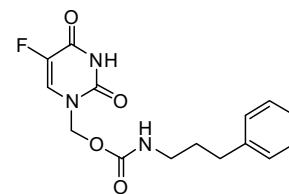
**(5-fluoro-2,4-dioxo-3,4-dihydropyrimidin-1(2H)-yl)methyl (4-nitrophenyl) carbonate, Product 14:**

Formaldehyde (278  $\mu\text{L}$ , 7.55 mmol) was added to 5-FU (164.5 mg, 1.26 mmol) and it left to react under stirring for 1h at 55°C. The resulted solution was evaporated until water was eliminated (Product 1). The obtained colorless oil [1] was dissolved in dry DCM (10 mL) and TEA (265  $\mu\text{L}$ , 1.89 mmol) was added. 5 min later, nitrophenylchloroformate (379 mg, 1.88 mmol) was also added as a solid. The reaction mixture was stirred and left overnight under reflux at 40°C. The product formation was confirmed by HPLC-MS. Final product was purified in a  $\text{SiO}_2$  column by flash chromatography using the elution system II and a gradient 5 $\rightarrow$ 80%B in 20 min. 21 mg were obtained as a white solid (0.06 mmol, yield: 4.8%). Purity by HPLC-MS: 65.2%.  $\text{Mw}_{\text{calc}}(\text{C}_{12}\text{H}_8\text{FN}_3\text{O}_7) = 325.07\text{g/mol}$ ,  $\text{ESI}_{\text{found}}[\text{M}+\text{H}]^+ = 325.12\text{ g/mol}$ .  $^1\text{H-NMR}$  (400 MHz,  $\text{DMSO-d}_6$ )  $\delta$ : 8.29 (d,  $J=8\text{Hz}$ , 2H), 8.08 (d,  $J=8\text{Hz}$ , 2H), 6.85 (d,  $J=8\text{Hz}$ , 2H), 5.87 (s, 2H), 5.66 (s, 2H). The product was used directly for the formation of product [15].



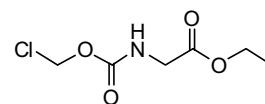
**(5-fluoro-2,4-dioxo-3,4-dihydropyrimidin-1(2H)-yl)methyl (3-phenylpropyl)carbamate, Product 15:**

To a solution of product 14 (21 mg, 0.07 mmol) in ACN (8 mL), 3-phenyl-1-propylamine (9.8 mg, 0.07 mmol) was added. The reaction mixture was left to react at 40°C during 1 h. Product formation was confirmed by HPLC-MS. Purity by HPLC-MS: 25.5% (not purified).  $\text{Mw}_{\text{calc}}(\text{C}_{15}\text{H}_{16}\text{FN}_3\text{O}_4) = 321.11\text{g/mol}$ ,  $\text{ESI}_{\text{found}}[\text{M}+\text{H}]^+ = 321.90\text{ g/mol}$ .



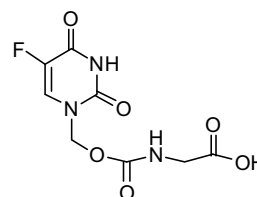
**Ethyl 2-(((chloromethoxy)carbonyl)amino)acetate, Product 16:**

To a solution of glycine ethyl ester (1000 mg, 7.13 mmol) in dry DCM (20 mL) TEA (1499.5  $\mu\text{L}$ , 10.72 mmol) was added, the mixture was stirred and it was left to react at -20°C for 5 min. Then, chloromethylchloroformate (692.5  $\mu\text{L}$ , 7.78 mmol) was added and the solution left to react under agitation during 10 min. The product formation was confirmed by HPLC-MS after that period of time.  $\text{H}_2\text{O}$  (10 mL) was added to quench the reaction. Aqueous and organic phases were separated. The organic phase was collected and washed with a NaCl saturated solution, evaporated under vacuum and 999.7 mg of product were obtained as a transparent oil (5.11 mmol, yield: 71.5%). Purity by HPLC-MS: 97.1%.  $\text{Mw}_{\text{calc}}(\text{C}_6\text{H}_{10}\text{ClNO}_4) = 195.6\text{ g/mol}$ ,  $\text{ESI}_{\text{found}}[\text{M}+\text{H}]^+ = 195.69\text{ g/mol}$ .  $^1\text{H-NMR}$  (400 MHz,  $\text{CDCl}_3$ ): 5.78 (s, 2H), 4.26 (q,  $J=4\text{Hz}$ , 2H), 4.01 (d,  $J=4\text{Hz}$ , 2H), 1.29 (t,  $J=4\text{Hz}$ , 3H).  $^{13}\text{C-NMR}$ : (101 MHz,  $\text{DMSO-d}_6$ )  $\delta$ : 65.80, 156.27, 42.21, 169.54, 61.8, 14.3.



**2-(((5-fluoro-2,4-dioxo-3,4-dihydropyrimidin-1(2H)-yl)methoxy)carbonyl)amino)acetic acid (5-FU-carbamate), Product 17:**

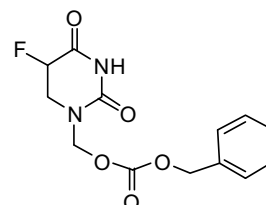
Product 22 (50 mg, 0.17 mmol) was dissolved in 6 mL of DCM:TFA (2/1) (v/v) solution. The reaction was stirred for 1 h at rt. Deprotection process



was confirmed by HPLC-MS. The solvent was evaporated under vacuum and a white solid obtained. 42.5 mg of product were obtained (0.16 mmol, yield: 93.8%). Purity by **HPLC-MS**: 97.2%.  $Mw_{calc}(C_8H_8FN_3O_6) = 261.16$  g/mol,  $ESI_{found}[M+H]^+ = 261.85$  g/mol.  $^1H-NMR$  (400 MHz,  $D_2O$ )  $\delta$ : 7.73 (d,  $J=4Hz$ , 1H), 5.64 (s, 2H), 3.68 (s, 2H).

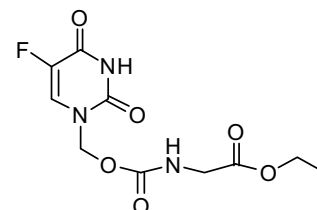
**Benzyl ((5-fluoro-2,4-dioxotetrahydropyrimidin-1(2H)-yl)methyl) carbonate, Product 18:**

To 5-FU (945.7 mg, 7.27 mmol) 1.69 mL of 37% HCHO in water were added. The mixture was stirred at 55°C for 1 h. The resulted solution was evaporated until water was eliminated. The obtained colorless oil product **1** was dissolved in dry ACN (20 mL) and TEA (1521.7  $\mu$ L, 10.91 mmol) was added. To the mixture, benzyl chloroformate (1557.47  $\mu$ L, 10.90 mmol) was added slowly and the reaction mixture was stirred overnight under Argon atmosphere. The product formation was confirmed by HPLC-MS and final product was purified in a  $SiO_2$  column by flash chromatography using the elution system II and a gradient 5 $\rightarrow$ 40%B in 15 min. 865.5 mg were obtained as a white solid (1.44 mmol, yield: 20.5%). Purity by **HPLC-MS**: 98.8%.  $Mw_{calc}(C_{13}H_{13}FN_2O_5) = 294.07$  g/mol,  $ESI_{found}[M+H]^+ = 294.89$  g/mol.  $^1H-NMR$  (400 MHz, DMSO- $d_6$ )  $\delta$ : 7.30 (d,  $J=8Hz$ , 2H), 6.58 (m, 5H), 4.82 (s, 2H), 4.39 (s, 2H).  $^{13}C-NMR$  (101 MHz, DMSO- $d_6$ )  $\delta$ : 157.18, 153.35, 149.19, 140.53, 134.93, 129.43, 129.09, 128.43, 128.23, 73.30, 69.43.



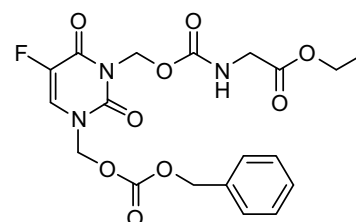
**Ethyl 2-(((5-fluoro-2,4-dioxo-3,4-dihydropyrimidin-1(2H)-yl)methoxy)carbonyl)amino)acetate, Product 19:**

5-FU (150.1 mg, 1.15 mmol) was dissolved in dry DMF (5mL) and TEA (1446  $\mu$ L, 10.3 mmol) was added. After 5 min, product **16** (253.98 mg, 1.30 mmol) was also mixed and left to react during 2 h at 50°C. Product formation was confirmed by HPLC-MS and then purified by flash chromatography using a  $SiO_2$  column, elution system II and a gradient 5 $\rightarrow$ 50%B in 25min. Finally, 176.8 mg of product **19** were obtained as a white solid (0.61 mmol, yield: 53.0%). Purity by **HPLC-MS**: 94.1%.  $Mw_{calc}(C_{10}H_{12}FN_3O_6) = 289.07$  g/mol,  $ESI_{found}[M+H]^+ = 289.99$  g/mol.  $^1H-NMR$  (400 MHz,  $CDCl_3$ )  $\delta$ : 7.69 (d,  $J=5.6Hz$ , 2H), 5.62 (s, 2H), 4.21 (q,  $J=8Hz$ , 3H), 3.95 (d,  $J=4Hz$ , 2H), 1.26 (m, 3H).



**Ethyl 2-(((3-(((benzyloxy)carbonyl)oxy)methyl)-5-fluoro-2,6-dioxo-2,3-dihydropyrimidin-1(6H)-yl)methoxy)carbonyl)amino)acetate, Product 20:**

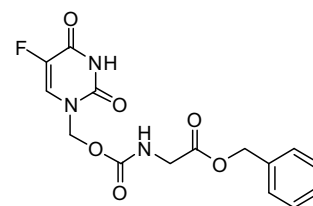
Product **18** (100 mg, 0.22 mmol) was dissolved in dry DMF (10 mL) and TEA (142.32  $\mu$ L, 1.03 mmol) was added. After 5 min, product **16** (79.59 mg, 0.4 mmol) was also added and the reaction mixture was left to react during 2 h at 50°C. Product formation was confirmed by HPLC-MS. Finally, 30.8 mg of product **20** were obtained as a white solid (0.06 mmol, yield: 20.5%). Purity by **HPLC-MS**: 95.6%.  $Mw_{calc}(C_{19}H_{20}FN_3O_9) = 453.1$  g/mol,  $ESI_{found}[M+H]^+ = 454.10$  g/mol.





**Benzyl**      **2-(((5-fluoro-2,4-dioxo-3,4-dihydropyrimidin-1(2H)-yl)methoxy)carbonyl)amino)acetate, Product 21:**

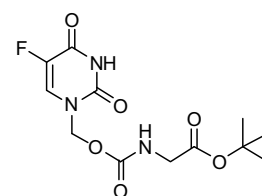
5-FU (64 mg, 0.49 mmol) was dissolved in dry DMF (5 mL) and TEA (1.9 mL, 1.44 mmol) was added. After 5 min, product **41** (152 mg, 0.59 mmol) was also added and the reaction mixture was left to react during 2 h at 50°C.



Product formation was confirmed by HPLC-MS and then purified by flash chromatography using a SiO<sub>2</sub> column, elution system II and a gradient 5→40%B in 30min. Finally, 85 mg of product **21** were obtained as a white solid (0.24 mmol, yield: 49.1%). Purity by **HPLC-MS**: 99.7%.  $Mw_{calc}(C_{15}H_{14}FN_3O_6) = 351.09$  g/mol,  $ESI_{found}[M+H]^+ = 352.05$  g/mol. **<sup>1</sup>H-NMR** (400 MHz, CDCl<sub>3</sub>) δ: 7.68 (d, J=4Hz, 1H), 7.34 (m, 5H), 5.61 (s, 2H), 5.18 (s, 2H), 4.00 (d, J=4Hz, 2H).

**Tert-butyl**      **2-(((5-fluoro-2,4-dioxo-3,4-dihydropyrimidin-1(2H)-yl)methoxy)carbonyl)amino)acetate, Product 22:**

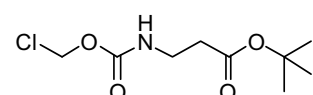
5-FU (169.3 mg, 1.3 mmol) was dissolved in dry DMF (5 mL) and TEA (1.6 mL, 11.7 mmol) was added. After 5 min, product **42** (348.1 mg, 1.56 mmol) was added and the reaction mixture was left to react during 2 h at 50°C. Product formation



was confirmed by HPLC-MS and purified by flash chromatography using a SiO<sub>2</sub> column, the elution system II and a gradient 5→50%B in 25min. Finally, 210 mg of 5-FU-GlytBut were obtained as a white solid (0.66 mmol, yield: 50.98%). Purity by **HPLC-MS**: 94.5%.  $Mw_{calc}(C_{15}H_{14}FN_3O_6) = 317.10$  g/mol,  $ESI_{found}[M+H]^+ = 318.00$  g/mol. **<sup>1</sup>H-NMR** (400 MHz, CDCl<sub>3</sub>) δ: 7.34 (d, J=8Hz, 1H), 5.64 (s, 2H), 3.86 (d, J=4Hz, 2H), 1.47 (s, 9H).

**tert-butyl 3-(((chloromethoxy)carbonyl)amino)propanoate, Product**

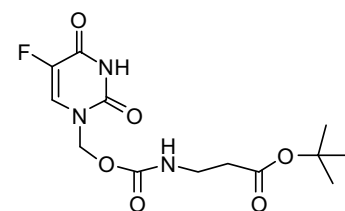
**23:** To a solution of β-Ala-OtBu (998.7 mg, 6.87 mmol) in dry DCM (20 mL) TEA (1.1 mL, 8.2 mmol) was added, the mixture was stirred and



left to react at -20°C for 5 min. Then, chloromethyl chloroformate (533 μL, 5.99 mmol) was added and the solution stirred during 10 min. Product formation was confirmed by HPLC-MS. The mixture was washed with saturated NaCl solution and the organic phase evaporated under vacuum. Product formation was confirmed by HPLC-MS. Purity by **HPLC-MS**: 63.6%.  $Mw_{calc}(C_9H_{16}ClNO_4) = 237.68$  g/mol,  $ESI_{found}[M-Boc+H]^+ = 181.0$  g/mol.

**Tert-butyl**      **3-(((5-fluoro-2,4-dioxo-3,4-dihydropyrimidin-1(2H)-yl)methoxy)carbonyl)amino)propanoate, (5-FU-Ala-OtBu) Product**

**24:** 5-FU (598 mg, 4.6 mmol) was dissolved in dry DMF (20 mL) and TEA (1.9 mL, 13.6 mmol) was added. After 5 min, product **23** (1.63 g, 6.88 mmol) was also mixed and left to react during 2 h at 50°C.

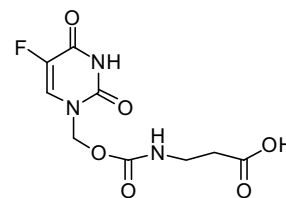


Product formation was confirmed by HPLC-MS and purified by flash chromatography using a SiO<sub>2</sub> column, elution system II and a gradient 5→60%B in 30min. Finally

1.02 g of product **24** were obtained as a white solid (3.08 mmol, yield: 67.5%). Purity by **HPLC-MS**: 97.4%.  $Mw_{\text{calc}}(\text{C}_{13}\text{H}_{18}\text{FN}_3\text{O}_6) = 331.3$  g/mol,  $\text{ESI}_{\text{found}}[\text{M-tBu+H}]^+ = 275.99$  g/mol.  $^1\text{H-NMR}$  (400 MHz,  $\text{CDCl}_3$ )  $\delta$ : 7.75 (d,  $J=4\text{Hz}$ , 1H), 5.56 (s, 2H), 3.43 (q,  $J=4\text{Hz}$ , 2H), 2.46 (t,  $J=4\text{Hz}$ , 2H), 1.49 (s, 9H).  $^{13}\text{C-NMR}$  (101 MHz,  $\text{DMSO-d}_6$ )  $\delta$ : 155.70, 150.93, 80.96, 67.00, 48.24, 36.35, 28.33.

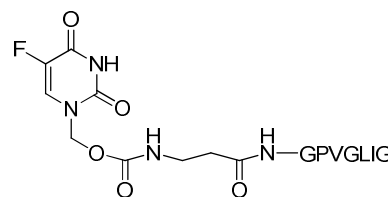
**3-(((5-fluoro-2,4-dioxo-3,4-dihydropyrimidin-1(2H)-yl)methoxy)carbonyl)amino)propanoic acid, (5-FU-Ala), Product 25:**

Product **24** (100 mg, 0.30 mmol) was dissolved in 6 mL of DCM:TFA (2/1) (v/v) solution. Reaction was stirred for 1 h at rt. The deprotection process was confirmed by HPLC-MS. Solvent was evaporated under vacuum and a white solid obtained. Finally, 79 mg of product were obtained (0.28 mmol, yield: 99%). Purity by **HPLC-MS**: 98.1%.  $Mw_{\text{calc}}(\text{C}_9\text{H}_{10}\text{FN}_3\text{O}_6) = 275.19$  g/mol,  $\text{ESI}_{\text{found}}[\text{M+H}]^+ = 275.92$  g/mol.  $^1\text{H-NMR}$  (400 MHz,  $\text{CDCl}_3$ )  $\delta$ : 7.84 (d,  $J=4\text{Hz}$ , 1H), 5.50 (s, 2H), 3.27 (t,  $J=4\text{Hz}$ , 2H), 2.45 (t,  $J=4\text{Hz}$ , 2H).  $^{13}\text{C-NMR}$  (101 MHz,  $\text{DMSO-d}_6$ )  $\delta$ : 158.21, 150.93, 88.12, 75.71, 36.21, 34.61.



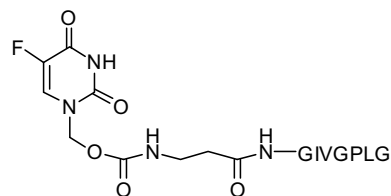
**5-FU-Ala-MMP9pept Product 26:**

To a solution n of product **9** (202 mg, 1  $\mu\text{mol}$ ) in dry DCM (10 mL), product **43** (160.1 mg, 0.36 mmol) dissolved in dry DCM (1 mL) was added. The pH of the final mixture was adjusted to pH=8 using DIEA and the reaction left overnight at rt under an inert atmosphere. Then, the product formation was confirmed by HPLC-MS and purified by semipreparative-HPLC-MS using a XBridge column, the elution system V and a gradient 25 $\rightarrow$ 50%B in 15 min. Finally, the product was collected and lyophilized leading to a slowly yellow product. 221 mg of product **26** were obtained with a 38% yield. Purity by **HPLC-MS**: 98.6%.  $Mw_{\text{calc}}(\text{C}_{37}\text{H}_{57}\text{FN}_{10}\text{O}_{13}) = 869.45$  g/mol,  $\text{ESI}_{\text{found}}[\text{M+H}]^+ = 870.1$  g/mol.

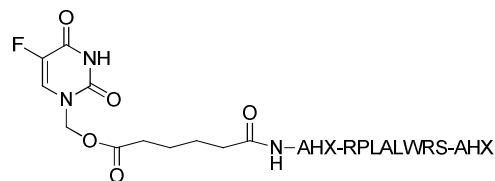


**5-FU-Ala-MMP9scram, Product 27:**

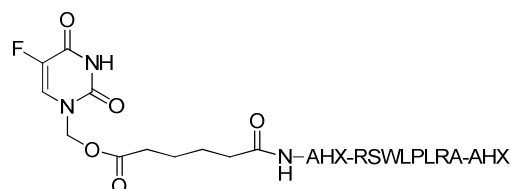
To a solution of product **10** (101 mg, 0.5  $\mu\text{mol}$ ) in dry DCM (10 mL), product **43** (80.1 mg, 0.18 mmol) dissolved in dry DCM (1mL) was added. The pH was adjusted to 8 using DIEA and the reaction was left to react overnight, at rt and under an inert atmosphere. Then, the product formation was confirmed by HPLC-MS and purified by semipreparative-HPLC-MS using a XBridge column, elution system V and a gradient 25 $\rightarrow$ 50%B in 15 min. Finally, the product was collected and lyophilized leading to a slowly yellow product. 121mg of **27** product were obtained with a 30% yield. Purity by **HPLC-MS**: 97.8%.  $Mw_{\text{calc}}(\text{C}_{37}\text{H}_{57}\text{FN}_{10}\text{O}_{13}) = 869.45$  g/mol,  $\text{ESI}_{\text{found}}[\text{M+H}]^+ = 870.1$  g/mol.



**5-FU-adipic-MMP7pept, Product 28:** To a solution of product **3** (20mg, 0.04 mmol) in dry DCM (5 mL), product **11** (46.7 mg, 0.038 mmol) dissolved in dry DMF (1mL) was added. The pH of the final mixture was adjusted to pH=8 with DIEA. The reaction was monitored by HPLC-MS and left to react under agitation overnight at rt. Product formation was confirmed by HPLC-MS and purified by semipreparative-HPLC using a BEH column, elution system IV and a gradient 5→5%B (2 min)→15%B (3min)→50%B (7min). Finally, 40.4 mg of product were obtained as a slightly yellow solid (0.021 mmol, 70% yield). Purity by **HPLC-MS**: 99.3%.  $Mw_{calc}(C_{69}H_{57}FN_{10}O_{17})= 1493.82$  g/mol,  $ESI_{found}[M+2H]^{2+}= 748.13$  g/mol.

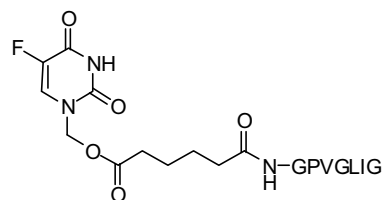


**5-FU-adipic-MMP7scram, Product 29:** To a solution of product **3** (21.1mg, 0.04 mmol) in dry DMF (5 mL), product **12** (49.5 mg, 0.04 mmol) dissolved in dry DMF (1mL) was added. The pH of the final mixture was adjusted to pH= 8 with DIEA. The reaction was monitored by HPLC-MS and left to react overnight at



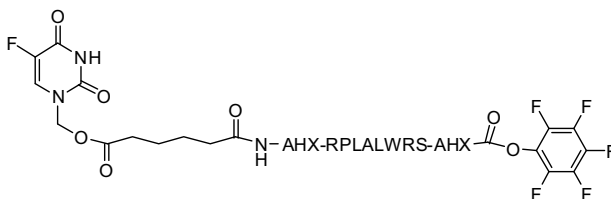
rt. Product formation was confirmed by HPLC-MS and purified by semipreparative-HPLC using a BEH column, elution system IV and a gradient 15→50%B in 12 min. Finally, 32.6 mg of product were obtained as a slightly yellow solid (0.021 mmol, 54% yield). Purity by **HPLC-MS**: 99.9%.  $Mw_{calc}(C_{69}H_{57}FN_{10}O_{17})= 1493.82$  g/mol,  $ESI_{found}[M+2H]^{2+}= 748.13$  g/mol.

**5-FU-adipic-MMP9pept, Product 30:** To a solution of product **3** (200.1mg, 0.44 mmol) in dry DMF (10 mL), product **9** (120.7 mg, 0.19 mmol) dissolved in dry DMF (1mL) was added. The pH of the final mixture was adjusted to pH=8 with DIEA. The reaction was monitored by HPLC-MS and left to react overnight at rt. Product formation was confirmed by HPLC-MS and purified by semipreparative-HPLC using a XSelect column, elution system IV and a gradient 20→60%B in 5 min. Finally, 88.8 mg of product were obtained as a white solid (0.1 mmol, 47% yield). Purity by **HPLC-MS**: 99.9%.  $Mw_{calc}(C_{39}H_{60}FN_9O_{13})= 881.3$  g/mol,  $ESI_{found}[M+H]^+= 882.41$  g/mol.



**5-FU-adipic-MMP7pept-5Fphenol, Product**

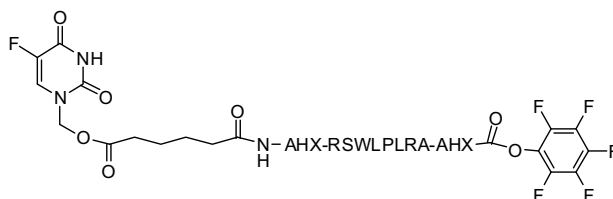
**31:** Product **28** (20 mg, 0.01 mmol) was dissolved in 5 mL of DCM and then 1.5 eq of pentafluorophenol (3.69 mg, 0.02 mmol), 1.5 eq of EDC (3.8 mg, 0.02 mmol) and 0.5 eq of DMAP (0.82 mg, 0.006 mmol) were added as a solid and the reaction mixture was left to react at room temperature under agitation during 2 h. Formation of product **31** was confirmed by HPLC-MS.



$Mw_{\text{calc}}(C_{75}H_{56}F_5N_3O_6) = 1660.76 \text{ g/mol}$ ,  $ESI_{\text{found}}[M+2H]^{2+} = 831.05 \text{ g/mol}$ . The product was directly used for the formation of product **33**.

**5-FU-adipic-MMP7scram-5Fphenol, Product**

**32:** Product **29** (20 mg, 0.01 mmol) was dissolved in 5 mL of DCM and then 1.5 eq of pentafluorophenol (3.69 mg, 0.02 mmol), 1.5 eq of EDC (3.8 mg, 0.02 mmol) and 0.5 eq of

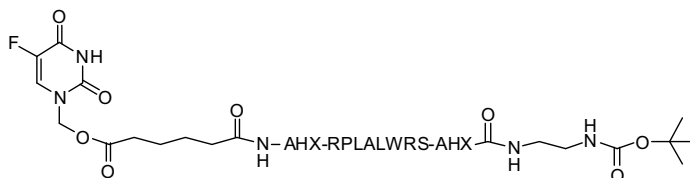


DMAP (0.82 mg, 0.01 mmol) were added as a solid and the reaction mixture was left to react at rt during 2 h. The product formation was confirmed by HPLC-MS.  $Mw_{\text{calc}}(C_{75}H_{56}F_5N_3O_6) = 1660.76 \text{ g/mol}$ ,  $ESI_{\text{found}}[M+2H]^{2+} = 831.05 \text{ g/mol}$ . The product was directly used for the formation of product **34**.

**5-FU-adipic-MMP7pept-**

**amideethyleneamine-Boc, Product 33:**

Product **31** (21.8 mg, 0.013 mmol) was dissolved in 5 mL of dry DMF. N-Boc-ethylenediamine (2.3  $\mu\text{L}$ , 0.09 mmol)

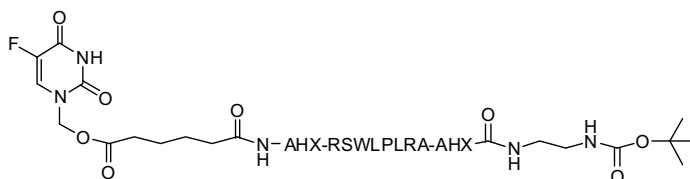


was dissolved in 1 mL of dry DMF and adjusted to pH=7 with acetic acid and then was added to the product **31** solution. The reaction was left to react overnight at rt. Product formation was confirmed by HPLC-MS and purified by semipreparative-HPLC using a XSelect column, elution system IV and a gradient 20 $\rightarrow$ 45% in 5 min. The product formation was confirmed by HPLC-MS. Finally, 1.1 mg of product were obtained as a slightly yellow solid (0.67  $\mu\text{mol}$ , 5.2% yield). Purity by **HPLC-MS**: 88.1%.  $Mw_{\text{calc}}(C_{76}H_{123}F_2N_{21}O_{18}) = 1636.91 \text{ g/mol}$ ,  $ESI_{\text{found}}[M+2H]^{2+} = 819.12 \text{ g/mol}$ .

**5-FU-adipic-MMP7scram-**

**amideethyleneamine-Boc, Product 34:**

Product **32** (21.8 mg, 0.013 mmol) was dissolved in 5 mL of dry DMF. N-Boc-ethylenediamine (2.3  $\mu\text{L}$ , 0.09 mmol)

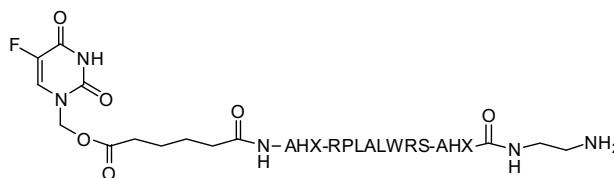


was dissolved in 1 mL of dry DMF and adjusted to pH=7 with acetic acid and then was added to the product **32** solution. The reaction was left to react overnight at rt. Product formation was confirmed by HPLC-MS and purified by semipreparative-HPLC using a XSelect column, elution system IV and a gradient 20 $\rightarrow$ 45%B in 5 min. Finally, 1.8 mg of product was obtained as a slightly yellow solid (1  $\mu\text{mol}$ , 8.5% yield). Purity by **HPLC-MS**: 75.1%.  $Mw_{\text{calc}}(C_{76}H_{123}F_2N_{21}O_{18}) = 1636.91 \text{ g/mol}$ ,  $ESI_{\text{found}}[M+2H]^{2+} = 819.12 \text{ g/mol}$ .

### 5-FU-adipic-MMP7pept-

#### amideethyleneamine, Product 35: Product 33

(1.1 mg, 0.67  $\mu\text{mol}$ ) was dissolved in a 3 mL solution of DCM:TFA (2:1, v/v). It was left to react during 1 h at rt. Product formation was

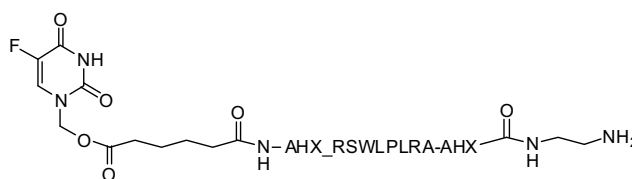


confirmed by HPLC-MS and the solvent was evaporated under vacuum. After solvent removal, colorless oil was obtained. Purity by **HPLC-MS**: 49.5%.  $Mw_{\text{calc}}(\text{C}_{71}\text{H}_{115}\text{FN}_{20}\text{O}_{16}) = 1536.79$  g/mol,  $ESI_{\text{found}}[\text{M}+2\text{H}-\text{H}_2\text{O}]^{2+} = 748.34$  g/mol. The product was directly used for the formation of product 37.

### 5-FU-adipic-MMP7scram-

#### amideethyleneamine, Product 36: Product 34

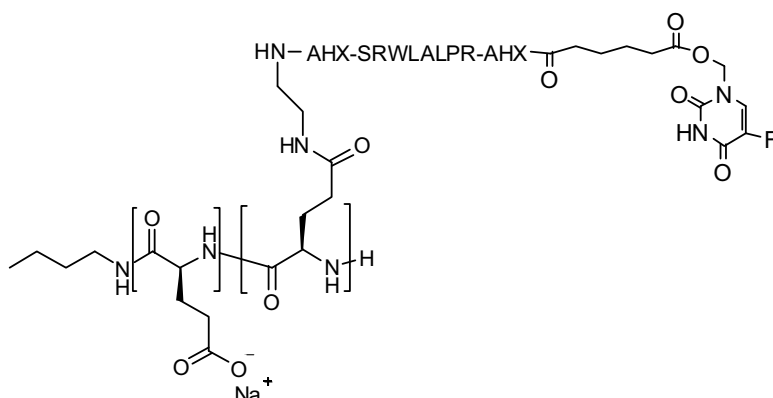
(1.8 mg, 0.1  $\mu\text{mol}$ ) was dissolved in a 3 mL solution of DCM:TFA (2:1, v/v). It was left to react during 1 h at rt. Product



formation was confirmed by HPLC-MS and the solvent was evaporated under vacuum. After solvent removal, colorless oil was obtained. Purity by **HPLC-MS**: 58.5%.  $Mw_{\text{calc}}(\text{C}_{71}\text{H}_{115}\text{FN}_{20}\text{O}_{16}) = 1536.79$  g/mol,  $ESI_{\text{found}}[\text{M}+2\text{H}-\text{H}_2\text{O}]^{2+} = 748.34$  g/mol. The product was directly used for the formation of product 38.

### PGA-MMP7pept-5FU, Product

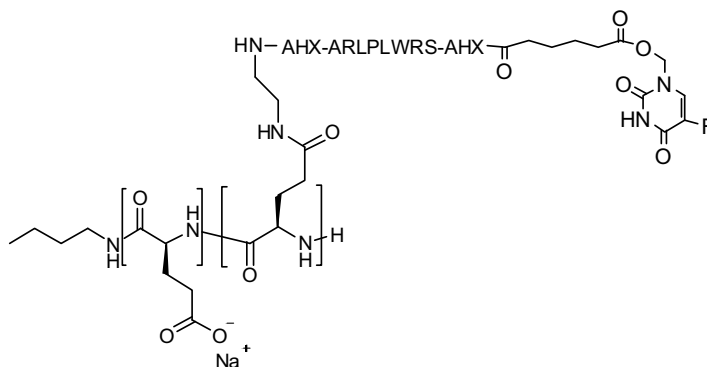
**37**: To a solution of PGA (10 mg, 0.78 mmol) in dry DMF (10 mL), DIC (27.7  $\mu\text{L}$ , 0.25 mmol) and HOBt (23.5 mg, 0.25 mmol) 5 minutes later were added as a solid. After 10 min, product 35 (195 mg, 0.11 mmol) was added. The pH was controlled and adjusted with DIEA to pH=8.



After 24h, same quantity of DIC was added again. The reaction was left to react during 36h at rt. DMF was evaporated under vacuum and a white solid was obtained and purified by dialysis. The crude was dissolved in 3 mL of a  $\text{NaHCO}_3$  0.1M (pH=7 adjusted with acetic acid) solution, introduced in the membrane (previously hydrated) and dialyzed against MilliQ- $\text{H}_2\text{O}$  (3 x5 L) for 24 h. Finally, the product was lyophilized and 95.4 mg of a yellow solid were obtained (yield=25%). TDL and FD were measured following the protocol described in section 2.3.1.1.2 by HPLC. TDL was 2.65% and a  $\text{FD} < 0.1\%$ .

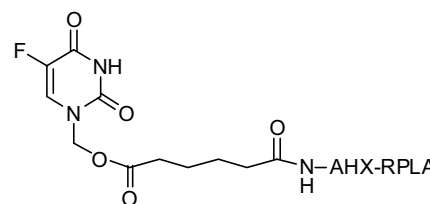
**PGA-MMP7Scram-5FU, Product 38:**

To a solution of PGA (3mg, 0.23 mmol) in dry DMF (5 mL), DIC (10.1  $\mu$ L, 0.09 mmol) was added and 5 min later HOBt (8.1 mg, 0.09 mmol) was also added as a solid. After 10 min, product **36** (50 mg, 0.065 mmol) was mixed. The pH was controlled and adjusted with DIEA to pH=8. After



24h, the same quantity of DIC was added again. The reaction was left to react during 36h at rt. DMF was evaporated under vacuum and a white solid was obtained. and purified by dialysis. The crude was dissolved in 3 mL of a  $\text{NaHCO}_3$  0.1M (pH=7 adjusted with acetic acid) solution, introduced in the membrane (previously hydrated) and dialyzed against MilliQ- $\text{H}_2\text{O}$  (3 x5 L) for 24 h. Finally, the product was lyophilized and 25.8 mg of a yellow solid were obtained (yield=15%). TDL and FD were measured following the protocol described in section 2.3.1.1.2 by HPLC. TDL was 0.73% and a FD< 0.1%.

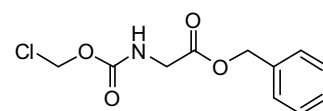
**5-FU-adipic-RPLA, Product 39:** Product **3** (10.1mg, 0.02 mmol) was dissolved in 5 mL and a solution of product **40** (11.48 mg, 0.02 mmol) in DMF (1 mL) was added. The mixture pH was adjusted to pH=8 with DIEA. The reaction was monitored by HPLC-MS and left to react overnight at rt.



Product formation was confirmed by HPLC-MS and purified by semipreparative-HPLC using a BEH column, elution system III and a gradient 0 $\rightarrow$ 40%B in 7 min. After the solvent removal, 16.2 mg of product were obtained as a slightly yellow solid (0.024 mmol, 53% yield). Purity by **HPLC-MS**: 99.8%.  $\text{Mw}_{\text{calc}}(\text{C}_{37}\text{H}_{58}\text{FN}_{10}\text{O}_{10}) = 838.92$  g/mol,  $\text{ESI}_{\text{found}}[\text{M}+\text{H}]^+ = 839.45$  g/mol.

**Peptide AHX-RPLA, Product 40:** The tetrapeptide was synthesized following the solid-phase synthetic route detailed in section 3.3.1. The synthesis was performed with 2 g of 2-chlorotrytil resin. Purification of both was performed by semipreparative-HPLC using a BEH column, elution system III and a gradient 0 $\rightarrow$ 40%B in 7 min. After the solvent removal by lyophilisation a white solid was obtained and 165.2 mg of product **40** were obtained. Purity by **HPLC-MS**: 91.9%.  $\text{Mw}_{\text{calc}}(\text{C}_{26}\text{H}_{45}\text{N}_8\text{O}_5) = 568.71$  g/mol,  $\text{ESI}_{\text{found}}[\text{M}+\text{H}]^+ = 569.28$  g/mol. The product was used for the synthesis of product **39**.

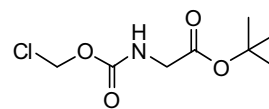
**Benzyl 2-(((chloromethoxy)carbonyl)amino)acetate, Product 41:** To a solution of Benzyl glycinate p-toluenesulfonate (200 mg, 0.59 mmol) in anhydrous DCM (20 mL) TEA (124  $\mu$ L, 0.88 mmol) was added, the



mixture was stirred and left to react at  $-20^\circ\text{C}$  for 5 min. Then, chloromethylchloroformate (57.4  $\mu$ L, 0.64 mmol) was added and the solution was stirred 10 min. The product formation was confirmed

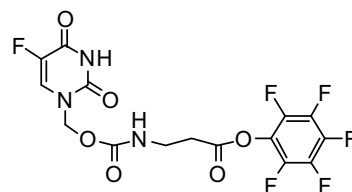
by HPLC-MS. Once it was confirmed, H<sub>2</sub>O (10 mL) was added to quench the reaction. Two phases were separated and the organic phase was cleaned with a saturated NaCl solution and then evaporated under vacuum. Finally, 114.2 mg of the chloro-derivate synthesized were obtained as transparent oil (0.44 mmol, yield: 75.1%). Purity by **HPLC-MS**: 99.7%.  $Mw_{\text{calc}}(C_{11}H_{12}ClNO_4) = 257.67$  g/mol,  $ESI_{\text{found}}[M+H]^+ = 257.96$  g/mol.

**Tert-butyl 2-(((chloromethoxy)carbonyl)amino)acetate, Product 42:** To a solution of Glycine *tert*-butyl ester hydrochloride (402 mg, 2.40 mmol) in



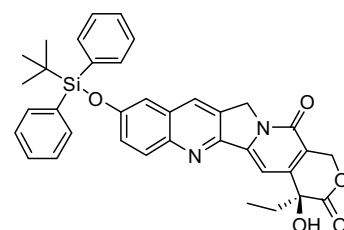
dry DCM (20 mL) TEA (498.73  $\mu$ L, 3.53 mmol) was added, the mixture was stirred and it was left to react at -20°C for 5 min. Then, chloromethylchloroformate (231.57  $\mu$ L, 2.58 mmol) was added and the solution was stirred during 10 min. Product formation was confirmed by HPLC-MS after that period of time H<sub>2</sub>O (10 mL) was added to quench the reaction. Two phases were separated and organic phase was cleaned with a saturated NaCl solution and then evaporated under vacuum yielding 348.1 mg of Product **42** as a transparent oil (1.56 mmol, yield: 65.1%). Purity by **HPLC-MS**: 94.8%.  $Mw_{\text{calc}}(C_8H_{14}ClNO_4) = 223.06$  g/mol,  $ESI_{\text{found}}[M+H]^+ = 223.86$  g/mol.

**Pentafluorophenyl 3-(((5-fluoro-2,4-dioxo-3,4-dihydropyrimidin-1(2H)-yl)methoxy)carbonyl)amino)propanoate, Product 43:**



Product **25** (281.7 mg, 0.97 mmol) was dissolved in 20 mL of DCM and then pentafluorophenol (269.8 mg, 1.46 mmol), EDC (227.3 mg, 1.16 mmol) and DMAP (89.25 mg, 0.06 mmol) were added as a solid. The reaction mixture was stirred at rt during 2 h. Product formation was confirmed by HPLC-MS. The crude was washed with saturated NaCl (3 x 20 mL) and secondly with saturated NaHCO<sub>3</sub> (3 x 20 mL). The organic phase was evaporated under vacuum yielding 398mg of product **43** as a white solid (yield=89.6). Purity by **HPLC-MS**: 97.0%.  $Mw_{\text{calc}}(C_{15}H_9F_6N_3O_6) = 454.03$  g/mol,  $ESI_{\text{found}}[M+H]^+ = 455.08$  g/mol. The product was directly used for the formation of products **26-27**.

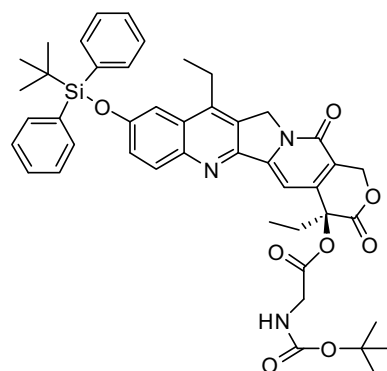
**SN-38-TBDPS, Product 44:** To a suspension of SN-38 (1 g, 2.55 mmol) in 50 mL of dry DCM, TEA (1.6 mL, 10.19 mmol) and *Tert*-butylchlorophenylsilane (2.6 mL, 11.47 mmol) were added. The reaction mixture was heated to reflux overnight. Once the reaction was finished, the crude was washed with 0.2N HCl (3 x 50 mL), saturated NaHCO<sub>3</sub> (3 x 50 mL) and saturated NaCl (3 x 50 mL). The



organic phase was dried over MgSO<sub>4</sub>, filtered and evaporated under vacuum. The residue was dissolved in DCM and product was precipitated by addition of hexane. The solid dissolved in DCM was absorbed in SiO<sub>2</sub> and purified by flash-chromatography, eluent system (A) DCM and (B) EtOH and a gradient 5 $\rightarrow$ 20%B in 15 min. Finally, 1.47 g of the product **44** was obtained as a yellow solid (2.3 mmol, yield 91%). Purity by **HPLC-MS**: 99.0%.  $Mw_{\text{calc}}(C_{36}H_{34}N_2O_5Si) = 630.80$  g/mol,  $ESI_{\text{found}}[M+H]^+ = 631.00$  g/mol. <sup>1</sup>H-NMR (400 MHz, CDCl<sub>3</sub>)  $\delta$ : 7.72 (d, J=9.2Hz, 1H), 7.43 (m, 5H), 7.23 (m, 6H), 6.92 (s, 1H), 6.74 (d, J=2.4Hz, 2H), 5.38 (d, J=12.4Hz, 1H), 4.94 (d, J=16.4Hz, 1H), 4.77 (s, 2H),

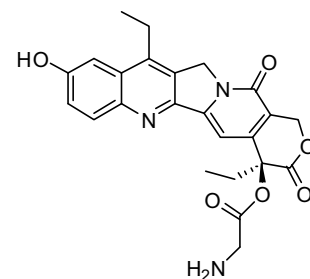
3.46 (s, 1H), 2.3 (q, J=7.6Hz, 2H), 1.54 (m, 2H), 0.84 (s, 9H), 0.69 (t, J=7.2Hz, 3H), 0.59 (t, J=15.2Hz, 3H).  $^{13}\text{C-NMR}$  (101 MHz,  $\text{CDCl}_3$ )  $\delta$ : 174.28, 157.99, 155.41, 150.56, 150.17, 147.60, 145.60, 144.08, 135.86, 132.51, 132.13, 130.69, 128.33, 128.13, 127.14, 126.25, 118.31, 110.37, 97.69, 73.13, 66.34, 49.70, 31.60, 26.96, 23.35, 20.04, 13.60, 8.13.

**SN-38-TBDPS-BocGly, Product 45:** To a solution of product **44** (SN-38 TBDPS) (1.47 g, 2.33 mmol) and Boc-Gly-OH (0.612 g, 350 mmol) in dry DCM (36 mL) at 0°C were added EDC (0.670 g, 3.5 mmol) and DMAP (0.142 g, 1.16 mmol). The reaction mixture was stirred at 0°C for 14h. Product formation and reaction completion were confirmed by HPLC-MS. The crude was washed with  $\text{NaHCO}_3$  0.5% (3 x20 mL), water (3 x20 mL), HCl 0.1N (3 x20 mL) and saturated NaCl (3 x20 mL) and finally the organic phase was dried over  $\text{MgSO}_4$ , filtered and evaporated under vacuum.



1.45 g of product **45** was obtained as a yellow solid (1.848 mmol, 79% yield). Purity by **HPLC-MS**: 100%.  $\text{Mw}_{\text{calc}}(\text{C}_{45}\text{H}_{49}\text{N}_3\text{O}_8\text{Si}) = 787.97$  g/mol,  $\text{ESI}_{\text{found}}[\text{M}+\text{H}-\text{Boc}]^+ = 688.31$  g/mol.  $^1\text{H-NMR}$  (400 MHz,  $\text{CDCl}_3$ )  $\delta$ : 8.04 (d, J=12Hz, 1H), 7.75 (m, 4H), 7.43 (m, 7H), 7.15 (s, 1H), 7.08 (d, J=2.8Hz, 1H), 5.65 (d, J=17.2Hz, 1H), 5.36 (d, J=17.2Hz, 1H), 5.10 (s, 2H), 4.10 (m, 2H), 2.64 (q, J=7.61Hz, 2H), 1.39 (s, 9H), 1.17 (s, 9H), 0.95 (t, J=7.2Hz, 3H), 0.89 (t, J=7.6Hz, 3H).  $^{13}\text{C-NMR}$  (101 MHz,  $\text{CDCl}_3$ )  $\delta$ : 169.65, 167.23, 157.59, 155.12, 149.69, 147.22, 145.69, 145.22, 143.97, 185.58, 132.14, 131.86, 130.15, 128.15, 129.91, 125.94, 119.26, 110.66, 95.59, 80.24, 67.15, 49.35, 42.46, 31.80, 28.33, 26.62, 22.80, 19.47, 13.29, 7.62.

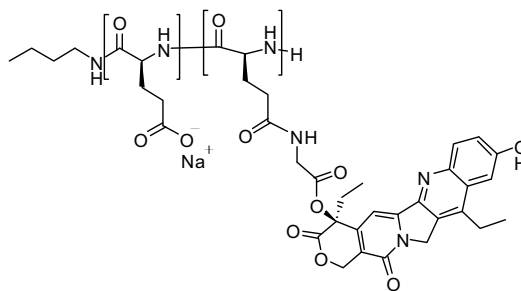
**SN-38-Gly, Product 47:** Product SN-38-TBDPS-GlyBoc **45** (100mg, 0.5 mmol) was dissolved in 200  $\mu\text{L}$  of THF and tetrabutylammonium fluoride solution (190  $\mu\text{L}$ , 0.7 mmol) and 190  $\mu\text{L}$  HCl 0.05 M were added in order to remove the TBDPS protecting group. The reaction mixture was stirred at 0°C on ice during 15 min. Then, the TBDPS removal was confirmed by HPLC-MS. Crude compound was washed with 5% HCl (3 x0.5 mL) solution in  $\text{H}_2\text{O}$  to remove the excess of tetrabutylammonium. The product obtained was SN-38-GlyBoc **46**.



Then, SN-38-GlyBoc **46** was dissolved in 4 mL of a solution HCl 4 M in 1,4-dioxane and it was left to react during 2h. The Boc removal was confirmed by HPLC-MS. 42.0 mg of product **47** was obtained as a yellow solid (0.093 mmol, 73.6% yield). Purity by **HPLC-MS**: 99%.  $\text{Mw}_{\text{calc}}(\text{C}_{24}\text{H}_{23}\text{N}_3\text{O}_6) = 449.46$  g/mol,  $\text{ESI}_{\text{found}}[\text{M}+\text{H}]^+ = 449.99$  g/mol. theoretical Mw: 449.46 g/mol, Mw detected by HPLC-MS: 449.99 g/mol.  $^1\text{H-NMR}$  (400 MHz,  $\text{DMSO-d}_6$ )  $\delta$ : 8.46 (s, 1H), 8.00 (d, J=8.8 Hz, 1H), 7.47 (m, 1H), 7.43 (m, 2H), 7.2 (s, 1H), 5.52 (s, 2H), 5.30 (d, J=4.8 Hz, 2H), 4.30 (m, 2H), 3.09 (d, J=6.8 Hz, 2H), 2.16 (m, 2H), 1.28 (t, J=7.6 Hz, 3H), 0.94 (t, J=7.6 Hz, 3H).



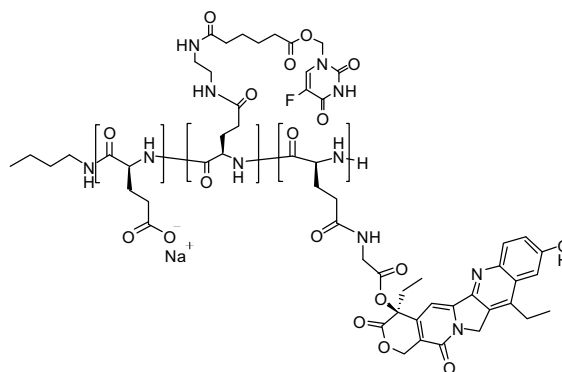
**PGA-SN38, Product 48:** To a PGA (100 mg, 0.77 mmol) solution in dry DMF (8 mL) DIC (178.85  $\mu$ L, 1.15 mmol) was added and 5 min later HOBt (156.04 mg, 1.15 mmol) was also added as a solid. After 10 min, product **46** (SN-38-Gly) (51.91 mg, 0.115 mmol) was also mixed. The pH was controlled and adjusted with DIEA to pH=8. After



24 h, the same quantity of DIC was added again. The reaction was left to react during 36h at rt under agitation. DMF was evaporated under vacuum and a white solid was obtained. Final conjugate was purified by dialysis (3x5L 24 h) dissolving previously the crude in 4mL of a  $\text{NaHCO}_3$  0.1M (pH=7 adjusted with acetic acid) solution. Finally, the product was lyophilized and 12.5 mg of a white foamy solid were obtained (yield=8%). TDL and FD were measured by UV-spectroscopy. TDL was 10.2% and a FD < 0.1%.

#### PGA-5FU-SN38, Product 49:

The conjugation of products **5** and **47** in a same PGA carrier was performed in solution by two different synthetic procedures. In both cases, product **5** was the first conjugated and secondly, product **47**. The former strategy consisted in a one pot reaction whereas in the second case the synthesis of PGA-5FU-SN38 was carried out in a two step process. It was observed that the second strategy allowed to control the ratio between both drugs, since it was quantified in between the TDL of 5-FU.



Below are detailed as an example the different strategies:

- **PGA-5FU-SN38 - One pot strategy:**

This experiment was performed with an estimated TDL of 5-FU and SN-38 of 10%.

To a solution of 100 mg of PGA-COOH in dry DMF (10 mL) DIC (27  $\mu$ L, 0.17 mmol) was added and 5 min later HOBt (120 mg, 1.06 mmol) was also added as a solid. After 10 min, product **5** (7.45 mg, 0.022 mmol) was also mixed. The pH was controlled and adjusted with DIEA to pH=8. The reaction was left to react during 24h at rt under agitation. After 24 h, the same quantity of DIC (27  $\mu$ L, 0.17 mmol) was added and 5 min later HOBt (120 mg, 1.06 mmol) was also mixed. After 10 min, product **47** (14.8 mg, 0.03 mmol) was also mixed. The pH was controlled and adjusted with DIEA to pH=8 and left to react 24 h. Then DMF was evaporated under vacuum and a yellow solid was obtained. Final conjugate was purified by dialysis (3x5L 24 h) dissolving previously the crude in 4mL of a  $\text{NaHCO}_3$  0.1M (pH=7 adjusted with acetic acid) solution. Finally, the product PGA-5FU-SN38 was lyophilized and 66.5 mg of a slightly yellow foamy solid was obtained (yield=70%). TDL and FD were

measured for each single drug. So, by means of HPLC it was quantified a FD below 0.1% and a TDL of 2.0% of 5-FU. The SN-38 quantification was performed by UV-spectroscopy with a TDL of 8.8% and a FD < 0.1%. The mM ratio of 5-FU against SN-38 attached to the polymeric chain was: 0.71 (5-FU:SN-38).

Table 3. 7 Summary of the synthesis of PGA-5FU-SN38 conjugate through the one pot strategy.

# Batch	Mass obtained (mg)	Synthetic methodology	TDL (5-FU)% (mg/mg)	TDL(SN-38)% (mg/mg)	Ratio 5-FU:SN-38
#1	66.5	One-pot	2.0%	8.8%	0.71

- **PGA-5FU-SN38 - Two step strategy:**

Different syntheses (Table 3. 8) were performed with the aim to achieve different 5-FU:SN-38 ratios.

Table 3. 8 Summary of PGA-5FU-SN38 conjugates family (PGA-5FU-SN38-(A,B,C,D) synthesized following a two step process.

# Batch	Mass obtained (mg)	TDL (5-FU)% (mg/mg)	TDL(SN-38)% (mg/mg)	mM 5-FU	mM SN-38	Ratio SN-38:5-FU
#A	140.1	3.05%	0.025%	10	0.03	1:300
#B	179.4	0.26%	0.02%	0.34	0.02	1:40
#C	123.5	3.27%	5.15%	42.3	2.20	1:20
#D	260	2.55%	0.025%	10	0.03	1:300

Below is detailed as an example the synthesis of a PGA-5FU-SN38 conjugate following the two step strategy.

To a solution of PGA-5-FU **6** (75 mg, 0.51 mmol) in dry DMF (10 mL) DIC (76  $\mu$ L, 0.48 mmol) and 5 min later HOBt (60 mg, 0.44 mmol) were added. After 10 min, product SN38-Gly **47** (83  $\mu$ g,  $1.8 \cdot 10^{-4}$  mmol) was also mixed. The pH was controlled and adjusted with DIEA to pH=8. After 24h, the same quantity of DIC was introduced and the reaction was left to react during 36h at rt. DMF was evaporated under vacuum and a white solid was obtained and purified by dialysis (3 x5 L 24 h) dissolving previously the crude in 2 mL of a NaHCO<sub>3</sub> 0.1M (pH=7 adjusted with acetic acid) solution. After lyophilized 140.1 mg of the final conjugate PGA-5FU-SN38, as a white foamy solid, were obtained. The SN-38 TDL and FD were measured by UV-spectroscopy and the TDL of 5-FU was confirmed also by HPLC once SN-38 was conjugated. The TDL of SN-38 was 0.025% and 3.05% for the 5-FU, the FD for both drugs was <0.1%. The mM ratio of 5-FU against SN-38 attached to the polymeric chain was: 333.33 (5-FU:SN-38).

### 3.9 *In vitro* validation techniques

*Techniques and methods using cell cultures were conducted at FVPR (CIBBIM-Nanomedicine, VHIR) and were analyzed by Helena Plà under the supervision of Dr. Ibane Abasolo.*

Cell work was performed in a class II biological safety cabinet, pre-sterilized by UV light and 70% v/v ethanol in double distilled water spray. All material used was sterile (bought sterile from the producer or autoclaved) and flushed with ethanol before putting it inside the cabinet.

In this work, two different human CRC cell lines were employed: HT-29.Fluc.C4 and HCT-116.Fluc2.C9 to which Firefly Luciferase (Fluc) gene was introduced in order to allow their *in vitro* monitoring by means of bioluminescence imaging.

*Table 3. 9 CRC cells: description and origin.*

CRC cell line	Origin	Source	Description
HCT-116	Homo sapiens, human	Colon tissue	Malignant cells isolated from a male with colonic carcinoma
HT-29	Homo sapiens, human	Colon tissue	Malignant cells isolated from a primary tumor from a female with a well-differentiated adenocarcinoma.

Below are described the conditions for the cell growth.

*Table 3. 10 Summary of conditions used for the cell growth.*

Cell line	Medium	Incubator Conditions
HT-29.Fluc.C4 (ref. ATCC®HTB-38™)	RPMI , 10% FBS, antibiotic and 2mM L-glutamine	37°C with 5% CO <sub>2</sub>
HCT-116.Fluc2.C9 (ref. ATCC®CLL-247™)	RPMI , 10% FBS, antibiotic and 2mM L-glutamine	37°C with 5% CO <sub>2</sub>

For cell passage a medium with antibiotic with 10% fetal bovine serum was used. To maintain the expression of Fluc reporters by Luciferase, Neomycin was added to the HT-29 and HCT-116 plates to a concentration of 500 µg/mL and 250 µg/mL, respectively.

### 3.9.1 MTT methodology to evaluate the cell viability

The MTT assay is a method that allows measuring cell viability, the proliferation of the cells (cell culture assays) and also determine and compare the cytotoxicity of drugs alone or conjugated to polymers. In the MTT procedure the proliferation of living cells is measured quantitatively via mitochondrial dehydrogenase activity: viable mitochondria reduce 3-[4,5-dimethylthiazol-2-yl]-2,5-diphenyl tetrazolium bromide or MTT, generating MTT formazan crystals that are spectrophotometrically measurable at 590 nm. The  $IC_{50}$  value is defined as the polymer-drug conjugate concentration at which cell growth is inhibited by 50%. MTT assays were carried out by triplicate in three different days, and in each experiment there were six wells per each treatment condition. Mean  $IC_{50}$  values were used to compare the cytotoxicity (so to say, efficacy) of each PDC and the corresponding free drug.

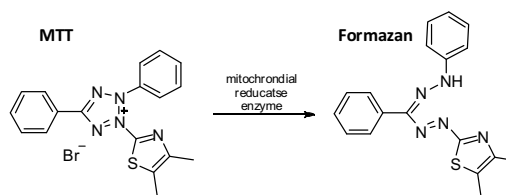


Figure 3. 4 Mitochondrial reductase reduces MTT to purple formazan dyes. This conversion is used to measure viable (living) cells.

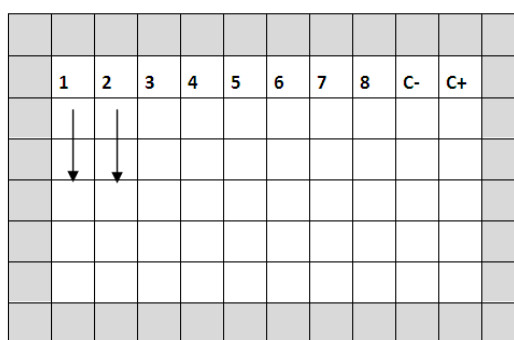


Figure 3. 5 Scheme of 96-well microtitre plate for an MTT assay. From left to right an increasing concentration of the product is tested. Column C- corresponds to a negative control, settled without treatment and Column C+ corresponds to a positive control (100% death). All the surrounding wells were filled with PBS, to avoid evaporation of cell media.

- On day 0, cells were seeded into sterile, flat-bottomed, 96-well plates (90  $\mu$ L/well, seeding densities of  $1 \cdot 10^6$ ) using complete medium without antibiotic. It was performed using a multi-channel pipette, and cells were allowed to settle for 24 h in the incubator at 37°C and 5%  $CO_2$ . 96-well plates were filled adding to the external well rows 200  $\mu$ L of PBS to prevent surrounding wells from dehydrating (Figure 3. 5).

On day 1, 24 h later, 8 different concentrations of the test product were prepared (Table 3. 11 ). 10  $\mu$ L of each prepared solution were added to each well of the plates, starting the lower concentration on the first column (Figure 3. 5). 10  $\mu$ L of medium without antibiotic were added to column C-, that corresponds to the cells without treatment (negative control) and 10  $\mu$ L of DMSO were added to column C+ wells, that corresponds to 100% death (positive control).

Table 3. 11 Summary of the concentration range studied for each polymer-drug conjugate.

Test product	Concentration range studied
PGA-5-FU	1.5-200 $\mu$ M (eq 5-FU)
PGA-MMPpept-5FU	1.5-200 $\mu$ M (eq 5-FU)
PGA-SN38	1·10 <sup>-5</sup> -1.4 $\mu$ M (eq SN-38)
PGA-5FU-SN38	0-300 $\mu$ M (eq 5-FU) and 0-1 $\mu$ M (eq SN-38)

- On day 4, 72 h after the addition of the treatment, 96-well plates were checked for cell confluence. Then, 10  $\mu$ L MTT of a 5 mg/mL solution in PBS was added to each well of the plate and cells incubated for 4 h. After this period of time, medium was removed using a multi-channel pipette avoiding contact with the bottom of the well and 180  $\mu$ L of DMSO was added to each well to dissolve the formazan crystals. The optical density of the solution was determined spectrophotometrically at 590 nm using a microtitre plate reader.
- Once absorbance at 590 nm was measured for treated and untreated cells, following the equation [1], cell viability expressed in% for each concentration was calculated. Cell viability is usually expressed as a percentage of the viable cells and as mean  $\pm$  standard error of the mean (SEM).

$$\text{Cell Viability (\%)} = (\text{Abs590x} \times 100) / \text{Abs590Control} \quad \text{Equation [1]}$$

Where, *Abs590x* is the absorbance measured for the compound at a polymer-drug concentration *x* and *Abs590Control* is the absorbance measured for control cells.

Finally, results were represented using the GraphPad Prism 6 Software in a dosage-response graphic (cell viability vs. concentration) and IC<sub>50</sub> values were also calculated using the same software.

### 3.9.2 Cell internalization

#### 3.9.2.1 Confocal fluorescence microscopy

Cell internalization of nanoconjugates labeled with CF (excitation and emission wavelengths 492/517 nm, respectively) was studied by confocal fluorescence microscopy to evaluate lysosomal co-localization and therefore establish if nanoparticle internalization followed the endocytic pathway. Different times were studied to evaluate the internalization of PGA-5-FU conjugate labeled with CF: 5 min, 30 min, 1 h and overnight. These experiments were performed in HCT-116.Fluc2.C9 and HT-29.Fluc.C4 cell lines.

- On day 0, cells were seeded at a density of  $5 \times 10^4$  cell/well, on 24-well plates with RPMI medium and allowed to seed for 24 -36 h.
- On day 1, PGA-5-FU-CF product [8] was added (100  $\mu$ M eq 5-FU). Experiments were performed after 5 min, 30 min, 1 h and overnight incubations at 37°C. Then medium was removed, and cells washed twice with PBS. LysoTracker Red (5  $\mu$ M) was added after that and incubated 30 min at 37 °C. Then cells were washed twice with PBS and paraformaldehyde (4%) was added to fix cells. Incubation was done 20 min at 4 °C and then cells washed twice with PBS. Cells were fixed with DAPI in a glass and visualized in the confocal microscope FV1000, Olympus.

### 3.9.2.2 Flow cytometry

Cellular uptake was studied by the flow cytometry technique, a technology that can simultaneously measure and analyze the relative fluorescence intensity of cells as they flow in a fluid stream through out a light beam.

Different times were studied to evaluate the internalization of PGA-5-FU conjugate labeled with CF: 2, 5, 10, 20, 40, 60, 120 min and overnight.

- On day 0 cells were seeded (density of  $7 \times 10^4$  cell/well) into a 24 well-plate using RPMI medium. They were allowed to settle for 24 to 36 h in an incubator at 37 °C and 5% CO<sub>2</sub>.
- On day 1, for the overnight measure, medium was removed and cells were treated with 250  $\mu$ L of PGA-5-FU-CF product [8] (0.25 mg/ml in PBS) and left at the incubator at 37°C and 5% CO<sub>2</sub>.
- On day 2, the product was added at specific times (120, 60, 40, 20, 10, 5 and 2 min before the end point) after removing the medium. End point cells were washed twice with cold PBS, trypsinized and analyzed by flow cytometry.

Absorption and emission wavelengths were set at 490 and 520 nm in the Facscalibur Becton Dickinson Cytometer, and results analyzed by FCSExpress software. Average internalized cells was measured at each time and represented as the average of positive cells vs. time.

### 3.10 *In vivo* studies

*All experiments carried out with animals were performed by personal of FVPR (CIBBIM-Nanomedicine, VHIR) under the supervision of Dr. Yolanda Fernandez. Animal experiments were performed following the protocols approved by the Animal Experimentation Ethical Committee of Vall d'Hebron.*

#### 3.10.1 Tumor-accumulation and whole-body biodistribution of PGA-5FU-AF750

Tumor-accumulation and whole-body biodistribution of product [7] was measured by means of *in vivo* and *ex vivo* fluorescence imaging (FLI) using the IVIS<sup>®</sup> Spectrum equipment. It is necessary to mention that the *in vivo* and *ex vivo* FLI results were confirmed by quantification of the therapeutic drug in the same organs by HPLC after homogenization (section 3.7).

Animals used in these experiments were 6-8 week-old athymic nude female mice (Hsd:Athymic Nude-Foxn1, Harlan). Two different biodistributions of PGA-5FU-AF750 were performed. In the first one (BD1), firefly luciferase expressing HCT-116.Fluc2-C9 human colorectal cancer cell line was used, whereas in the second experiment (BD2), firefly luciferase expressing HT-29.Fluc-C4 human colorectal cell line was used.

Mice received subcutaneous (s.c.) tumor cell injection ( $2 \times 10^6$  cells/100  $\mu$ L PBS) into the rear right flank. Body weight and tumor were measured twice a week by caliper measurements, and the tumor volume was calculated according to the formula  $Dxd^2/2$ . Once the tumors reach a defined volume (133-158  $mm^3$ ), mice were randomized accordingly to their tumor volume.

Mice were separated in 5 different groups: G0, G1a, G1b, G2a and G2b. G0 correspond to the non-treated group, G1a and G1b correspond to the 5-FU treated groups and G2a and G2b to the PGA-5FU-AF750 treated groups. Two mice without tumor were included in groups G1a, G1b, G2a and G2b. For the BD2 an additional group was added for the AF750 evaluation containing 1 animal without tumor.

Thereafter, mice were treated with test substances by intravenous administration (i.v.) in a single dose. At the specified times post-administration, tumor, plasma, liver, spleen, kidneys, lung, heart, brain, muscle and kin were collected and frozen for 5-FU quantification by HPLC. Furthermore, in the group of animals treated with fluorescent labeled compound, tumor-accumulation and whole-body biodistribution were measured non-invasively by FLI from ventral, lateral and dorsal views. The fluorescence signal was quantified in radiant efficiency units. In addition, at different end-time points, tumor- and tissue-accumulations of compound were determined by *ex vivo* FLI.

The *in vivo* FLI time-points for the BD1.HCT-116 experiment were 1, 4, 9, 24 and 48 h post-administration, and 4, 8 and 24 h post-administration for the BD2.HT-29 experiment. Experimental groups, administered doses, end points of the experiment and *ex vivo* FLI time points for each group are summarized in Table 3.12 of 5-FU, PGA-5-FU and AF750 for both biodistribution experiments.

Table 3. 12 Summary of the two biodistribution experiments performed with product [7].

Experiment	Group	Treatment (unique dose)	n (animals)	End point
<b>BD1. HCT-116</b>	G0	Non-treated	4	4 and 48 h
	G1a	5-FU (50 mg/kg)	8	4 h
	G1b	5-FU (50 mg/kg)	8	48 h
	G2a	PGA-5FU-AF750 (50 mg/kg)	8	4 h
	G2b	PGA-5FU-AF750 (50 mg/kg)	8	48 h
<b>BD2. HT-29</b>	G0	Non-treated	4	4 and 48 h
	G1a	5-FU (50 mg/kg)	8	4 h
	G1b	5-FU (50 mg/kg)	8	24 h
	G2a	PGA-5FU-AF750 (50 - 25 mg/kg)	8	4 h
	G2b	PGA-5FU-AF750 (25 mg/kg)	8	24 h
	G4	AF750 (0.3 – 0.15 mg/kg)	4	24 h

### 3.10.2 Tumor growth inhibition of PGA-5-FU

The tumor growth inhibition of HCT-116.Fluc2-C9 colorectal cells induced by 5-FU or PGA-5-FU [6] was followed by measuring the tumor volume using a caliper.

Animals used in these experiments were 6-8 week-old athymic nude female mice (HSd:Athymic Nude-Foxn1, Harlan). Mice received subcutaneous (s.c.) tumor cell injection of HCT-116.Fluc2-C9 cells ( $2 \times 10^6$  cells/100  $\mu$ L PBS) into the rear right flank.

Body weight and tumor volume were measured twice a week by caliper means, and tumor volume calculated according to the formula  $D \times d^2 / 2$ . Once tumors reach a defined volume (132 mm<sup>3</sup>, median), mice were randomized accordingly.

Mice were separated in 3 different groups (10 animals/group): G1, G2 and G3. G1 corresponds to the control group, injected with the vehicle (PBS); G2 group were treated with 5-FU and G3 group were treated with PGA-5-FU.

The treatment consisted in i.v. administration during 40 days, twice a week (binary representation; 1001000).

Body weight change over time (measures twice per week) was recorded to evaluate toxicity associated to the product. At the end of the experiment, *ex vivo* tumor volume was also measured to study inhibition of the tumor growth.





---

## 4. Results

---

As mentioned before, the main objective of this thesis is the design of a set of new polymer-drug conjugates to improve the efficacy of the actual treatment for mCRC disease.

Since the difference between different PDC is found on the type of linkers used in the tripartite structure as well as in the number of drugs conjugated to the polymeric carrier, the results obtained during this work have been structured according the characteristics of the different nanoconjugates.

For this reason, the results are presented individually for each type of PDC, and as for the objectives, and therefore, discussion and conclusions for each PDC type are shown separately.



---

## 4.1 Polymer-drug conjugates based on Poly-(L-glutamic acid) and 5-Fluorouracil

---

Even though 5-FU is used as first-line treatment in CRC since 50 years ago, its use has several drawbacks. One of the most relevant is related with its short plasma half-life (10 -20 min), thus requiring the administration of high doses to reach efficacy. On the other hand, 5-FU sensitivity has been associated to genetic alteration that upregulate DPD and TS levels. Gene amplification of TS has been observed in cell lines resistant to 5-FU treatment<sup>11</sup>. In addition, its non-specific distribution in tumor and healthy tissues is responsible for toxic side effects on bone marrow (myelosuppression) and the gastrointestinal tract, stomatitis, toxicity in the intestinal mucosa and severe brain neurotoxicity reaction<sup>99</sup>. As mentioned in the Introduction of this thesis, polymer-drug conjugates are a great alternative for delivering anticancer drugs to tumor sites. It has been demonstrated that PDC enhance the accumulation of the novel macromolecular systems in the damage tissue thanks to the EPR effect. This prompts the accumulation of drugs in cancerous tissues, reducing side-effects. For this reason, this promising systems are a good alternative to the actual cytotoxic treatment for mCRC based on 5-FU as a single agent.

Besides the innovation on 5-FU selectivity introduced with the 5-FU prodrugs generally for oral administration, 5-FU has been conjugated or entrapped in different nanocarriers in order to achieve a selective drug release while at the same time increasing its therapeutic activity. 5-FU entrapped in liposome carriers<sup>99</sup> can be an alternative to the 5-FU injected as a single agent in terms of reducing its non-specific biodistribution<sup>100</sup>. Another example of 5-FU encapsulation are Eudragit-coated microspheres containing the cytotoxic drug for colon targeting<sup>101</sup> that show colon-specific delivery of 5-FU once administered orally. Also, pH dependent hydrogels for targeted delivery of 5-FU in CRC cells have been published in the literature, in which a release of 5-FU by diffusion, produce cellular apoptosis in HCT-116 and HT-29 CRC cell lines<sup>102</sup>.

Concerning the conjugation of 5-FU through a covalent linkage to the nanocarrier different polymers have been reported. A pectin conjugate (polysaccharide natural polymer) containing 5-FU covalently linked (5-FU-pectin)<sup>103</sup> showed the reduction of systemic absorption and effectively delivery of 5-FU in the colon as well as its accumulation in the tumor. 5-FU-Chitosan nanoparticles<sup>104</sup> for the treatment of liver cancer provided a sustained release in the liver. Effective drug exposure time against hepatic cancer cells was increased in comparison with the observed in 5-FU *in vivo*. PDC of poly( $\alpha$ -malyc acid) and 5-FU also showed increased survival rates and decreased *in vivo* toxicity in mice<sup>105</sup>. 5-FU has been also linked to dendrimers through covalent bonds or ionic interactions<sup>106,107</sup>. As another example, the conjugation of 5-FU to macromolecules of PEG and dextran are described. This conjugate causes an increase in the concentration of 5-FU in colon tissues in comparison to the administration of 5-FU alone<sup>108</sup>. It also

has been reported the conjugation to the biodegradable poly(D,L-lactic-co-glycolic acid) (PLGA) polymer<sup>109</sup> containing a Translocatorprotein (TSPO) ligand and 5-FU for a selective targeting in CRC cells overexpressing TSPO, showing an enhanced toxicity against human cancer cells due to the synergistic effect of the TSPO ligand and 5-FU. A further example on 5-FU conjugation to polymer is the HPMA-5-FU system containing the GPLG linker<sup>110</sup>. In this study the therapeutic evaluation demonstrated that the treatment with the HPMA-5-FU conjugate displayed stronger tumor growth inhibition in comparison to 5-FU alone. Even though it is a promising carrier for improving the therapeutic activity of 5-FU, it is worth mentioning that HPMA is not a biodegradable polymer.

In all these examples, 5-FU linked to a polymeric carrier showed improvements on the stability, specificity and toxicity against tumor cells in comparison to the 5-FU administered as a single agent.

Thereby, in the present section it is studied the conjugation of the chemotherapeutic agent 5-FU to a biodegradable polymeric chain of PGA through a covalent linkage. Since it is true that several administration cycles of the new polymer-drug conjugate will be necessary for the chemotherapeutic treatment of mCRC, biodegradable polymers has become the alternative to those (e.g. HPMA or PEG) that can accumulate in the body once administered when its Mw is high and renal elimination cannot be guaranteed.

The selection of the appropriate linkage between the drug and the carrier was based on the previous research done in the UQC group by M. Melgarejo. The kinetic release of 5-FU covalently linked to PEG-based dendrimers (with different linkages) was evaluated and it was found that carbamate bond was too stable and did not allow sustained release of 5-FU. On the other hand, the ester bond in first-generation PEG dendrimers showed high lability in plasma but higher stability in acid conditions.

With all this information in hands, and knowing that polymer randomly coiled at  $pK < 5$  (i.e. within tumors), in this section we proposed the evaluation of the 5-FU conjugation to PGA through an ester bond. We consider that the conformation of the macromolecular polymer-drug conjugate would protect the ester linkage thus avoiding unspecific release during transport to the target tumor site. In addition, taking profit also of the EPR effect, we expected that our new polymer-drug conjugate would accumulate in the tumor, ensuring that most drug release would happen there.

#### **4.1.1 Synthesis optimization of PGA-5-FU conjugates**

##### **4.1.1.1 Synthesis of PGA-5-FU conjugate**

###### **4.1.1.1.1 5-FU derivatization**

*Since 2008, several studies carried out by Lorena Simón, Daniel Pulido and Marta Melgarejo at the UQC group have been focused on the conjugation of 5-FU to PEG-based dendrimers<sup>111</sup>. The knowledge gained in this field has been very useful for this thesis, specifically regarding the chemical modification of 5-FU for its conjugation to the PGA carrier.*

Derivatization of 5-FU for the synthesis of prodrugs normally takes place through the reactive nitrogens of the uracil cycle (N1 and N3, Figure 4. 1). The literature describes several substituents that can be introduced into N1 and N3 position of 5-FU, but it has been reported that N1 is much more reactive than N3<sup>112,113,114</sup>, which makes synthesis much easier.

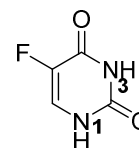
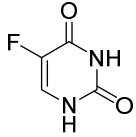


Figure 4. 1 Chemical structure of 5-FU.

Table 4. 1 summarizes the different substituent's that can be linked to 5-FU, classified according to their antitumor activity, toxicity and relative stability<sup>115</sup>. Among all substituents, 5-FU is the most active, but also the more toxic and less stable.

Table 4. 1 Types of 5-FU prodrug and its antitumoral activity, toxicity and stability.(adapted from Ozaki et al)<sup>115</sup>.

	Antitumor activity	Toxicity	Stability
(a) H	↑	↑	↓
(b) COCOR			
(c) COR			
(d) COOR			
(e) CONHR			
(f) CONR2			
(g) C(O)SR			
(h) SO2R			
(i)CH2OR			
(j) CH2SR			
(k) CH2SOR			
(l) CH2SO2R			
(m) CH2COR			
(n) CH2COOR			
(o) CH2NHCOR			
(p) CH2CH2R			

The most common prodrugs of 5-FU using the N1 position are the N-alkylcarbonyl-5-FU compounds (Table 4. 1 (b and c), Figure 4. 2 (b)). They have very similar properties to 5-FU because they undergo a rapid decomposition once administered orally due to the acidic conditions of the stomach<sup>116,117</sup>. These compounds show a high release of 5-FU but also low stability in the presence of water or protic solvents. On the other end of the table, we found compounds that show lower anticancer activity but higher stability. Since they do not decompose to give the 5-FU, these compounds, such the alkyl derivatives N-alkyl-5-FU (Table 4. 1

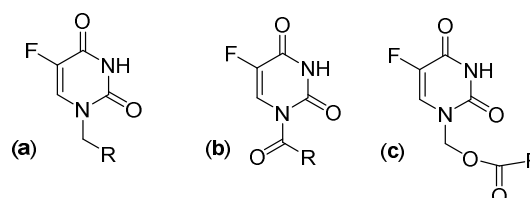


Figure 4. 2 Structure of the N-alkyl-5-FU (a), N-alkylcarbonyl-5-FU (b) and (c) N-alkylcarboxymethyl-5-FU derivatives.

entries p, o, n, m, l, k and j; Figure 4. 2 (a))<sup>118,119,112</sup>, are inactive and non-toxic. In order to achieve a better release, N-alkylcarboxymethyl-5-FU prodrugs were studied (Figure 4. 2 (c)). It has been reported for acetyl and butyryloxymethyl-5-FU derivatives that plasma half life increases at pH 7.4<sup>123</sup>, and they are also reasonably stable compounds in protic solvents. This is due to the introduction of an oxygen atom that makes the N-C bond more labile in respect to the N-alkyl-5-FU derivatives<sup>120,121,122</sup>. For this reason the N-alkylcarboxymethyl-5-FU derivatives are considered a good alternative for the synthesis of 5-FU pro-drugs.

The hydrolysis steps of N3-alkylcarboxymethyl-5-FU derivatives are shown in Figure 4. 3. The first step consists on the hydrolysis of the ester bond by a mechanism of addition-elimination and the second step is the loss of formaldehyde from the N-hydroxymethyl-5-FU intermediate to rend 5-FU rapidly. The estimated half-life of the N-hydroxymethyl-5-FU intermediate is 0.4 s<sup>123</sup>.

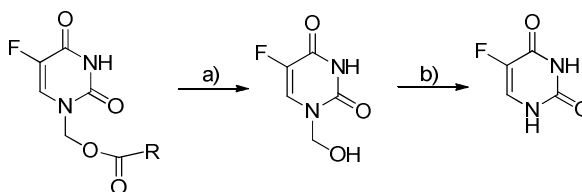


Figure 4. 3 Mechanism of 5-FU release from N3-alkylcarboxymethyl-5-FU derivatives.  
(a) Addition-elimination reaction (b) Rapid elimination of formaldehyde.

A previous work performed by L. Simón in the UQC group studied the N3-alkylcarboxymethyl-5-FU derivatization of 5-FU. In detail, the conjugation of 5-FU to a PEG-based dendrimer an ester bond in the N3 position was studied. Although N3-alkylcarboxymethyl-5-FU prodrugs are more difficult to synthesize and require a much more elaborate synthetic strategy<sup>124</sup>, they are chemically more stable (3.75 times) but more enzymatically labile (5 times) than the prodrug of N1-alkylcarboxymethyl-5-FU<sup>123</sup>. The reason behind the high stability of N3 derivatives relays in the number of oxygen atoms with negative charge distributed in the uracil ring in the ionized form, which is close to the point of the nucleophilic attack on the ester (e.g. hydroxyl attack).

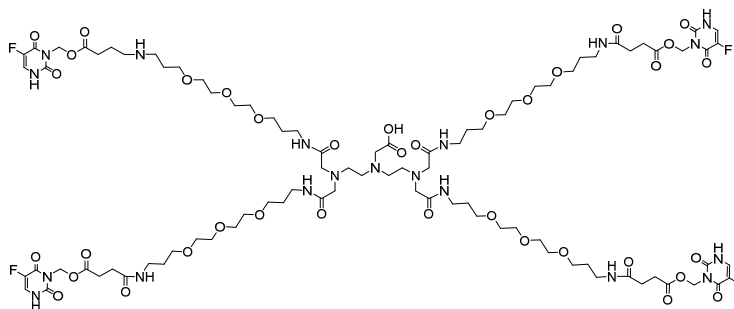


Figure 4. 4 Chemical structure of the dendrimers studied by L.Simón with N3-alkylcarboxymethyl-5-FU substitution<sup>111</sup>.

In order to achieve the N3-alkylcarboxymethyl-5FU, it was necessary to protect the more reactive N1 position prior to the 5-FU conjugation to the dendrimer. Therefore, L. Simón proposed a succinic acid molecule as a spacer between the drug and the carrier to ensure the generation of an ester bond. Although the substitution on N3 position was achieved, decomposition of the 5-FU modified molecule (Figure 4. 4) prevented further use of the molecule. Additional research, by M. Melgarejo

and D. Pulido revealed that the decomposition problems could be avoided using a longer spacer (adipic acid) and that it was not possible to obtain the N3 derivative.

With all the knowledge gained, the conjugation of 5-FU to PGA was proposed, in this thesis, through the carboxylic groups of the monomer units of glutamic acid. This conjugation was done through an amide bond because this linkage ensures the stability of the final conjugate. But, as mentioned, the ester bond was selected for the 5-FU associated release. This ester bond was introduced in an initial 5-FU derivatization prior to its conjugation to PGA. For this reason the strategy of 5-FU modification proposed consisted on a multi step reaction (Figure 4. 5).

First, the derivatization of 5-FU through the N1 position incorporating an adipic acid molecule lead the ester bond required. It was achieved in a two step process; first 5-FU was mixed with a formaldehyde solution to obtain the 5-FU derivative [1] during 1 h at 55°C. This product is very unstable so, it was necessary to complete the procedure fastly. Once the product was dried, it was mixed with adipic acid in the presence of DCC (3 eq) and DMAP (0.5 eq) in anhydrous DMF and the reaction was left at rt overnight. The crude of this reaction was dirty and the yield was relatively low (33%). Different purification methods were evaluated in order to improve this result. The product was purified by semipreparative-HPLC, manual SPE using an OASIS (C18) column and by flash chromatography in a SiO<sub>2</sub> column. The best results were achieved with the first option, by means of semipreparative-HPLC. The product **5-FU-adipic** [2] was finally obtained in a high purity (98.1%)(Figure 4. 6).

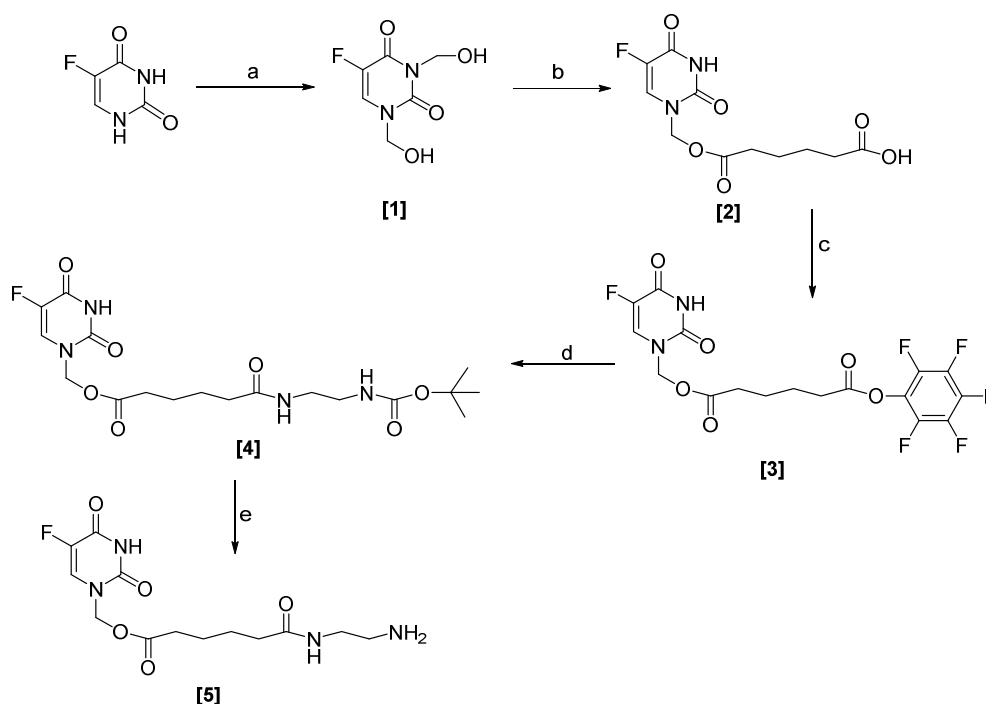


Figure 4. 5 Synthesis scheme of product [5]. Conditions: a) HCOOH 37% (6 eq), 1 h, 55°C; b) Adipic acid, DCC (3eq), DMAP(0.5 eq), DMF, overnight, rt; c) 5-F-pheno (1.5 eq), EDC (1.5 eq), DMAP (0.5 eq), DCM, 3 h, rt; d) N-Boc-ethylenamino (1.1 eq), pH=7, DMF, overnight, rt; e) TFA/DCM (1:3), 1 h, rt.



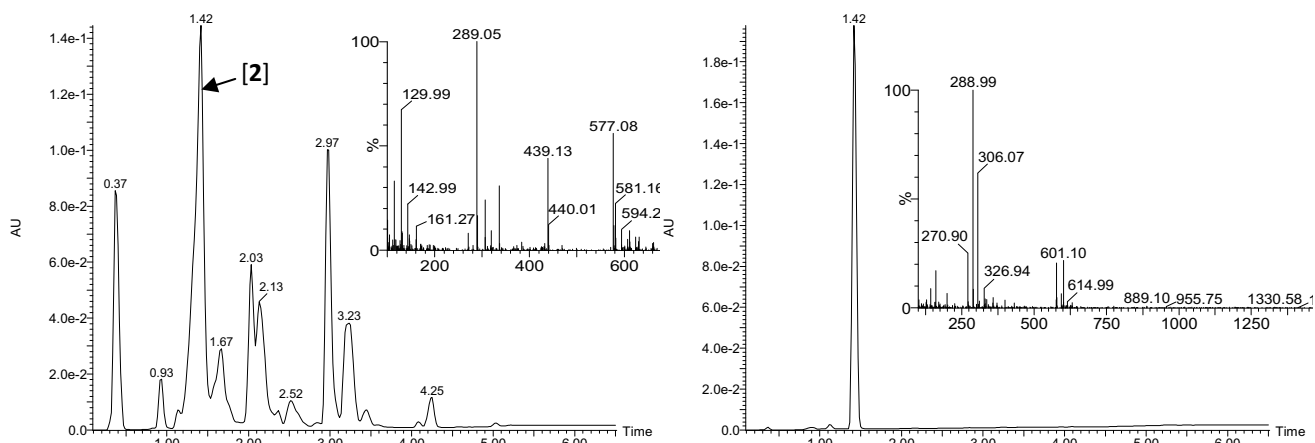


Figure 4. 6 HPLC-MS chromatograms of product [2] crude (left) and product [2] purified (right).

Once the purification of 5-FU derivative was carried out, the next step consisted on the modification of product [2] by adding a N-Boc-ethylenediamine to obtain the 5-FU derivative [4]. To achieve this product, the strategy consisted on the activation of the carboxylic group of the 5-FU derivative [2] as pentafluorophenol ester. Product [3] was obtained in a reaction of product [2] in the presence of EDC and DMAP in DCM during 3 h at rt. The product was purified by a simple extraction process.

The coming next step consisted on the reaction of the 5-FU derivative [3] and N-Boc-ethylenediamine to obtain product [4]. Ethylenediamine was chosen with one amino group protected with the Boc group in order to avoid the formation of by-products. It is necessary to mention that the amine has a pH of 11, so prior to its addition the pH was adjusted to pH=6 using acetic acid to avoid the ester hydrolysis of product [3] once added. Purification was carried out in a very reproducible and easy flash-chromatography process in a SiO<sub>2</sub> column obtaining high yields (90%) and also a pure product (99.3%).

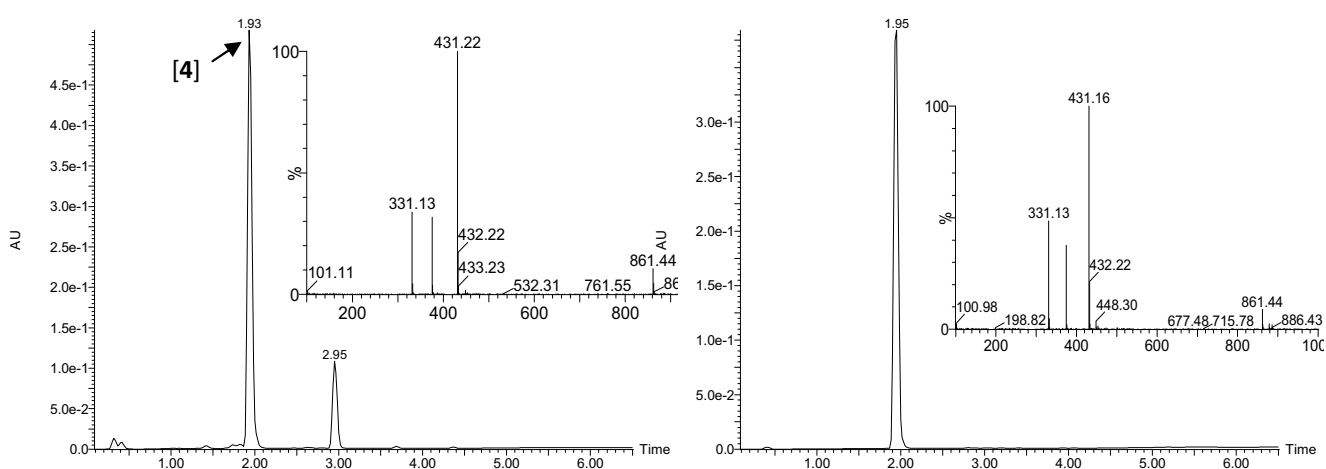


Figure 4. 7 HPLC-MS chromatograms of product [4] crude (left) and product [4] purified (right).

For the final conjugation of the 5-FU derivative [4] to the PGA polymeric chain it was necessary to eliminate the Boc group (Figure 4. 8), thus, the amide bond between the  $\gamma$ -carboxylic units of glutamic acid and the 5-FU derivative [5] could occur.

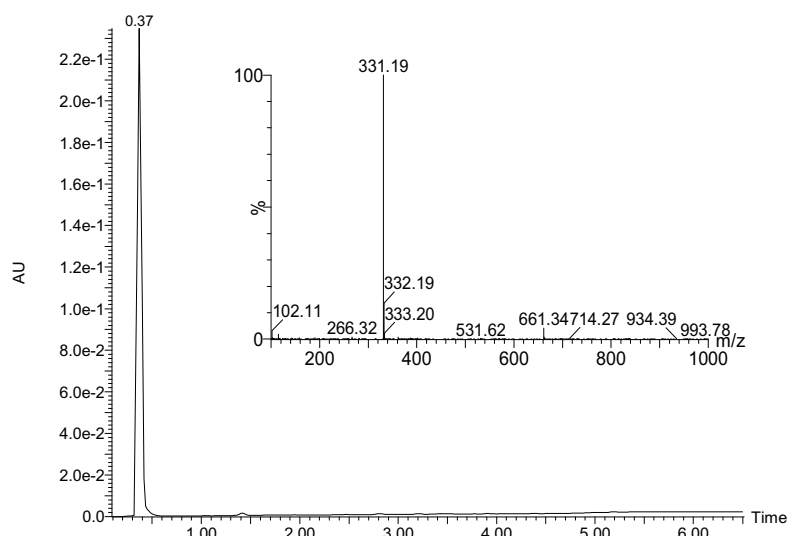


Figure 4. 8 HPLC-MS chromatogram of product [5].

#### 4.1.1.1.2 Conjugation of the 5-FU derivatized to PGA

Once 5-FU was modified through the N1 position leading an ester bond derivative and a free amino group, product [5] was conjugated to PGA.

PGA was purchased as poly-L-glutamic acid sodium salt form (PGA-COONa). To carry out the conjugation of product [5] to the carboxylic groups of the polymeric chain it was necessary to convert the PGA-COONa to its acidic form (PGA-COOH). Two strategies were followed: the use of a  $H^+$  exchange resin (Amberlite®)<sup>125</sup> or the precipitation of PGA-COOH through the acidification of a PGA-COONa solution with HCl 1 M<sup>126</sup>. In this later case, the product precipitated at pH below 5. The second strategy was selected since it was simpler and faster.

Several syntheses were carried out in order to optimize the experimental conditions. Throughout the optimization process, high Total Drug Loading (TDL) and low Free Drug (FD) values were aimed. The TDL corresponds to the average of drug that is conjugated to the polymeric carrier through a covalent bond. The FD corresponds to the average of drug that is entrapped in the structure due to the random coiled conformation of the polymer, without any chemical conjugation and should be ideally below 2%. TDL and FD were measured by means of RP-HPLC using an UV detector set at 254 nm, before and after the hydrolysis of PGA-5-FU (0.1 mg/mL solution in H<sub>2</sub>O) with NaOH 1 M which released all the 5-FU covalently bound to the polymer (Figure 4. 9).

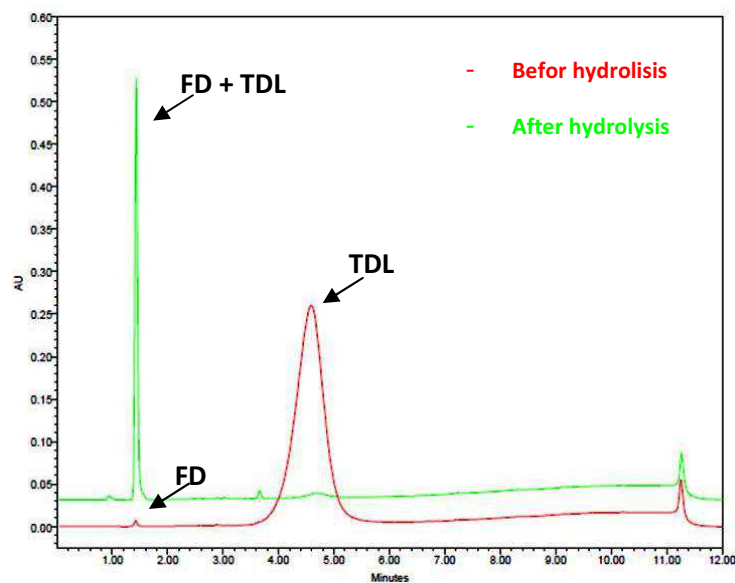


Figure 4. 9 Example of the chromatograms obtained before and after the hydrolysis of the ester bond in the PGA-5-FU conjugate. The red trace corresponds to the non-hydrolyzed conjugate. The green trace corresponds to the chromatogram of the hydrolyzed PGA-5-FU where the 5-FU is released. The area of TDL corresponds to the difference between the areas of FD+TDL and FD peaks. Both, TDL and FD are expressed in a mass average or a molar average. The higher TDL is, the lower doses of PDC will be administered, so, this value was really relevant through the optimization process.

Table 4. 2 summarizes the different synthetic batches performed with the final TDL, yield and the amount obtained.

Table 4. 2 Summary of the different reactions performed to set up the methodology for the synthesis of PGA-5-FU. All the experiments were performed with the objective to obtain conjugated with an estimated 5-FU TDL of 15%.

# Batch	TDL% (mg/mg)	Mass obtained (mg)	Yield%
#1	1.6	28.5	27%
#2	7.63	22.5	27%
#3	10.2	32	22%
#4	3.29	168	25%
#5	7.23	102.1	40%
#6	11.89	103.6	48%
#7	9.06	40.5	37%
#8	12.82	246.9	28%
#9	9.18	250	35%

The first coupling conditions (batch #1 in Table 4.2) evaluated consisted in 1.5 eq of DIC and a catalytic amount of DMAP in DMF, yielding a very low TDL (1.6%). In batch #2, the coupling reagents used were 1.5 eq of DIC and 1.5 eq of HOBt, in DMF adjusting the final pH at 8 with DIEA. With these conditions, TDL (7.63%) was greatly improved (Figure 4.10).

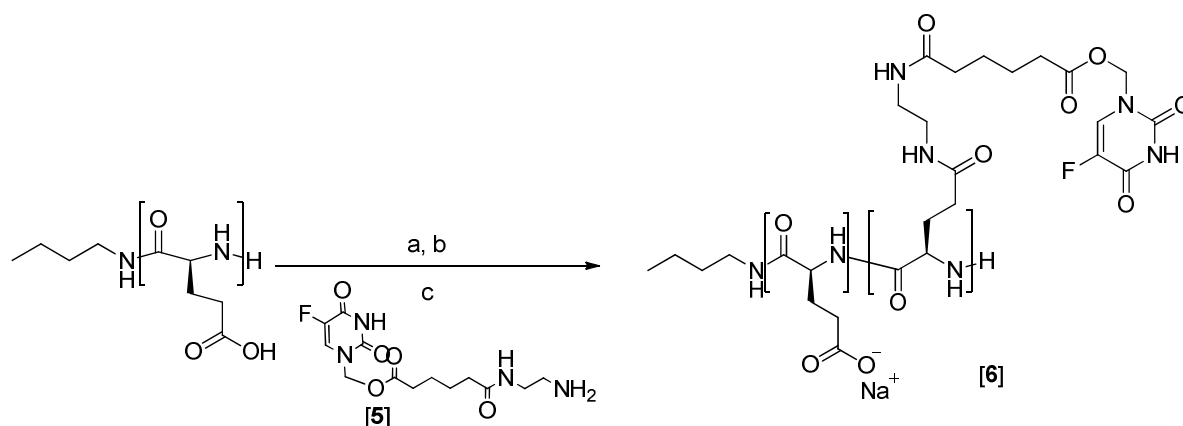


Figure 4.10 Synthesis scheme of PGA-5-FU [6]. Conditions: a) DIC (1.5 eq) 5min; b) HOBt (1.5 eq), 10 min; c) product [5] (1 eq), 36 h (24 h readdition DIC (1.5 eq)), rt.

The established procedure consisted on the precipitation of PGA-COOH aqueous solution using a solution of HCl 1 M following a centrifugation process (3500 rpm, 10 min) because it was necessary to eliminate the aqueous phase for the coupling of 5-FU derivative [5] in anhydrous DMF. The dry pellet was lyophilized and then PGA-COOH was dissolved in DMF. Once a clear solution was obtained, 1.5 eq of DIC were added and once mixed, 1.5 eq of HOBt were added 5 min later. The mixture was left to react for 10 min, and then product [5] was added to the reaction vessel. The pH was carefully adjusted to 8 with DIEA to avoid the hydrolysis of the ester bond in product [5]. It was left to react under agitation during 36 h, and at 24 h 1.5 eq of DIC were added. Finally, the crude was dried under vacuum and dissolved in a NaHCO<sub>3</sub> (0.1 M adjusted to pH 7 with HCl 1 M). In this step, the exchange of H<sup>+</sup> and Na<sup>+</sup> lead again the PGA sodium salt form for those monomers where the 5-FU derivative [5] was not attached. Once the product was dissolved, it was purified by means of dialysis against distilled water for 24 h, followed by lyophilization and further characterization of TDL and FD by HPLC. This strategy ensures the stability of the ester bond during the synthesis of the PGA-5-FU conjugate and yields pure PGA-5-FU conjugates.

Batches #1 to #3 were performed with a PGA sodium salt (Mw between 15 and 50 kDa) purchased from Sigma-Aldrich. Even though batches #2 and #3 showed a higher TDL, very low yields were obtained. These results could be related with the high polydispersity index (PI) of Sigma's polymer. A SEC-MALS-IR analysis of this polymer (section 4.1.2.3), revealed an average Mw of 70.9 kDa (far from the theoretical 15 – 50 kDa range) and a PI of 3.43. To solve this problem, a PGA sodium salt (Mw of 15 kDa) was purchased to Polypeptide Solutions S.L. (PPS), since they guaranteed a PI around 1.1. This is very important factor in order to achieve higher and reproductive TDL result, higher yields in the reactions and also permits working in a large scale. On batch #4 the coupling conditions were DIC/HOBt and the PGA used was from PPS. Although the TDL of this batch was

lower than 5%, the crude was more soluble, fact that facilitated the purification of product [6]. Batch #5 showed higher a TDL (7.23%) and also higher yields (40%). Batches #8 and #9 were performed in a large scale with 800 mg of PGA-COOH as starting product to evaluate the reproducibility of the established conditions. TDL higher than 10% were achieved, low yields were obtained (28 and 35% respectively).

Different batches of a higher amount of starting product were synthesized and pooled in order to achieve the necessary quantity of 5-FU eq drug in PGA-5-FU conjugate to perform all physico-chemical characterization and the *in vitro* and *in vivo* biodistribution and efficacy studies with a unique “single batch”.

Table 4.3 summarizes all batches (#batch) that were pooled and analyzed as a single final batch in terms of TDL, FD and further physic-chemical characterizations and *in vitro* and *in vivo* assays. Prior to the final mixture, the TDL, FD and cytotoxicity of each batch was evaluated (section ). As shown in the table, higher yields were achieved when working in a big large scale, and TDL around 10% were obtained in most of the reactions. The final batch used for the characterization and *in vitro* and *in vivo* validation, corresponds to the **PGA-5-FU pool [6]** and has a TDL of 7.66% and a FD <0.1%.

Table 4.3 Summary of all PGA-5-FU batches pooled for the obtainment of PGA-5-FU-pool. \*PGA-5-FU pool [6] corresponds to the final product used to perform all the *in vitro* and *in vivo* validation experiments.

# Batch	TDL% (mg/mg)	Mass obtained (mg)	Yield%
#8	12.82%	246.9	28%
#9	9.18%	250	35%
#10	10.2%	1203	61%
#11	9.51%	245	55%
#12	5.04%	175	66%
#13	1.92%	153.8	20%
#14	6.27%	509.2	42%
#15	5.68%	808.9	58%
#16	8.70%	586.2	68%
<b>PGA-5-FU pool [6]*</b>	7.66%	4175	-

#### 4.1.1.2 Synthesis of an AF750 labeled PGA-5-FU conjugate

Fluorescent based techniques applied to the diagnosis and detection of diseases or monitorization of certain treatments *in vivo* has become a powerful tool for researchers and clinicians. Labeling the compound with a fluorophore through a stable bond is mandatory to ensure the localization of the studied product through imaging techniques. With the aim to study whole body biodistribution and tumor accumulation of the PGA-5-FU conjugate *in vivo*, product [6] was labeled with a fluorophore dye.

For *in vivo* imaging a fluorophore sensitive to the near infrared is required in order to avoid interferences produced by autofluorescence from tissues. Accordingly, AlexaFluor750®(AF750) was chosen as labeling fluorophore for *in vivo* experiments. Its emission and excitation spectra (Figure 4.11) are in the range of UV until the infrared wavelength. AF750 compounds are considered more photostables, bright and less sensitive to pH than other fluorophores with similar emission and excitation wavelengths.

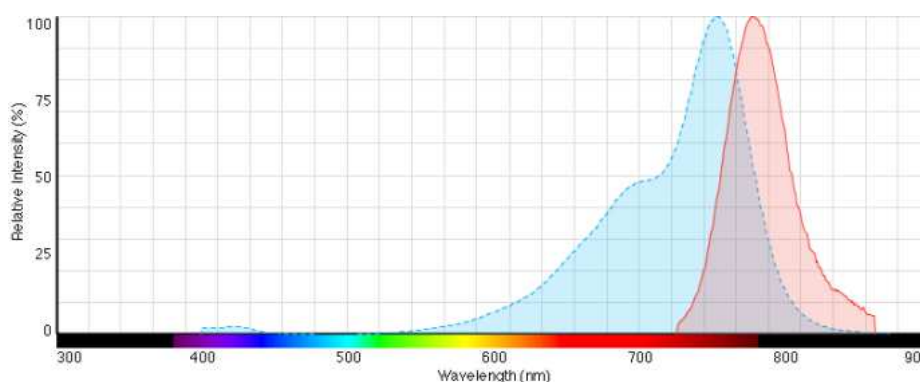


Figure 4. 11 Emission and excitation spectra of AF750.  $\lambda_{ex}$ =749 nm (blue) and  $\lambda_{em}$ = 775 nm (red).

AF750 was purchased from Life Technologies™, in the form of succinimidyl ester. We approached the labeling through the N-terminal free amino group position of the PGA chain. Because a very low amount of dye has to be conjugated in comparison to 5-FU (only 0.1% of the TDL of 5-FU), we expected that this minority free amino groups in the PGA chains should be enough to reach the necessary amount of AF750 required. In addition, as AF750 has an expensive price and a high Mw (~1300 g/mol), it was preferable to conjugate it directly, thus, avoiding the chemical modification to make it reactive with the free carboxylic groups of the PGA chain and also reducing its cost.

Therefore, the linkage of the AF750 dye and the PGA-5-FU-pool [6] was made through an amide bond that also offers the advantage of a higher stability, thus limiting the unspecific release of the dye once administered to the animal.

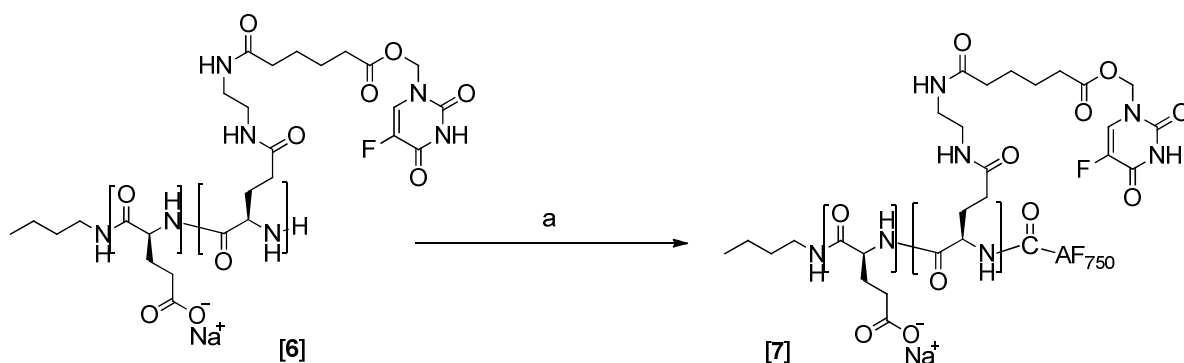


Figure 4. 12 Synthesis scheme of PGA-5FU-AF750 [7]. Conditions: a) AF750 (0.06% (w/w) of 5-FU TDL in product [6]), DMF, ovrn, rt, light protected.

Table 4. 4 Summary of the different reactions performed for the synthesis of PGA-5FU-AF750. BD stands for biodistribution.

# Batch	Product code	Mass obtained (mg)	AF750 $\mu\text{g}$	<i>In vivo</i> experiment
#1	PGA-5FU-AF750-1	410.88	206.6	BD1 in HCT-116
#2	PGA-5FU-AF750-2	426.0	150	BD2 in HT-29

Table 4. 4 summarize the two different syntheses of PGA-5FU-AF750 performed. Each synthetic product was used for a different biodistribution *in vivo* experiment (section 4.1.6.1). Both syntheses were performed following the same methodology and using as a starting product PGA-5-FU-pool [6]. PGA-5-FU-pool [6] was dissolved in DMF and AF750 (0.06% (w/w) of 5-FU) was added. The reaction vessel was protected from light and it was left to react overnight under agitation. Then, DMF was removed under vacuum and the crude was dissolved in 1 mL of water to purify it. Purification was performed by SEC using a PD10 column in water. Fractions of 1 mL were collected and then lyophilized, always light-protected. Then the unreacted AF750 was discarded and the amount of dye conjugated to PGA-5FU-AF750 [7] was quantified.

In order to quantify the amount of AF750 conjugated different techniques were evaluated. The first strategy was carried out by HPLC using a fluorescence detector. Unfortunately, some problems appeared due to the low intensity detected by our fluorescence detector and imprecise results were achieved. Moreover in the HPLC we found out an additional problem; the methodology followed for the 5-FU TDL quantification contains a hydrolysis step with NaOH that was not capable to cleave the amide bond formed between the PGA-5-FU and AF750. For this reason, narrow peaks able to be integrated were not obtained and thus it was not possible to quantify it by HPLC. Since the maximum of emission of this dye is 775 nm, we tried to measure the AF750 content by UV-spectroscopy. A calibration curve of AF750 was performed at  $\lambda=775$  nm. Although product PGA-5FU-AF750 [7] showed, for both syntheses performed, a maximum in its UV spectra at 775 nm, the exact contain of AF750 was not possible to determine. It was due to the lowest limit of detection of the UV-spectrophotometer and the  $\lambda$  selected for the detection is near to the high UV limit of the lamp. Even though this problems, an approximate result (206.6  $\mu\text{g}$  and 150  $\mu\text{g}$ , batch #1 and #2,

respectively) were obtained, and it was possible to monitor both biodistribution experiments using a Xenogen IVIS® Spectrum system, that is a high-quality and low-noise imaging system that allows visualization, monitoring and quantification *in vivo* in real time. Further, this equipment allows *in vitro*, *in vivo* and *ex vivo* images, with both fluorescence and bioluminescence. To proceed, in the FVPR Laboratory (CIBBIM-Nanomedicine, VHIR) they performed an FLI measurement to ensure that the amount of AF750 was enough to monitor the experiment. In both cases the product contained sufficient dye.

Concerning all difficulties found in the quantification of the conjugates dye, it was proposed as an alternative the quantification by means of the Xenogen IVIS® Spectrum system. Thereby, by preparing a calibration curve in a 96-well plate it would be possible to quantify the AF750 content in a solution at a known concentration of product [7] in PBS. However, with our product this alternative was not used.

#### 4.1.1.3 Synthesis of a carboxyfluoresceine labeled PGA-5-FU conjugate

For cell internalization studies *in vitro* in the different cell lines studied it was necessary also to label the PGA-5-FU conjugate. For this purpose the typical dyes used are fluoresceine derivatives that have the emission wavelength at 521 nm and the excitation wavelength at 494 nm. In concrete, 6-carboxyfluoresceine (CF) was select as the appropriate dye for the *in vitro* studies.

Whereas the dye was different, the synthetic strategy was the same: the conjugation of the dye to the N-terminal free amino group of the PGA chains.

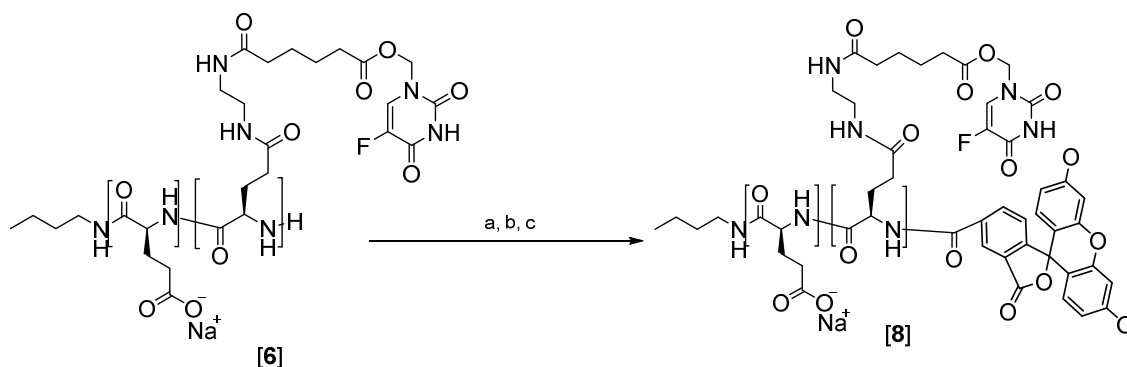


Figure 4. 13 Synthesis scheme of PGA-5FU-CF [8] obtainment. Conditions: a) DIC (1.5 eq) 5min; b) HOBt (1.5 eq), 10 min; c) 6-Carboxyfluoresceine (1 eq), ovrn, rt.

The synthesis of product [8] was performed using as a starting product PGA-5-FU-pool [6]. PGA-5-FU-pool [6] was dissolved in DMF and then DIC and HOBt were added and the mixture was left to react for 10 min. Then, 6-carboxyfluoreceine was added, the reaction vessel was protected from light and stirred overnight. Then, DMF was removed under vacuum and the crude was dissolved in 1 mL of water to purify it. Purification was performed by SEC using a PD10 column in water. Fractions of 1 mL were collected and then lyophilized, always light-protected. Then the unreacted CF was discarded and the amount of dye conjugated to product [8] was quantified (7.5 mg obtained).



This quantification was performed by means of Nanodrop spectrophotometry. A calibration curve in the range of 0 to 0.1 mg/mL was performed ( $\lambda=492$  nm) and the absorbance of a solution of PGA-5FU-CF (24 mg/mL) was analyzed. The CF content was calculated using the calibration curve and it was expressed as a mass average. The amount of CF conjugated to PGA-5FU-CF product [8] was 0.0325%.

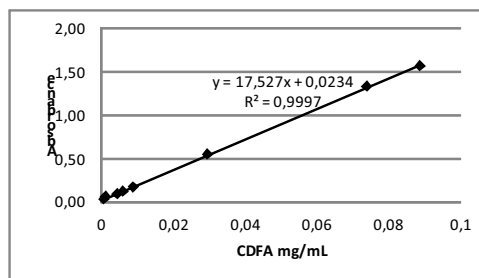


Figure 4. 14 Calibration curve of CF at 492 nm by Nanodrop spectrophotometry.

#### 4.1.2 Physico-chemical characterization of PGA-5-FU conjugates

The particle size of PGA-5-FU-pool conjugate [6], its aggregation in solution in different mediums and the average molecular weight results are shown in this section.

##### 4.1.2.1 Determination of PGA-5-FU size by Dynamic Light Scattering (DLS)

DLS was used to measure the particle size of PGA-5-FU conjugate. DLS measurements were performed in a ZetaSizer Malvern Instrument at 25°C. PGA-5-FU conjugate was dissolved in MilliQ H<sub>2</sub>O (0.1 mg/mL), the solution was filtered through a 0.22  $\mu$ m cellulose membrane before the analysis and the average size of the product was measured. Results corresponding to the micelle size distribution by volume (%) were expressed as the diameter of the nanoparticles (nm). Results were achieved by an n=3 measurement.

The synthesized PGA-5-FU conjugate [6] showed a particle size of 89.23 nm and a polydispersity of 0.267 measured by means of DLS in H<sub>2</sub>O (Figure 4. 15). Therefore, the product adopts a conformation in a water solution that leads to nanoparticles with a size below 100 nm and very narrow peaks.

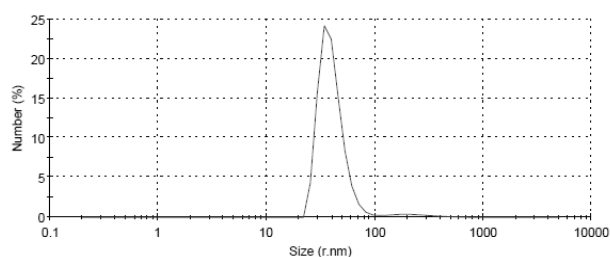


Figure 4. 15 Size distribution by intensity of PGA-5-FU conjugate (measured at 0.1 mg/mL in H<sub>2</sub>O).

Because the product will be administered *in vivo* in a solution of PBS at pH 7.4, it was also studied the particle size in that conditions. Although the study of its size would be more realistic if performed in plasma, the biomolecules that it contains do not allow obtaining clear peaks. To proceed, a solution of PGA-5-FU [6] in PBS was prepared (0.1 mg/mL), also filtered through a 0.22

$\mu\text{m}$  cellulose membrane and then, analyzed by DLS. The synthesized product PGA-5-FU [6] showed a particle size of 85.55 nm and a polydispersity of 0.321 in a solution of PBS (Figure 4. 16). In both mediums, the product showed an average size below 100 nm, but it is in PBS where a higher polydispersity (represented in wider peaks) was found.

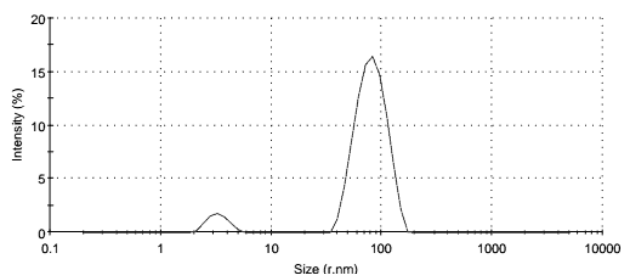


Figure 4. 16 Size distribution by intensity of PGA-5-FU conjugate (measured at 0.1 mg/mL in PBS pH 7.4) .

#### 4.1.2.2 Study of the aggregation of PGA-5-FU conjugate in solution measured by DLS

Conjugating an insoluble drug to a polymeric carrier helps to increase the dosage in intravenous injections. Low maximum solubility values of several drugs, such as 5-FU, can be increased by their conjugation to a water soluble polymer, such as PGA. Once the PGA-5-FU was obtained, the maximum solubility in PBS and water were evaluated.

In order to evaluate the best way for the storage of PGA-5-FU [6] solutions for *in vivo* efficacy experiments, a study of the conjugate aggregation by DLS was designed over a range of concentrations, in a period time of one month. It was decided to study a long period because efficacy trials *in vivo* last for about one month. Moreover, the range of concentrations studied was chosen according to the value of maximum solubility found for two different media: PBS at pH 7.4 (in which the samples will be injected) and H<sub>2</sub>O. It was decided to study also the aggregation in water to confirm if salts present in PBS buffer could induce faster aggregation. The range of concentrations tested contained the concentration corresponding to the maximum solubility of the conjugate, dilutions of it and a higher concentration in order to confirm the presence of aggregates in suspensions of PGA-5-FU conjugate [6].

During this period of time, solutions were stored at 4°C and before the measurement they were shaken in a vortex. For each concentration 3 different samples were prepared. The time measurement points correspond to: 0 min and 3, 24, 72, 168, 240 and 640 h.

Calculation of the maximum solubility was performed by weighting 1 mg of the product and sequentially adding volumes of 20  $\mu\text{L}$  to the medium studied (PBS or H<sub>2</sub>O). After each addition, centrifugation at 1350 rpm was performed and it was finalized when no solid was observed in the transparent solution. It was found that PGA-5-FU [6] in H<sub>2</sub>O showed a maximum solubility of 174.3 mg/mL and 105.21 mg/mL in PBS.

The concentration range studied in the aggregation study was from 4.7 mg/mL to 200 mg/mL in H<sub>2</sub>O and from 7.4 mg/mL to 150 mg/mL in PBS. The average particle size used for this representation corresponded to the peak with a higher intensity. In some cases bi- or trimodal profiles were observed.

Figure 4. 17 (A and B) shows the profile of the aggregation in H<sub>2</sub>O and PBS respectively of product [6] over time. In both cases it was found that at concentrations higher than the maximum solubility the synthetic nanoconjugate aggregate and larger particle sizes (up to 250 nm) were generated. Also, it was seen that the average particle size during all measurements, except the last one at 640 h, showed a quite stable evolution around 100 nm from 37.5 mg/mL solutions onwards. Because aggregates appeared almost one month later when the solution was kept at 4°C between measurements, it was decided to prepare PGA-5-FU solutions for *in vivo* experiments at the concentration corresponding to the maximum solubility in PBS and keep them in the freezer to ensure its stability and avoid aggregates.

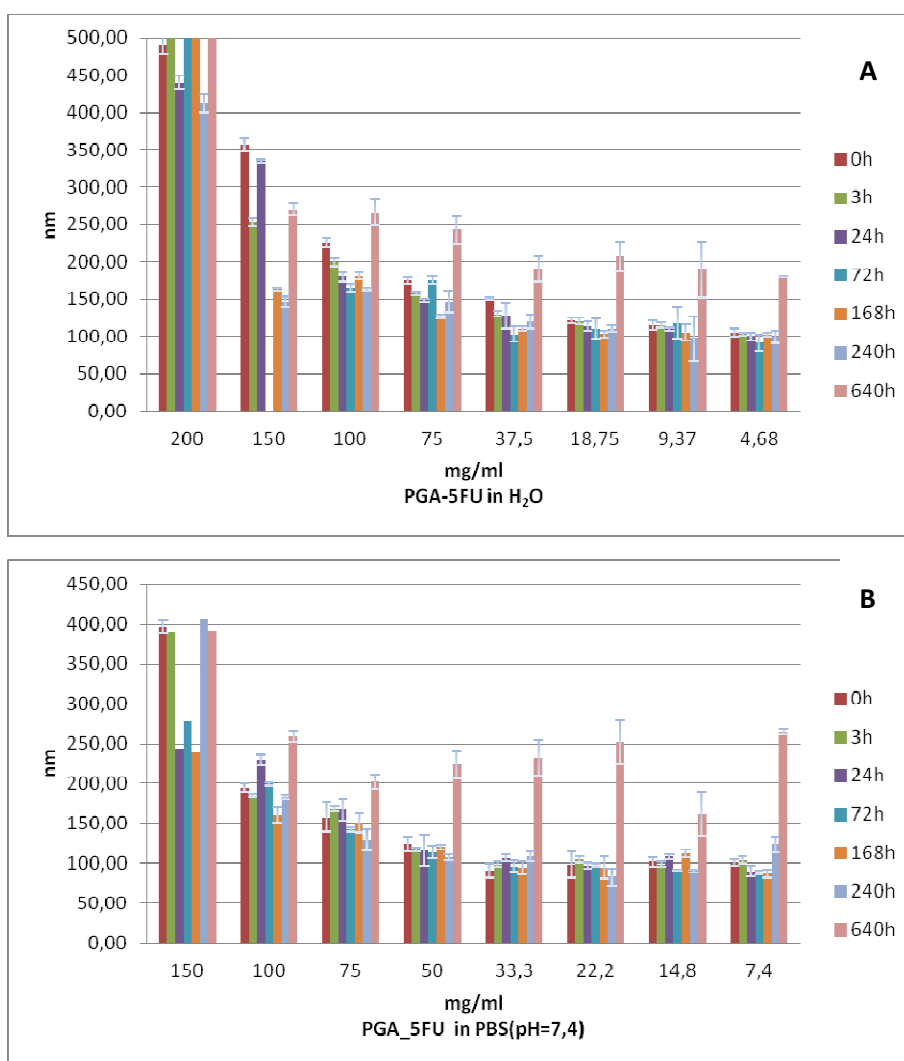


Figure 4. 17 Representation of the aggregation study of PGA-5-FU by DLS in two different mediums, A: H<sub>2</sub>O and B: PBS.

Figure 4. 18 shows an example of the general behavior the results obtained for a PGA-5-FU solution (50 mg/mL in PBS) in the different measurements. Overtime width peak increases as well as the outcome of other particle size populations. Average particle size (of the peak of highest intensity in the graphics in Figure 4. 18) showed a double increase: initially it had a value around 90 nm and at the end of the experiment the particle size was in the range of 200 nm (Table 4. 5). For solutions with a higher concentration this behavior was abrupt.

Table 4. 5 Summary of the average particle size and its Pdl at each measured time (in PBS).

Time / h	Size / nm (Pdl)	Time / h	Size / nm (Pdl)
0 h	91.21 (0.21)	168 h	117.85 (0.45)
3 h	91.89 (0.59)	240 h	127.33 (0.63)
24 h	97.40 (0.65)	640 h	223.41 (0.91)

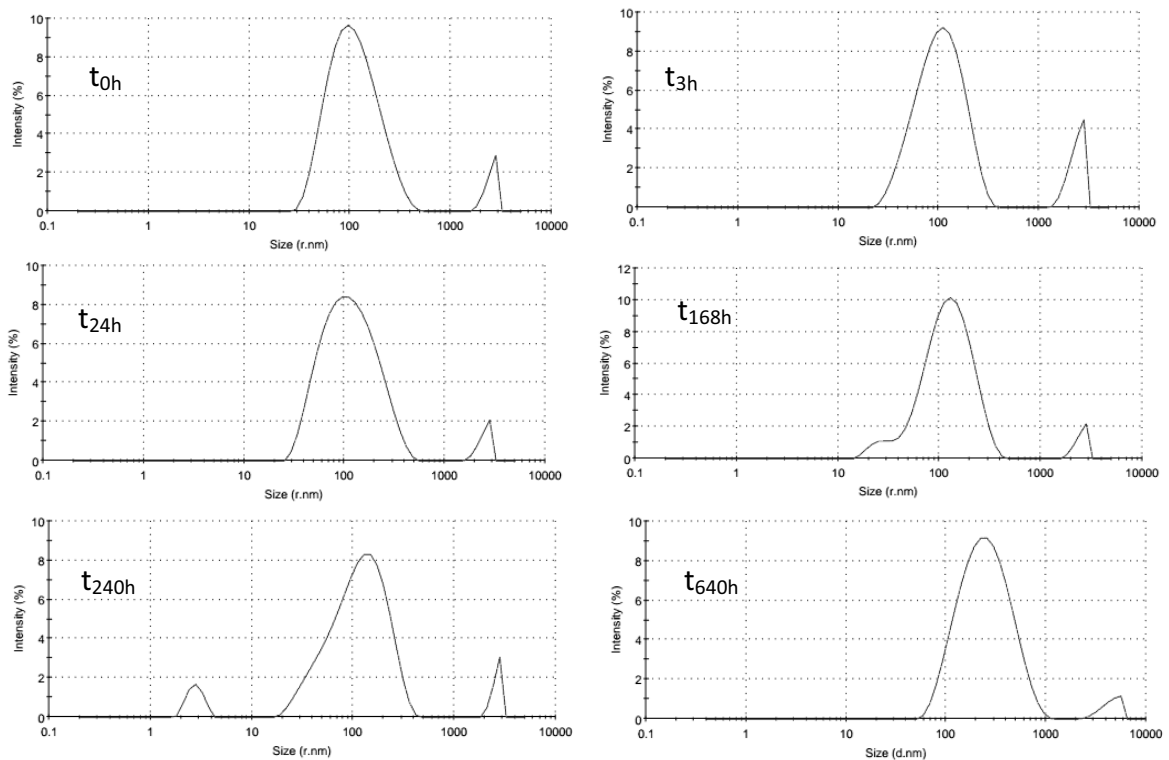


Figure 4. 18 DLS traces of a PGA-5-FU solution over the time (50 mg/mL in PBS).

#### 4.1.2.3 Determination of the Molecular Weight and the Polydispersity Index of PGA-5-FU conjugate by SEC-MALS-IR

Using a Size Exclusion Chromatography (SEC) system connected to a Multiangle light Scattering (MALS) and a Refractive Index (RI) detectors it is possible to obtain information about the size and the Mw of a particle or macromolecule by comparing the light that interacts with it by light scattered as a result of this interaction.

The analysis of PGA-5-FU nanoconjugate [6] by SEC-MALS-RI was performed using as an elution system of NaHCO<sub>3</sub> 50 mM buffer (isocratic flow 0.7 mL/min) in a SEC column (Symmetry 4.6 x250 mm, 5 μm from WATERS), a MALS detector recorded the amount of light scattered at different angles. Next, a second detector (RI) allows estimating sample concentration. Thus it was possible to measure the average molecular weight (Mw) and the polydispersity (PI) of the polymeric samples.

It was carried out also the analysis of both commercial PGA used as starting products for the reactions (from Sigma and PPS, S.L). The analysis of the PGA from Sigma Aldrich (5 mg/mL) showed a Mw = 70.9 kDa and polydispersity of 3.43. Mw result is so far from the one gave by Sigma-Aldrich (15 -50 kDa). Figure 4. 19 shows the superposition of MALS (red line) and RI (green line) traces. MALS trace indicates that there is not a unique population because between minutes 7 to 18 a superposition of peaks is showed. It is observed a high percentage at the beginning, thus increasing the Mw value. Once it was analyzed by SEC-MALS-IR and seeing the low reproducibility in synthesis carried out with this PGA, it was confirmed the need of a better PGA in term of polydispersity and lower Mw.

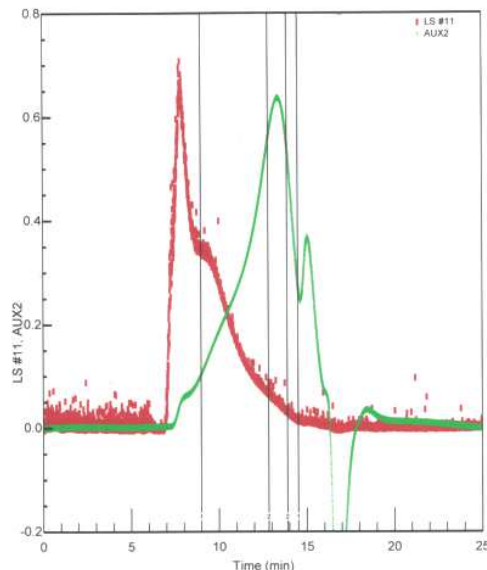


Figure 4. 19 Light Scattering and Refraction index traces of PGA-COONa from Sigma-Aldrich. (MALS (red line) and RI (green line) chromatograms).

As mentioned, PGA from PPS, S.L. showed better reproducibility in the reactions developed with higher yields and higher TDL of 5-FU in the nanoconjugates obtained. The Mw found for this PGA was Mw= 13.2 kDa and a PI= 1.3. These results are really similar to those gave by the commercial source (Mw= 15.2 kDa and a PI= 1.18).

PGA-5-FU product [6] was analyzed by SEC-MALS-RI (10 mg/mL) and the Mw found was Mw= 15.2 kDa and a PI= 1.49. Figure 4. 20 represents the superposition of MALS and IR traces for PGA-COOH (from PPS, S.L, red color) and PGA-5-FU (product [6], blue color). An increase on the retention time of PGA-5-FU ( $t_{rPGA-COOH}=11 - 13.4$  min and  $t_{rPGA-5-FU}=10 - 14.2$  min) is observed suggesting a slightly increase on its size, what is confirmed with the Mw and PI obtained. Dotted lines in Figure 4. 20 represent the diminution of the molar mass through the time because in SEC molecules with higher size exit first than the small ones. Although it is obtained a double population in PGA-5-FU nanoconjugates the PI obtained is similar to PGA-COOH.

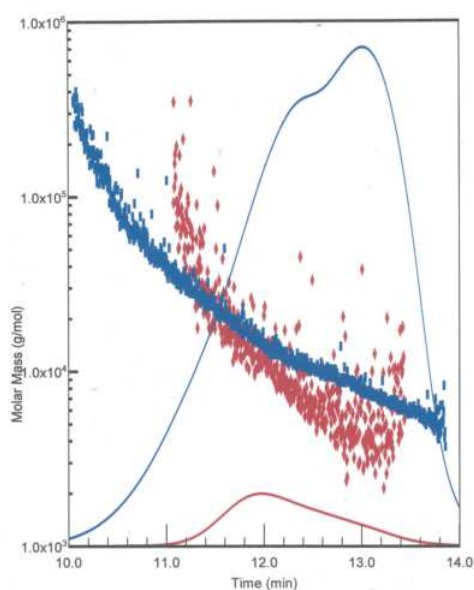


Figure 4. 20 Representation of Mw vs. time of PGA-COONa (red) from PPS and PGA-5-FU (blue).

#### 4.1.2.4 Stability studies *in vitro* of PGA-5-FU conjugate

PGA-5-FU-pool [6] was fully characterized in terms of stability and degradability *in vitro* before *in vitro* and *in vivo* validation studies. Even though several variables appears *in vivo*, and also in cell medium, mimicking some specific conditions (such as different pHs or plasma environment) gives us powerful information to understand the behavior of the synthesized product once inside the body. So, it would be possible to hypothesize if the polymer-drug conjugate would be stable while transport through the blood stream, if the polymer conformation would protect the ester bond between the drug and the linker, as well as the behavior of the PGA-5-FU in different pHs. All this information would let us know the unspecific release of the drug while transport and also the stability of product [6].

In particular, the variables studied are **plasma**, **different pHs** and **Cathepsin B**. Regarding plasma stability studies, PGA-5-FU-pool nanoconjugate [6] was incubated in mice plasma (from animals of the FVPR Laboratory (CIBBIM-Nanomedicine, VHIR)) as well as in human plasma (from Sigma-Aldrich) (10 mg/mL). In the case of pH dependant degradation studies, product [6] (10 mg/mL) was

incubated at three different pHs: 5.5, 6.5 and 7.4. The highest value was evaluated to mimic the pH in which the conjugate will be once injected through the i.v. administration route. It is well known that tumors have a lower pH than healthy tissues and that the vesicles generated in the endocytic pathway have also an acid pH<sup>127</sup>. For this reason, it is a relevant information the degradation and stability of the conjugate at low pH. Moreover, because it is expected internalization through the endocytic pathway, the degradation of the nanoconjugate PGA-5-FU [6] (10 mg/mL) by Cathepsin B present in lysosomes (5  $\mu$ L, 10 units/mL using PBS 7.4 buffer) will be studied, because it is well known that this enzyme is responsible for the PGA degradation<sup>128</sup>.

All experiments were performed according to the methodology described in section 3.6 and the amount of 5-FU released in the specific conditions were quantified by RP-HPLC at 254 nm using a C18 column. Integrated peaks of 5-FU detected were interpolated in a calibration curve of standard 5-FU. Experiments were performed at 37°C in triplicate and Resorcinol was used as an internal standard.

Figure 4. 21 shows the degradation curves of PGA-5-FU over the time in the different mediums studied.

- In **plasma** experiments it was observed a similar behavior between human and mice plasma, nevertheless in mice plasma PGA-5-FU [6] showed a slightly higher unspecific release of 5-FU. It was also observed that the 5-FU kinetic release from the PGA-5-FU nanoconjugate in mice plasma was very fast during the first 30 min of study and then, it reached a plateau of around 8% of 5-FU released. In the release curve corresponding to human plasma the plateau was slightly lower (6%). Therefore, it is confirmed a high plasma stability of the nanoconjugate [6]. This positive result led us to confirm that the conformational structure that the nanoconjugate will adopt in solution protects the ester bond between the drug and the carrier, what is a very important issue due to the high lability of ester bonds in the presence of plasma esterases. Moreover, since 5-FU has a very short half-life (10 -20 min) in plasma circulation, a prolonged half-life of PGA-5-FU is positive for the treatment.
- In experiments at different **pHs** it was also observed a low dependant release of 5-FU from product [6] over time. A very low difference was seen when comparing the curves obtained for the different pH studied, however a higher release at pH 7.4 was observed. This is related also with the nature of the linkage between 5-FU and the polymeric chain: ester bonds are more labile to basic pH than acidic environments. Nevertheless, the amount of drug released (less than 5%) at neutral pH was lower than in plasma. As it is known that tumors and cell compartment in the endocytosis internalization have an acidic pH, with this data we confirm that a very low released of 5-FU will be produced exclusively by the low pH. For this reason, we hypothesize that other enzymes inside the cell will produce the major release of the drug once internalized.

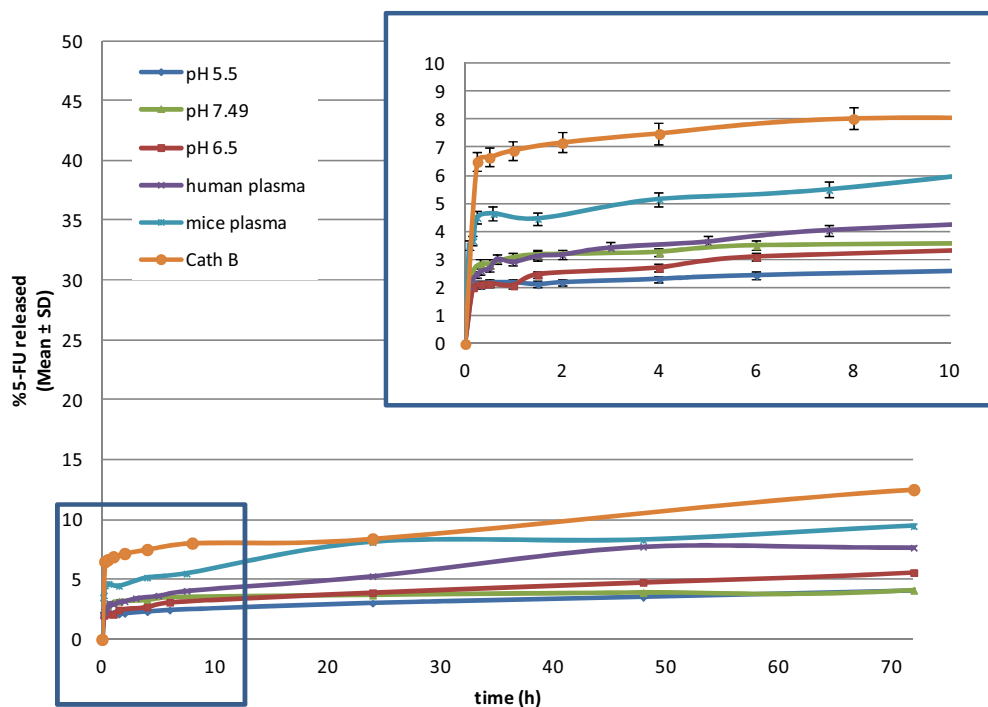


Figure 4.21 Degradation curves of PGA-5-FU over the time in different incubation mediums. The blue box corresponds to an enlargement area of the first 10 h of the experiments.

- In **Cathepsin B** experiment it was observed higher release than in plasma, but it was not very pronounced. Around 10% of 5-FU release was achieved from the first 24 h and the maximum result observed does not exceed 15%. It was expected that nanoconjugates based on PGA experiments showed degradation of the polymeric chains by Cathepsin B. In this experiment 5-FU released was measured, confirming the low 5-FU dependant release by Cathepsin B. With this data obtained it could be said that the degradation of the polymer by this enzyme has a lower kinetic profile. As mentioned, the experiment was performed in PBS, therefore if the degradation of the polymer was higher, smaller moieties of the polymeric chain would be released faster and thus, the ester bond would remain more accessible than in the experiment at pH 7.4 and the release of the drug would be higher. It can be confirmed that the nanoconjugate is biodegradable but the process is not fast.



### 4.1.3 *In vitro* cytotoxicity assays in HT-29 and HCT-116 colorectal cancer cell lines

*In vitro* efficacy studies were conducted at FVPR Laboratory (CIBBIM-Nanomedicine, VHIR) and were analyzed by Helena Plà under the supervision of Dr. Ibane Abasolo.

The evaluation of the cytotoxicity of the different PGA-5-FU batches was performed using the standard MTT assay in HT-29.Fluc.C4 and HCT-116.Fluc2.C9 cells.

Table 4.6 summarizes the IC<sub>50</sub> values of the different PGA-5-FU batches in both CRC cell lines as well as the values of free drug (5-FU) and PGA-5-FU-pool [6]. Initially, MTT evaluation was performed for all PGA-5-FU batches, but once we found that the efficacy was similar in all batches, MTT assay was only conducted with the product PGA-5-FU[6] batches (#8 to #16) that were pooled together.

In general, PDC showed lower cytotoxicities (higher IC<sub>50</sub> values) than 5-FU in both CRC lines studied. IC<sub>50</sub> of free 5-FU was 4.88 μM in HCT-116 and 14.21 μM in HT-29, while PGA-5-FU-pool [6] values were 82.25 and 33.38 μM for these cell lines. This can be explained due to the macromolecular conformation of the new polymeric drug, that can contribute to the slower release of 5-FU. In addition, the endocytosis process of polymer-drug conjugates is much slower than the diffusion of free drug through cellular membrane<sup>129</sup>. Interestingly, cytotoxicity of PGA-5-FU conjugates did not only depend on the conformational structure of the monomer, but also on 5-FU content, being slightly different when loadings below 5% are compared with those above. Hence, with higher the TDLs, higher IC<sub>50</sub> values are achieved.

Between both cell lines, IC<sub>50</sub> values of 5-FU of all PGA-5-FU tested were higher in HT-29 than in HCT-116 cell line. Therefore, HCT-116 cell line resulted more sensitive to 5-FU and PGA-5-FU treatment. Encouragingly, PGA-5-FU-pool [6] showed a similar IC<sub>50</sub> as those single batches used for its obtainment. Figure 4. 22 represents the cytotoxicity curves of PGA-5-FU-pool and 5-FU in both cell lines studied.

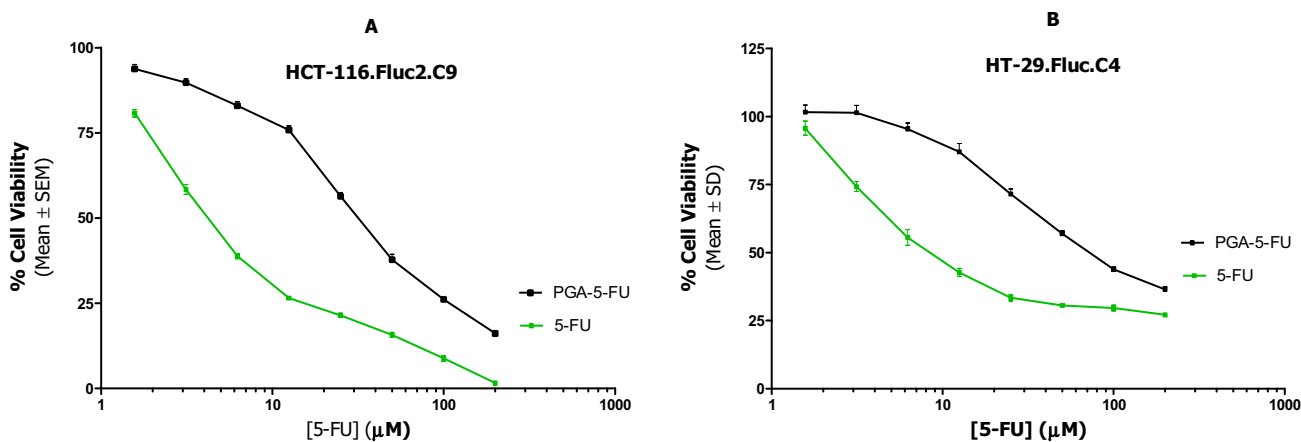


Figure 4. 22 Cytotoxicity of PGA-5-FU measured by MTT assay after 72 h incubation. (A) HCT.166.Fluc2.C9 cells (B):HT-29.Fluc.C4 cells.

Table 4. 6 Summary of all PGA-5-FU products synthesized showing the  $IC_{50}$  values in both CRC studied. Results are expressed as Mean  $\pm$  SD.

# Batch	TDL (%)	$IC_{50}$ $\mu$ M HT-29. Fluc.C4	$IC_{50}$ $\mu$ M HCT-116. Fluc2.C9
#1	1.6	-	-
#2	7.63	128.62 $\pm$ 0.02	34.58 $\pm$ 0.01
#3	10.2	108.73 $\pm$ 0.02	88.95 $\pm$ 0.01
#4	3.29	22.42 $\pm$ 0.03	10.65 $\pm$ 0.01
#5	7.23	29.33 $\pm$ 0.01	23.61 $\pm$ 0.01
#6	11.89	292.79 $\pm$ 0.02	157.81 $\pm$ 0.02
#7	<b>9.06</b>	24.23 $\pm$ 0.01	12.02 $\pm$ 0.01
#8	<b>11.82</b>	134.17 $\pm$ 0.02	32.31 $\pm$ 0.02
#9	<b>9.8</b>	105.96 $\pm$ 0.01	23.10 $\pm$ 0.01
#10	<b>10.2</b>	106.96 $\pm$ 0.03	33.21 $\pm$ 0.05
#11	<b>9.51</b>	-	-
#12	<b>5.04</b>	-	-
#13	1.92	-	-
#14	6.27	-	-
#15	5.68	45.69 $\pm$ 0.01	19.48 $\pm$ 0.01
#16	8.70	-	-
<i>PGA-5-FU-pool</i>	7.66	82.25 $\pm$ 0.02	33.38 $\pm$ 0.01
<b>5-FU</b>		14.21 $\pm$ 0.04	4.88 $\pm$ 0.01

#### 4.1.4 Cell internalization studies of PGA-5FU-CF conjugate

Cell internalization studies were carried out at the FVPR Laboratory (CIBBIM-Nanomedicine, VHIR) under the supervision of Dr. Ibane Abasolo.

As complementary *in vitro* studies, cell internalization experiments were carried out with product [8] also in HCT-116 and HT-29 cell lines. The lysosomal co-localization of the compound was studied by confocal microscopy and the quantification of the internalization was carried out by flow cytometry.

#### 4.1.4.1 Confocal fluorescence microscopy studies of PGA-5FU-CF

Confocal microscopy allows the analysis of samples at different wavelengths. Thus, when analyzing plates containing treated cells, it is possible to distinguish cell nuclei, which has been previously stained with DAPI (blue color), lysosomes previously marked with LysoTracker red DND-99 (red color), and product [8] labeled with the fluorophore CF (green color). By overlaying these images, it is possible to identify the lysosomal co-localization (yellow color) produced when the product [8] internalizes.

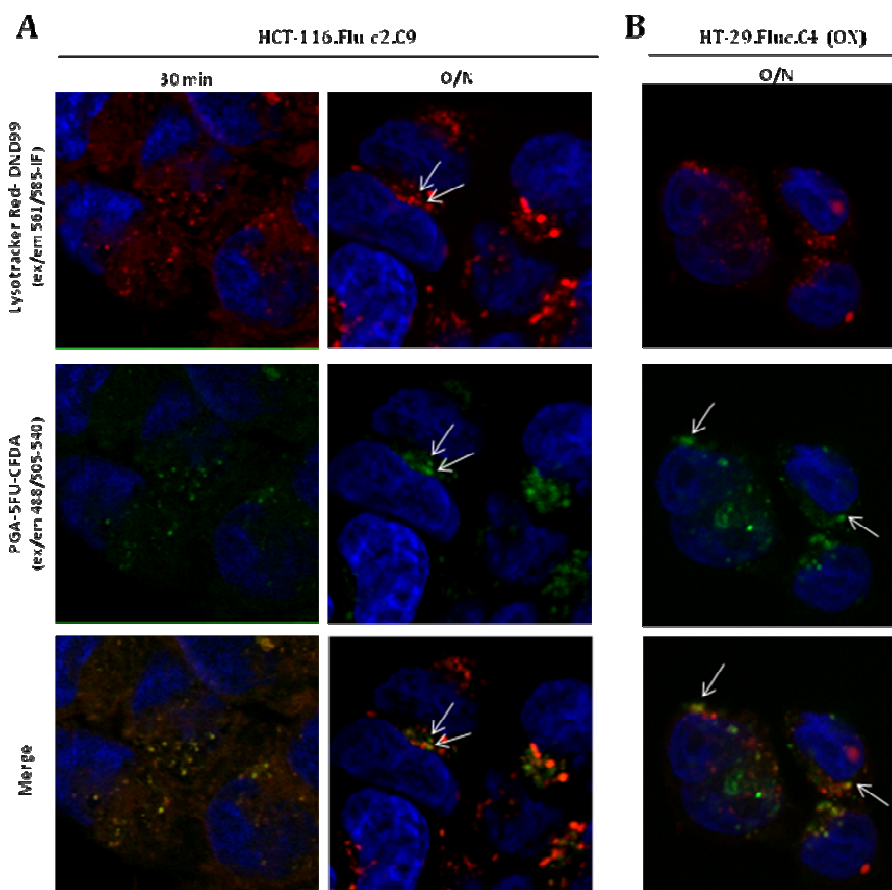


Figure 4. 23 Confocal microscopy images taken from live HCT-116.Fluc2.C9 and HT-29.Fluc.C4 cells. (A) HCT-116.Fluc2.C9 cells at 100 mM 5-FU eq of product [8] after 30 min and overnight incubation (B) HT-29.Fluc.C4 cells at 100 mM 5-FU eq of product [8] after overnight incubation. LysoTracker-Red was employed as lysosomal marker (in red, first line) and the polymer-drug conjugate was labelled with CF (in green, second line). Co-localization is seen in yellow (third line).

Experiments were performed at different incubation times (30, 120 min and overnight) with PGA-5FU-CF [8] (100  $\mu$ M eq of 5-FU) and LysoTracker red (5  $\mu$ M). Figure 4. 23 shows microscope confocal images after 30 min and overnight incubation. In both cell lines, HCT-116 and HT-29, the product [8] was localized within the lysosomal compartment, with no clear difference between them. In both cell lines, greater internalization was seen by increasing the incubation time.

#### 4.1.4.2 Flow cytometry studies of PGA-5FU-CF

Cell-uptake experiments of product [8] were performed by flow cytometry in HT-29.Fluc.C4 and HCT-116.Fluc2.C9 CRC cell lines by comparing the efficiency of internalization at different times by flow cytometry.

A range of concentrations of product [8] were tested (0.25, 1.75, 2.5 mg eq 5-FU/mL) at 2 h incubation, in order to observe the degree of internalization of the product in both cell lines. As shown in Figure 4. 24, at concentrations above 1.75 mg eq 5-FU/mL a 90 -100% internalization was reached in both cell lines, indicating that at high concentrations of product [8] internalization increased in the same way in both cell lines. As expected, internalization was dose dependent. However, when the concentration of study was 0.25 mg eq 5-FU/mL a large difference in internalization between both cell lines was observed, 20% in HT-29.Fluc-C4 and about 40% in HCT-116.Fluc2-C9. For this reason 0.25 mg/mL was chosen as the concentration for subsequent internalization assay.

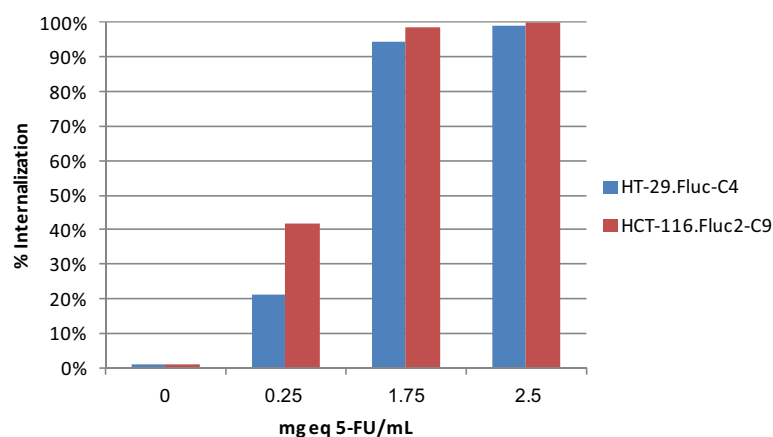


Figure 4. 24 Internalization quantification at different concentrations of PGA-5FU-CF in HT-29.Fluc.C4 and HCT-116.Fluc2.C9 cell lines. % internalization refers to the average of positive cells (fluorescent) in a fluid stream measured by flow cytometry.

Further, cell-uptake experiments of PGA-5FU-CF (0.25 mg eq 5-FU/mL) were performed in both CRC cell lines at different times: 2, 5, 10, 20, 40, 60, 120 min and overnight. As shown in Figure 4.24, PGA-5FU-CF product [8] showed cell-uptake in both CRC studied. However, a clear difference between HCT-116 and HT-29 cell lines was observed. In the former one, product [8] internalized faster. After 30 min incubation, 50% of HCT-116 cells showed positive CF signal, while for the HT-29 CRC cell line, only the 15% of cells had CF after 2 h. Thereby, cell-uptake properties are directly related to the cell line tested.

Regarding the cytotoxicity studies of product PGA-5-FU [6] (section 4.1.3), it was found that the IC<sub>50</sub> ratio between product [6] and free drug 5-FU was lower in HCT-116 cell line than in HT-29. This could have direct relationship with a more rapid internalization of product [8] in HCT-116 cells. However, it is important to note that the MTT assays were done at 72 h, whereas the internalization studies were performed after 2 h of incubation.

It was also assessed if differences in the amount of product [8] internalized in both CRC cell line were observed. Figure 4.25 shows the total mean intensity (level of fluorescence) over time for

both cell lines. It was confirmed that besides product [8] was internalized more rapidly in HCT-116 cells, higher amounts of the product were also internalized in this CRC cell line.

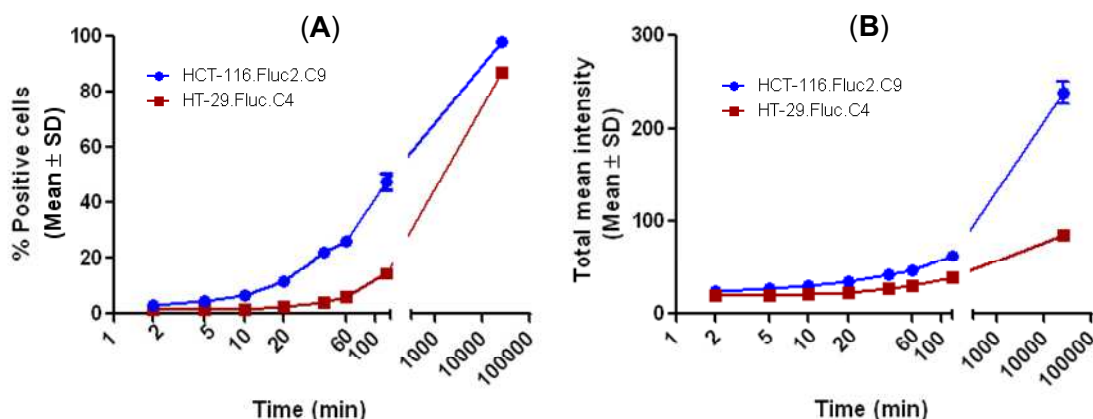


Figure 4.25 Representation of internalization of PGA-5FU-CF product [8] in HCT-116.Fluc2.C9 and HT-29.Fluc.C4 cell lines, only measuring positive cells (A) and the total mean intensity (B).

#### 4.1.5 5-FU quantification in tissue and plasma: HPLC method development and validation

A sensitive method for 5-FU quantification in plasma and tissues from the *in vivo* experiments (section 0) was needed in order to (i) evaluate the benefit of 5-FU conjugation to a macromolecular polymer and (ii) correlate the FLI measurements with real drug concentration values.

Several publications describe 5-FU quantification mostly in plasma but also in tissues by different techniques such as HPLC-MS<sup>130,131,132</sup>, HPLC-MS/MS<sup>133</sup>, HPLC-UV<sup>134,135,136</sup>. In our case, it was chosen to combine HPLC with a UV detector set at 254 nm because all 5-FU quantifications performed previously (FD and TDL measurements) were done with this equipment.

Besides homogenization, biological samples injected in HPLC equipment require a pre-treatment process to remove interferences of unwanted biological metabolites that produce dirty chromatograms or HPLC contaminations, low selectivity of 5-FU peaks, and reduce the lifetime of the columns. Accordingly, the final validated method had three consecutive steps: (i) homogenization of tissues; (ii) pre-treatment of tissue homogenates to remove interferences and (iii) HPLC analysis.

##### 4.1.5.1 Method validation: Tissue homogenization

**Tissue homogenization** was performed using the FastPrep 24 (MP Biomedicals) as described in section 3.7. Tissue homogenates were first treated in acid conditions (HCl 0.1 M) and secondly, the solid residue was treated in a basic digestion (NaOH 0.02 M). In both cases, a next step was added to precipitate proteins with trichloroacetic acid (TCA 5%).

#### 4.1.5.2 Method Validation: Pre-treatment of tissue homogenates

The **pre-treatment of the tissue homogenates** was studied through different methods once all tissues were homogenized a part from the protein precipitation by TCA<sup>137,134</sup>.

Two different approaches were tested, one based on liquid-liquid extractions<sup>137</sup> and the other on liquid-solid extraction<sup>138</sup>. However, 5-FU could not be extracted from tissue homogenates. Having the need to remove biological interferences from homogenates before HPLC injection, a mechanical technique was also tested. Wang *et al*<sup>134</sup> described a simple and rapid method for 5-FU quantification from tissues by HPLC including an ultrafiltration process (10 K cutoff membrane) to remove interferences. To evaluate the recovery of the ultracentrifugation process, 100 µL of 5-FU (0.1 mg/mL in PBS) were added to tissue homogenates and plasma from a control animal. Then, Amicon Ultra centrifugal filter units (4 mL) of 3 K and 10 K from Merck Millipore were compared for each group of samples (40 min x 2, 4000 rpm). Collected samples were analyzed by HPLC and the recovery was calculated by comparison of the 5-FU peak areas and the theoretical content. In both cases, 3 K and 10 K, the recovery was > 90%. The selectivity of 5-FU peaks increased considerably. Finally, it was selected an Amicon Ultra 4 centrifugal tube with a 3 K cutoff membrane for the ultracentrifugation of plasma and tissue homogenates. Thus, the interference peaks surrounding 5-FU peak disappeared and the selectivity of 5-FU peaks increased considerably.

#### 4.1.5.3 Method Validation: HPLC

**HPLC method validation** was performed once the tissue homogenization and the pre-treatment process were established. The following validation parameters were set up: selectivity, linearity, limit of detection (LOD), limit of quantification (LOQ) and recovery.

- **Sample Preparation:**
  - **Stock solution of 5-FU** was prepared dissolving an accurately weighed amount in PBS to achieve a theoretical concentration of 1000 µg/mL.
  - **Stock solution of Resorcinol (Internal Standard)** was prepared by dissolving an accurately weighed amount in H<sub>2</sub>O to achieve a theoretical concentration of 1000 µg/mL.

- **Chromatographic conditions:**

HPLC separation of tissue homogenates was done with a C-18 reverse phase column (XSelect HSS T3 3.5 mm, 4.6 x 250 mm, Waters). A guard column packed with the same material was used to protect the column. 5-FU and Resorcinol (internal standard) were detected at 254 nm wavelength. The elution system was A: H<sub>2</sub>O and B: MeOH. Flow rate was 0.6 mL/min and the gradient was: 100%A from 0 to 30 min, 20%A - 80%B from 30 to 45 min, 20%- 80%B during 5 min, 100%B until 56 min, then it was necessary to equilibrate the column during 25 min with 100%A. The injection volume was 20 µL. Retention times: 5-FU (15 min) and Resorcinol (42 min). Thus it was confirmed the system suitability.

- **Selectivity** was evaluated through the chromatographic analysis of plasma, tumor, liver, spleen, kidney and lung tissue homogenates. It was concluded that neither the matrix effect or degradation products generated peaks in the chromatogram that could interfere with 5-FU.
- The **Limit of Detection** was determined from the peak and standard deviation of the noise level (SN). The LOD corresponds to concentrations of 5-FU that resulted in peak heights three fold higher than Signal Noise (SN) and was 3.25 ng 5-FU/mL.
- The **Limit of Quantification** was determined from the peak and standard deviation of the noise level (SN). The LOQ corresponds to concentrations of 5-FU that resulted in peak heights tenfold higher than SN and was 10.0 ng 5-FU/mL.
- **Linearity** was evaluated through a calibration curve using the peak area of 5-FU dissolved in water and resorcinol as an internal standard. 5-FU concentration range was: 10 ng/mL to 25000 ng/mL ( $y = 71.62x - 594.78$   $R^2=0.9999$ ).
- **Recovery** of 5-FU was calculated by comparing the concentration obtained from extracts of three Quality Control Samples (QC) with the theoretical concentration of 5-FU and resorcinol standard compounds. QC levels representing low, middle and high 5-FU contents (Table 4.7). Recovery was studied for plasma, tumor, liver, kidney, spleen and lung tissues. For each concentration the process was repeated three times and all results were given as Mean  $\pm$  SD.

*Table 4. 7 Summary of the three different concentrations of 5-FU studied.*

	Low (L)	Medium (M)	High (H)
ng 5-FU/mL	8.125	750	7500

A standard solution (SS) containing the analyte and the IS (32.5 5-FU  $\mu$ g/mL, 1.2 mg resorcinol/mL) was used for the addition of QC.

To proceed, tissue was washed with PBS and dried with a filter paper. Then ~200 mg of sample were placed in bead-containing 2 mL homogenizer tubes (lysing matrix D, MP Biomedicals). A known amount of 5-FU and resorcinol were added in three different concentrations: L, M and H (0.5  $\mu$ L, 46  $\mu$ L and 461.5  $\mu$ L of SS, respectively). A volume of 100  $\mu$ L of 0.1M HCl and 900  $\mu$ L of PBS were added to each tube. The tissue was homogenized following the methodology detailed in section 3.7. The supernatant was ultrafiltrate to remove the interference components for quantitative determination of 5-FU in mice plasma and tissue samples using 4 mL ultrafiltration cell with a 3 K cut-off membrane (Merck). The supernatant was placed in the cell and three consecutive centrifugation processes at 4000 rpm at 4°C were carried out. 2 mL of filtrate were obtained, 20  $\mu$ L of it were analyzed by HPLC following the methodology described above and the rest were kept in the refrigerator (-20°C).

In the case of plasma analysis, 5-FU and Resorcinol were added to 200  $\mu$ L of plasma in three different concentrations (QC): L, M and H (0.5  $\mu$ L, 46  $\mu$ L and 461.5  $\mu$ L of SS, respectively).

The solution was reconstituted to 2 mL with PBS. The mixture was ultracentrifugate following the methodology explained for tissue samples.

HPLC analysis showed different recoveries concerning each QC and the different tissues. Table 4.8 summarizes 5-FU recoveries expressed as Mean  $\pm$  SD for all concentration points tested. Since the QC Low represented a theoretical concentration of 8.125 ng 5-FU/mL that is slightly lower than the LOQ (10 ng 5-FU/mL) this QC could not be analyzed. It is necessary to mention that only 0.5  $\mu$ L of the solution SS were added, what correspond to a very small amount of 5-FU (150 ng). Moreover, almost none of the chromatograms showed the 5-FU peak, and if it was observed it was below the LOD. Regarding the QCs Medium and High (Table 4.8 and Figure 4. 26) good recoveries were achieved. All of them higher than 70% except for the lung and spleen in the QC medium.

Table 4. 8 Summary of 5-FU recoveries (%) for each QC concentration in different tissues and plasma expressed as mean  $\pm$  SD.

	QC - Low	QC – Medium	QC - High
<b>Kidney</b>	< LOQ	90.87 $\pm$ 5.30	76.82 $\pm$ 4.64
<b>Tumor</b>	< LOQ	91.19 $\pm$ 12.32	73.15 $\pm$ 3.88
<b>Spleen</b>	< LOQ	32.88 $\pm$ 2.87	82.88 $\pm$ 15.98
<b>Lung</b>	< LOQ	48.83 $\pm$ 1.31	78.51 $\pm$ 12.16
<b>Plasma</b>	< LOQ	75.87 $\pm$ 10.53	84.04 $\pm$ 14.07
<b>Liver</b>	< LOQ	88.97 $\pm$ 15.70	85.36 $\pm$ 6.99

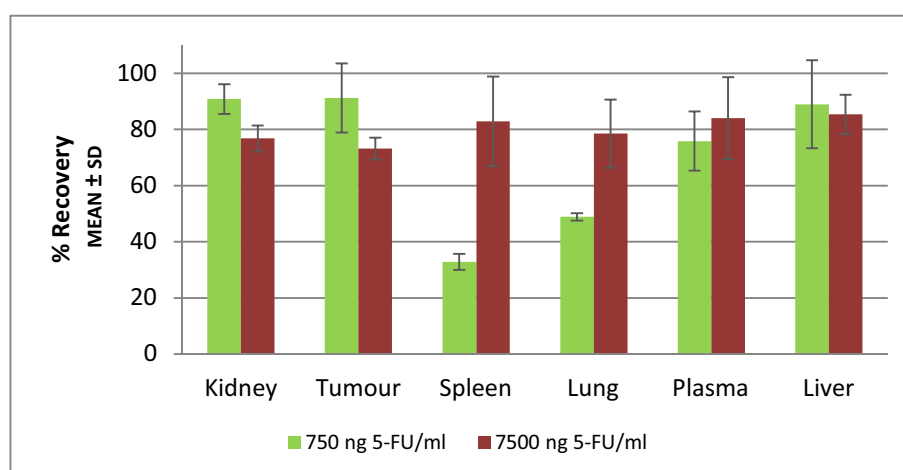


Figure 4. 26 Representation of 5-FU recovery at three QC concentrations.



#### **4.1.6 *In vivo* studies in xenograft mice models**

*In vivo* studies were carried out at the FVPR Laboratory (CIBBIM-Nanomedicine, VHIR) and the animal facilities of the Vall d'Hebron Research Institute under the supervision of Dr. Yolanda Fernández. All experimental procedures were approved by Vall d'Hebron Animal Experimentation Ethical Committee.

##### **4.1.6.1 Tumor-accumulation and whole-body Biodistribution in athymic nude female mice bearing CRC tumors**

To evaluate tumor-accumulation and whole-body biodistribution of PGA-5-FU labeled with fluorophore AF750, two different *in vivo* experiments were carried out in animals bearing subcutaneous (s.c.) tumors grown from HCT-116.Fluc2-C9 or HT-29.Fluc-C4 cells. In both cases, the PGA-5FU-AF750 tumor and whole-body biodistribution were measured by means of *in vivo* and *ex vivo* fluorescence imaging (FLI) using an IVIS® Spectrum equipment at specified times. The monitorization of the FLI *in vivo* using an IVIS® Spectrum is possible by using a fluorophore in the near-infrared (NIR) region, thus, avoiding the interferences caused by the autofluorescence of tissues. The fluorescence signal was quantified in radiant efficiency units. In addition, PGA-5FU-AF750 distribution was studied through the quantification of 5-FU in different tissue homogenates and plasma by means of HPLC following the methodology set up in section 4.1.5.3.

##### **4.1.6.2 Tumor-accumulation and whole-body biodistribution on subcutaneous HCT-116.Fluc2-C9 human CRC tumors growing in athymic nude female mice (BD1)**

Animals (n=6) received a unique i.v. administration dose of PGA-5FU-AF750-1 product [7] (50 mg eq 5-FU/kg in PBS) or 5-FU (50 mg eq 5-FU/kg), respectively. It is important to note that the administration of equivalent doses of 5-FU allows the comparison of results obtained between the animals injected with the nanoconjugate and those injected only with 5-FU.

It was well-tolerated and adverse side-effects were not observed up to 48 h post-administration. At the end of treatment, treated to control (T/C) values of body weight were 10% and 8% for the PGA-5FU-AF750-1 and 5-FU treated-groups, respectively. These indicate that PGA-5-FU-AF750-1 and 5-FU did not induce acute weight loss.

In the BD1 experiment, *in vivo* FLI measurements were performed at 4, 9, 24 and 48 h, and *ex vivo* FLI and 5-FU HPLC quantification were done to plasma, tumor, liver, kidney and lung of animals sacrificed at 4 and 48 h.

Two animals without tumor were also included as control animals. Differences between these animals and those bearing tumors are expected regarding the biodistribution of the injected polymeric nanoconjugate product.

#### 4.1.6.2.1 *In vivo* FLI (BD1)

In BD1 experiment the AF750 tumor-accumulation was monitored and quantified at 1, 4, 9, 24 and 48 h post-administration. *In vivo* FLI showed that the PGA-5FU-AF750-1 tumor-accumulation was maximal at 4 h post-administration, decreased very rapidly within the first 24 h, and then it was maintained low for up to 48 h. Interestingly, *in vivo* tumor-accumulation kinetic images (Figure 4. 27) show a clear localization of product [7] in the whole animal, detecting a higher fluorescence in tumors.

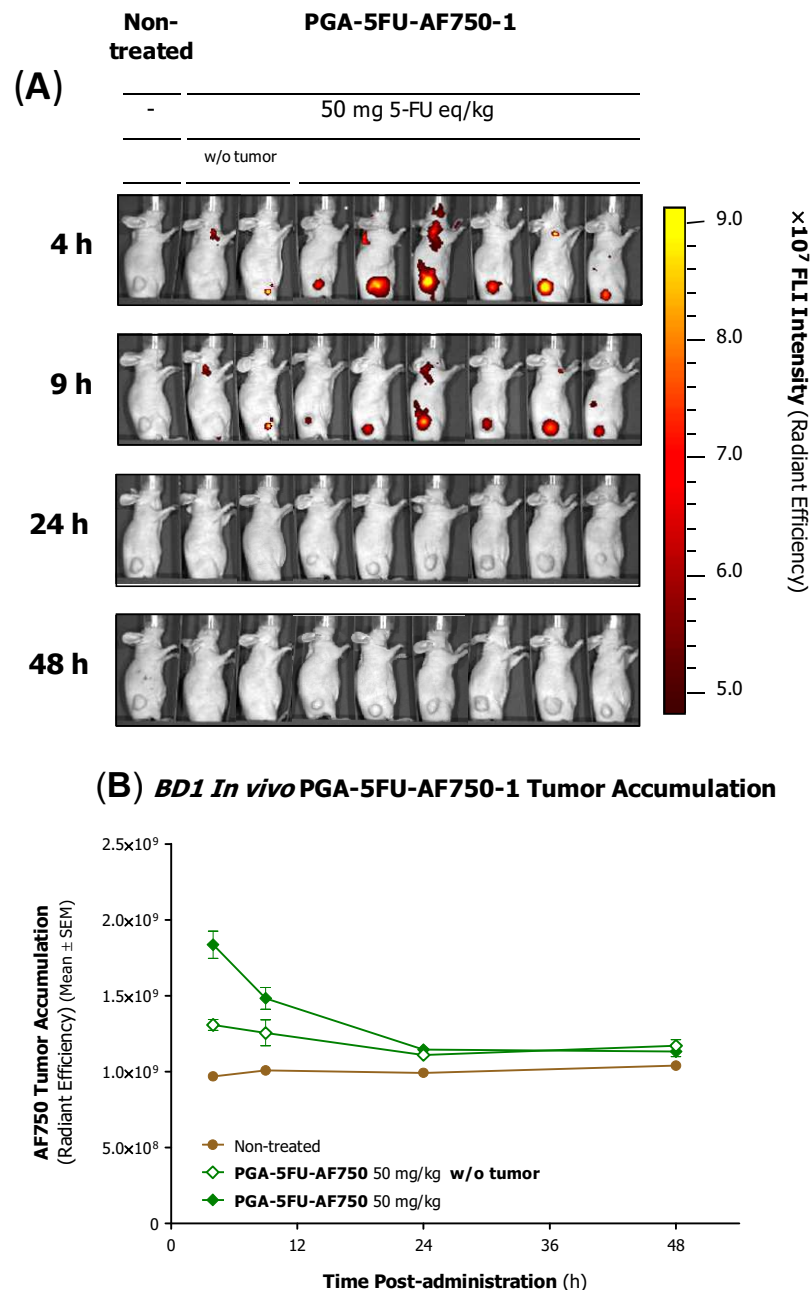


Figure 4. 27 Non-invasive monitoring of PGA-5FU-AF750 tumor-accumulation over time. *In vivo* FLI tumor-accumulation of s.c. HCT-116.Fluc2-C9 colon tumor-bearing mice after i.v. administration of PGA-5FU-AF750-1. Pseudocolor scale bars were consistent for all images in order to show relative changes over time. **A)** Lateral mouse view. **B)** AF750 quantification by measurements of AF750 FLI intensity (Radiant Efficiency). Mean values  $\pm$  SEM are displayed over time.

#### 4.1.6.2.2 Ex vivo FLI (BD1)

BD1 *ex vivo* FLI analysis at different end-time points (4 and 48 h) were performed for all tissues. The *ex vivo* FLI images allow to determine more precisely the location of the compound of interest and its quantification. Figure 4. 28 and 4.29 show *ex vivo* FLI images of tumors and kidneys, the only organs in which the fluorescent signal was quantifiable above background levels. In good agreement with the *in vivo* FLI images, this data confirmed the accumulation in tumors, but also the excretion of the conjugate **PGA-5FU-AF750-1** through the renal route. Figure 4. 30 include the graphs of AF750 FLI quantification over the time of the rest of tissues and plasma. Clearly, FLI accumulation in these tissues (liver, spleen, lung, heart, brain, muscle, skin and plasma) is not significant. For this reason, unforeseen toxicities of the tested product in these tissues have not to be expected.

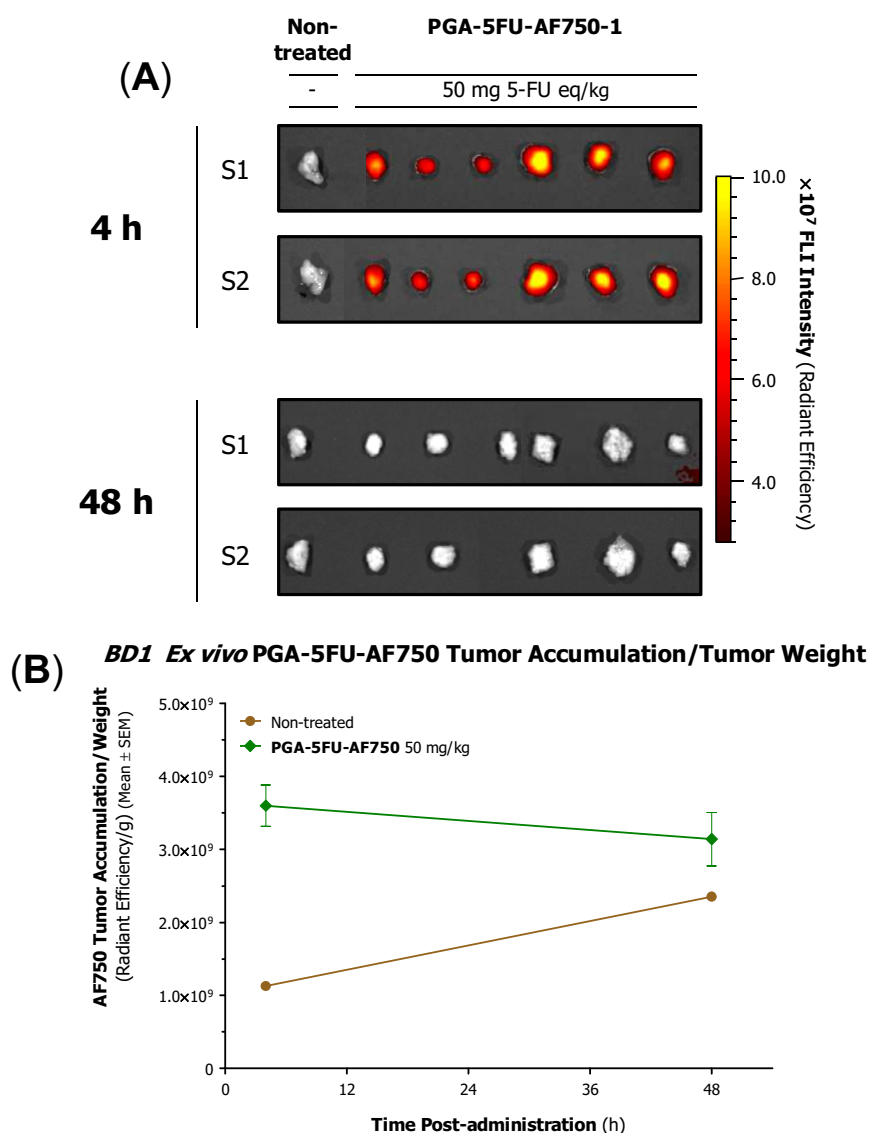


Figure 4. 28 (A) *Ex vivo* tumor FLI at 4 and 48 h post-administration of PGA-5FU-AF750-1 of s.c. HCT-116.Fluc2-C9 colon tumor-bearing mice after i.v. administration of the test compound. Pseudocolor scale bars were consistent for all images in order to show relative changes from 4 to 48 h. (B) AF750 tissue-accumulation per tissue weight were quantified by measurements of AF750 FLI intensity (Radiant Efficiency). Mean values  $\pm$  SEM are displayed at each corresponding end point. S1 and S2 stands for Side 1 and 2 of the imaged tissues.

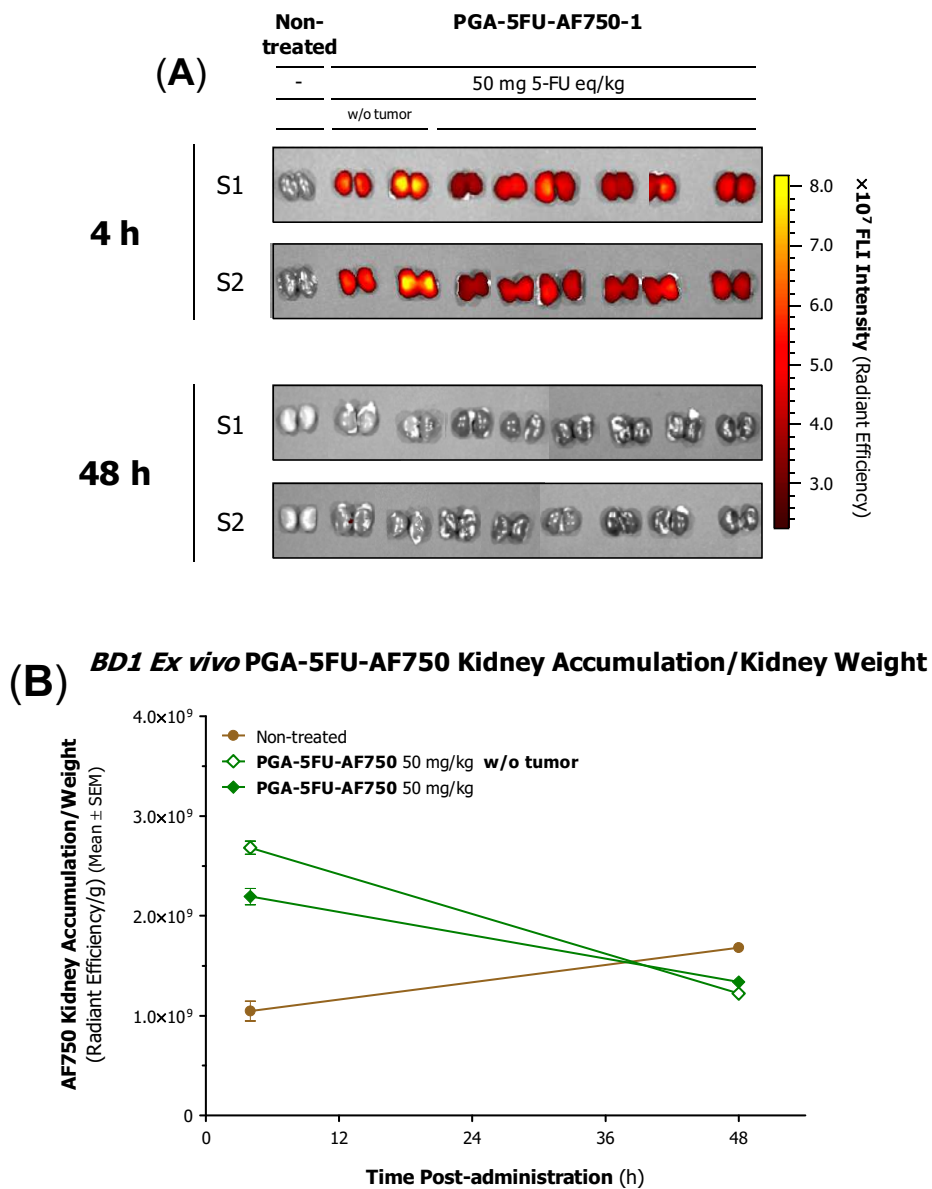


Figure 4. 29 (A) Ex vivo kidney FLI at 4 and 48 h post-administration of PGA-5FU-AF750-1 of s.c. HCT-116.Fluc2-C9 colon tumor-bearing mice after i.v. administration of the test compound. Pseudocolor scale bars were consistent for all images in order to show relative changes from 4 to 48 h. (B) AF750 tissue-accumulation per tissue weight were quantified by measurements of AF750 FLI intensity (Radiant Efficiency). Mean values ± SEM are displayed at each corresponding end point. S1 and S2 stands for Side 1 and 2 of the imaged tissues.

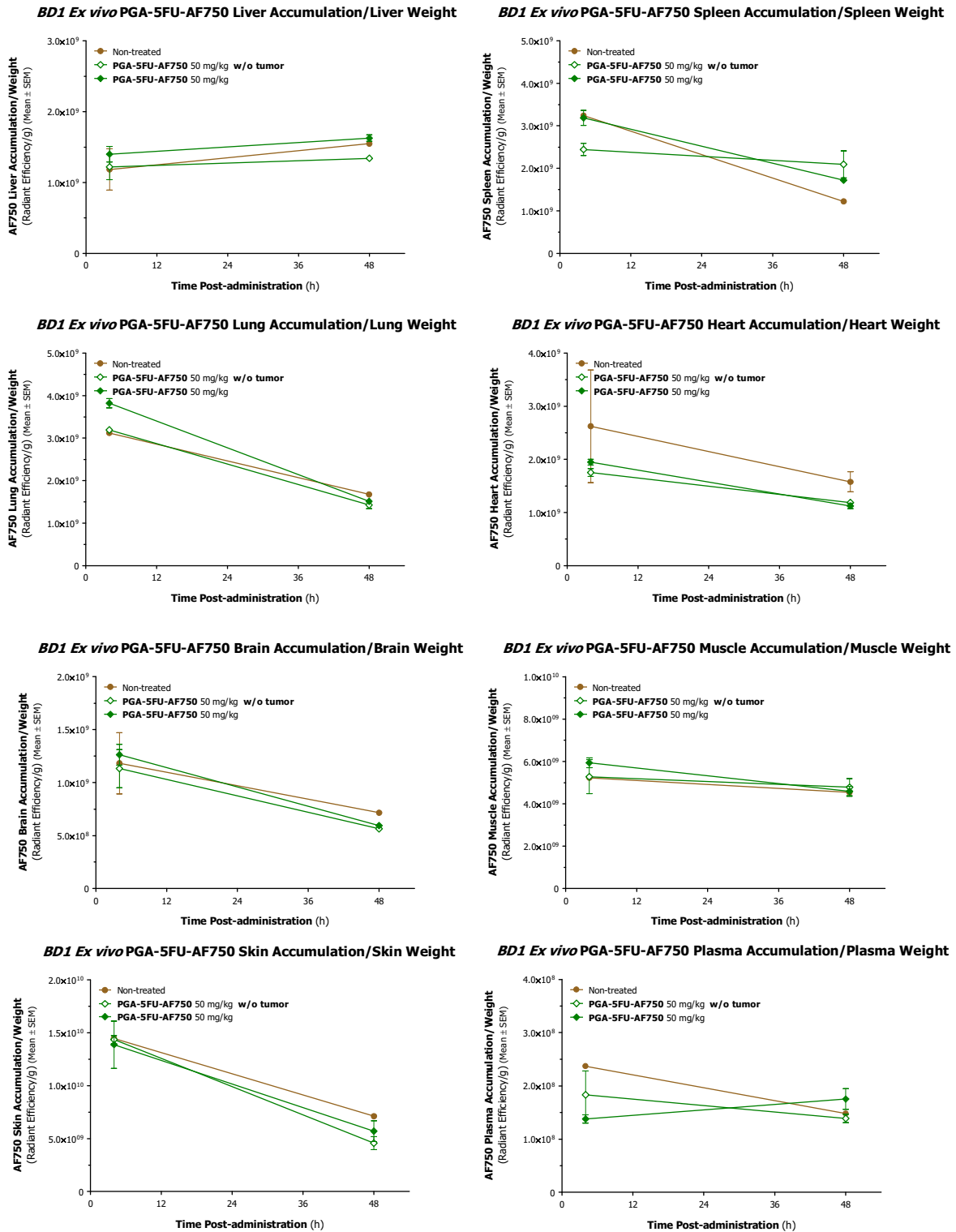


Figure 4. 30 AF750 quantification by measurements of AF750 FLI intensity (Radiant Efficiency) in liver, spleen, lung, heart, brain, muscle, skin and plasma. Mean values  $\pm$  SEM are displayed over time.

#### 4.1.6.2.3 Ex vivo 5-FU quantification by HPLC (BD1)

5-FU quantification by HPLC in plasma, liver, kidney, lung and tumor of 5-FU and PGA-5FU-AF750-1 injected groups was determined following the methodology set up in section 4.1.5. The measurements were performed with six different samples of each tissue in a unique determination per sample. Results are expressed as mean value  $\pm$  SEM deviation. As the recovery found in spleen (Figure 4. 26) was very low, it was not included in the list of tissues to be analyzed in the biodistribution study.

In the PGA-5FU-AF750 group, an additional step for the complete hydrolysis of the ester linkage between the 5-FU and the carrier was performed (NaOH 2 M) for the quantification of the PGA-5FU-AF750-1 conjugate accumulation. After ultrafiltration of tissue homogenates and plasma carried out for the removal of interferences in the chromatogram, samples were lyophilized. Finally the residue was redissolved in 2 mL of PBS (pH 5) and 20  $\mu$ L of the clear solution were analyzed by HPLC using a C-18 reverse phase column (XSelect HSS T3 3.5  $\mu$ m, 4.6 x 250 mm, Waters) and the conditions detailed in section 3.7.

A calibration curve in the range of 10 to 25000 ng/mL of 5-FU was used to quantify the drug content in tissue and plasma samples. Table 4. 9 shows the results expressed as %ID/g tissue for the HPLC quantification of 5-FU. Percentage of ID value of each tissue was multiplied with the corresponding recovery factor (QC Medium, Table 4.8) determined in the validation of the method in section 4.1.5.3. Very low amounts of 5-FU were detected suggesting that the majority could be excreted during the first 4 h of the BD1 experiment and also metabolized in the liver.

Table 4. 9 PGA-5FU-AF750-1 and 5-FU tissue biodistribution and 5-FU levels quantification measured by HPLC at 4 and 48 h post-administration in BD1 experiment.

		5-FU Tissue Accumulation/Weight : ng 5-FU/g tissue (Mean $\pm$ SEM)				
		Tumor	Liver	Kidney	Lung	Plasma
5-FU	4 h	0.027 $\pm$ 0.012	0.023 $\pm$ 0.003	0.031 $\pm$ 0.003	0.007 $\pm$ 0.004	0
	48 h	0	0.025 $\pm$ 0.004	0.007 $\pm$ 0.003	0	0
PGA-5FU-AF750-1	4 h	0.015 $\pm$ 0.005	0.002 $\pm$ 0.002	0.025 $\pm$ 0.003	0.010 $\pm$ 0.004	0.050 $\pm$ 0.018
	48 h	0.005 $\pm$ 0.004	0.004 $\pm$ 0.003	0.006 $\pm$ 0.002	0.011 $\pm$ 0.003	0

The 5-FU quantification by HPLC of tissue homogenates and plasma gave us a deeper detail of the complete biodistribution of 5-FU in animals injected either with 5-FU or PGA-5FU-AF750-1. Figure 4. 31 represents the comparison within the 5-FU and PGA-5FU-AF750-1 injected animals at 4 and 48 h.

**% ID / g tissue- BD1 (HCT-116.Fluc2-C9)**  
Measured by HPLC

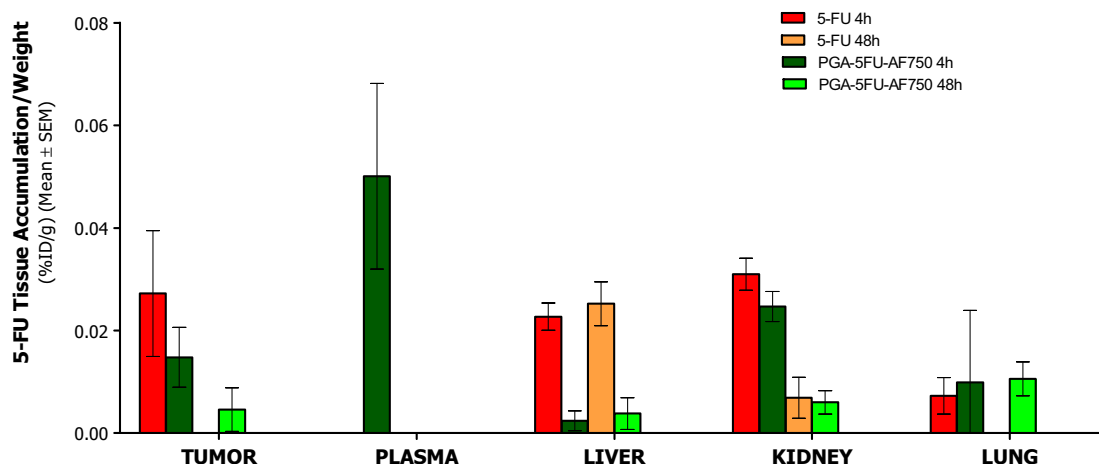


Figure 4. 31 PGA-5FU-AF750-1 and 5-FU tissue biodistribution and 5-FU levels quantification measured by HPLC at 4 and 48 h post-administration in BD1 experiment.

In good agreement with the *in vivo* and *ex vivo* FLI results, the tumor accumulation of 5-FU was confirmed by HPLC 5-FU quantification. Although it is true that at 4 h post-administration a higher amount of 5-FU was detected for those animals injected with the free drug, we confirmed that the conjugate still remains accumulated in the tumor up to 48 h thanks to the EPR effect whereas the free drug was not detected at that time.

Interestingly, animals treated with PGA-5FU-AF750-1 conjugate showed high levels of 5-FU in plasma at 4 h post-administration, while no 5-FU was detected for those animals injected with free drug. It is known that 5-FU has a very short half-life in plasma (10-20 min)<sup>11</sup> and for this reason no 5-FU was detected in plasma at 4 h, suggesting that the conjugation to the PGA carrier increases the plasma half-life of 5-FU.

HPLC 5-FU quantification confirmed the excretion of the conjugate through the renal route, seen by FLI imaging. *Ex vivo* liver imaging did not show a significant accumulation of the conjugate in this organ, however, by 5-FU HPLC measurements quantifiable 5-FU levels were observed in the liver, suggesting that PGA-5FU-AF750-1 was also excreted through the liver. It is remarkable that 5-FU content of liver and kidney in animals administered with the free drug is considerably higher than in animals that received the nanoconjugate. Yuan *et al.*<sup>110</sup> described the *in vivo* biodistribution of the HPMA-5FU conjugate and showed that the preferential accumulation of those animals injected with free drug (24 mg 5-FU/kg) at 4 h post-administration was in the liver tissue (0.065 %ID), followed by the tumor (0.035 %ID), plasma (0.018 %ID) and kidney (0.010 %ID). In contrast, in our experiment it was found out that the free drug was equally distributed between tumor, kidney and liver tissues at 4 h post-administration time. In the case of the liver, it can be considered a positive result because it is described that up to 80% of administered 5-FU is broken down by DPD in the liver<sup>11</sup>. Moreover, with these results in hand, when comparing the % ID detected in tumors and kidneys-livers at 48 h post-administration, we confirmed that the amount of accumulated product was similar to the quantity of excreted product.

Regarding 5-FU quantifications in lung tissues, a higher 5-FU accumulation was observed in animals that received the PGA-5FU-AF750-1 compared to those administered with the free drug. This result might suggest aggregation of the polymeric nanoconjugate before or after the i.v. administration. These aggregates would be sequestered in lung capillaries and would be dissolving over time without negative consequences to the animal.

#### **4.1.6.3 Tumor-accumulation and whole-body biodistribution on subcutaneous HT-29.Fluc-C4 human CRC tumors growing in athymic nude female mice (BD2)**

Animals (n=6) received a unique i.v. administration dose of 5-FU (50 mg eq 5-FU/kg) and it was well-tolerated and adverse side effects were not observed up to 24 h post-administration. However a unique i.v. administration dose of PGA-5FU-AF750-2 at 50 mg eq 5-FU/kg caused mouse death immediately after therapeutic agent administration, unlike in BD1 experiment where PGA-5FU-AF750-1 was well-tolerated. The death of the animal was caused by a pulmonary collapse. As mentioned before, particle aggregates can be sequestered in lung capillaries after the i.v. administration. For this reason we suspected that before the injection the PGA-5FU-AF750-2 product might aggregate. Unfortunately, the average particle size of the product could not be analyzed by DLS since this technique could not be used with fluorophore substances. Consequently, the 5-FU injected dose was decreased to 25 mg eq 5-FU/kg, which was well tolerated and no adverse side effects were observed up to 24 h post-administration. Moreover, the same amount of free AF750 (0.30 mg AF750 eq/kg) loaded into the PGA-5FU-AF750-2 was injected in an additional group of animals (n=6) and it did not cause death or any side effects, indicating that the fluorophore was not inducing the toxicity observed.

In the BD2 experiment, *in vivo* FLI measurements were performed at 4, 8 and 24 h, and *ex vivo* FLI and 5-FU HPLC quantification were done of plasma, tumor, liver, kidney and lung of animals sacrificed at 4 and 24 h. The second end-point of this experiment was forwarded compared to the BD1 experiment because no fluorescence was detected *ex vivo* at 48 h post-administration in the first biodistribution assay.

##### **4.1.6.3.1 *In vivo* FLI (BD2)**

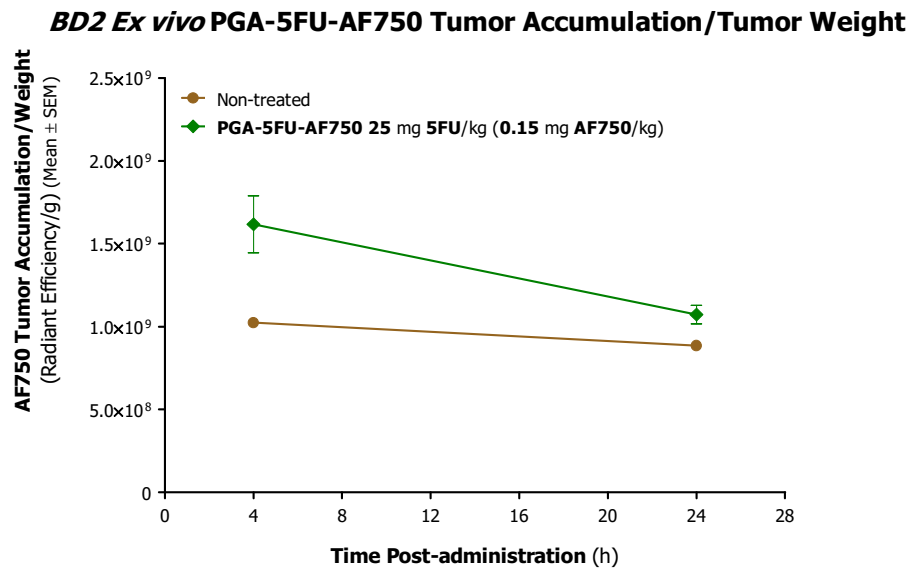
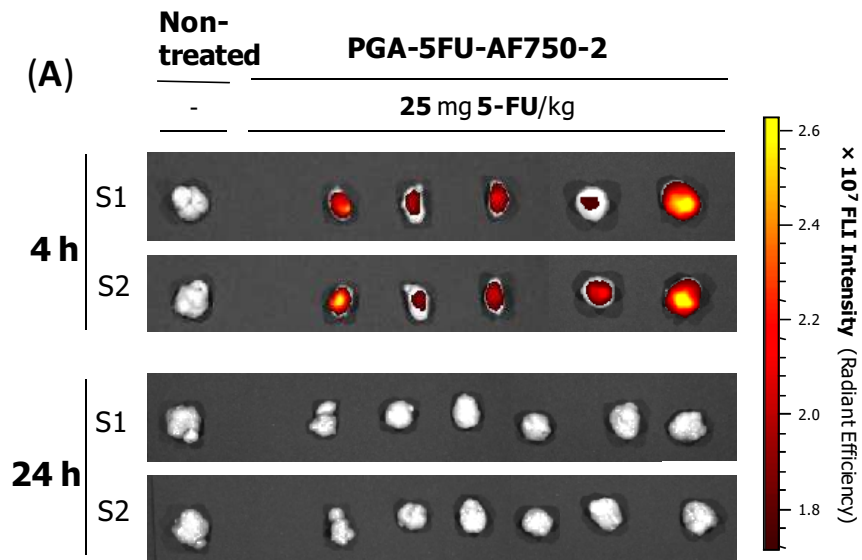
Since the administered dose of PGA-5FU-AF750-2 was reduced to 25 mg eq 5-FU/kg in the BD2 experiment, the amount of AF750 resulted also reduced (0.15 mg eq AF750/kg). Accordingly, *in vivo* FLI showed that 0.15 mg eq AF750/kg was not sufficient for the detection of noninvasive accumulations of AF750 *in vivo*.

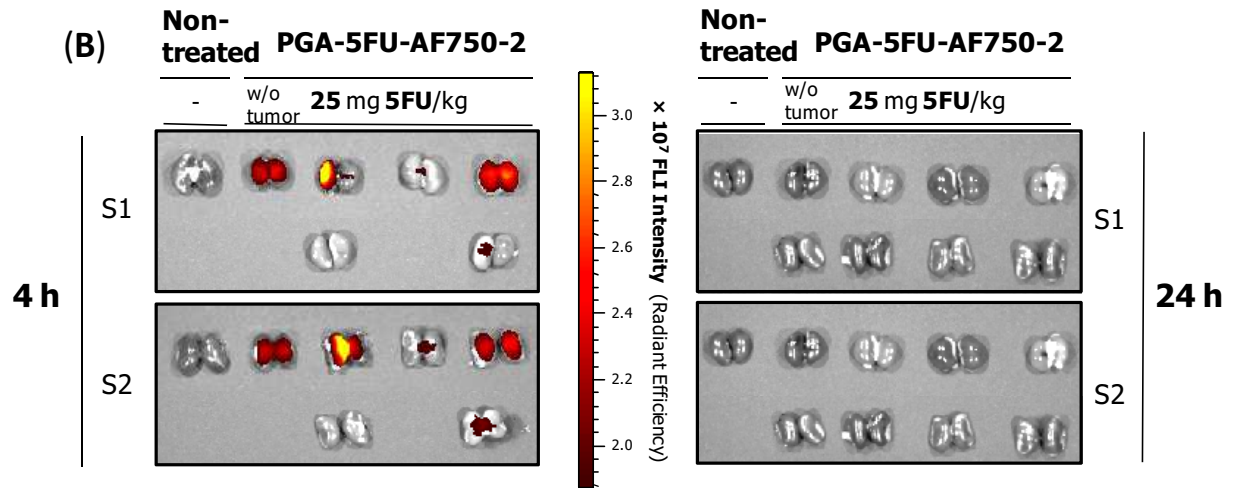
##### **4.1.6.3.2 *Ex vivo* FLI (BD2)**

BD2 *ex vivo* FLI analysis at different end-time points (4 and 24 h) was performed for all tissues. Figure 4. 32 show the *ex vivo* FLI images of tumors (A), kidneys (B) and liver (C). *Ex vivo* FLI PGA-5FU-AF750-2 fluorescence was detected mainly in kidney and liver. Kidney and liver-accumulations were maximal at 4 h post-administration and decreased rapidly within the first 24 h, indicating that PGA-5FU-AF750-2 was quickly excreted through both, renal and hepatic routes (see Figure 4. 32 B

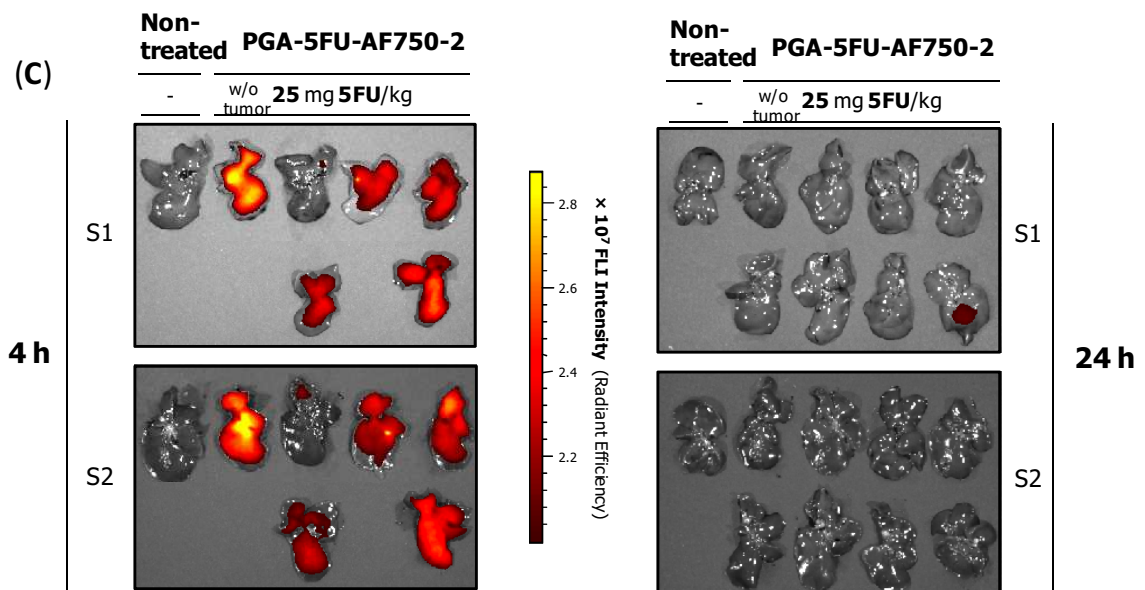
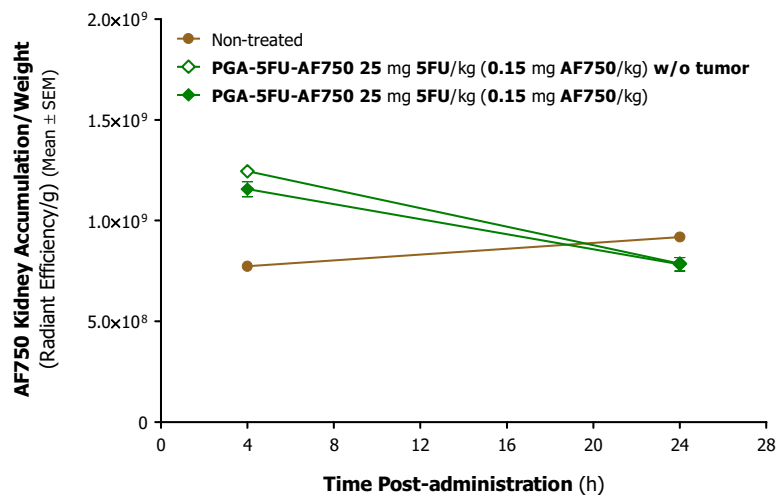


and C, respectively). In addition, it was observed that the non-tumor bearing mice that received the PGA-5FU-AF750-2 showed similar kidney and liver-accumulation than tumor-bearing mice.





**BD2 Ex vivo PGA-5FU-AF750 Kidney Accumulation/Kidney Weight**



### BD2 Ex vivo PGA-5FU-AF750 Liver Accumulation/Liver Weight

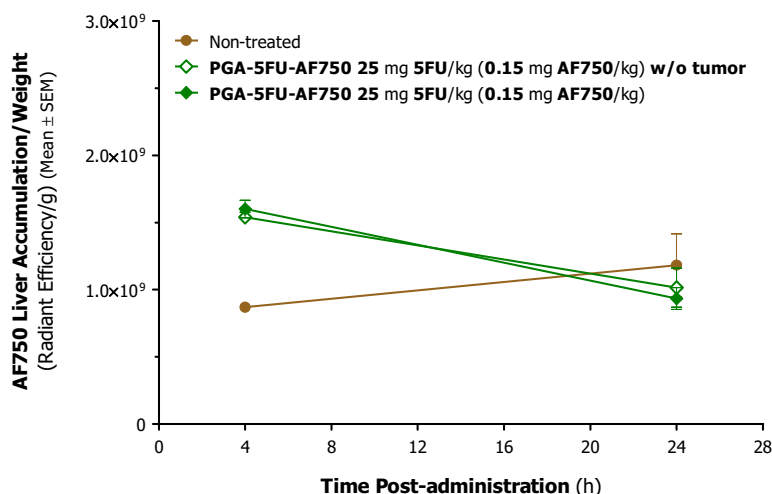
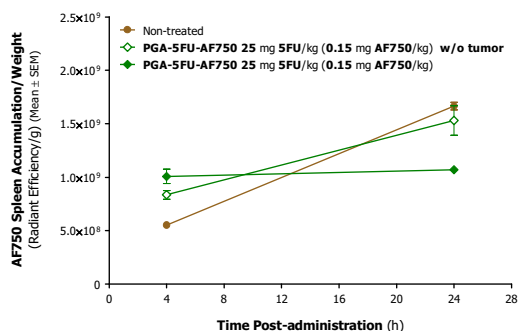
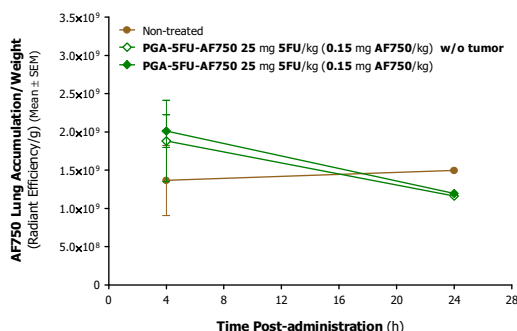


Figure 4. 32. PGA-5FU-AF750, tumor and tissue-accumulations in s.c. HT-29.Fluc-C4 colon tumor-bearing mice after i.v. administration of the test compound. Ex vivo tumor (A), kidney (B), liver (C), FLI at 4 and 24 h post-administration of PGA-5FU-AF750. Pseudocolor scale bars were consistent for all images in order to show relative changes from 4 to 24 h. AF750 tissue-accumulation per tissue weight were quantified by measurements of AF750 FLI intensity (Radiant efficiency). Mean values ± SEM are displayed at each corresponding end point. S1 and S2 stands for Side 1 and 2 of the imaged tissue.

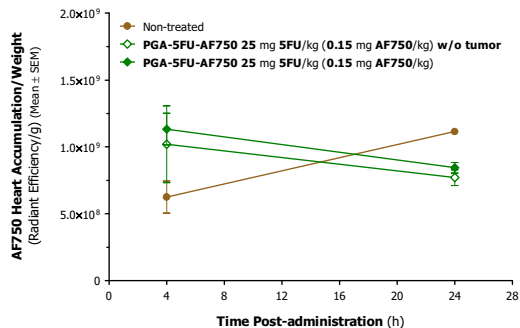
### BD2 Ex vivo PGA-5FU-AF750 Spleen Accumulation/Spleen Weight



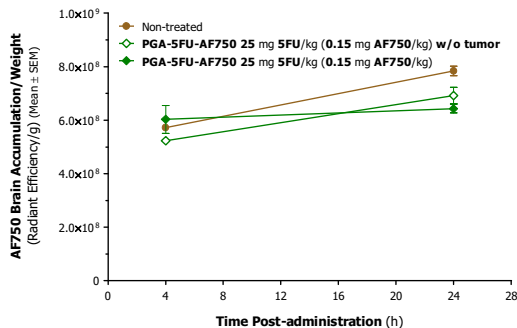
### BD2 Ex vivo PGA-5FU-AF750 Lung Accumulation/Lung Weight



### BD2 Ex vivo PGA-5FU-AF750 Heart Accumulation/Heart Weight



### BD2 Ex vivo PGA-5FU-AF750 Brain Accumulation/Brain Weight



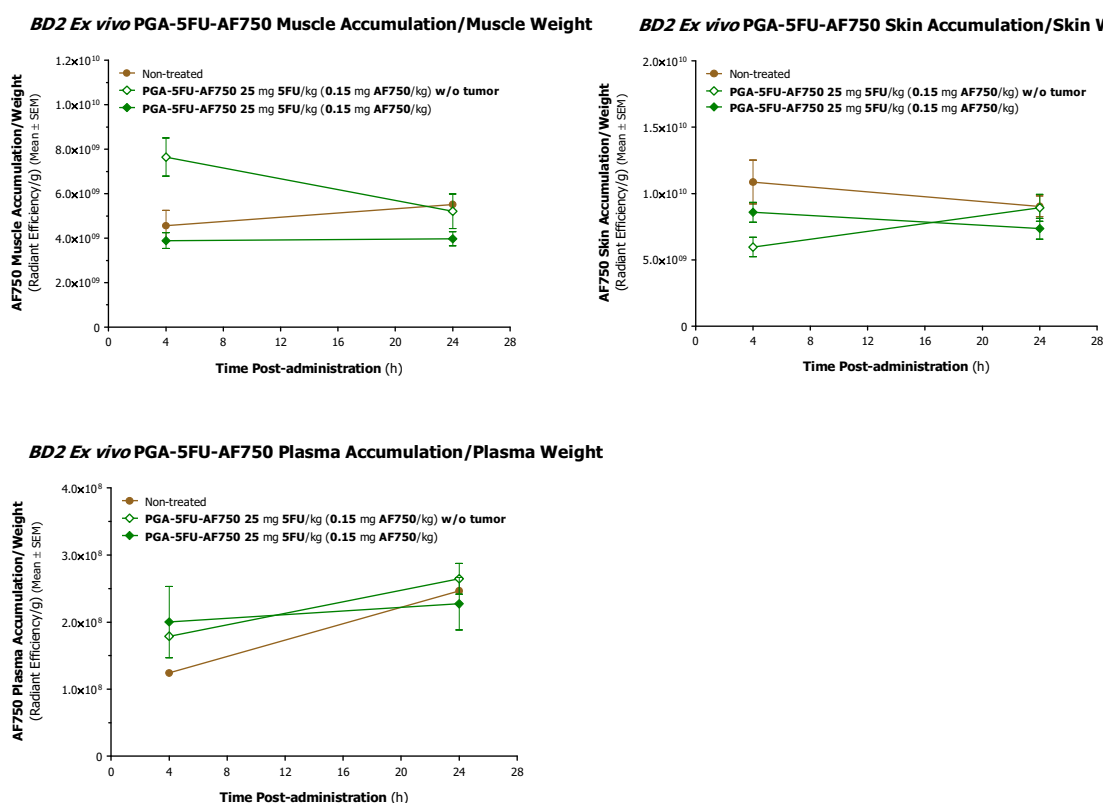


Figure 4.33 PGA-5FU-AF750, tumor, kidney, spleen, lung, plasma, muscle, skin and liver-accumulations. Ex vivo spleen, lung, heart, brain, muscle, skin and plasma FLI at 4 and 24 h post-administration of PGA-5FU-AF750-2. Pseudocolor scale bars were consistent for all images in order to show relative changes from 4 to 24 h. AF750 tissue-accumulation per tissue weight were quantified by measurements of AF750 FLI intensity (Radiant efficiency). Mean values  $\pm$  SEM are displayed at each corresponding end point. S1 and S2 stands for Side 1 and 2 of the imaged tissues.

#### 4.1.6.3.3 Ex vivo 5-FU quantification by HPLC (BD2)

5-FU quantification by HPLC in plasma, liver, kidney, lung and tumor of 5-FU and PGA-5FU-AF750-2 injected groups was determined following the methodology detailed in section 3.7. The methodology followed was the same explained for the BD1 experiment in section 4.5.1.1.3. As the recovery found in spleen (Figure 4.26) was very low, it was not included in the list of tissues to be analyzed in the biodistribution study.

Table 4.10 shows the results of HPLC quantifications expressed as %ID/g tissue. Percentage of ID value of each tissue was multiplied with the corresponding recovery factor (QC Medium, Table 4.8) determined in the validation of the method in section 4.1.5.3. Very low amounts of 5-FU were detected suggesting that the majority of the drug might be excreted/metabolized during the first 4 h.

5-FU quantification by HPLC of tissue homogenates and plasma gave us a deeper detail of the complete biodistribution of 5-FU in animals injected either with 5-FU or PGA-5FU-AF750-2. Figure 4.34 represents the comparison between 5-FU and PGA-5FU-AF750-2 injected animals.

Table 4. 10 PGA-5FU-AF750-2 and 5-FU tissue biodistribution and 5-FU levels quantification measured by HPLC at 4 and 24 h post-administration in BD2 experiment.

		5-FU Tissue Accumulation/Weight : ng 5-FU/g tissue (Mean ±SEM)				
		Tumor	Liver	Kidney	Lung	Plasma
5-FU	4 h	0.030 ± 0.005	0.030 ± 0.007	0.145 ± 0.011	0.049 ± 0.006	0
	24 h	0.019 ± 0.004	0	0.047 ± 0.005	0.034 ± 0.004	0
PGA-5FU-AF750-2	4 h	0.060 ± 0.027	0.050 ± 0.016	0.233 ± 0.064	0.073 ± 0.006	0.009 ± 0.004
	24 h	0.032 ± 0.010	0.031 ± 0.014	0.049 ± 0.020	0.057 ± 0.007	0.026 ± 0.013

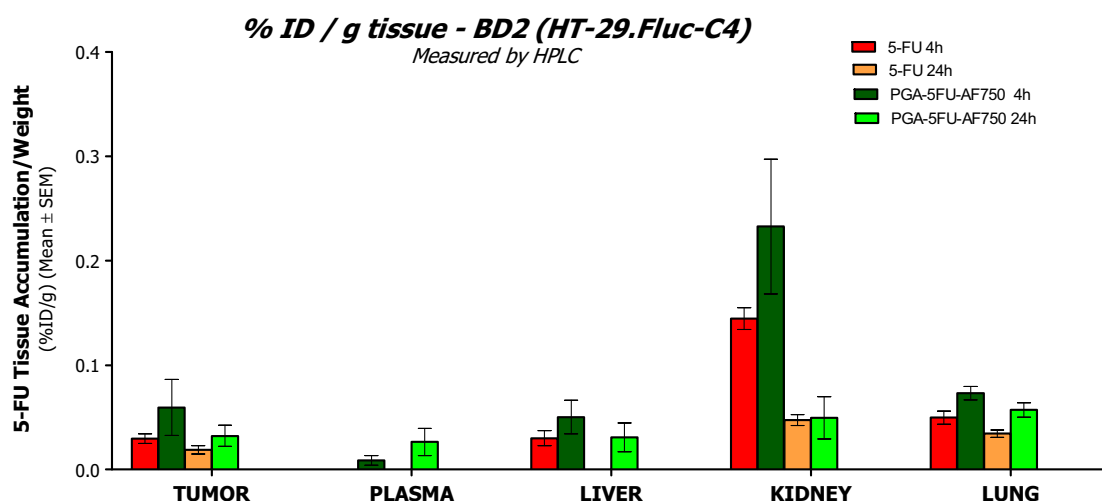


Figure 4. 34 PGA-5FU-AF750-2 and 5-FU tissue biodistribution and 5-FU levels quantification measured by HPLC at 4 and 24 h post-administration in BD2 experiment.

In good agreement with the *ex vivo* FLI results, with the HPLC 5-FU quantification it was possible to confirm the tumor accumulation up to 24 h, as well as the excretion of the conjugate through the renal and hepatic routes.

Regarding the 5-FU content in tumors from those animals that received an injection of PGA-5FU-AF750-2, it was observed a maximum accumulation at 4 h post administration. At 24 h post-administration 50% of the 5-FU detected at 4 h still remained accumulated in the tumor, confirming the EPR effect. Contrary to the amount of 5-FU quantified at 4 h for the animals that received a 5-FU injection in the BD1 experiment, in the BD2 the amount of 5-FU detected was lower than the quantified for the PGA-5FU-AF750-2 injected animals. It is necessary to mention that at 24 h post-administration 5-FU injected as a free drug still remained in tumors in the BD2 experiment whereas at 48 h was not detected in the BD1 experiment.

Regarding kidney accumulation it is remarkable that at 4 h post-administration a high amount of conjugate and 5-FU were excreted but it decreased up to 24 h. In a very low proportion, the same

behavior was observed in the liver, confirming a higher hepatic excretion during the first hours of the experiment for PGA-5FU-AF750-2 and 5-FU.

A positive finding was the detection of 5-FU in plasma up to 24 h, confirming the stability of the conjugate PGA-5FU-AF750-2 in circulation.

Finally, it was confirmed that the higher particle size of the conjugate could induce to an accumulation in lungs after the i.v. injection.

#### 4.1.6.4 Comparison of the BD1 and BD2 experiments

It is noteworthy the difference between the percentages of ID values in both BD experiments performed in two different xenograft models (HCT-116 (BD1) or HT-29 (BD2)). The lower results were obtained for the first analysis (BD1). It could be attributed to the better manipulation of the samples in the BD2 experiment, that can be attributed to the experience gained when the second experiment BD2 was carried out. For this reason, the level of 5-FU of those animals injected with the free drug of the second biodistribution assay (BD2) should be considered more representative.

In addition, the administered dose resulted different (BD1/BD2, 2:1) since the PGA-5FU-AF750-2 conjugate was toxic at the same dose in which was performed the BD1 experiment. Since both PGA-5FU-AF750 conjugates were synthesized in two different reactions using as a starting product the PGA-5-FU-pool [6], we hypothesized the toxicity associated to the PGA-5FU-AF750-2 to any interference during the synthetic or lyophilization processes. It is necessary to mention that we tried to measure the particle size of the administered solution, because animals died due to a pulmonary collapse, usually associated to the administration of conjugates with a high particle/aggregate size. Unfortunately, using the DLS system it was not possible to find out the presence of aggregates because the fluorophore dye produced interferences in the reflection light system. But when analyzing the relation of tumor vs. liver accumulations in BD1 and BD2 experiments it was observed that higher amounts of PDC were accumulated in the liver in the BD2 experiment in comparison to the tumor accumulation. This confirmed the difference of both products and the aggregating process that was hypothesized at the beginning of the BD2 assay.

In the study of the *in vivo* biodistribution of the HPMA-5FU conjugate<sup>110</sup> mentioned before, *Yuan et al* showed that the conjugate accumulation in tumor (0.035% ID) at 4 h post-administration was lower than in the liver (0.065% ID). They also confirmed the excretion through the renal route and the accumulation in spleen (0.002% ID), lung (0.001% ID) and plasma (0.018% ID). Our results suggest that the use of our polymeric system loaded with the same drug could produce a benefit in the biodistribution in comparison to the HPMA-based system. The liver accumulations of the PGA-5FU-AF750 system are in BD1 and BD2 experiments lower than in the tumor. Thus, the undesired metabolization of 5-FU in the liver is expected to be reduced. In addition, our system is composed by a biodegradable polymeric carrier of poly-(glutamic acid) whereas HPMA is non-biodegradable and can accumulate in the body once administered, particularly when its Mw is high and renal elimination cannot be guaranteed.

As mentioned before, free 5-FU is immediately distributed and metabolized in tissues such as liver, kidney and intestine after i.v. injection, which is the main reason for its low *in vivo* antitumor activity<sup>11</sup>. With both techniques (FLI and HPLC) used to quantify the biodistribution of PGA-5FU-AF750 it is suggested that by conjugating a PGA chain to 5-FU, 5-FU can be protected from a rapid metabolism within the body and accumulate in the tumor up to 24 and 48 h post-administration. This data suggests that an increased retention in tumor and lower renal elimination would benefit PGA-5-FU antitumor efficacy. Although we detected 5-FU at 4 h post-administration in all tissues, the study of the biodistribution at shorter time's post-administration is needed in order to understand the behavior of our PDC after i.v. injection.

#### 4.1.6.5 *In vivo* tumor growth inhibition studies

Due to the promising results observed in the BD1 experiment performed in animals bearing CRC tumors grown from HCT-116.Fluc2-C9, as well as the encouraging results in the *in vitro* experiments performed in the same CRC cell line, we decided to study the tumor growth inhibition in HCT-116.Fluc2-C9 tumor-bearing mice.

Athymic 6-8 week-old female mice (HSd:Athymic Nude-Foxn1, Harlan) were injected subcutaneously (s.c.) with  $2 \times 10^6$  cells HCT-116.Fluc2-C9 into the rear right flank. Tumor volume measured using a caliper, *in vivo* (twice per week), according to the formula  $D \times d^2 / 2$ .

Once tumors reached an average volume of 132 mm<sup>3</sup> (median), the animals were randomized in 3 different groups and treatment consisted in the i.v. administration of 5-FU, PGA-5-FU or vehicle twice a week (1001000), during 5 weeks:

- **G1 - Control Group/Vehicle:** PBS injected i.v. (schedule 1001000), n=10 animals.
- **G2 - 5-FU Group:** 5-FU injected i.v., 30 mg 5-FU/kg (schedule 1001000), n=10 animals.
- **G3 – PGA-5-FU Group:** PGA-5-FU injected i.v., 30 mg eq 5-FU/kg (schedule 1001000), n=10 animals.

The i.v. administration dose of 5-FU (G2) at 50 mg eq 5-FU/kg was well-tolerated and adverse effects were not observed up to 24 h post-administration. However, the first administration of PGA-5-FU (G3) at 50 mg eq 5-FU/kg caused mouse death immediately after the administration. Consequently, the 5-FU injected dose was reduced to 25 mg eq 5-FU/kg for the next four administrations in both groups. Once the average body weight was stabilized (see Figure 4. 35), the administered dose was increased to 40 mg eq 5-FU/kg. However, after administration of 40 mg eq 5-FU/kg, body weight of animals in G2 (PGA-5-FU) dropped dramatically. Therefore, the injected dose was maintained at 30 mg eq 5-FU/kg until the end of the experiment for both groups.

The death of the animal administered with 50 mg eq 5-FU/kg of PGA-5-FU was produced due to a pulmonary collapse, as it happened in BD2 experiment (section 4.1.6.3). Since it is known that particle aggregates might block pulmonary capillaries, we suspected that the PGA-5-FU-pool

product suffered unexpected alterations during the storage period that could negatively contribute to the increase of the particle size of the PGA-5-FU-pool product (See section 4.1.6.5.1)

A part from the above mentioned toxicities associated to PGA-5-FU administration at 40 or at 50 mg eq 5-FU/kg, no other toxicity sign was observed during the course of the experiment and no significant body weight loss was observed (Figure 4.35).

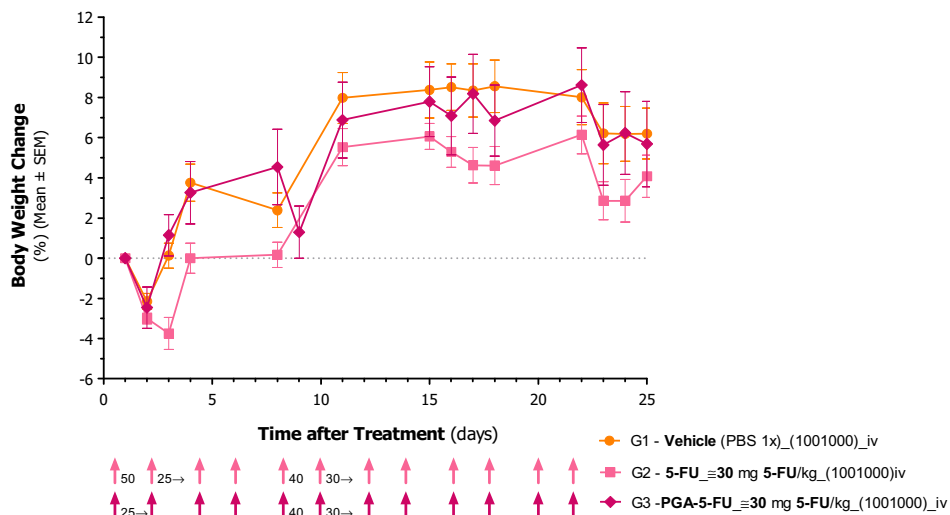


Figure 4.35 Body weight profiles of treated mice of G1, G2 and G3 groups monitored along the experiment. The arrows in the bottom correspond to the dose administered.

Tumor-growth measurement for each animal was carried out *in vivo*. In addition, at the end point (day 45), *ex vivo* tumor volume and tumor weight measurements were performed (Figure 4.37, Figure 4.38, respectively). Figure 4.36 represents the evolution of tumor volume until 25 days, when the major differences between groups were observed. However, at this point the differences between groups are not statistically significant.

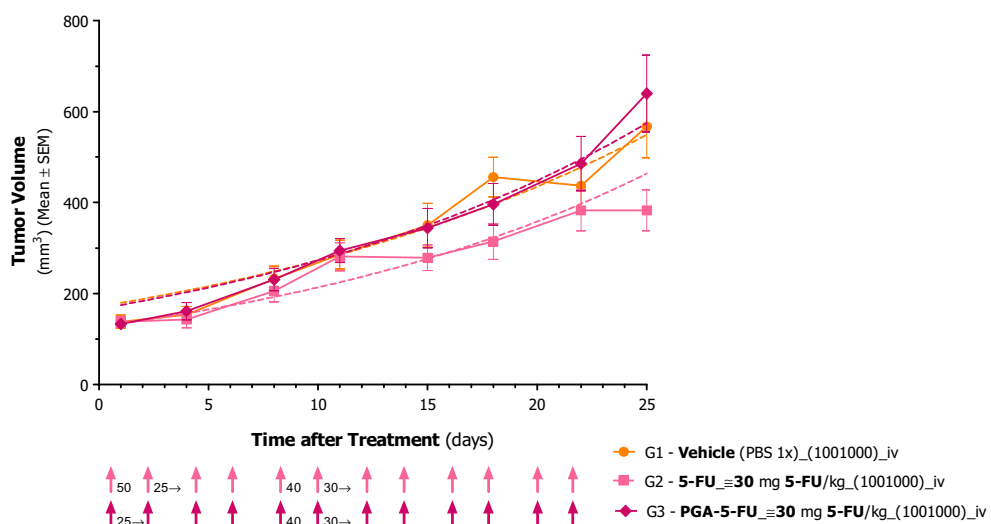


Figure 4.36 Tumor volume profiles of mice in G1, G2 and G3 groups monitored along the experiment. The arrows in the bottom correspond to the dose administered.



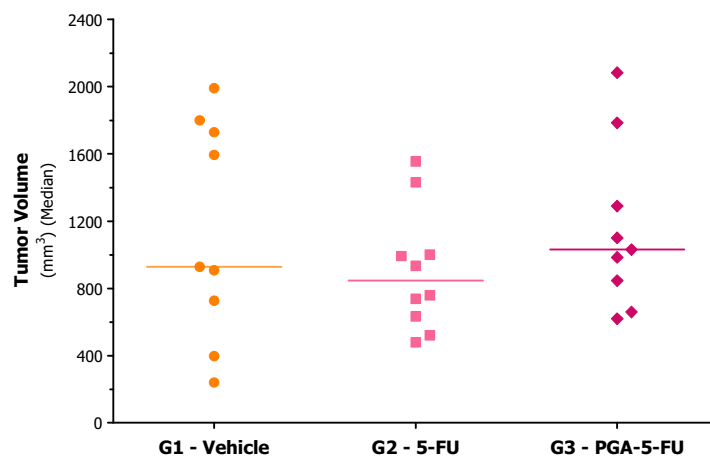


Figure 4. 37 Effect of the 5-FU or PGA-5-FU on tumor volume at the end of the experiment (day 45). Scatter plots of tumor volumes are shown with the median value represented by a line. Statistical analysis was done using a Dunn's Multiple Comparison test and no statistical differences were observed.

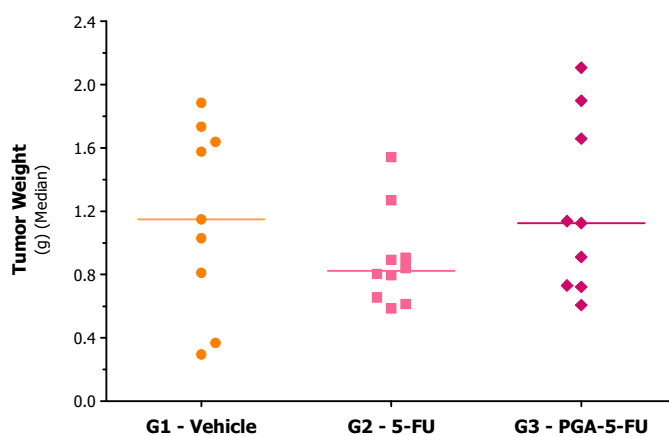


Figure 4. 38 Effect of the 5-FU or PGA-5-FU on tumor weight at the end of the experiment. Scatter plots of tumor weight are shown with the median value represented by a line. Statistical analysis was done using a Dunn's Multiple Comparison test and no statistical differences were observed.

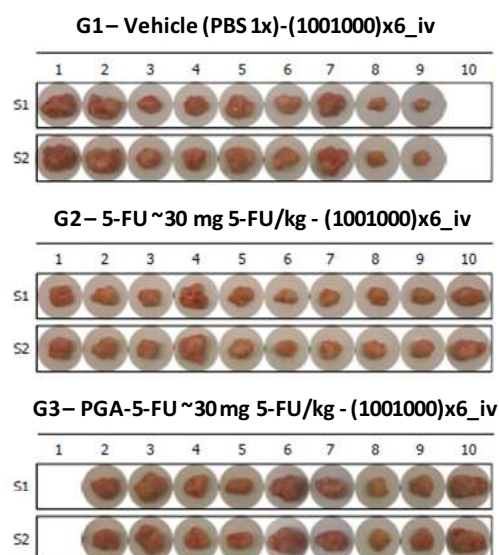


Figure 4. 39 Tumor photographs of treated animals. Comparative pictures of HCT-116 xenograft tumors excised at the end of the experiment.

Table 4.11 and Table 4.12 summarize the ratios between the treated vs. control groups (T/C ratios) to evaluate the reduction of the tumor volume or tumor weight, respectively. As it can be seen, only 5-FU treated animals have lower T/C values than the control.

Table 4. 11 T/C ratios of tumor volume measured *ex vivo* by means of caliper measurements.

Tumor Volume <i>ex vivo</i> (mm <sup>3</sup> )	G1 Vehicle	G2 5-FU	G3 PGA-5-FU
<b>Median</b>	928.9	846.4	1031.0
<b>Mean</b>	1146.0	904.0	1155.0
<b>SEM</b>	215.4	113.9	164.6
<b>T/C ratio (%)</b>	<b>100</b>	<b>91</b>	<b>111</b>

Table 4. 12 T/C ratios of tumor weight measured *ex vivo*.

Tumor Volume <i>ex vivo</i> (mm <sup>3</sup> )	G1 Vehicle	G2 5-FU	G3 PGA-5-FU
<b>Median</b>	1.1490	0.8222	1.1240
<b>Mean</b>	1.1640	0.8903	1.2100
<b>SEM</b>	0.1961	0.0949	0.1829
<b>T/C ratio (%)</b>	<b>100</b>	<b>72</b>	<b>98</b>

Collectively these results (*in vivo* and *ex vivo* tumor volume and *ex vivo* tumor weights) indicate that the administration of 30 mg eq 5-FU/kg twice a week does not induce a significant growth inhibition, either when the 5-FU is administered as a free drug vehiculized along with PGA. If the initial dose of 50 mg eq 5-FU/kg were maintained, a significant tumor growth inhibition could have been recorded at least for the 5-FU control group (G2). However, the toxicity seen for PGA-5FU forced us to reduce the dose in both PGA-5-FU and 5-FU treated groups and although slight differences are observed between vehicle and 30 mg/kg 5-FU treated groups such differences are not significant.

On the other hand, the absence of a significant effect in the PGA-5-FU treated group is due to the alteration of the product during its storage. This detail, further explained in section 4.1.6.5.1, was only detected after re-analyzing the PGA-5FU pool product, once the first toxicity effect were recorded in the *in vivo* efficacy assay.

The evaluation of the efficacy of PGA-5-FU would therefore require performing additional experiments where (i) PGA-5-FU is maintained stable (without aggregates or significant 5-FU release) from its synthesis until its administration *in vivo* and (ii) 50 mg/kg of 5-FU can be administered safely.

#### **4.1.6.5.1 Characterization of the PGA-5-FU injected into animals in the *in vivo* tumor growth inhibition experiment**

To better understand the low efficacy in the growth inhibition experiment and the toxicity observed when administered 50 mg eq 5-FU/kg of PGA-5-FU-pool [6] the remaining product of the injection solution (kept at -20°C after its solubilisation in PBS) at: 50 mg eq 5-FU/kg and 25 mg eq 5-FU/kg was further analyzed. As mentioned before, we suspected that the formation of aggregates in the solution injected into animals could be the cause of death by pulmonary collapse.

Therefore, the PGA-5-FU [6] (7.5 mg eq 5-FU/mL) solution prepared for the i.v. administration at the FVPR Laboratory (CIBBIM-Nanomedicine, VHIR) was analyzed by DLS. Interestingly, the product at a concentration of 3.75 mg 5-FU/mL that showed a particle size around 100 nm as detailed in Figure 4. 15 carried out after the purification process, showed an average particle size of 364.11 nm (see Figure 4. 40), confirming the aggregation of the PGA-5-FU [6] in the i.v. administered solution.

Therefore, the aggregation of the nanoconjugate might be the reason of the animal death in the tumor growth inhibition experiment, because pulmonary collapse is normally associated to particles with bigger nanometric size. In addition, we suspect that the toxicity observed in the BD2 experiment was due to the same aggregation problem, although PGA-5FU-AF750-2 product could not be analyzed by means of DLS.

An HPLC-MS analysis of the aggregate product was performed to determine its stability during storage. We expected some 5-FU release because the PGA-5-FU [6] conjugate was dissolved in PBS and, during almost 1 h, it remained at rt before storage at -20 °C, but when we analyzed the product, we detected the presence of 5-FU-adipic [2] (Mw=288 g/mol) released from PGA-5-FU (Figure 4. 41).

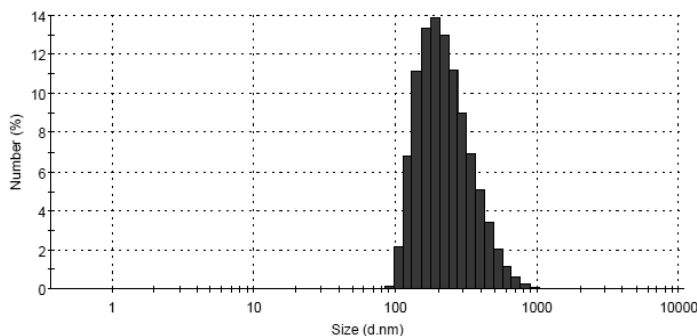


Figure 4.40 Size distribution by intensity of PGA-5-FU conjugate after the growth inhibition experiment, measured at the concentration injected into animals (25mg eq 5-FU/kg).

Regarding the structure of the PGA-5-FU [6] conjugate and the products detected in the HPLC-MS analysis, we suggest that part of the 5-FU-adipic [2] linked to the polymeric carrier was released leading free amino groups in some monomers of the PGA chain. Moreover, the conjugate synthesized had a very low TDL (7.06%) and for this reason, we considered that the carboxylic groups of the non-loaded glutamic acid monomers could interact with the free amino groups and thus, produce an unexpected aggregation of the nanoconjugate.

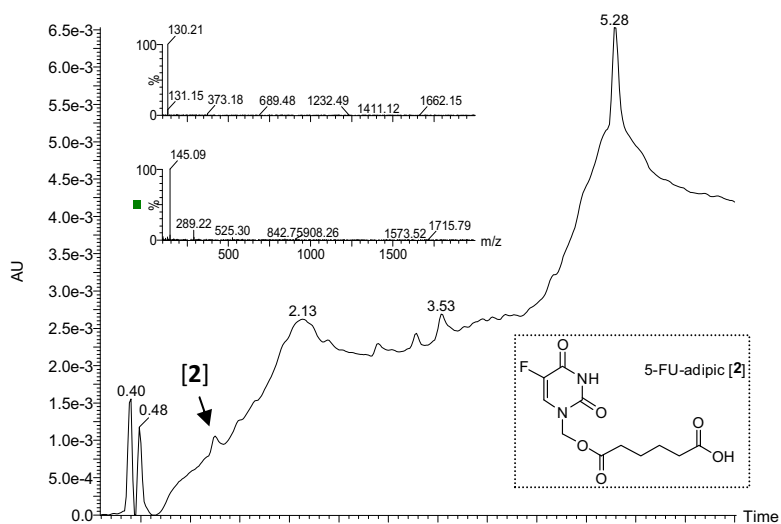


Figure 4.41 HPLC-MS chromatogram of the PGA-5-FU [6] injected into animals in the tumor growth inhibition experiment of section 2.6 (50 mg eq 5-FU/kg) and chemical structure of 5-FU-adipic product [2].

To avoid this type of problems in the future, each batch of product should be tested immediately after its synthesis, and if necessary stored at  $-20^{\circ}\text{C}$  under argon, to eliminate any possible degradation and avoid an aggregation of the nanoconjugate during storage for a long period of time. In addition, quality controls (including particle size and HPLC-MS analysis) should be performed to each batch stored at  $-20^{\circ}\text{C}$  before its administration into animals.

#### 4.1.7 Conclusions

This study indicated that the conjugation of 5-FU to a polyglutamic acid carrier with a molecular weight of 15 kDa through an ester bond showed therapeutic activity *in vitro* in the HCT-116.Fluc2-C9 and HT-29.FlucC4 CRC cell lines.

Additionally, the cellular uptake assays performed with the PGA-5-FU nanoconjugate labeled with a carboxyfluorescein fluorescent probe indicated that the internalization of the conjugate was through the endocytic pathway, and this internalization proved to be more rapid and efficient in HCT-116.Fluc2-C9 cell line compared to HT-29.Fluc-C4 cells.

The *in vivo* biodistribution experiments performed in murine models of CRC, with animals carrying tumors grown from HCT-116.Fluc2-C9 or HT-29.FlucC4 injected subcutaneously, confirmed a greater accumulation of the PGA-5-FU nanoconjugate labeled with AF750 at longer times in tumor in comparison to 5-FU levels detected in animals injected only with 5-FU as a free drug, confirming the EPR effect of the polymeric PGA-5-FU in these specific models. The studies also indicated that conjugation of 5-FU to a PGA polymer allow to increase the plasma half-life of 5-FU, which is in the range of min, up to 24 h after i.v. administration. Finally, BD assays also showed that the product was preferentially excreted through the kidney, but it was also removed by the liver in smaller amounts.

Finally, after the unexpected results observed in the *in vivo* tumor growth inhibition studies it was confirmed that the storage conditions of the PGA-5-FU conjugate are of significant importance to prevent the degradation of the conjugate and consequently the alteration of the nanoconjugate size producing aggregates. Such aggregates seem to be the reason behind the toxicity observed in the animals administered with PGA-5-FU.

---

## 4.2 Polymer-drug conjugates based on Poly-(L-glutamic acid) and 5-Fluorouracil sensitive to Matrix Metalloproteinases

---

In this section a new class of PGA-based PDC with **MMP-9** and **MMP-7** sensitive peptides was studied. The rationale behind using these enzyme-sensitive peptides relies on the increased expression and activity of these enzymes in the extracellular microenvironment of CRC.

While PGA-5-FU [6] conjugate will accumulate in the tumor thanks to a passive targeting, PGA polymers with MMP-cleavable linkers will combine passive targeting into the tumors with active release of the drug due to the presence of MMP enzymes within tumor microenvironment. So, we hypothesize that the new MMP-sensitive PDC would preferably accumulate in tumor areas thanks to the EPR effect, but also, would improve the extracellular 5-FU release in tumor tissues, thus increasing its therapeutic efficacy.

Given the good results of the ester linkage between 5-FU and PGA in the previous section (high stability while transport leading a very low unspecific release and higher tumor accumulation *in vivo*), we decided to explore this type of bond between 5-FU and the MMP-sensitive peptides. However, we also explored a carbamate linkage between 5-FU and the MMP-sensitive peptides in order to determine the best kinetic release conditions regarding MMP-mediated release.

### 4.2.1 Synthesis of MMP sensitive peptides

As mentioned in the Introduction (section 1.3.2.2.1), two different peptidyl sequences were selected from the literature as substrates for MMP-9 and MMP-7.

The peptide linker composition sensitive to MMP-9 (**GPVGLIG**) was selected based on the work published by *Turk et al*<sup>139</sup> and *Langer et al*<sup>51</sup>. *Turk et al* built a combinatorial library of oligopeptides as MMP substrates and scored (regarding its selectivity) all amino acids at each position between 8 different possibilities (P4-P3-P2-P1-P1'-P2'-P3'-P4', where the cleavage occurs between P1 and P1'). Based on this study, *Langer et al*<sup>141</sup> selected the PVGLIG sequence because it formed a MMP-9 sensitive hexapeptide (P3-...-P3') without any functional side chains, and introduced it into a new dextran polymer. Interestingly, the new Dextran-PVGLIG-Methotrexate conjugate showed sensitivity to the target enzyme MMP-9 and stability in systemic circulation. As detailed in Table 1.2, this sequence was also successfully used in a MMP sensitive PEGylated-peptide-conjugate adriamycin<sup>140</sup>. Taking this information into account, we decided to use the PVGLIG sequence and to add a Glycine as an extra amino acid to the N terminal of the sequence, to have a secondary

amine instead of a primary amine, thus enhancing its reactivity. Thus, the final MMP-9 cleavable peptide used in the MMP sensitive PDC corresponds to the sequence **GPVGLIG**.

On the other hand, in the area of optical *in vivo* fluorescence imaging research, novel entities have been designed as proteolytic beacons selective for specific enzymes<sup>141,142</sup> including MMPs. In detail, AHX-RPLALWRS-AHX sequences (where AHX stands for aminohexanoic acid) were used as the MMP-7 substrates in PAMAM-dendrimers labeled with the fluorophore dye Cy5<sup>141</sup>. Indeed, already in 1995, *Welch et al*<sup>143</sup> described that the best substrate for MMP-7 was the peptidyl sequence Dnp-RPLALWRS (where Dnp stands for dinitrophenyl). Therefore, the MMP-7 cleavable peptide selected in our project to design the MMP-7 sensitive PDC (PGA-MMP7pept-5FU) corresponded to this sequence: **AHX-RPLALWRS-AHX**.

In addition to the two specific MMP cleavable sequences, two additional peptides composed by the same amino acids (type and number) in a different order (scrambled peptides) were also synthesized, as negative controls for MMP sensitivity (Table 4. 13).

Table 4. 13 Different MMP-sensitive peptides and its corresponding scrambled peptide.

	MMP-9	MMP-7
<b>MMP-Sensitive Peptide</b>	GPVGLIG [9]	AHX-RPLALWRS-AHX [11]
<b>Scrambled Peptide</b>	GIVGPLG [10]	AHX-RSWLPLRA-AHX [12]

The synthesis of these four peptides was carried out in solid phase using 1-1.5 g of 2-chlorotrytil resin (1.6 mmol/g peptide) using Fmoc-protected amino acids. The peptides were grown from C to N terminal and the Fmoc group protected temporally the  $\alpha$ -amine of the coupled amino acid. Figure 4. 42 represents the SPPS scheme followed in the synthesis of the GPVGLIG peptide.

Once the peptide sequence was finally achieved, the peptidil-resin was treated with an acidic solution of DCM:TFA (95:5, v/v). The next step consisted on the evaporation of TFA and the precipitation of the peptide in cold diethyl ether. For peptides [9] and [10] no further purification was necessary. In the case of the MMP-7 and scrambled-MMP-7 peptides, it was necessary to remove all the side-chain protecting amino groups with an overnight treatment with a solution of TIS/H<sub>2</sub>O/EDT/TFA (1:2.5:2.5:94, v/v/v/v). Removal of protecting groups was monitored by HPLC-MS and once completely eliminated, TFA solution was evaporated. Peptides were purified by RP-HPLC-semipreparative. All synthesis steps were controlled following the Kaiser test and the Choranyl tests.

Following this strategy peptides [9-12] were synthesized and purified. Peptide formation was confirmed by HPLC-MS and MALDI-TOF, confirming the Mw of the desired products. A total amount of 305.6 mg of GPVGLIG [9] and 149.8 mg of GIVGPLG [10] were obtained, with a purity of 97.3% and 96.8%, respectively. In the case of MMP-7 sensitive peptides, after semi-preparative HPLC purification 139.1 mg of AHX-RPLALWRS-AHX peptide [11] and 170.1 mg of AHX-RSWLPLRA-AHX peptide [12] were obtained, with a purity of 97.7% and 97.8% respectively.

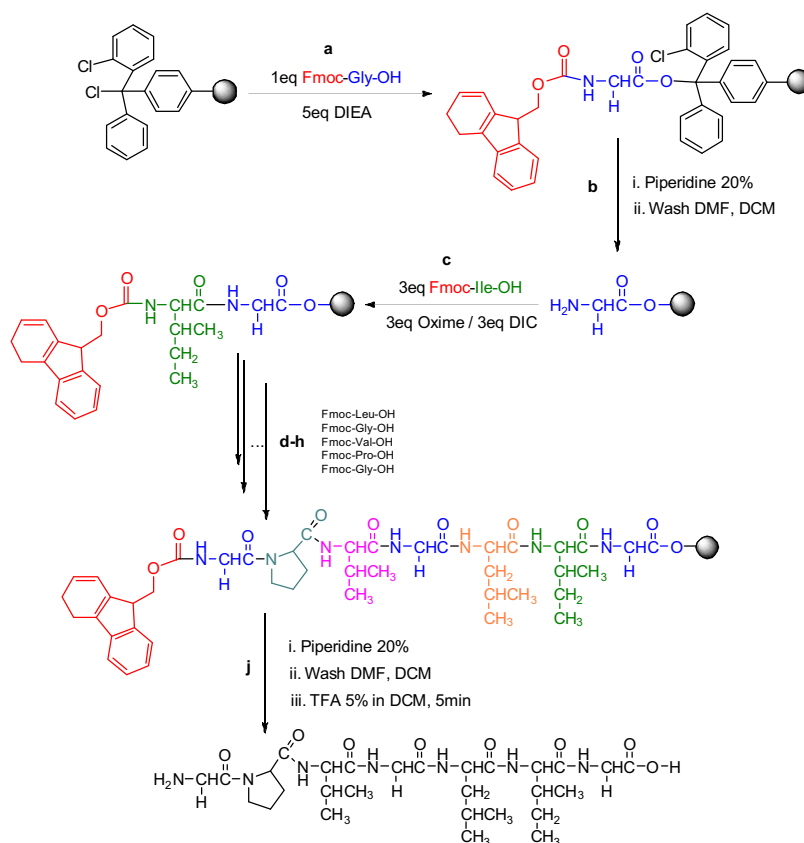


Figure 4.42 Synthesis scheme of GPVGLIG peptide by SPPS. Conditions: Cleaning and resin conditioning 5 x 1min DMF and 5 x 1 min DCM ; using 10 mL of solvent per gram of resin; a) Fmoc-Gly-OH (1eq), DIEA (5eq) in DCM, 45 min; b) (DMF (5 x 1 min) , Piperidine / DMF (2:8) ( 1 x 1 min , 2 x 20 min) , DMF (5 x 1 min) , DCM (5 x 1 min); c) Fmoc-Ile-OH (3eq), oxime (3eq), DIC (3eq) in DCM, 2h; d-h) repeat b) and c) steps for each amino acid; j) (DMF (5 x 1 min) , Piperidine / DMF (2:8) ( 1 x 1 min , 2 x 20 min) , DMF (5 x 1 min) , DCM (5 x 1 min) , TFA 5% in DCM (5min).

#### 4.2.1.1 Sequence recognition cleavage assay of the MMP-sensitive peptides synthesized

The specificity of the enzymes for the selected sequences was tested in an assay where the peptides were incubated against MMP-9 and MMP-7 enzymes. The experiment was carried out also with the scrambled sequences to confirm that they were not MMP substrates.

To proceed, 1 mg of peptides [9-12] was dissolved in PBS and MMP-9 (1µg/mL) for [9-10] peptides or MMP-7 (0.1 mg/mL) for [11-12] peptides was added, thermomixed at 37°C during 24 h and analyzed by HPLC-MS.

Figure 4.43 shows HPLC-MS chromatograms, before and after incubation of the GPVGLIG peptide [9] with MMP-9. As expected, the enzymatic activity of MMP-9, breaks down the PVGLIG peptide [9] (Mw 612.35 g/mol) into two fragments of Mw 329.19 g/mol (GPVG [9-i]) and 302.19 g/mol (LIG [9-ii]).

Similarly, the incubation of AHX-RPLALWRS-AHX peptide [11] (Mw 1224.50 g/mol) with MMP-7, resulted in two peptide fragments: 569.3 g/mol (AHX-RPLA [11-i]) and 674.3 g/mol (LWRS-AHX [11-ii]) as shown by HPLC-MS chromatograms.

In the case of the scrambled peptides (products [10] and [12]) no cleavage was observed, further confirming the specificity of selected peptide sequences ([9] and [11]).



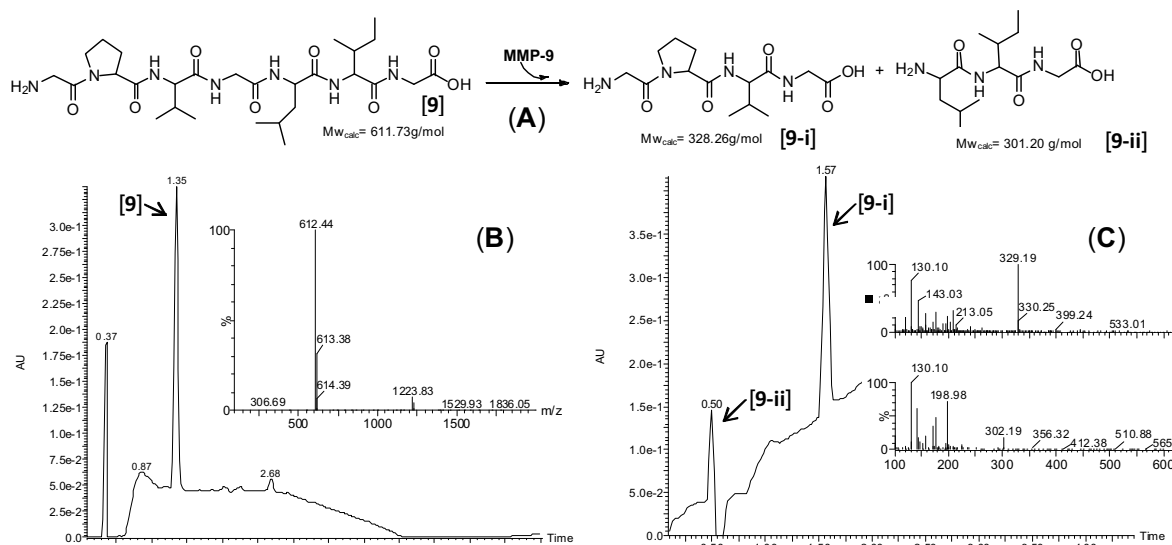


Figure 4. 43 Sequence recognition cleavage assay with the MMP-9 human enzyme of GPVGLIG. (A) Cleavage reaction; (B) HPLC-MS analysis of the GPVGLIG peptide before incubation with MMP-9 enzyme and (C) Crude HPLC-MS analysis of the incubation of GPVGLIG peptide with MMP-9 enzyme.

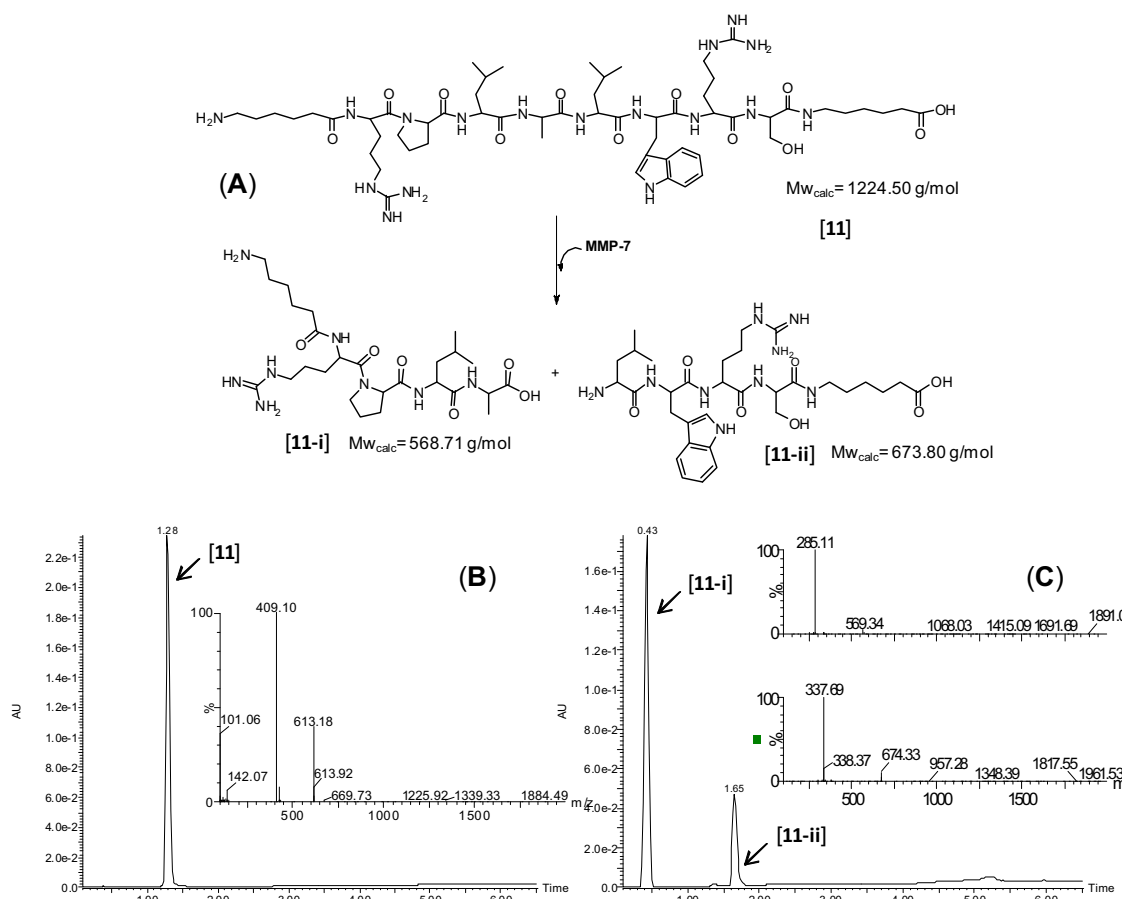


Figure 4. 44 Sequence recognition cleavage assay with the MMP-7 human enzyme of AHX-RPLALWRS-AHX. (A) Cleavage reaction; (B) HPLC-MS analysis of the AHX-RPLALWRS-AHX peptide before incubation with MMP-7 enzyme and (C) Crude HPLC-MS analysis of the incubation of AHX-RPLALWRS-AHX peptide with MMP-7 enzyme.

## 4.2.2 Study of the bond nature between the drug and the MMP-sensitive peptide

The PGA-MMPpept-5FU conjugates were designed as a tripartite structure composed by: the PGA carrier, the MMP-linker and the anticancer drug 5-FU. In section 4.1, the linker in the PGA-5-FU system was an adipic acid molecule attached to 5-FU through an ester bond.

In the case of PGA-MMPpept-5FU conjugates, in addition to the ester bond, the carbamate bond between 5-FU and the N-terminal of the peptides [9-12] was studied to evaluate the kinetic release of 5-FU. It is worth mentioning that in these conjugates we expected the release of 5-FU produced by the activity of the MMPs and that corresponding to the hydrolysis of the bond between the drug and the MMP-sensitive linker.

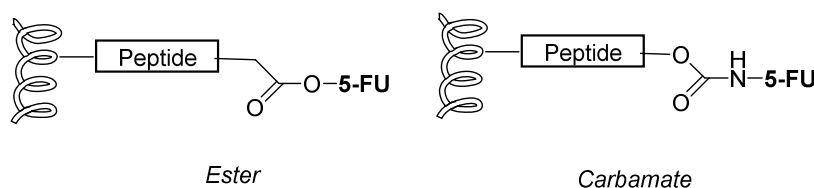



Figure 4. 45 Drug-peptides bonds studied, where  represents the polymer backbone.

### 4.2.2.1 Methodology for the synthesis of the 5-FU conjugated to the MMP-sensitive peptide containing a carbamate bond

The MMP-9 sequence was used in the first stage of the project to set up the synthetic methodology to achieve the carbamate bond between the drug and the peptide. Once obtained, it was possible to evaluate the suitability of the carbamate bond for the final conjugate in the *in vitro* tests (plasma and pHs) and in the study of its cytotoxicity in the HCT-116 CRC cell line.

Unexpectedly, different strategies were checked to get the drug-peptide moiety (5FU-GPVGLIG) containing the carbamate bond.

#### 4.2.2.1.1 Carbamate bond formation: Strategy 1

The first strategy consisted on the activation of 5-FU to get an intermediate product that will further react directly in the N-terminal of the peptide through a carbamate bond formation. Two different alternatives were studied.

- The **first alternative** consisted on the formation of product [13] through the activation of 5-FU with DSC. Then, in a second step this intermediate would react with the N-terminal of the peptide forming the carbamate bond.

Initially, the reaction was performed with only 1.2 eq of DSC. Unlikely, it did not run and it was evaluated an excess of 3 and 10 eq of DSC in the presence and absence of TEA. Finally product formation was observed by HPLC-MS ( $Mw_{calc} = 301.3$  g/mol,  $ESI_{found}[M+H]^+ = 301.95$  g/mol) when using 10 eq of DSC and TEA. In order to evaluate the formation of the carbamate bond, it was left to react overnight with 3-phenyl-1-propylamine. This product

was used in this initial stage of the project to check the carbamate bond formation in a small scale and thus avoid the peptide consumption. However, the desired product was not obtained.

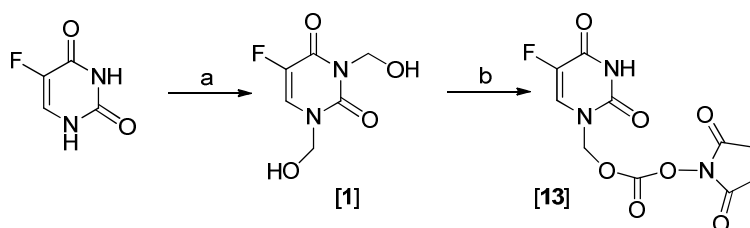


Figure 4.46 Synthesis of 5-FU derivative with DSC. Conditions: a) HCHO 37% (6eq), 1h, 55°C; b) DSC (10 eq), TEA (10 eq), 2h, rt, ACN.

- o The **second alternative** consisted on the formation of product [14] through the activation of 5-FU with nitrophenylchloroformate<sup>144</sup>. Then, the carbamate bond formation was expected through the reaction of the nitrophenyl activated 5-FU and the N-terminal of the peptide.

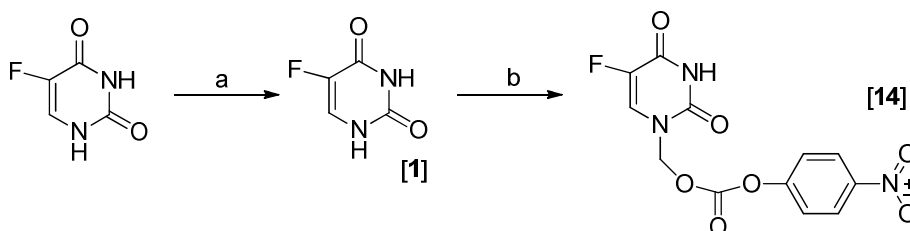


Figure 4.47 Synthesis of 5-FU derivative with nitrophenylchloroformate [14]. Conditions: a) HCHO 37% (6eq), 1h, 55°C; b) TEA (1.5 eq), nitrophenylchloroformate (1.5 eq), ACN (anhydrous), ovr, rt.

Once product [1] was obtained, a first test was performed with nitrophenylchloroformate and TEA in anhydrous ACN. The reaction mixture was left to react overnight at rt. Product [14] was detected by HPLC-MS ( $Mw_{calc} = 325.21$ ,  $ESI_{found}[M+H]^+ = 326.1$ ). In order to check the carbamate formation it was left to react with 3-phenyl-1-propylamine at 40 °C, during 1 h in anhydrous ACN. In this case the product [15] was obtained ( $Mw_{calc} = 321.30$ ,  $ESI_{found}[M+H]^+ = 321.90$ ) but conversion was very low.

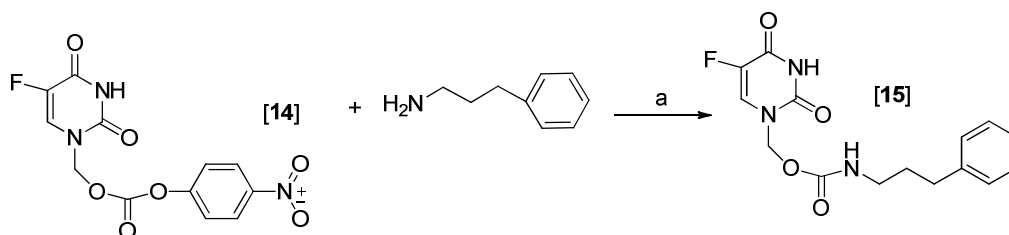


Figure 4.48 Synthesis of product [15]. Conditions: a) 3-phenyl-1-propylamine (1.5 eq), ACN (anhydrous) 1 h, 40°C.

Regarding the dirty crude obtained in the product [14] formation, it was decided to optimize the reaction conditions to avoid the purification step of the intermediate reagent. A first test was performed in anhydrous pyridine<sup>145</sup> as a solvent and 2 eq of nitrophenylchloroformate. In this case even dirtier crude was obtained. Then, it was tested the formation of 4-o-p-nitrophenyl-oxycarbonyl-5-FU<sup>145</sup>, product [14] by stirring the

reaction mixture in anhydrous DCM under reflux (40 °C) overnight. Product was successfully obtained ( $Mw_{\text{calc}} = 325.21$ ,  $ESI_{\text{found}}[M+H]^+ = 326.1$ ) and purified by flash-chromatography. In the same manner as in the previous test, the product was made to react with 3-phenyl-1-propylamine, and, although the product was detected by HPLC-MS, conversion was very low and the crude was dirtier.

#### 4.2.2.1.2 Carbamate bond formation: Strategy 2

Since it was not possible to obtain the carbamate bond directly on the N-terminal position of the peptide, a second strategy was thought in a two steps process (Figure 4. 49). The first step consisted on the modification of 5-FU in the N1 position to get a 5-FU-derivative containing a carbamate bond and a free carboxylic group that will further react in the second step of the process with the N-terminal of the peptide.

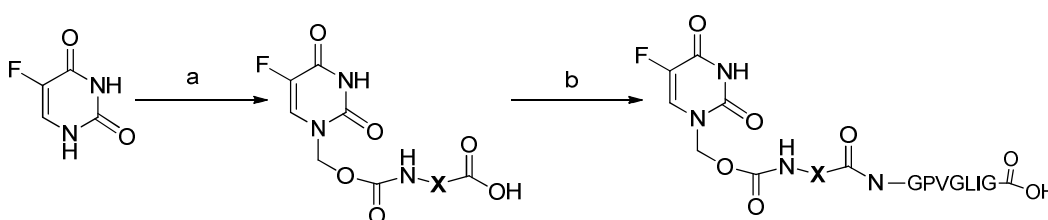


Figure 4. 49 Scheme of the synthesis strategy process proposed for the obtention of 5-FU-GPVGLIG moiety through a carbamate bond. a) Corresponds to the formation of the 5-FU-derivative containing the carbamate bond in the N1 position of 5-FU. b) Corresponds to the linkage of 5-FU-derivative to the N-terminal of the peptide through an amide bond.

In order to get the 5-FU derivative containing the carbamate bond it was necessary to synthesize product [17] through the reaction of chloromethyl chloroformate and a glycine protected in the X position<sup>146</sup>. Initially, to evaluate the suitability of the methodology the glycine ethyl ester was selected.

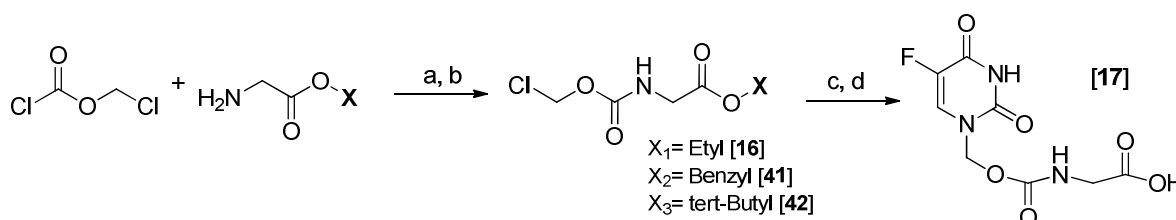


Figure 4. 50 Synthesis of product [17]. Different protecting groups were studied: ethyl, benzyl and tert-butyl (X). Conditions detailed are based on the definitive conditions find out with tert-butyl protected glycine. Conditions: a) Glycine tertbutyl ester (1eq), TEA (1.5 eq), 10 min, -20°C, anhydrous DCM; b) chloromethylchloroformate (1.1 eq), 10 min, -20 °C. Work up in H<sub>2</sub>O and collection of the organic phase; c) 5-FU (0.8 eq), TEA (2.5 eq), 50°C, 3h, DCM, flash chromatography purification SiO<sub>2</sub> column DCM /Ethyl Acetate ; d) TFA/DCM (1:3), 1h, rt.

To proceed, glycine ethyl ester hydrochloride was dissolved in anhydrous DCM and TEA (1.5 eq) added. The mixture was left at -20°C during 5 min and then chloromethyl chloroformate (1.1 eq) was added. The reaction was left at -20°C for 10 min and product formation confirmed by HPLC-MS ( $Mw_{\text{calc}} = 195.6$  g/mol,  $ESI_{\text{found}}[M+H]^+ = 195.69$  g/mol) and purified through liquid-liquid extraction in H<sub>2</sub>O and saturated NaCl. Product [16] was obtained with a high purity.

Based on the results obtained previously in our group by L. Simón, prior to the reaction of product [16] with 5-FU, it was decided to explore the carbamate formation also in the N3 position of 5-FU. In spite of the fact that the N1 position of 5-FU is more reactive, derivatives through the N3 position are more stable<sup>112,113,114</sup> though more difficult to synthesize. To reach the N3 substitution, it is necessary to protect N1 position. L. Simón worked with 1-benzyloxycarbonyloxymethyl-5-FU [18] to perform N3 substitutions on 5-FU, followed by a hydrogenation process to remove the Z protecting group. With all this information in hands, the substitution on N1 position, performing the reaction of product [16] with 5-FU directly was intended, as well as with product [18] to substitute the N3 position.

The product 1-benzyloxycarbonyloxymethyl-5-FU [18] was obtained following the synthesis process detailed in Figure 4. 51, and the crude was purified by flash chromatography.

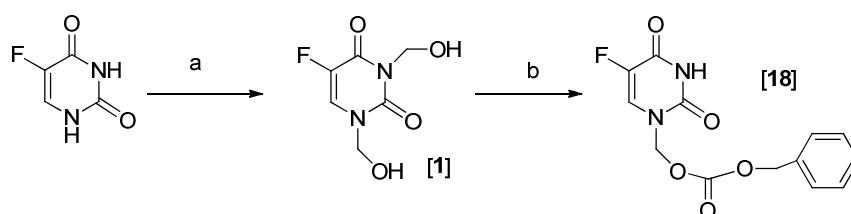


Figure 4. 51 Synthesis of product [18]. Conditions: a) HCHO 37% (6eq), 1h, 55°C; b) Benzyl chloroformate (1.5 eq), TEA (1.5 eq), o/n, rt, anhydrous ACN.

At that point, product [16] was made to react with 5-FU and product [18] using different reaction conditions. First, product [16] (1.2 eq) was mixed with 5-FU or product [18] (1 eq) in DMF with potassium carbonate (1 eq) and the reaction was left at 50°C overnight. None of the reactions worked properly. Then, TEA (3 eq) was used instead of potassium carbonate, either at rt or at 50°C, for both 5-FU and product [18]. Final product formation was confirmed by HPLC-MS after 3 h reaction at rt. Products [19] and [20] were obtained when reactions were performed at 50°C. Reaction for product [20] ran slowly, due to the lower reactivity of the N3 amino group of 5-FU (Figure 4.52), and therefore working with this product was discontinued. In the case of the reaction with 5-FU, once the product [19] was formed it was also detected the 5-FU disubstituted product (in N1 and N3 positions) in a very little quantity. In this case, product [19] was easily purified by flash-chromatography and obtained in a high purity (98.6%).

Figure 4. 53 shows the <sup>1</sup>H-NMR spectra of product [19] prior to be hydrolyzed with Ba(OH)<sub>2</sub>, and Figure 4. 54 shows the <sup>1</sup>H-NMR spectra of the [19] hydrolysis crude performed with Ba(OH)<sub>2</sub>. In both cases, the presence of free 5-FU confirmed the low stability of the carbamate bond in these conditions.

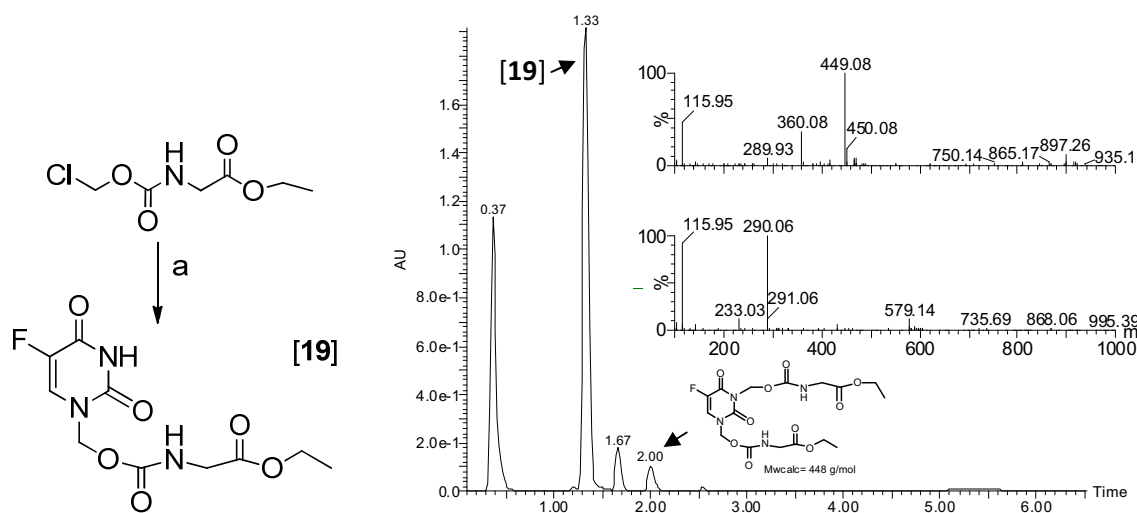


Figure 4.52-A HPLC-MS Chromatogram of product [19]. Conditions: a) product [16] (1.2 eq), 5-FU (1 eq), TEA (3 eq), DMF, 3 h, 50 °C.

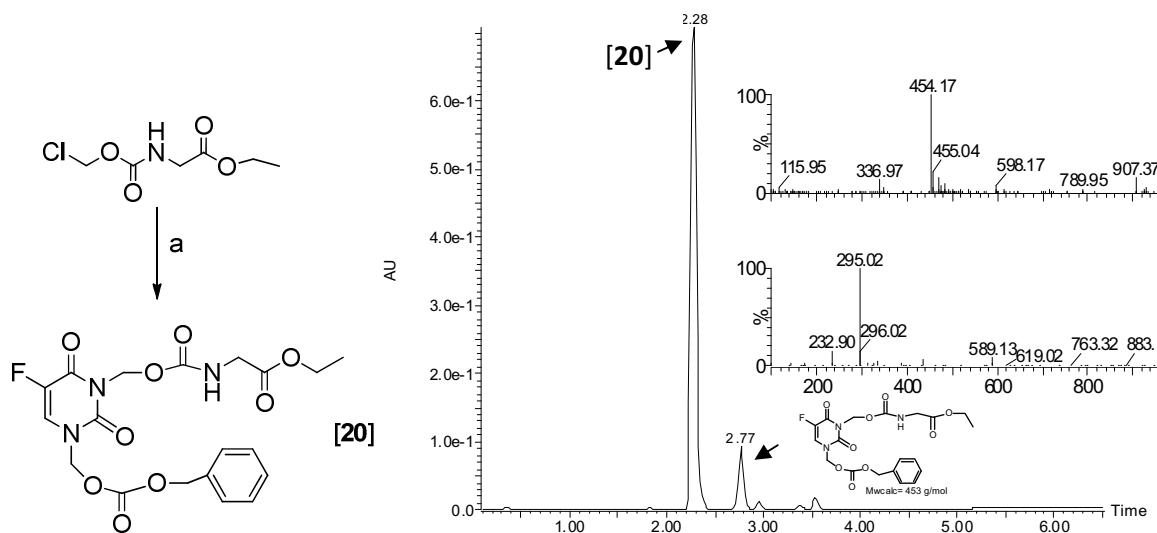


Figure 4.52 HPLC-MS Chromatograms of products [19] and [20]. Conditions product [19]: a) product [16] (1.2 eq), 5-FU (1 eq), TEA (3 eq), DMF, 3 h, 50 °C. Conditions product [20]: a) product [16] (1.2 eq), Product [18] (1 eq), TEA (3 eq), DMF, 3 h, 50 °C.

Table 4.14 Summary of the different hydrolysis conditions tested for the ethyl ester elimination of product [19].

Hydrolysis conditions for <chem>R-C(=O)OCC</chem>
Ba(OH) <sub>2</sub> (1.5 eq), 1 h, rt, H <sub>2</sub> O/THF (1:1)
LiOH (1 and 3 eq), 1 h, rt H <sub>2</sub> O/THF (1:3),
NaOH (1 eq), o/vn, rt, THF/H <sub>2</sub> O (3:1) // NaOH (1 eq) in MeOH <sup>147</sup>
Trimethylsilane, 80°C and rt, 2 h, ACN reflux

Once clear the difficulty of removing the ethyl protecting group without releasing free 5-FU, different protecting groups not labile in basic conditions as well as the coupling of not protected Glycine were checked.

When using not protected Glycine, the product generated in the reaction with chloromethyl chloroformate corresponded to the addition of two glycines. Even though it was made to react with 5-FU and a dirty crude was obtained and discarded for purification. Alternative protecting groups to the ethyl ester were checked.

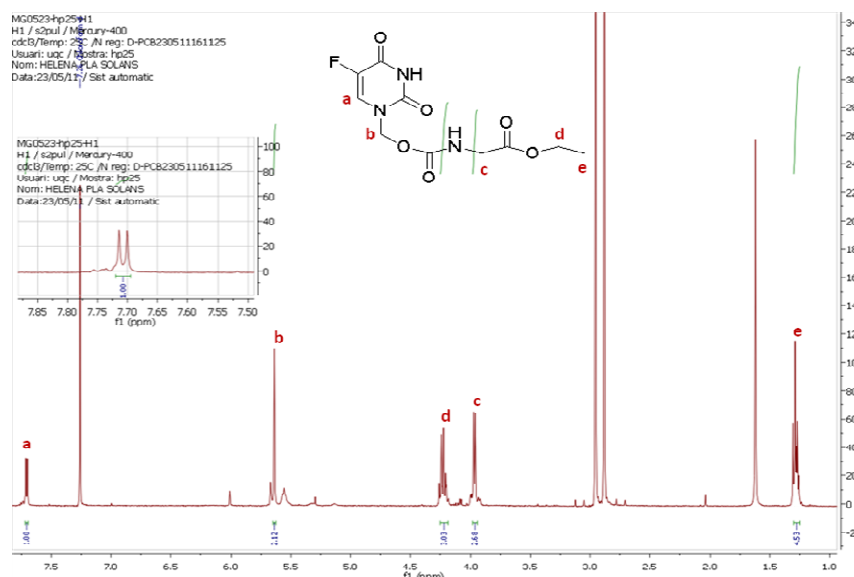


Figure 4. 53  $^1\text{H-NMR}$  of product **[19]** (400 MHz,  $\text{CDCl}_3$ )  $\delta$ : 7.69 (d,  $J=5.6\text{ Hz}$ , 2H), 5.62 (s, 2H), 4.21 (q,  $J=8\text{ Hz}$ , 3H), 3.95 (d,  $J=4\text{ Hz}$ , 2H), 1.26 (m, 3H).

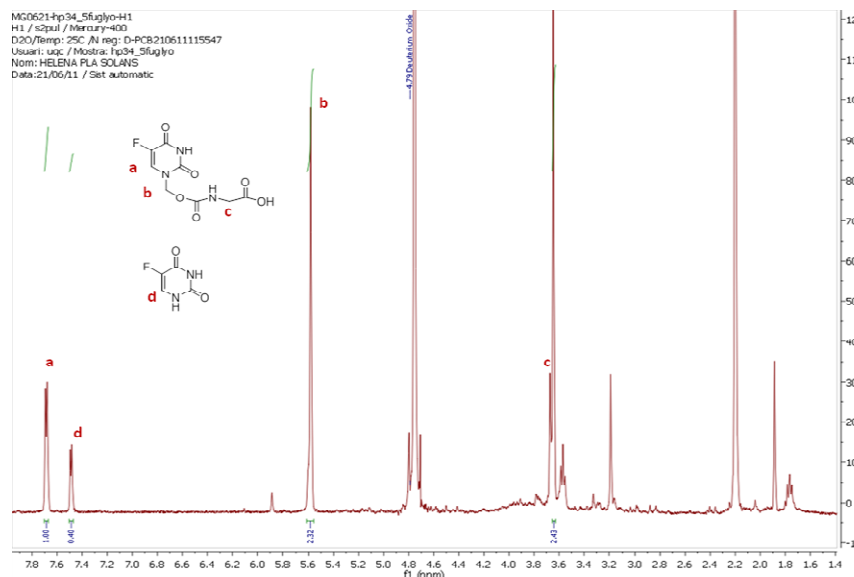


Figure 4. 54 Example of  $^1\text{H-NMR}$  of product **[19]** hydrolyzed in  $\text{Ba}(\text{OH})_2$  conditions. As observed, product **[19]** was hydrolyzed giving two different products: product **[17]** and 5-FU.

Therefore, benzyl and *tert*-butyl protecting groups were evaluated. Both 5-FU derivatives [21] and [22] (Figure 4. 55) were synthesized according to the previous conditions set up for the synthesis of product [19] and also purified by flash chromatography.

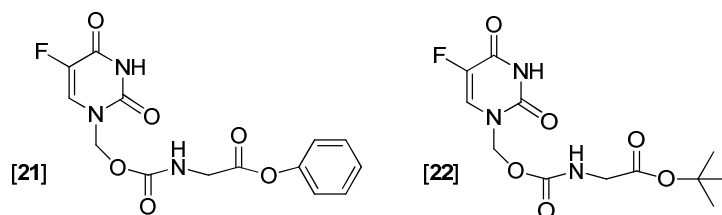


Figure 4. 55 Chemical structure of products [21] and [22].

Table 4. 15 summarizes the reaction conditions tested for the deprotection of the benzyl and *tert*-butyl groups. Successfully, the hydrolysis of product [22] with TFA 95% the carbamate bond between 5-FU and Glycine was stable and no 5-FU was released. This result was confirmed by <sup>1</sup>H-NMR.

Table 4. 15 Summary of the different protecting groups and the conditions tested for the deprotection of product [21-22].

Protecting Group	Hydrolysis conditions
	LiOH (1 and 3 eq), 1 h, rt, H <sub>2</sub> O/THF (1:3)
	HCl 4M in 1,4-dioxane, ovn, rt TFA 95%, ovn, rt

Then, the use of  $\beta$ -alanine *t*-butyl ester (Figure 4. 56) instead of glycine *t*-butyl ester since  $\beta$ -alanine is a better spacer moiety was explored. The deprotection was evaluated in a mixture of TFA/DCM (1:3) and analyzed after 1 h. Product [24] (5-FU-Ala-OtBu) was completely hydrolyzed leading product [25] (5-FU-Ala) and the carbamate bond remained stable. This result was also confirmed by <sup>1</sup>H-NMR and HPLC showing a high pure product (97.37%) (Figure 4. 57).

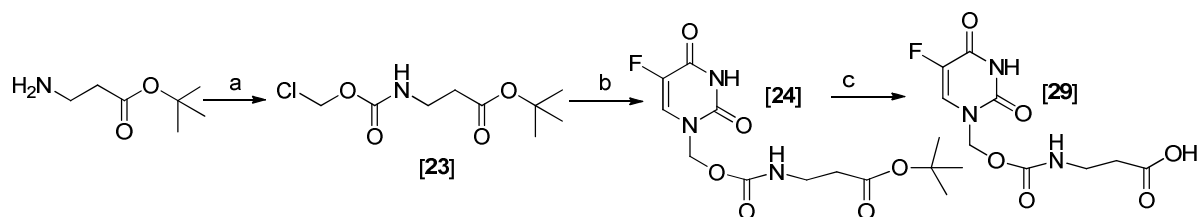


Figure 4. 56 Synthesis of product [29]. Conditions: a)  $\beta$ -alanine *t*-butyl ester (1eq), TEA (1.5 eq), 10 min, -20°C, anhydrous DCM, chloromethylchloroformate (1.1 eq), 10 min, -20 °C. Work up in H<sub>2</sub>O and collection of the organic phase; b) 5-FU (0.8 eq), TEA (2.5 eq), 50°C, 3 h, DCM; c) TFA/DCM (1:3), 1 h, rt.



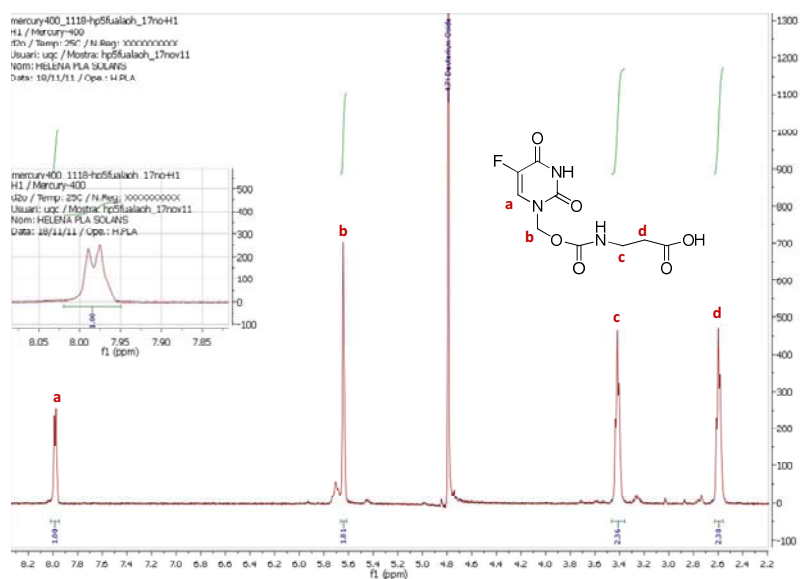


Figure 4.57  $^1\text{H-NMR}$  of product [25] obtained after the hydrolysis of product [24] in TFA/DCM (1:3), 1h, rt.  $^1\text{H-NMR}$  (400 MHz,  $\text{CDCl}_3$ )  $\delta$ : 7.84 (d,  $J=4$  Hz, 1H), 5.50 (s, 2H), 3.27 (t,  $J=4$  Hz, 2H), 2.45 (t,  $J=4$  Hz, 2H).

#### 4.2.2.1.3 Conjugation of the 5-FU modified through a carbamate bond and the MMP-sensitive peptides

The following step consisted on conjugation of product 5-FU-Ala [25] and the MMP-sensitive peptide. As mentioned before, the evaluation of the carbamate linkage was carried out with the MMP-9 sensitive peptide and its corresponding scrambled peptide. To proceed, product 5-FU-Ala [25] was activated with pentafluorophenol previously to the amide bond formation with the N-terminal of products [9-10].

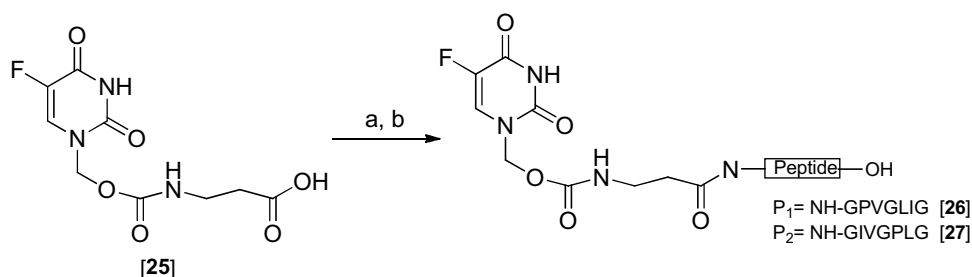


Figure 4.58 Synthesis of products [26] (5-FU-Ala-MMP9pept) and [27] (5-FU-Ala-MMP9scram). Conditions: a) Activation (1.5 eq pentafluorophenol, 1.5 eq EDC, 0.5 eq DMAP in DCM, 3h, rt); b) peptide [9]/[10] (0.9 eq), pH= 8 adjusted with DIEA, DCM, ovn, rt.

Both N-substituted peptides [26] (5-FU-Ala-MMP9pept) and [27] (5-FU-Ala-MMP9scram) were purified by means of semi-preparative HPLC in  $\text{H}_2\text{O}:\text{ACN}$  in acid media, finally obtaining purities of 98.7% and 97.5%, respectively.

#### 4.2.2.1.4 Stability tests of the 5-FU-Ala-MMP9 product [26] containing a carbamate bond

Although the degradation of a PDC and a linker-drug moiety in media (plasma, pHs or cell medium) is expected to be different since the conformation of both systems is clearly distinct. In section 4.1.2.4 we confirmed that the ester bond present in the PGA-5-FU system remains stable in plasma thanks to the conformation of the polymer-drug conjugate, whereas it is labile when the linker-

drug moiety is not conjugated to the polymer. At this stage of the project, the use of the carbamate bond was new, so we decided to evaluate the stability and degradability of the linker-drug moiety (product 5-FU-Ala-MMP9pept [26]), as an informative assay.

The kinetic release of 5-FU and the cytotoxicity of product [26] in HCT-116.Fluc CRC cell line was addressed. It is necessary to mention that, besides the evaluation of product 5-FU-Ala-MMP9pept [26] as a substrate for MMP-9, it is really important to know if the released product has a cytotoxicity comparable to 5-FU. The product of the MMP-9 activity corresponds to a peptidyl drug unit, containing 4 amino acids (GPVG) linked through a carbamate bond to 5-FU that ideally should be degraded releasing free 5-FU. Therefore, it is important to study the stability of product (5-FU-GPVG), hence the facility of the carbamate bond to release 5-FU.

- **pH stability:** 1 mg of product 5-FU-Ala-MMP9 [26] was incubated at 37°C in 100 µL of PBS at 3 different pH (5.5, 6.5 and 7.3) and the amount of 5-FU released after 24 h incubation was analyzed by HPLC-UV. Resorcinol was used as an internal standard.

As shown in Figure 4. 59 only 0.5 % of 5-FU was released after 24 h of incubation at pH 7.3. No detectable 5-FU release was observed at pH 5.5 or 6.5. This confirmed the high stability of the carbamate bond at the pHs tested, in contrast to the high lability observed in basic conditions (Table 4.14).

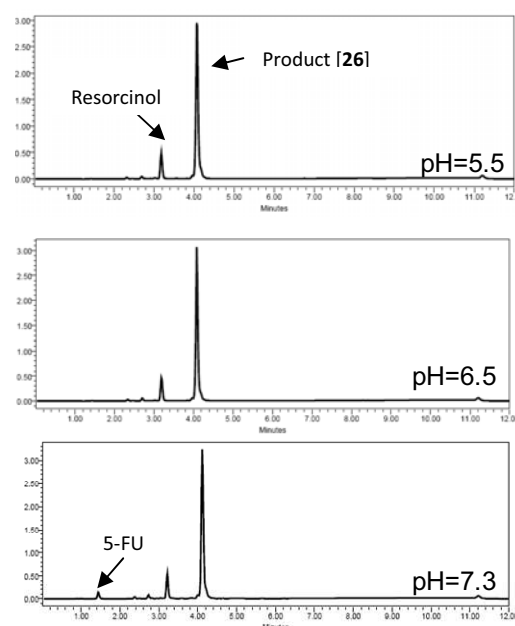


Figure 4. 59 HPLC chromatograms after 24 h of incubation at 37 °C of product 5-FU-Ala-MMP9pept [26] at different pH. Three different peaks can be distinguished: 5-FU (purple), Resorcinol (IS) (green), product [26] (red). Only at pH= 7.3 a 5-FU release is detected.

- **MMP-9 responsiveness:** 1 mg of product 5-FU-Ala-MMP9pept [26] was dissolved in H<sub>2</sub>O and MMP-9 (10 µg/mL) was added. Aliquots of 5 µL were taken at different times and analyzed by HPLC-MS to detect the 5-FU-GPVG Mw. Furthermore, the analysis by HPLC allowed the quantification of the kinetic release of the peptidyl 5-FU. Figure 4. 60 represents the release of 5-FU-GPVG, and as it can be clearly seen, product 5-FU-Ala-MMP9 [26] was able to be cleaved by MMP-9. Interestingly, the release was not too fast and it confirmed that the carbamate bond remained unaffected by the enzyme MMP-9.

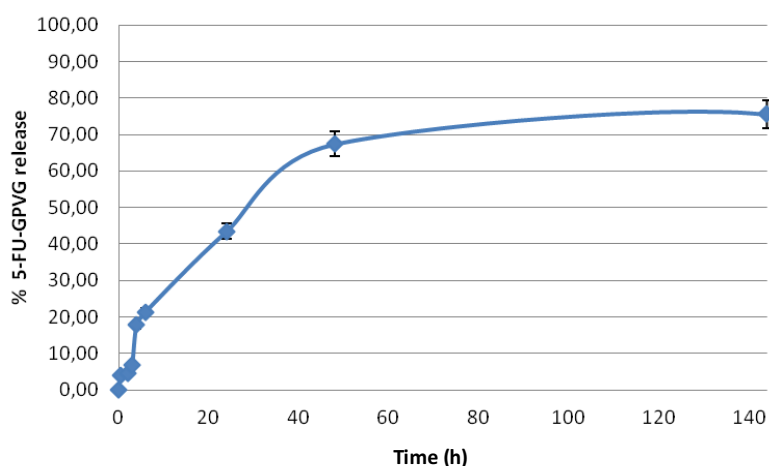


Figure 4. 60 Kinetic release of 5-FU-GPVG from product 5-FU-Ala-MMP9 [26] over the time when incubated with MMP-9. The quantification was performed by HPLC.

- **Cytotoxicity of product 5-FU-Ala-MMP9 [26] in HCT-116 CRC cell line:** As mentioned before, although it was necessary to evaluate if the synthesized product was a substrate for MMP-9, it was important to test its cytotoxicity to check if the released 5-FU peptidyl product (5-FU-GPVG) was still effective in the inhibition of CRC cells proliferation.

An MTT experiment was performed in HCT-116 CRC cell line. Even though the experiment could be done in CRC cells with MMP-9 overexpression, it was considered that the cytotoxicity associated to the product would be also associated to the lability of the carbamate bond, and therefore, the experiment in CRC cells without MMP-9 overexpression could

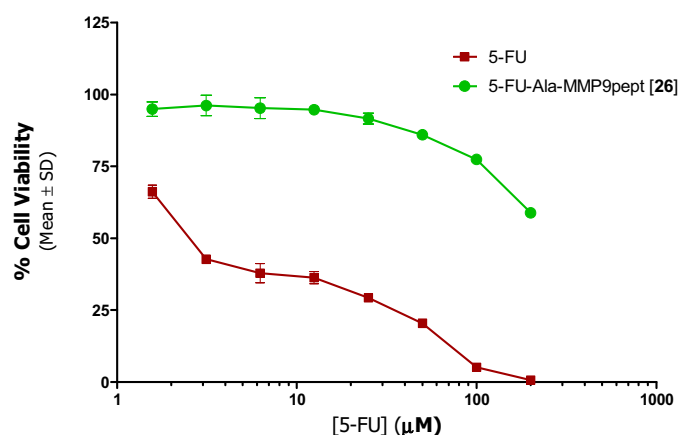


Figure 4. 61 Cytotoxicity curves of product [26] and 5-FU in HCT-116 CRC cell line.

give enough information to evaluate the suitability of the carbamate bond in the final polymer-drug conjugate sensitive to MMP-7 or MMP-9.

The cytotoxicity of product 5-FU-Ala-MMP9pept [26] was performed following the MTT methodology with 72 h incubation time (section 3.9.1). The maximum concentration tested was 200 μM eq of 5-FU. At the concentrations tested, when increasing product 5-FU-Ala-MMP9pept [26] concentration the cell viability decreased. Nevertheless, still the maximum concentration tested (200 μM eq 5-FU) was not sufficient to achieve significant toxicity. Unfortunately, the stability of the carbamate linkage was too high, greatly limiting its activity as a cytotoxic drug, similar to free 5-FU ( $IC_{50}$  (5-FU):  $3.36 \pm 0.04 \mu M$ ;  $IC_{50}$  (5-FU-Ala-

MMP9pept):  $323.20 \pm 0.03 \mu\text{M}$ ). Although the experiment was not performed in CRC cells overexpressing MMP-9 and despite when we performed the incubation of product 5-FU-Ala-MMP9 [26] with MMP-9 we saw a good sustained release associated to the MMP-9 cleavage.

In addition, a parallel work performed in our group (M. Melgarejo) with a 5-FU-PEG molecule containing also a carbamate linkage between the carrier and 5-FU, demonstrated that the stability of the carbamate bond in plasma was too high, and a very little amount of 5-FU was released.

With these results in hand it was decided to evaluate the suitability of an ester bond between the drug and the carrier and abandon the carbamate bond strategy.

#### 4.2.2.2 Conjugation of 5-FU to the MMP-sensitive peptide through an ester bond

As shown above, the study of the feasibility of using a carbamate bond in a PGA-MMPpept-5FU conjugate was carried out with the MMP-9 sensitive peptide. However, for the study of the ester bond we performed most of the work with the peptide sensitive to MMP-7. The reason for this decision was the higher prevalence/selectivity of MMP-7 in CRC tissues. In addition to its overexpression in CRC tissues, MMP-9, is also present at sites of inflammation. Thus, we decided to focus mainly on the MMP-7 enzyme that is more exclusive of CRC tissues.

As for the carbamate bond, the feasibility of the ester linkage was evaluated with a model that consisted in the drug conjugated to the peptide linker. Therefore, it was necessary to synthesize products [28-30] that corresponded to 5-FU conjugated to the N-terminal of the peptides [9,11,12] through an ester bond. Products [28], [29] and [30] were named: 5-FU-adipic-MMP7pept [28], 5-FU-adipic-MMP7scram [29] and 5-FU-adipic-MMP9pept [30].

Figure 4. 62 shows the synthetic route that started from product 5-FU-adipic [2] used in section 4.1 for the synthesis of PGA-5-FU conjugates. The free carboxylic group of product [2] was activated with pentafluorophenol (1.5 eq) in a reaction performed at rt with EDC (1.5 eq) and DMAP (0.5 eq) in DCM. Then, the conjugation to the N-terminal of the peptides was carried out in DMF and DIEA at rt. Products [28-30] were purified by semipreparative HPLC, and were obtained in a high purity (99.3%, 99.9%, 99.9%, respectively).

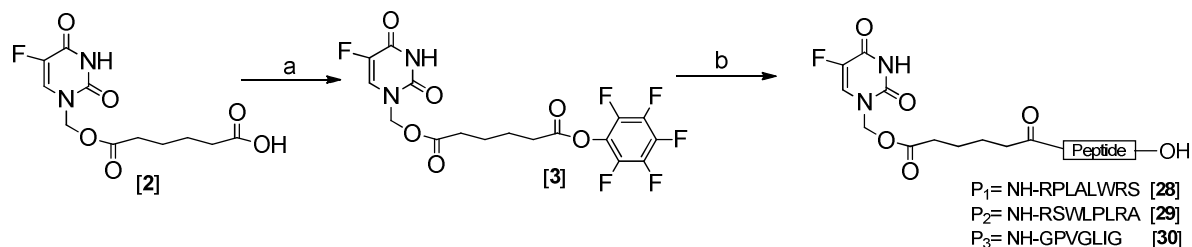


Figure 4. 62 Synthesis of products [28-30]. Conditions: a) pentafluorophenol (1.5 eq), EDC (1.5 eq), DMAP (0.5 eq), DCM, 3 h, rt; b) Peptide [9]/[11]/[12] (0.9 eq), pH=8 adjusted DIEA, o/vn, rt, DMF.

#### 4.2.2.3 Stability tests of the unit 5-FU-peptide moiety conjugated through an ester bond

Once the products were synthesized, the stability and degradation experiments were performed in different mediums: plasma, 3 different pHs (in PBS) and in the presence of MMP-7 or MMP-9. In addition, *in vitro* experiments were carried out in CRC cell lines in order to evaluate the cytotoxicity of the synthesized products.

##### 4.2.2.3.1 Stability tests of the 5-FU-adipic-MMP7pept and 5-FU-adipic-MMP7scram [28-29]

- pHs: 1.5 mg of product 5-FU-adipic-MMP7pept [28] was incubated at 37°C in 100 µL of PBS at 3 different pH (5.4, 6.53 and 7.47), aliquots of 5 µL were taken at scheduled times and analyzed by HPLC-UV to quantify the amount of 5-FU released, as previously described.

Table 4. 16 summarizes the average release of 5-FU from product 5-FU-adipic-MMP7scram [29] after 24 h and 72 h of incubation at 3 different pHs. As expected due to the nature of the ester bond, confirming that the linkage remained stable in these conditions.

Table 4. 16 Summary of the % of 5-FU released from product [29] when incubated at different pH.

	Time /h	pH 5.40	pH 6.53	pH 7.47
% 5-FU release	24 h	0.34%	0.45%	0.63%
	72 h	0.40%	0.55%	1.21%

- **Plasma:** 1 mg of products [28-29] was dissolved in 100 µL of mice plasma, aliquots of 5 µL were taken at scheduled times and analyzed by HPLC-UV to quantify the amount of 5-FU released. As shown in Figure 4.63, the stability of the ester bond was really low in plasma. This could be explained due to the presence of esterases in plasma. However, it is important to note that the PDC is a tripartite structure and that this experiment evaluated the stability of the peptide-drug conjugate previous to its union to the polymeric carrier.

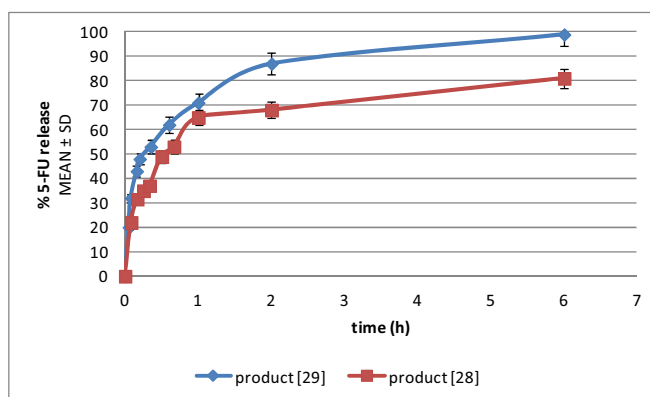


Figure 4. 63 Kinetic release of 5-FU over the time when incubating product 5-FU-adipic-MMP7 [28] (red line) and product 5-FU-adipic-ScramMMP7 [29] (blue) in plasma. 5-FU quantification was performed by HPLC.

- **MMP-7 responsiveness:** With the aim of evaluating the specificity against MMP-7 of product [28], a sequence recognition cleavage assay with MMP-7 enzyme was performed. To proceed, 1mg of product [28] was dissolved in PBS and then MMP-7 (0.1 mg/mL) was added. It was left at 37°C during 24 h and then it was analyzed by HPLC-MS.

Figure 4.64 shows chromatograms of the starting product 5FU-peptide derivative and the crude after incubation with the MMP-7 enzyme. The starting product [28] has a Mw of 1494.71 g/mol and the HPLC-MS detected a Mw of 748.20 g/mol that corresponds to the  $[M+2H]^{2+}$  ion. After 24 h of incubation with MMP-7, when the crude was analyzed by HPLC-MS two new peaks appeared (one of them is double peak with the same ionogram). The main peak showed a Mw of 839.38 g/mol that corresponds to the  $[M+H]^+$  of the 5-FU-RPLA released product. Therefore, it was confirmed that the conjugation of the drug to the MMP-7-sensitive linker did not avoid the MMP-7 enzymatic activity in product [28].

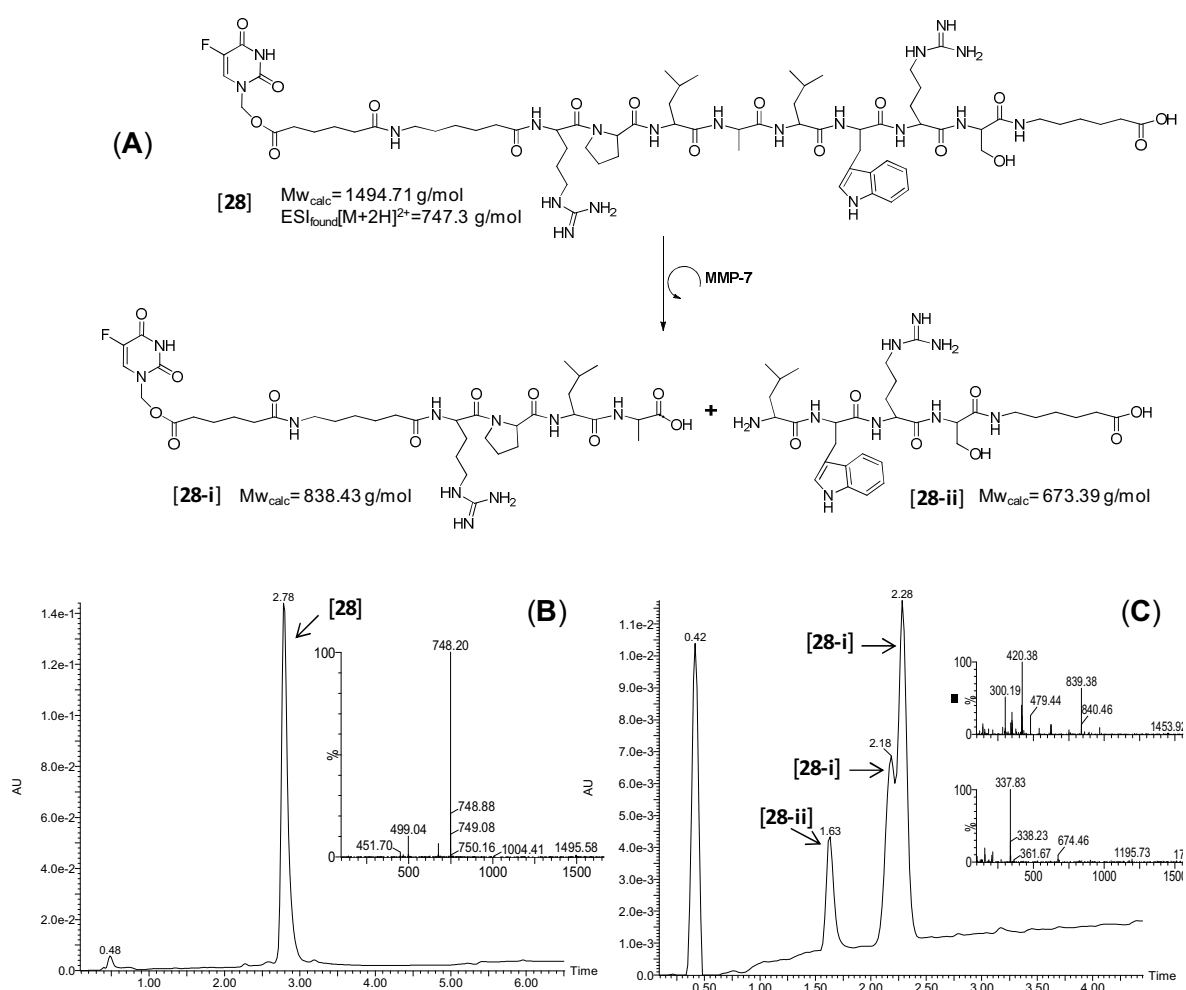


Figure 4. 64 Sequence recognition cleavage assay with MMP-7 human enzyme of product [28]. (A) Cleavage reaction; (B) HPLC-MS analysis of product [28] and (C) Crude HPLC-MS analysis of the incubation of product [28] with MMP-7 enzyme.

- **Cytotoxicity of products 5-FU-adipic-MMP7pept [28] and 5-FU-adipic-MMP7scram [29] against HT-29 CRC cell line overexpressing MMP-7:** The cytotoxicity evaluation of the MMP-7-sensitive product [28] and scrambled control [29] 5-FU-adipic-MMP7scram was performed in HT-29 CRC cells overexpressing MMP-7 at the FVPR Laboratory (CIBBIM-Nanomedicine, VHIR). MMP-7 overexpression was accomplished by incubating the HT-29 cells with Tumor Necrosis Factor (TNF $\alpha$ ) (100 ng/mL)<sup>148</sup>, as further confirmed by a Western Blot analysis of HT-29 cell lysates and conditioned media.

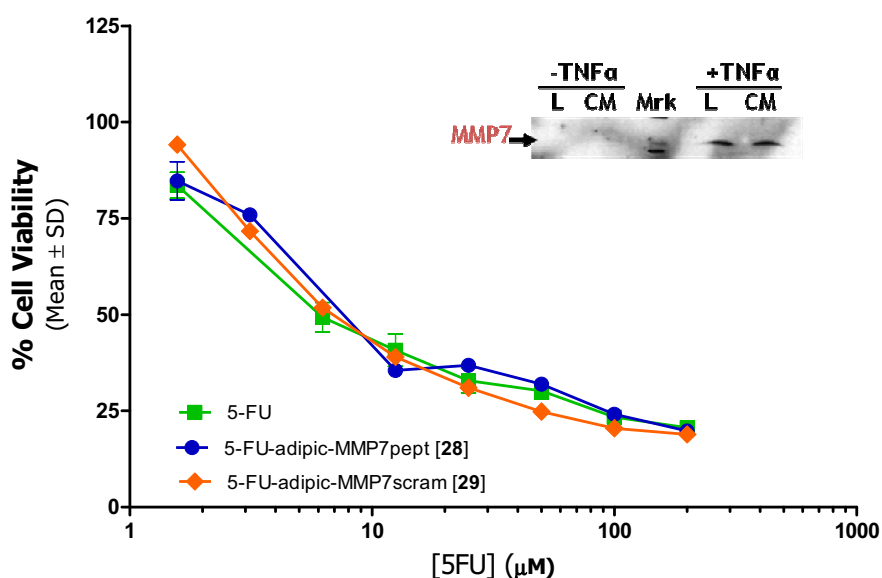


Figure 4. 65 Cytotoxicity curves of products [28], [29] and 5-FU in HT-29 CRC cell line overexpressing MMP-7. On top is shown the Western Blot of HT-29 cell lysates (L) and conditioned media (MC) showing signal when incubating with TNF $\alpha$ , thus demonstrating MMP-7 overexpression.  $IC_{50}(5-FU)$ :  $9.29 \pm 0.06 \mu M$ ;  $IC_{50}(5-FU-adipic-MMP7)$ :  $16.20 \pm 0.007 \mu M$ ;  $IC_{50}(5-FU-adipic-ScramMMP7)$ :  $10.8 \pm 0.04 \mu M$ .

The cytotoxicity of products [28,29] was performed following the MTT methodology with 72 h incubation time (section 3.9.1) The maximum concentration tested was 200  $\mu M$  eq of 5-FU. At the concentrations tested, it was noted that when increasing product [28,29] concentration the cell viability experimented the same behavior to 5-FU. Nonetheless, the same behavior was observed for the MMP-sensitive product and the negative control (scrambled peptide). Thus, it could be confirmed that the low stability of the ester linkage produced a fast kinetic release of 5-FU. For this reason, the evaluation of the influence of the MMP-7 overexpression on the cytotoxic activity when comparing products [28] and [29] could not be accomplished.

#### 4.2.2.3.2 Stability tests of the 5-FU-adipic-MMP9pept [30] containing a ester bond

*The experiments on this section were partially performed by a Master student (Bárbara González) under our supervision.*

- **pHs:** 1.5 mg of product [30] was incubated at 37 °C in 100  $\mu L$  of PBS at 3 different pH (5.4, 6.53 and 7.47), aliquots of 5  $\mu L$  were taken at scheduled times and analyzed by HPLC-UV, to

quantify the amount of 5-FU released as previously described. The product was stable at all pHs and at 24 h, 5-FU release was 4.1% at pH = 7.4, 2.53% at pH= 6.5 and 1.76% at pH=5.5. However, none of the 3 pHs display an important released of drug.

- **Plasma:** 1 mg of product 5-FU-adipic-MMP9pept [30] was dissolved in 100  $\mu$ L of mice plasma, aliquots of 5  $\mu$ L were taken at scheduled times and analyzed by HPLC-UV to quantify the amount of 5-FU released. As shown in Figure 4. 66, the stability of the ester bond was really low in plasma. Product 5-FU-adipic-MMP9pept [30] was rapidly degraded releasing more than the 80% of 5-FU after 10 min incubation. This experiment also confirmed that enzymes present in plasma did not affect the stability of the MMP-9-sensitive peptide since no fragmentation of this peptide was detected. This result would indicate that more than 80% of product 5-FU-adipic-MMP9pept [30] would be degraded when administrated intravenously. However, it is important to note that the PDC is a tripartite structure and that this experiment evaluated the stability of the peptide-drug conjugate previous to its union to the polymeric carrier.

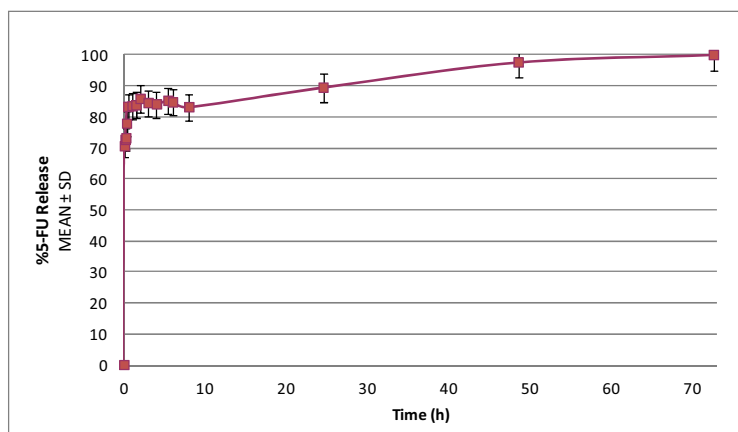


Figure 4. 66 Kinetic release of 5-FU over the time when incubating product 5-FU-adipic-MMP9pept [30] in plasma. 5-FU quantification was performed by HPLC.

- **MMP-9 responsiveness:** With the aim of evaluating the specificity against MMP-9 of product 5-FU-adipic-MMP9pept [30], a sequence recognition cleavage assay against MMP-9 enzyme was performed. To proceed, MMP-9 (10 $\mu$ g/mL) was added to 1 mg of product 5-FU-adipic-MMP9pept [30] and analyzed by HPLC-MS 24 h later. Unfortunately, no cleavage was achieved for product 5-FU-adipic-MMP9 [30]. Although as previously confirmed products GPVGLIG [9] and 5-FU-Ala-MMP9 [26] were cleaved by MMP-9, when the GPVGLIG peptide [9] was conjugated with 5-FU through an ester bond no specific peptide cleavage was observed. The experiment was performed in the same conditions as before, and in addition, new MMP-9 was used to eliminate the suspect of the loose of enzyme activity due to mishandling. Thus, there could be a hydrophobic attraction between the adipic acid and the peptide in product 5-FU-Ala-MMP9pept [26], that blocks the access of MMP-9 enzyme to the cleavage site.



- **Cytotoxicity of product 5-FU-adipic-MMP9pept [30] in HCT-116 and HT-29 CRC cell line:** Although in the sequence recognition experiment the product did not showed a MMP-9 selective release, we continued with the evaluation of the cytotoxicity of product [30] in HT-29 and HCT-116 cell lines, following the methodology previously described. MTT assays revealed that, as for the product 5-FU-adipic-MMP7pept [28], the 5-FU-adipic-MMP9pept [30] had a very similar behavior to the free 5-FU thus, confirming the low stability of the ester linkage in the cell culture conditions.

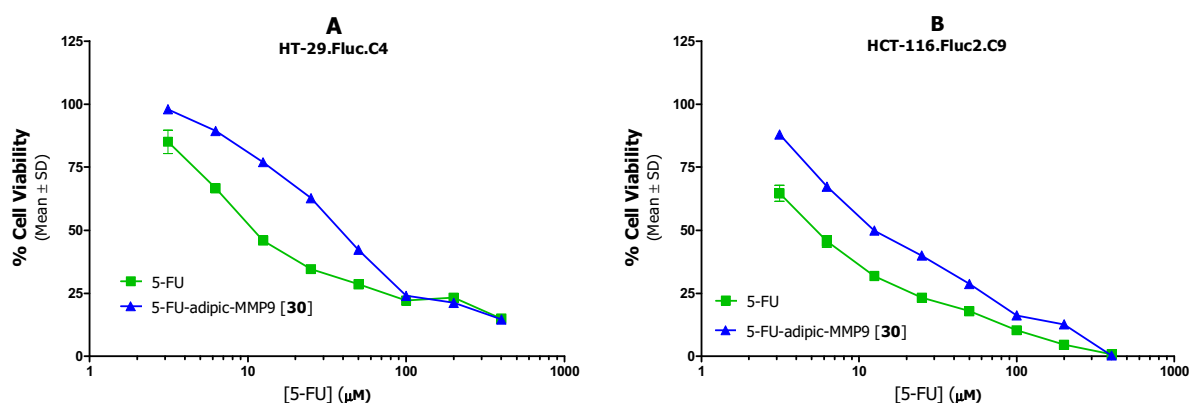


Figure 4.67 MTT cell viability assays of product [30] in HT-29 (A) and HCT-116(B) CRC cells.

Table 4.17  $IC_{50}$  ( $\mu M$ ) values of 5-FU and product [30] after 72 h incubation in HCT-116 and HT-29 cells. Results are expressed as mean  $\pm$  SD.

	Compound	HCT-116. Fluc2.C9	HT-29. Fluc.C4
$IC_{50}$ ( $\mu M$ )	5-FU	6.10 $\pm$ 0.01	27.47 $\pm$ 0.03
	5-FU-adipic-MMP9pept [30]	17.67 $\pm$ 0.03	43.38 $\pm$ 0.02

In good agreement with the results obtained when incubating products [26,28,30] in plasma, cell culture experiments showed that the ester bond was not stable, releasing the 5-FU rapidly. However, it was decided to stick to this type of bond for PGA-MMPpept-5FU conjugates based in our experience with PGA-5FU conjugates, where the conformational structure of the PGA protects the hydrolysis of the ester bond.

#### 4.2.3 Synthesis of the PGA-based polymer-drug conjugate sensitive to MMP-7: PGA-MMP7pept-5FU

Two different PDC were synthesized to evaluate their cytotoxicity in CRC cell cultures, the PGA-MMP7pept-5FU conjugate [37] with the MMP-7-specific AHX-RPLALWR-AHX [11] linker and the PGA-MMP7Scram-5FU conjugate [38] that contained the scrambled sequence.

The synthetic methodology followed for the obtainment of both PDC was the same used for PGA-5-FU [6] (section 4.1.1.1.2). The drug-linker moiety was modified in order to have an amino group that would further react with the carboxylic groups of the PGA polymeric chain through an amide bond. Hence, using as starting products 5-FU-adipic-MMP7pept [28] and 5-FU-adipic-MMP7scram [29] previously purified by semipreparative HPLC, the synthesis of products [35-36] was carried out in a multistep process (Figure 4. 68).

Therefore, products [28] and [29] were activated by pentafluorophenol and reacted with N-Boc-ethylenediamine (at pH=6 adjusted previously) to obtain products [33] and [34], respectively. The purification of products [33] and [34] was carried out by semipreparative HPLC in a XSelect column, yielding purities of 88.1% and 89.1%, respectively.

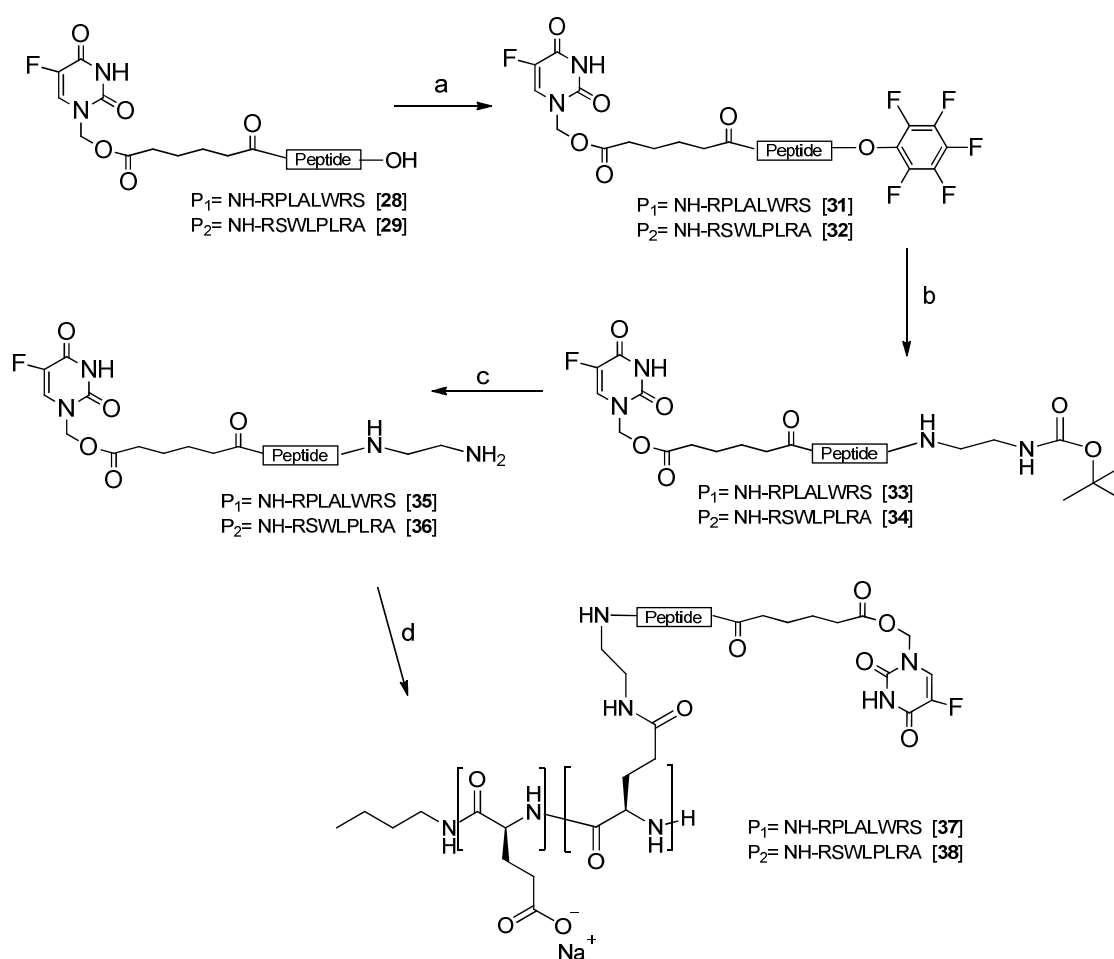


Figure 4. 68 Synthesis of products PGA-MM7pept -5FU [37] and PGA-MMP7scram-5FU [38]. Conditions: a) pentafluorophenol (1.5 eq), EDC (1.5 eq), DMAP (0.5 eq), DCM, rt, 3 h; b) N-Boc-ethylenediamine (1.1 eq), pH=7, DMF, overnight, rt; c) TFA/DCM (1:3), 1 h, rt d) PGA-COOH in DMF, DIC (1.5 eq) 5 min, HOBT (1.5 eq), 10 min; product [35]/[36] (1 eq), 36 h (24h readdition DIC (1.5 eq)), rt.

The amine protecting group (Boc) was eliminated with a mixture of TFA/DCM (1:3) during 1 h at rt to get products [35] and [36] to finally conjugate them to the PGA chain. Then, 10 mg (0.76 mmol) of PGA-COOH were dissolved in DMF and activated with DIC plus HOBT, as detailed before. The mixture was left to react for 10 min, and then products [35] and [36] were added and pH was

adjusted to 8 with DIEA. It was left to react under agitation during 36 h, and at 24 h DIC was added yielding PGA-MMP7pept-5FU [37] and PGA-MMP7scram-5FU [38], respectively. The crude was dried under vacuum and dissolved in a NaHCO<sub>3</sub> (0.1 M adjusted to pH 7 with HCl 1 M). In this step, the exchange of H<sup>+</sup> and Na<sup>+</sup> lead again the PGA sodium salt. The crude was dissolved, purified by dialysis against distilled water and finally lyophilized for the further characterization of TDL and FD by HPLC. The synthetic strategy used ensures the stability of the ester bond during the synthesis and the achievement of pure conjugates.

Table 4. 18 summarizes the different syntheses performed to get the products. Unlike PGA-5-FU [6], products [37] and [38] presented a surprisingly low TDL, around 1%. This could be explained due to the nature and length of the peptides, which might have produced a steric hindrance and would have not allowed the conjugation of more 5-FU-peptide units, and could have affected the PDC conformation in solution.

Table 4. 18 Summary of the different reactions performed to get products [37] and [38].

Compound	TDL% (mg/mg)	Mass obtained (mg)
PGA-MMP7pept-5FU [37]	2.65%	111.8
PGA-MMP7scram-5FU [38]	0.73%	25.1

#### 4.2.3.1 Determination of the particle size of PGA-MMP7pept-5FU conjugate [37]

DLS was used for the measurement of the particle size of PGA-MMP7pept-5FU conjugate [37]. DLS measurements were performed in a ZetaSizer Malvern Instrument at 25°C following the same methodology used for the PGA-5-FU conjugate [6].

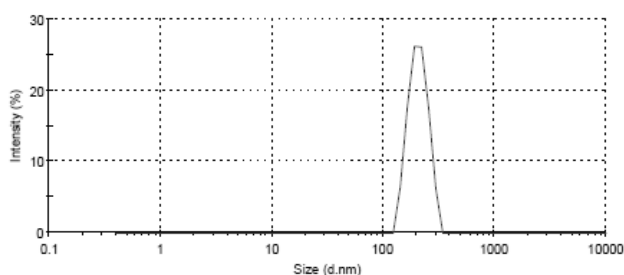


Figure 4. 69 Size distribution by intensity of PGA-MMP7pept-5FU conjugate [37] (measured at 0.1 mg/mL in H<sub>2</sub>O).

PGA-MMP7pept-5FU conjugate [37] showed a particle size of 208.2 nm and a polydispersity of 0.566 measured by means of DLS in H<sub>2</sub>O (Figure 4. 69). In comparison to the results achieved in product [6] analysis (89.23 nm), product [37] showed a slightly higher particle size. This could be related with the conformation that the longer linkers (peptides) produce to the final conjugates.

#### 4.2.3.2 Stability studies *in vitro* of PGA-MMP7pept-5FU [37] conjugate

PGA-MMP7pept-5FU [37] conjugate was characterized in terms of stability and degradability *in vitro* before the study of the cytotoxicity in HCT-116 and HT-29 CRC cell lines. The stability and degradability tests were performed at 3 different pHs (in PBS), in mice and human plasma and incubated with MMP-7.

All the experiments were performed according the methodology explained in section 3.6 and the amount of 5-FU released in the specific conditions were quantified by RP-HPLC in a C18 column with a UV detector set at 254 nm. Integrated peaks of 5-FU detected were interpolated in a calibration curve of standard 5-FU. Experiments were performed at 37 °C in triplicate and Resorcinol was used as an internal standard. In the case of the MMP-7 incubation experiment, a part from the 5-FU quantification, it was quantified the amount of 5-FU-RPLA released.

##### 4.2.3.2.1 Stability studies: Plasma and different pHs

To check the degradability of product PGA-MMP7pept-5FU [37] against 3 different pHs (5.5, 6.5 and 7.4) product [37] (10 mg/mL) was incubated in 100 µL of PBS at the corresponding pH. Regarding the plasma experiments, PGA-MMP7pept-5FU [37] was incubated in mice and human plasma (10 mg/mL). The aim of these experiments was to test if the polymer-drug conjugate would be stable while transport through the bloodstream, and thus confirm if the polymer conformation would protect the ester bond that showed low stability in the experiments performed with products 5-FU-adipic-MMP7pept [28] and 5-FU-adipic-MMP7scram[29].

Figure 4. 70 represents the degradation curves of PGA-MMP7pept-5FU [37] in the different pHs and in plasma over the time.

Degradation studies in **plasma** showed a similar behavior in human and mice plasma, nevertheless in human plasma product [37] showed a slightly higher unspecific release of 5-FU compared to mice plasma, contrary to the results obtained for product PGA-5-FU [6]. It was also observed that 5-FU was released during the first 30 min, and then 5-FU release reached a plateau of 10% and 14% in mice and human plasma, respectively. This positive finding confirmed that no more than 15% of the 5-FU conjugated to the PGA-MMP7pept-5FU would be released in plasma circulation. So, it suggested that the conjugate could reach the target tissue (CRC overexpressing MMP-7) without suffering an important unspecific release of the active drug in circulation.

Regarding the **pH** degradation curves, a very low pH-dependent release of 5-FU was observed with product [37] at acidic (5.5 and 6.5) and physiological (7.4) pHs. This suggests that when the PGA-MMP7pept-5FU conjugate will reach the tumor, the release produced by the acidic environment, typical in cancerous tissues might be low. This is a positive finding since the product was designed for being sensitive to MMP-7 overexpressed in tumors.

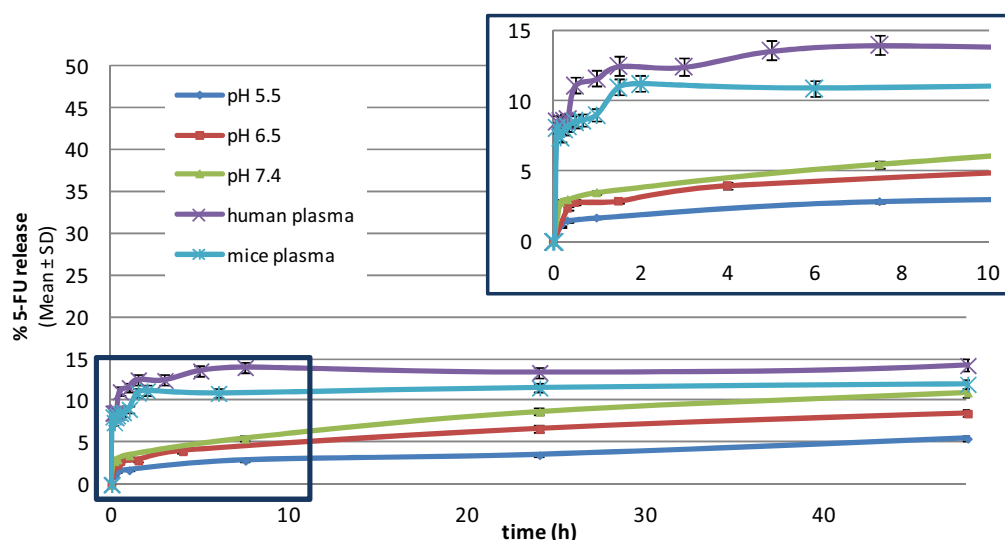


Figure 4. 70 Degradation curves of PGA-MMP7pept-5FU in different mediums of incubation over the time. The blue box corresponds to an area enlargement of the first 10 h of the experiments.

#### 4.2.3.2.2 Stability studies: MMP-7 responsiveness

The degradation of PGA-MMP7pept-5FU was studied against MMP-7 enzyme to determine the selectivity of the PDC. To proceed, 2 mg of PGA-MMP7pept-5FU [37] were dissolved in H<sub>2</sub>O and MMP-7 (0.1 mg/mL) was added. It was left at 37°C during 72 h and at scheduled times (0, 5, 15 and 30 min, 1, 4, 6, 24, 48 and 72 h) aliquots of 5 µL were taken and analyzed by HPLC-MS and HPLC-UV.

To measure the amount of the 5-FU-RPLA released, a calibration curve was performed with 5-FU-RPLA (product [39]). Product [39] was synthesized following the same methodology used for the synthesis of products [28-30]. Previously the tetrapeptide AHX-RPLA [40] was synthesized by SPPS using 100 mg of 2-chlorotrytil resin (1.6 mmol/g peptide) and Fmoc protected amino acids (see protocol in section 3.3.1). Product AHX-RPLA [40] was finally obtained in a high purity (91.9%).

Then, following the same conditions explained in section 4.2.3 the product [39] was obtained and also purified by semipreparative HPLC in a BEH column in acid (HCOOH). The product was obtained in a high purity (99.8%).

The calibration curve of 5-FU-RPLA [39] was set with the same conditions used for the 5-FU standard calibration curve. Therefore, HPLC analysis could be used to quantify either 5-FU ( $t_r = 1.8$  min) or 5-FU-RPLA ( $t_r = 5.8$  min).

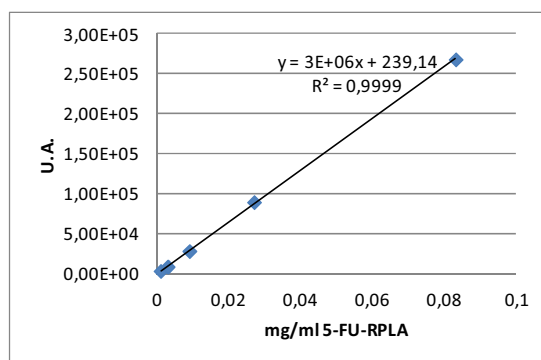


Figure 4. 71 Calibration curve of 5-FU-RPLA performed by HPLC.

Figure 4. 72 represents the degradation curve of PGA-MMP7pept-5FU [37] corresponding to the release of 5-FU-RPLA. During the first hours almost the 50% of 5-FU was released from the conjugate PGA-MMP7pept-5FU [37], reaching a maximum of 80% during the next two days. No free 5-FU was detected when PGA-MMP7pept-5FU [37] was incubated with MMP-7 (data not shown).

Thus, the conformation that the polymer-drug conjugate PGA-MMP7pept-5FU [37] adopted in solution made the peptide chain very accessible for the MMP-7 enzyme, allowing its hydrolysis even when conjugated to the macromolecular polymer. On the other hand, the product released is 5-FU linked to a tetrapeptide, instead of the bioactive drug 5-FU. For this reason, it was very important to study the cytotoxic profile in CRC cells overexpressing MMP-7, in order to determine if 5-FU-RPLA offered a cytotoxicity comparable to the free 5-FU.

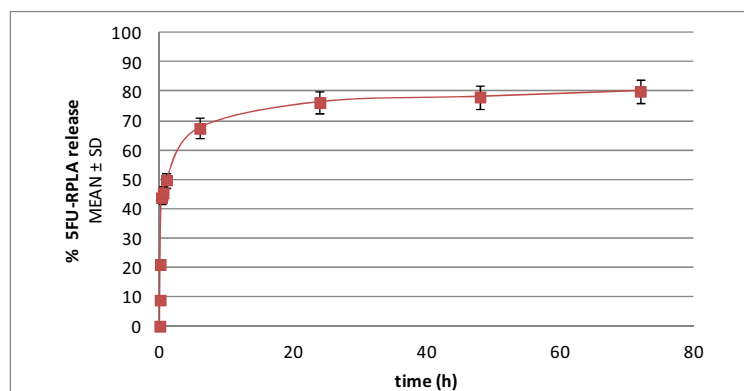


Figure 4. 72 Kinetic release of 5-FU-RPLA from product [37] over the time when incubated with MMP-7. Product [39] is the 5-FU-RPLA, the released moiety due to the cleavage produced by MMP-7. The quantification was performed by HPLC.

#### 4.2.3.3 Cytotoxicity assays of PGA-MMP7pept-5FU conjugate

*In vitro* efficacy studies were carried out at the FVPR laboratory (CIBBIM Nanomedicine, VHIR) under the supervision of Dr. Ibane Abasolo.

The evaluation of the cytotoxicity of PGA-MMP7pept-5FU product [37] was performed using the MTT assay, as previously detailed. In addition, for PGA-MMP7pept-5FU [37] and PGA-MMP7Scram-5FU [38] the MTT assay was also performed in HCT-116 and HT-29 CRC cell lines overexpressing the MMP-7 enzyme.

##### 4.2.3.3.1 Cytotoxicity assays of PGA-MMP7pept-5FU conjugate *in vitro* in HT-29 and HCT-116 cell lines

In the evaluation of the cytotoxicity of PGA-MMP7pept-5FU [37], PGA-5-FU [6] and 5-FU were also analyzed in the same experiment.

The MTT assay was performed in HCT-116 and HT-29 CRC cell lines and the maximum concentration tested was 200  $\mu$ M eq of 5-FU for all products. The IC<sub>50</sub> values were compared after 72 h of incubation with products [6] and [37].

Table 4. 19 summarizes these results and Figure 4. 73 shows the cytotoxicity curves for the tested compounds in both CRC cell lines. Both PDC showed IC<sub>50</sub> higher than 5-FU, being lower for product PGA-MMP7pept-5FU [37]. In good agreement with the stability and degradation experiments discussed previously, the lower IC<sub>50</sub> of product [37] could be related with the conformation of the conjugate containing the peptide. This suggests that it was easier to release free 5-FU than 5-FU-RPLA [39] from the conjugate PGA-MMP7pept-5FU [37].

Table 4. 19 IC<sub>50</sub> ( $\mu$ M) values of 5-FU, product PGA-5-FU [6] and PGA-MMP7pept-5FU [37] in HCT-116 and HT-29. Results are expressed as Mean  $\pm$  SD.

	Compound	HCT-116. Fluc2.C9	HT-29. Fluc.C4
IC <sub>50</sub> ( $\mu$ M)	5-FU	4.88 $\pm$ 0.01	14.21 $\pm$ 0.05
	PGA-MMP7pept-5FU [37]	9.11 $\pm$ 0.05	55.92 $\pm$ 0.03
	PGA-5-FU [6]	33.38 $\pm$ 0.01	82.25 $\pm$ 0.02

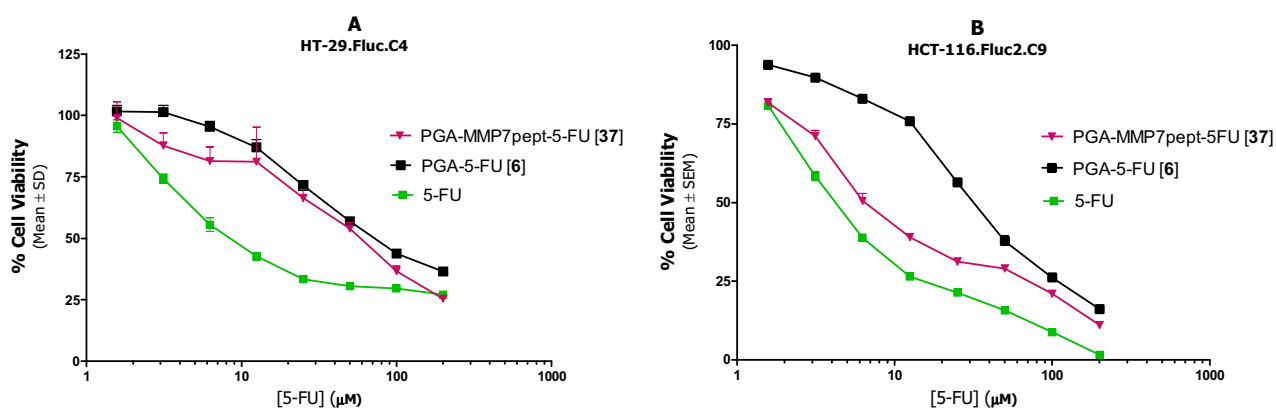


Figure 4.73 Cell viability of 5-FU and products PGA-5-FU [6] and PGA-MMP7pept-5FU [37] carried out by MTT in HT-29 (A) and HCT-116(B) CRC cells.

#### 4.2.3.3.2 Cytotoxicity assays of PGA-MMP7pept-5FU conjugate *in vitro* in HT-29 and HCT-116 cell lines overexpressing MMP-7

The cytotoxicity of product PGA-MMP7pept-5FU [37] was studied in HCT-116 and HT-29 CRC cell lines overexpressing MMP-7 and product PGA-MMP7Scram-5FU [38] was included as a negative control.

The mentioned cells were treated with  $\text{TNF}\alpha$  to induce the MMP-7 overexpression, what was confirmed through a Western Blot analysis. The cytotoxicity was studied following the MTT assay, described previously, and the maximum concentration tested was 100  $\mu\text{M}$  eq of 5-FU. The experiment was also performed without  $\text{TNF}\alpha$ .

Table 4.20 summarizes the  $\text{IC}_{50}$  values obtained in both cell lines for the product PGA-MMP7pept-5FU [37] and PGA-MMP7Scram-5FU [38] and 5-FU and the cytotoxic profiles are showed in Figure 4.74. No significant difference was observed between both treatments regardless MMP-7 overexpression. None of the tested compounds offered the typical cytotoxic profile of PDC in these conditions. Often, for the  $\text{IC}_{50}$  of the PDC is slightly higher than the  $\text{IC}_{50}$  of the free drug due to the internalization process and consecutive release of the drug. Previous PGA-MMP7pept-5FU [37] degradation assays (section 4.2.3.2.2) showed that the product released was 5-FU-RPLA [39]. Thus, after the cytotoxic study of product PGA-MMP7pept-5FU [37], it was confirmed that, even though the released product when MMP-7 was overexpressed was the 5-FU linked with the tetrapeptide RPLA, a fast hydrolysis of the ester bond should be occurring in cell cultures leaving 5-FU alone. Indeed, the cytotoxic profile of products [37,38] (PGA-MMP7pept-5FU and PGA-MMP7Scram-5FU) was very similar to that observed for products [28,29] (5-FU-adipic-MMP7pept and 5-FU-adipic-MMP7scram) in an MTT experiment in the HT-29 CRC cell line overexpressing MMP-7 (section 4.2.2.3.1).



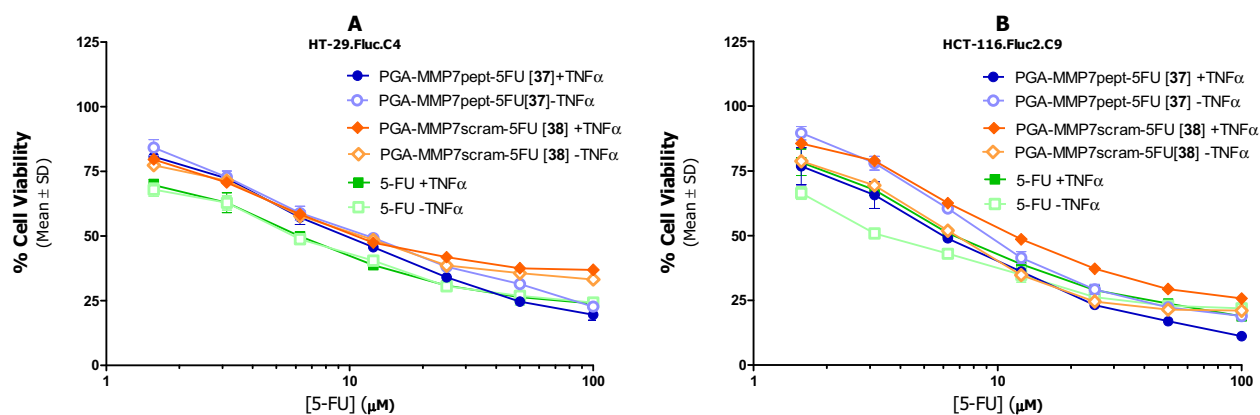


Figure 4.74 Cell viability graphics of 5-FU and products [37] and [38] carried out by the MTT procedure in HT-29 (A) and HCT-116(B) CRC cells overexpressing MMP-7.

Table 4. 20  $IC_{50}$  values ( $\mu M$ ) of 5-FU, product PGA-MMP7pept-5FU [37] and PGA-MMP7scram-5FU [38] in HCT-116 and HT-29 were MMP-7 overexpression was induced by  $TNF\alpha$ . Results are expressed as Mean  $\pm$  SD.

	Compound	Treatment	HCT-116. Fluc2.C9	HT-29. Fluc.C4
$IC_{50}$ ( $\mu M$ )	5-FU	$TNF\alpha$	$7.88 \pm 0.02$	$6.80 \pm 0.05$
	5-FU	--	$4.08 \pm 0.04$	$6.64 \pm 0.03$
	PGA-MMP7pept-5FU [37]	$TNF\alpha$	$6.42 \pm 0.02$	$10.47 \pm 0.01$
	PGA-MMP7pept-5FU [37]	--	$10.77 \pm 0.03$	$13.15 \pm 0.02$
	PGA-MMP7scram-5FU [38]	$TNF\alpha$	$14.37 \pm 0.03$	$16.46 \pm 0.05$
	PGA-MMP7scram-5FU [38]	--	$7.36 \pm 0.03$	$14.28 \pm 0.04$

These data confirm that the proposed design for a PGA-MMP7-sensitive polymer-drug conjugate was not suitable to ensure an enzyme specific release of 5-FU. Although degradation studies showed that the system was selective for MMP-7, a very fast 5-FU release from both, sensitive and insensitive MMP-7 PDC ([37] and [38] respectively), was observed. These results also suggest that once the product will find MMP-7 in the environment, the 5-FU-RPLA unit would be released from the conjugate, and then, a fast hydrolysis of the ester bond would be produced. On the other hand, since the same cytotoxicity for the non-sensitive-MMP-7 PDC (PGA-MMP7scram-5FU) was demonstrated, it is considered that the undesirable fast drug release is not due to MMPs uniquely, but rather to the high exposure of the ester bond to the microenvironment.

#### 4.2.4 Conclusions

In the study of a new PDC sensitive to MMP to deliver 5-FU we confirmed that it is of significant importance the type of link between the MMP-sensitive peptide and the bioactive agent 5-FU. Previous to the conjugation to the PGA carrier, it was confirmed through cytotoxic experiments of the (MMP-9 sensitive peptide)-drug unit that the carbamate union was too stable *in vitro*, opposite to the ester bond behavior, resulting as an undesirable linkage for their use in polymeric nanoconjugates designed to release drugs gradually.

In this section data confirmed through *in vitro* therapeutic efficacy studies performed in HCT-116.Fluc2-C9 and HT-29.Fluc-C4 cells overexpressing MMP-7, that the conjugation of 5-FU linked to MMP7-sensitive peptide AHX-RPLALWRS-AHX through an ester bond, to a polyglutamic acid carrier with a molecular weight of 15 kDa lead a PDC that adopted a conformation in solution that resulted very accessible for the MMP7 enzyme and esterases. Thus, the cleavage of the sensitive peptide and the ester bond were produced faster than expected.

When analyzing the results observed for the control nanoconjugate synthesized with a scrambled sequence not sensitive to MMP-7, it was confirmed that the ester linkage for this type of nanoconjugates was not a suitable option since it remained very exposed in the structure. For this reason, it is suggested the study of different linkages between the peptide and the drug to enhance the selectivity of the PGA-MMPpept-5FU conjugate, as well as the use of polymers with a higher molecular weight to better protect the peptide-drug bond.



---

## 4.3 Polymer-drug conjugates based on Poly-(L-glutamic acid), 5-Fluorouracil and SN-38

---

Encouraged for the interesting results described for the combination of 5-FU and Irinotecan (CPT-11) as free drugs, this section explores this combination in a single polymeric chain carrying 5-FU and the active metabolite of Irinotecan (CPT-11), the SN-38 (7-ethyl-10-hydroxyl-camptothecin)<sup>24,31,167</sup>.

As mentioned in the introduction, Irinotecan (CPT-11) is used in clinics nowadays, nonetheless it has several limitations and it is suggested that the direct delivery of the active metabolite SN-38 may improve the antitumor efficacy while limiting the gastrointestinal toxicity<sup>14</sup>.

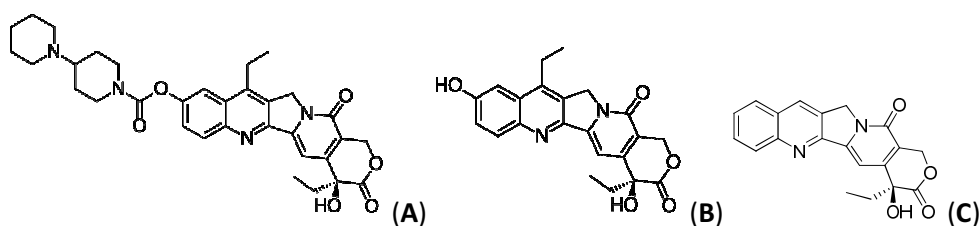


Figure 4. 75 Chemical structures of Irinotecan (CPT-11) (A), SN-38(B) and CPT(C).

Drug delivery systems carrying 5-FU have been explored and discussed in section 4.1. Regarding CPT, the literature describes different drug delivery systems carrying 20(S)-Camptothecin (CPT) or biologically active CPT (such as SN-38) with the aim of improving the specificity and efficacy of the Irinotecan based chemotherapeutic treatment.

Direct linkage of CPT was explored by *Bhatt et al*<sup>149</sup>, who designed a family of PGA-X-CPT conjugates (where X stands for the linker) exploring different kind of linkers. Within all the conjugates studied (PGA-CPT, PGA-Gly-CPT, PGA-Ala-CPT, PGA-( $\beta$ -Ala)-CPT, PGA-(4-NH-butyryl)-CPT, PGA-(2-O-acetyl)-CPT, PGA-(4-O-butyryl)-CPT, PGA-( $\gamma$ -Glu)-CPT), it was found an improved efficacy of PGA-Gly-CPT in HT-29 colon and NCI-H460 lung carcinoma cells. Further, they also found that higher CPT loadings (above 47% of TDL) on the PDC were traduced in a reduction of the aqueous solubility. However, the *in vivo* pharmacokinetic studies examining plasma and tumor levels of CPT showed a 6-fold improvement in exposure of tumor tissue to CPT in comparison to free CPT.

Much research has been focused on the development of new CPT derivatives with the aim of enhancing its solubility, ensuring the stabilization of the lactone ring and keeping its anticancer properties. CPT derivatives can function as CPT pro-drugs to release CPT *in vivo* and enhance its pharmacokinetic, biodistribution and toxicity profiles. As a result of these investigations, two CPT

analogues, Topotecan and Irinotecan, that have been approved by the FDA for the treatment of colon and ovarian cancers.

SN-38 shows a higher cytotoxicity than Irinotecan (CPT-11) against tumor cells *in vitro* (it is 100- to 1000-fold more potent), but it is very insoluble. For this reason SN-38 loaded drug delivery systems have been extensively studied. One of the most interesting drug delivery systems is the pegylated conjugate of SN-38, named PEG-SN38 (EZN-2208), that is being evaluated in phase II Clinical trials in patients with metastatic colorectal and breast cancers and a phase I/II study in pediatric patients with cancer since it showed enhanced tumor accumulation and anticancer activity in comparison to Irinotecan (CPT-11) administered alone. Its conjugation also allowed an enhancement of SN-38 solubility allowing its systemic administration<sup>150,151</sup>. Another example that has reached clinical trials is the SN-38 encapsulated in liposomes (LE-SN38)<sup>152</sup>. SN-38 has also been loaded in polymeric micelles showing an increase of its solubility and anticancer activity in cancer cells<sup>153</sup>. Complexes of SN-38 and PAMAM dendrimers are another drug delivery system proposed that shown promising results for oral delivery to minimize gastrointestinal toxicity<sup>154</sup>. SN-38 has also been conjugated to HPMA<sup>155</sup> and albumin<sup>156</sup> showing in both cases a good solubility and stability while retaining its *in vitro* cytotoxicity. A part from the incorporation of SN-38 into drug delivery systems, a new pro-drug of SN-38 showed to improve the therapeutic window of Irinotecan (CPT-11) when conjugating SN-38 to a cationic peptide via an esterase cleavable linker<sup>157</sup>. A new antibody-drug conjugate for the therapy of hematologic malignancies (Epratuzumab-SN38) also showed promising results in lymphoma and leukemia<sup>158</sup>.

In all these examples, the stabilization of SN-38 by its conjugation or encapsulation showed improvements on the stability, specificity and toxicity against tumor cells in comparison to the Irinotecan (CPT-11) administered as a single agent. Thereby, the present chapter will study the conjugation of two chemotherapeutic agents: 5-FU and SN-38 to a biodegradable polymeric chain, PGA, through a covalent linkage since PGA-Gly-CPT<sup>60</sup> also showed improved anticancer activity.

As a preliminary step for the development of the PGA-5FU-SN38 conjugate with an optimal loading of both drugs and adjusted kinetic release, it was decided to explore as a first trial the ester linkage between the drug and the carrier for both bioactive agents.

### 4.3.1 Synthesis of PGA-SN38

With the aim of verifying the attachment of SN-38 to the polymeric carrier, it was first synthesized a PDC based on PGA conjugated to SN-38 as a single agent. This initial trial is aimed to confirm the synthetic methodology the SN-38 loading to PGA for the further design of the PDC combining both drugs.

#### 4.3.1.1 SN-38 derivatization

*The product [47] was synthesized in a large scale in our laboratory by Rosario Ramón.*

Camptothecins have a particular characteristic in its chemical structure: the lactone ring of the 20(S)-Camptothecin and its analogues. Figure 4. 76 represents the conversion of the SN-38 (active

form, E-Ring, [I]) to the lactone hydrolyzed carboxylate form of SN-38 (inactive form, [II]) by opening of this ring. Although the conversion is reversible, in human blood the hydrolyzed carboxylate form did not occur because it binds preferentially to human albumin<sup>60</sup> avoiding the possibility to return to lactone form. At equilibrium in human plasma, less than 0.2% of the CPT is in the lactone hydrolyzed carboxylate form<sup>159</sup>. In addition, 24 h after Irinotecan (CPT-11) infusion in humans, about 25-30% and 50-64% of CPT-11 and SN-38, respectively, are in the lactone form compared with the total amount of both anticancer agents<sup>150</sup>.

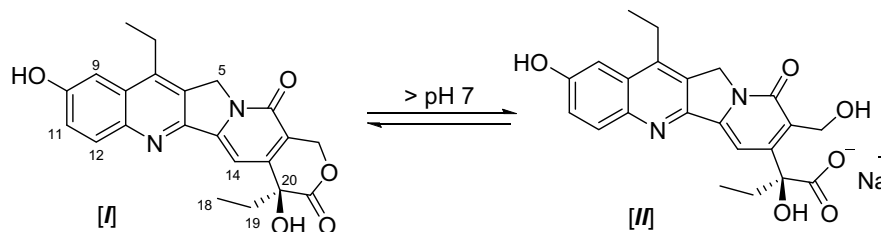


Figure 4. 76 pH dependant conversion of SN-38 [I] to the lactone hydrolyzed carboxylate form [II].

A clinical trial was performed by Muggia *et al*<sup>160</sup> with the hydrolyzed form of CPT to evaluate its anticancer activity, showing also toxicity and a weak activity in patients. In addition, it was found that the carboxylate was a relatively inactive antitumor agent *in vitro*, compared to CPT<sup>161</sup>. Considering these results, and the fact that the regeneration of the lactone ring does not take place in human blood, the use of CPT as a chemotherapeutic agent was discarded.

Among all the CPT analogues discussed in the literature, special emphasis has to be put in those called: **20(S)-O-acylated CPT derivatives**, (Figure 4. 77) that has better toxicity associated. The 20(S)-hydroxyl group is believed to participate in the enhanced rate of lactone hydrolysis to the carboxylate form. For this reason, the acylation of this hydroxyl group to stabilize the lactone ring is beneficial to block its participation in the hydrolysis by inhibiting the conversion, increasing its therapeutic benefit<sup>162</sup>. For this reason, we decided to use in our PDC containing SN-38 this strategy to avoid the lactone-carboxylate equilibrium in favor of the less active carboxylate form.

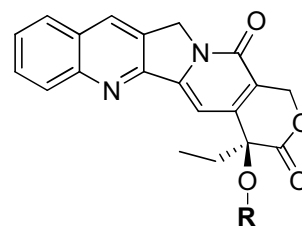


Figure 4. 77 Chemical structure of the 20(S)-O-acylated CPT derivatives.

To ensure the obtainment of a 20(S)-O-acylated derivative of SN-38, it was necessary to protect first the 10-OH hydroxyl group because it is more active than the 20-OH group. In the literature it can be found different protecting groups (t-butylcarbonyl (Boc), *tert*-butyldimethylsilyl (TBDMSO), t-butyl diphenylsilyl (TBDPSO))<sup>150,163</sup> have been used for this purpose. In the specific case of the above mentioned, PEG-SN38 (EZN-2208) Zhao *et al*<sup>150</sup> showed that the 10-OH group with the TBDPSO protecting group was the best approach to scale up the synthesis.

The conjugation of the SN-38 derivative and the PGA polymeric chain was proposed through the  $\gamma$ -carboxylic groups of the glutamic acid units, as it was carried out in the previous PDC synthesized in this thesis. For this reason, a free  $\text{NH}_2$  group in the SN-38 derivative is necessary to ensure the amide bond formation. We hypothesized that this type of conjugation would enhance the solubility of the drug, while improving its E-ring stability.

Since the 20(S)-O-acylation of SN-38 was the key aspect of the SN-38 derivatization, we proposed to conjugate to the 20-OH group a Boc-glycine molecule after the TBDPSO protection of the 10-OH group. Thus, the lactone stability and the limitation of side-reactions with the 10-OH group were guaranteed. Figure 4. 78 shows the synthetic procedure followed for the SN-38 derivatization.

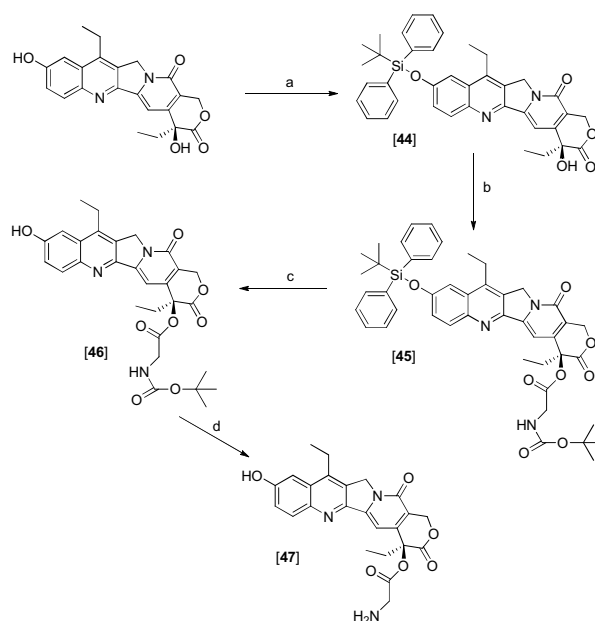


Figure 4. 78 Synthetic scheme of product [47]. Conditions: a) TEA (4 eq), TBDPSO (4.5 eq), DCM, reflux, o/n; b) Boc-Gly-OH (1.5eq), EDC (1.5 eq), DMAP (0.5 eq), DCM, 0°C, 14 h; c) TBAF (1.5 eq), HCl (0.5 M), THF, 15 min, 0°C; d) HCl 4 M in 1-4-dioxane, 2 h, RT.

To proceed, first the SN-38 was protected with the TBDPSO group to obtain product SN-38-TBDPSO [44]. The reaction was performed in DCM using TEA and TBDPSO (4 eq) in a reaction performed overnight under reflux. After purification, the product was obtained with a high purity (99.0%). The following step was the incorporation of Boc-glycine to the 20-OH group of product SN-38-TBDPSO [44] to yield product SN-38-TBDPSO-GlyBoc [45] using EDC as an activator agent. Final product was obtained with a high purity (97.9%).

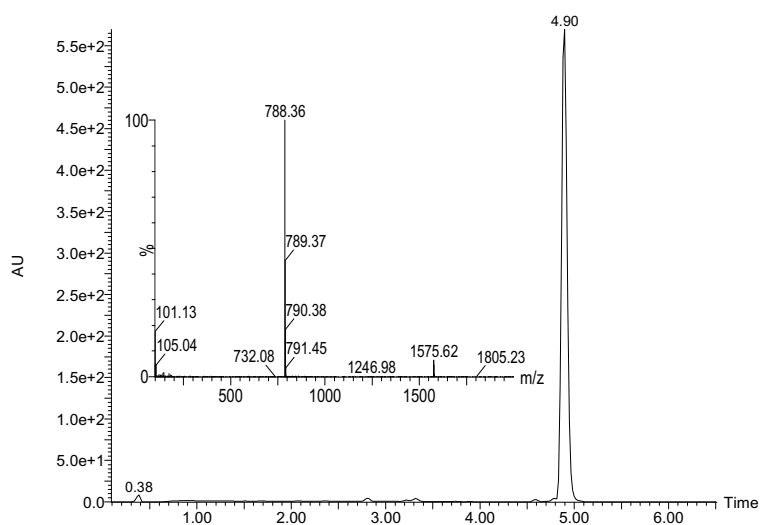


Figure 4. 79 HPLC-MS chromatogram of product SN-38-TBDPSO-GlyBoc [45].

#### 4.3.1.2 Conjugation of the SN-38 derivatized to PGA (PGA-SN38)

Synthesis of the PDC PGA-SN38 (product [48]) required the following synthetic step. First, product SN-38-TBDPSO-GlyBoc [45] was deprotected and the removal of TBDPS and Boc protecting groups was achieved in a two step process. Product [45] was treated with tetrabutylammonium fluoride (1.0 M in THF) and HCl (0.05 M) at 0°C on ice during 15 min to remove the TBDPS protecting group. Then, the Boc removal was achieved 2 h after treatment with HCl 4.0 M in 1,4-dioxane. Once product SN-38-Gly [47] was obtained, it was conjugated with PGA following the same procedure set up for the PGA-5-FU synthesis in section 4.1.1.

To proceed, 100 mg of PGA in the acidic form (previously precipitated in HCl), were dissolved in anhydrous DMF and carboxylic groups were activated with DIC (5 min) and HOBT (10 min). Then, product SN-38-Gly [47] was added and pH was adjusted to 8. The aim was to obtain a TDL of 15%. After purification by dialysis, PGA-SN38 (Product [48]) was lyophilized and 12.5 mg of a white foamy solid were obtained with a very low yield (8%).

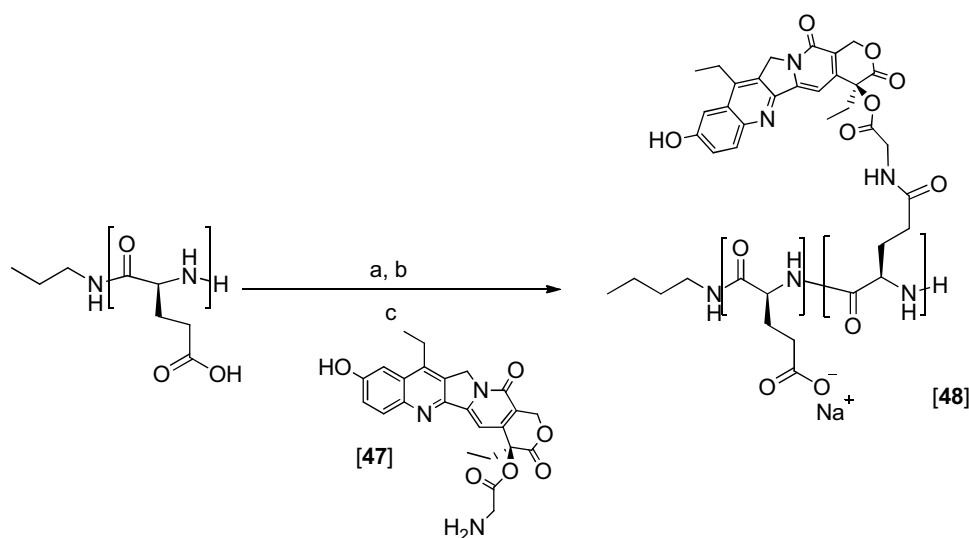


Figure 4. 80 Synthesis scheme of PGA-SN38 [48]. Conditions: a) DIC (1.5 eq) 5 min; b) HOBT (1.5 eq), 10 min; c) Product [47] (1 eq), 36 h (24 h readdition DIC (1.5 eq)), RT.

Since the final objective of this synthesis was the development of the methodology for the synthesis of the PDC containing 5-FU and SN-38, an alternative way to quantify the total drug loading of SN-38 in this PDC was explored. In the PDC carrying both drugs it would be useful to have two different techniques for measuring the amount of drugs loaded. For this reason the quantification of the SN-38 in the PGA-SN38 conjugate [48] was performed by UV-spectroscopy. The SN-38 UV-spectra has different maximums of absorbance (Figure 4. 81), in this case, the  $\lambda=378$  nm was selected as the set wavelength to perform absorbance measurements<sup>164</sup>.



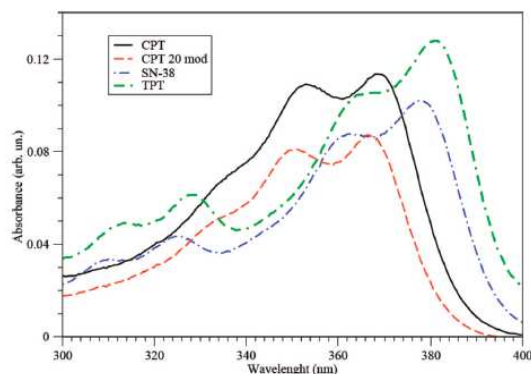


Figure 4. 81 UV-vis experimental spectra of 5  $\mu\text{M}$  CPT, CPT derivatized in the 20-OH position, SN-38 and Topotecan (TPT) in aqueous solution in the 300-400 nm region. Adapted from Sana et al<sup>164</sup>.

For the SN-38 TDL quantification, a calibration curve was used at  $\lambda=378$  nm in the range of 0-0.1 mg/mL. Two solutions containing PGA-SN38 conjugate [47] (0.23 mg/mL and 0.55 mg/mL) were analyzed. The total TDL of SN-38 in the PGA-SN38 conjugate [48] was found to be 10.2%. To measure the amount of Free Drug entrapped in the PDC structure, both solutions were mixed with NaOH (1 M) and then the analytical process was repeated. By comparing both results obtained it was possible to confirm a TDL of 10.2% and a FD < 0.1%.

This confirmed that the same methodology followed for the conjugation of 5-FU to the PGA carrier was useful for the attachment of the 20(S)-O-acylated SN-38 derivative [47].

#### 4.3.1.2.1 PGA-SN38 characterization

Although product [48] was synthesized as a preliminary step to ensure the conjugation of product SN-38-Gly [47] to PGA, a complete physicochemical characterization was performed.

#### 4.3.1.2.2 Determination of PGA-SN38 size by DLS

DLS was used for the measurement of the particle size of PGA-SN38 conjugate [48] following the same methodology explained in the section 3.5 with the ZetaSizer Malvern Instrument at 25°C.

The synthesized PGA-SN38 conjugate [48] showed a particle size of 79.63 nm and a PDI of 0.195 measured by means of DLS in PBS at pH= 7.4 (Figure 4. 82). The product adopted a conformation in a water solution that leads to nanoparticles with a size below 100 nm and very narrow peaks.

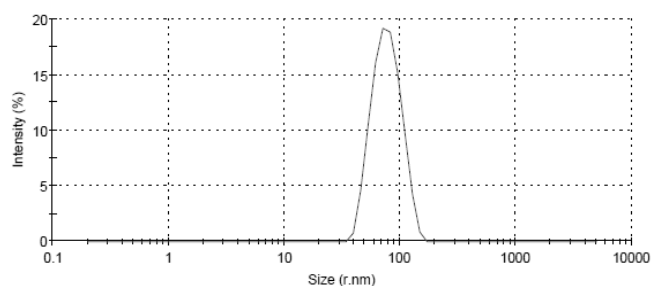


Figure 4. 82 Size distribution by intensity of PGA-SN38 [48] (measured at 0.1 mg/ml in PBS at pH= 7.4).

#### 4.3.1.2.3 Stability studies *in vitro* of conjugate PGA-SN38 [48]

PGA-SN38 conjugate [48] was fully characterized in terms of stability and degradability *in vitro*.

In particular, the different variables studied were **plasma**, **pH** and **Cathepsin B**. Regarding plasma stability studies, PGA-SN38 [48] was incubated in mice plasma (from animals of FVPR Laboratory (CIBBIM-Nanomedicine, VHIR), 1.5 mg/mL). For pH dependant degradation studies, product PGA-SN38 [48] (1.5 mg/mL) was incubated at 3 different pHs: 5.5, 6.5 and 7.4. Finally, it was studied the degradation of the nanoconjugate [48] (1.5 mg/mL) by Cathepsin B present in lysosomes (5  $\mu$ L, 10 units/mL using PBS 7.4 as a solvent).

All the experiments were performed according to the methodology explained in section 3.6 and the amount of SN-38 released in the specific conditions were quantified by HPLC-UV at  $\lambda = 378$  nm. Integrated peaks of SN-38 detected were interpolated in a calibration curve of standard SN-38. Experiments were performed at 37°C in triplicates and Resorcinol was used as an internal standard.

Figure 4. 83 represents the degradation curves of PGA-SN38 in the different mediums studied over time.

- In **plasma**, a very low release of SN-38 during the time analyzed was observed. A faster release of SN-38 was expected because the drug was linked to PGA by an ester bond as was in the case of PGA-5-FU and PGA-MMPpept-5FU conjugates. The release of SN-38 was less than 2% after 2 h of incubation. The plasma stability curve did not reach a plateau as it was observed in previous experiments (PGA-5-FU and PGA-MMPpept-5FU). Nonetheless, the maximum of drug released in plasma was less than 10% after 96 h of incubation. This was a promising result since it demonstrated a very low unspecific release of the drug when circulating in plasma.

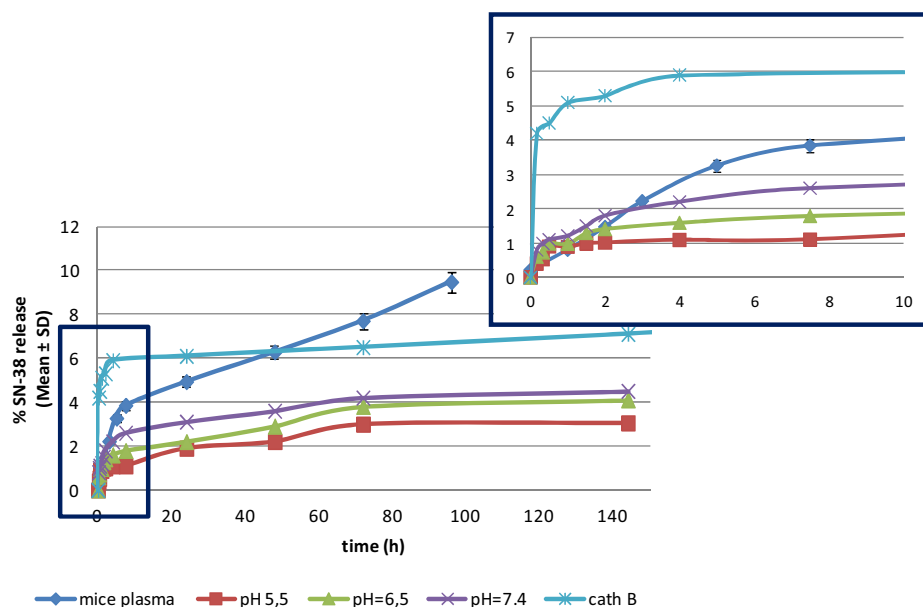


Figure 4. 83 Degradation curves of PGA-SN38 [48] in different mediums over the time. The blue box corresponds to an area enlargement of the first 10 h of the experiment.

- In **pH** experiments a low dependant release of SN-38 from product PGA-SN38 [48] overtime was observed. Drug release curves obtained for the different pH were similar, being the highest at pH 7.4. This could be related also to the nature of the linkage between SN-38 and the polymeric chain: ester bonds are more labile to basic pH than to acidic environments. Nevertheless, the amount of drug released (less than 5%) at neutral pH was lower than in plasma. Thus, the conjugate showed high pH stability.
- Contrary to the results obtained with PGA-5-FU conjugate [6] (section 4.1) in this experiment a higher drug release in the presence of **Cathepsin-B** was observed than in plasma during the first 10 h of the experiment. Around 6% of SN-38 release was achieved during the first 24 h and drug release did not exceed 10%. Thus, the degradation of the polymeric chain by Cathepsin has a lower kinetic profile, suggesting a biodegradation process.

#### 4.3.1.3 Cytotoxicity assays of PGA-SN38 [48] *in vitro* in HT-29 and HCT-116 CRC cell lines

*In vitro* efficacy studies were carried out at the FVPR Laboratory (CIBBIM Nanomedicine, VHIR) and analyzed by Helena Plà under the supervision of Dr. Ibane Abasolo.

The evaluation of the therapeutic activity of the PGA-SN38 [48] was performed using the MTT assay (section 3.9.1). Figure 4.84 represents the cytotoxicity curves of product [48] and free SN-38 in HCT-116 and HT-29 CRC cell lines.

As expected, in both cases the free drug showed a lower IC<sub>50</sub> than the PDC. But values did not differ much, indicating that the PGA-SN38 [48] offers a similar therapeutic activity against CRC cells than the single drug.

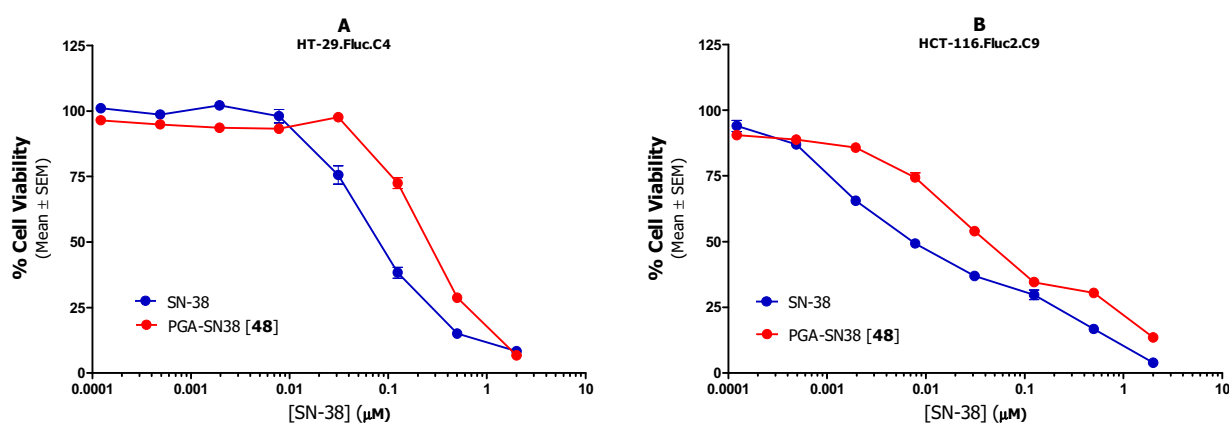


Figure 4. 84 Cytotoxicity of PGA-SN38 [48] measured by MTT assay after 72 h of incubation. (A) HT-29.Fluc.C4 cells; (B) HCT-116.Fluc2.C9 cells.

Table 4. 21 Summary of the  $IC_{50}$  ( $\mu M$ ) values obtained in the HCT-116 and HT-29 CRC cells. Results are expressed as Mean  $\pm$  SEM.

	Compound	HCT-116. Fluc2.C9	HT-29. Fluc.C4
$IC_{50}$ ( $\mu M$ )	SN-38	0.013 $\pm$ 0.050	0.092 $\pm$ 0.038
	PGA-SN38 [48]	0.051 $\pm$ 0.040	0.261 $\pm$ 0.028

### 4.3.2 Design and synthesis of a PGA-5FU-SN38 family with different loadings of 5-FU and SN-38

After confirming the suitability of the methodology proposed for the conjugation of the 20(S)-O-acylated SN-38 through a linker containing an ester bond to the PGA carrier, next step was to conjugate 5-FU and SN-38 in a single PDC.

The conjugation of the modified 5-FU and the 20(S)-O-acylated SN-38 in a single polymeric carrier through an ester bond was evaluated and a small family of PGA-5FU-SN38 conjugates carrying different ratios of both drugs synthesized.

Taking into account the slightly constant loading of 5-FU achieved in PGA-5-FU [6], the lower price of the 5-FU and the expensiveness of SN-38, 5-FU was conjugated before SN-38. Related to this, the synthesis of a PDC carrying more than one agent can be performed in two different ways: through a one-pot reaction or in two steps synthesizing and purifying first the PGA-5-FU and then, conjugating the SN-38. The main difference between both processes is the intermediate purification of PGA-5-FU and the TDL of 5-FU quantification prior to the SN-38 conjugation.

#### 4.3.2.1 Optimization of PGA-5FU-SN38 production

The PGA-5FU-SN38 [49 #1] was the first trial synthesized. In this trial, PGA-5FU-SN38 conjugate was synthesized through a one-pot reaction (Table 4. 22).

Table 4. 22 Summary of the reaction performed for the synthesis of the PGA-5FU-SN38 conjugate (PGA-5FU-SN38 [49#1]).

# Batch	Mass obtained (mg)	Synthetic methodology	TDL (5-FU)% (mg/mg)	TDL(SN-38)% (mg/mg)	Ratio 5-FU:SN-38
#1	66.5	One-pot	2.0%	8.8%	0.71

The batch #1 was performed with the aim of achieving a TDL of 10% (wt/wt) for both drugs. Although SN-38 was more toxic than 5-FU, the synthesis was mainly intended to evaluate the synthetic methodology. To proceed 80 mg of PGA-COOH were dissolved in anhydrous DMF and carboxylic groups were activated with DIC (5 min) and HOBt (10 min). Then, product [5] (5-FU-adipic) was added and pH was adjusted at 8 with DIEA. It was left to react 24 h at rt and then DIC and HOBt were added. After 10 min, product SN-38-Gly [46] was added and the pH was adjusted again at 8 with DIEA, left to react at rt during 24 h. The crude was dissolved in 0.1M  $NaHCO_3$  (pH=7

adjusted with acetic acid) solution and then purified by dialysis. Finally, the product PGA-5FU-SN38 was lyophilized and 66.5 mg of a slightly yellow foamy solid were obtained (Product [49 #1]). 5-FU HPLC measurements quantified a FD below 0.1% and a TDL of 2.0%. SN-38 quantification was done by UV-spectroscopy, rendering a TDL of 8.8% and a FD < 0.1%. The mM ratio of 5-FU against SN-38 attached to the polymeric chain was 1.40 (SN-38:5-FU).

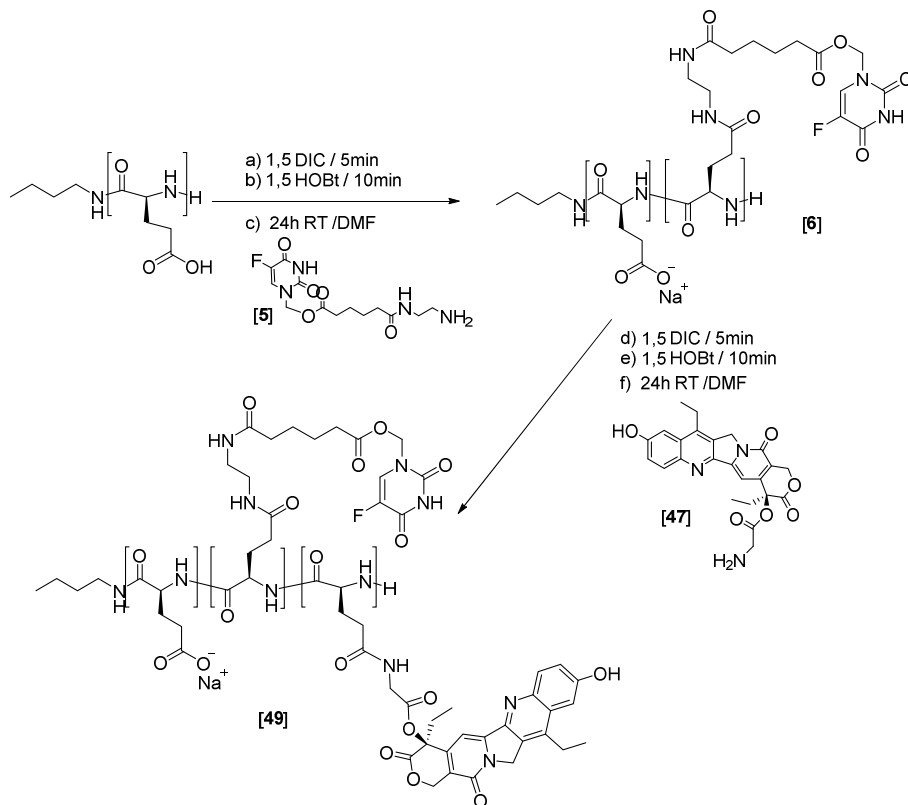


Figure 4.85 Synthesis scheme of the methodology followed for the obtention of product [49 #1]. For the one-pot reaction no purification and TDL of PGA-5FU was performed. Conditions: a) DIC (1.5 eq) 5min; b) HOBt (1.5 eq), 10 min; c) product [5] (1 eq), 24h, RT; d) DIC (1.5 eq) 5min; e) HOBt (1.5 eq), 10 min; f) product [47] (1 eq), 24h, RT.

Synthetic efforts were so far aimed to achieve the same TDL for both drugs. Unsuccessfully a problem arose related with the low TDL of 5-FU. During the second pH adjustment with DIEA (pH=8), a considering amount of the conjugated 5-FU was released. Thus, using this one-pot strategy the initial 5-FU loading previous to the SN-38 conjugation was not maintained. Therefore, the following reactions (# batch A-D in Table 4. 22) were performed in a multistep process quantifying the amount of 5-FU TDL before and after the 20(S)-O acylated SN-38 conjugation.

#### 4.3.2.1.1 *In vitro* cytotoxicity of PGA-5FU-SN38 [49 #1]

It was decided nonetheless, to evaluate product [49 #1] cytotoxicity against HCT-116 and HT-29 CRC cell lines and compare the cytotoxicity curves and the  $IC_{50}$  values with 5-FU, SN-38 and PGA-SN38 [48].

In this experiment the cytotoxic profile of the combination of the single drugs at the same molecular ratio was also evaluated.

Regarding the cytotoxicity curves of the products studied *in vitro* (Figure 4. 86), some findings were observed. If we focus in the 5-FU profile, it was not observed in both cells lines studied any activity. 5-FU did not show efficacy. This was expected because the maximum concentration tested was 1.4  $\mu$ M eq of 5-FU, and  $IC_{50}$  value for 5-FU in the cell lines was in the range of 5-10  $\mu$ M (section 4.1.3).

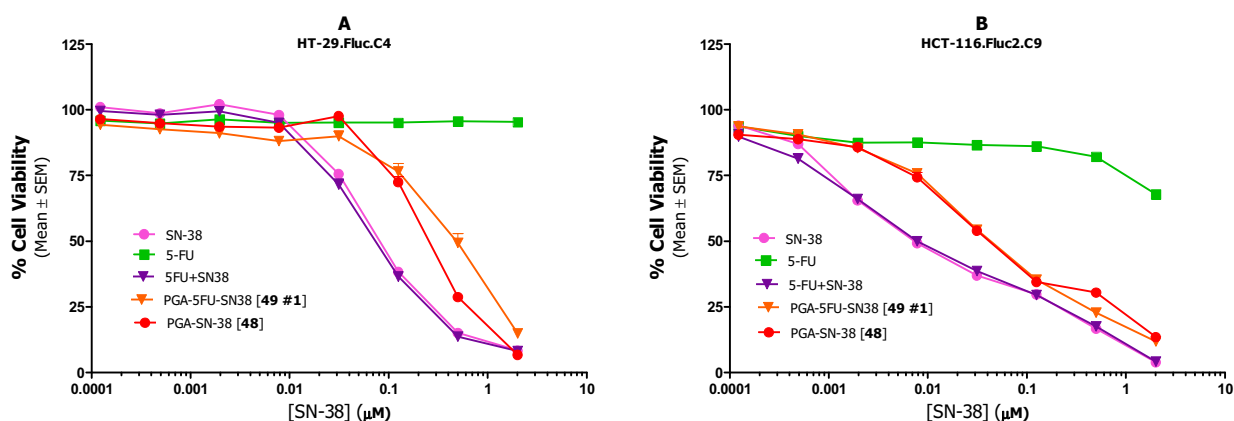


Figure 4. 86 Cytotoxicity of PGA-5FU-SN38 [49#1] measured by MTT assay after 72 h of incubation. (A) HT-29.Fluc.C4 cells; (B) HCT-116.Fluc2.C9 cells. (A)  $IC_{50}$ (5-FU) >2  $\mu$ M,  $IC_{50}$ (SN-38):0.148  $\pm$  0.038  $\mu$ M,  $IC_{50}$ (5-FU+SN-38) :0.11  $\pm$  0.023  $\mu$ M,  $IC_{50}$ (PGA-5FU-SN38 [49#1]): 0.647  $\pm$  0.064  $\mu$ M, PGA-SN38[48]: 0.320  $\pm$  0.028  $\mu$ M; (B)  $IC_{50}$ (5-FU)>2 $\mu$ M,  $IC_{50}$ (SN-38): 0.018  $\pm$  0.05  $\mu$ M,  $IC_{50}$ (5-FU+SN-38): 0.013  $\pm$  0.057  $\mu$ M,  $IC_{50}$ (PGA-5FU-SN38 [49#1]): 0.059  $\pm$  0.044  $\mu$ M, PGA-SN38[48]: 0.059  $\pm$  0.050  $\mu$ M.  $IC_{50}$  values are expressed as a  $\mu$ M of SN-38 eq.

In contrast, SN-38 and 5-FU+SN-38 showed activity although the combination of the single drugs did not show a significant improvement. Regarding the PDC studied, in both CRC cells the  $IC_{50}$  values obtained are in the same order of magnitude to the corresponding one of the single drug SN-38, showing in both cases a lower activity in comparison to the SN-38 or the combination of both drugs 5-FU+SN-38 (ratio: 1.40 (SN-38:5-FU)). Although the PDC with a combination therapy showed anticancer activity, the combination of both drugs in the polymeric carrier in a molar proportion of 0.71 did not show any synergistic effect.

On the other hand it has to be mentioned that the activity of the SN-38 is extremely higher than the activity of 5-FU, thus, the cytotoxic activity of PGA-5FU-SN38 [49 #1] was not due to the 5-FU activity, but to the SN-38 anticancer agent.

#### 4.3.2.2 Synergism experiments of 5-FU and SN-38 as single drugs

*The synergism experiments of 5-FU and SN-38 as single drugs were performed by personal of FVPR Laboratory (CIBBIM-Nanomedicine, VHIR) under the supervision of Dr. Ibane Abasolo.*

Synergy refers to the efficacy of a multidrug therapy when is greater than the sum of each drug alone if used separately. However, often the result of a multidrug therapy is different from the summation of the effect of each drug by its own. Therefore, when the sum of the effect of all drugs is the same as the final effect as applying the multidrug therapy, it would be called additive effect. When it is lower, there would be antagonism between these drugs. Finally, there would be synergism if the effect is greater than the additive effect.

The experiments performed to find out the appropriate proportion of 5-FU and SN-38 (administered as single agents) in HCT-116 and HT-29 CRC cell lines to achieve a synergistic effect, were done in parallel to the synthesis and *in vitro* evaluation of the first PGA-5FU-SN38 [49 #1] conjugate.

As a summary, different MTT assays were conducted testing different concentrations of both drugs in combination. 5-FU concentration range covered from 0.052  $\mu\text{M}$  to 200  $\mu\text{M}$ , whereas SN-38 was studied from  $5.2 \cdot 10^{-5}$   $\mu\text{M}$  to 0.2  $\mu\text{M}$ . In the MTT analysis, the minimum concentration of both drugs that showed the lower cell viability was selected as the synergic concentration. It was found that both drugs administered as single agents showed a synergistic effect at this proportion: 5-FU (1-8  $\mu\text{M}$ ):SN-38 (0.0332  $\mu\text{M}$ ), that corresponds to a **1:240** (SN-38:5-FU) ratio.

In good agreement with the  $\text{IC}_{50}$  values obtained in the MTT experiment performed with the PGA-5FU-SN38 conjugate [49 #1] explained above, we confirmed that the synthesized conjugate carrying both drugs must have a higher TDL of 5-FU than the corresponding for SN-38. Therefore, it was also confirmed the need of an accurate synthetic methodology to achieve specific ratios of TDL of both drugs in the final PDC.

#### 4.3.2.3 Design of a small family of PGA-5FU-SN38 conjugates carrying different ratios of drugs

##### 4.3.2.3.1 Synthesis of the PGA-5FU-SN38 family

Regarding the results obtained in the screening experiments, the synthesis of a small family of different PGA-5FU-SN38 conjugates was performed trying to reach the expected loadings in a two step process with the purification and quantification of the intermediate product PGA-5-FU.

It was expected that the conjugation of a concrete amount of SN-38 to an intermediate PGA-5-FU conjugate could be more precise if the total 5-FU attached in the first reaction was quantified first. In addition, the ratio founded has two orders of magnitude of difference, and thus, it would be necessary to work on a very small proportion of SN-38 to reach the desired ratio of both drugs.

Two different batches of PGA-5-FU (**-A** and **-B**) were synthesized with a different TDL. The products were synthesized and purified in the same manner as done in section 4.1.1. Concretely, these batches were named **PGA-5-FU-A** and **PGA-5-FU-B**, and the TDL was measured by HPLC. For PGA-5-FU-**A**, 445.4 mg were obtained with a TDL of 4.05%, whereas for the PGA-5-FU-**B** we obtained 112.3 mg and the TDL was 0.50%. For both PDC the FD was < 0.1%.

These two PGA-5-FU conjugates were used as the starting reagents for the family of PGA-5FU-SN38 conjugates. Precisely, the conjugates were named PGA-5FU-SN38-**X**, where **X** stands for A, B, C and D. The difference between them is the ratio SN-38:5-FU.

The starting material for PGA-5FU-SN38-(**A,C,D**) was PGA-5-FU-**A**, and PGA-5-FU-**B** was used for the combined conjugate PGA-5FU-SN38-(**B**). In all cases, the methodology followed for the conjugation of the 20(S)-O-acylated SN-38, was the same detailed in section 4.3.1.5 for the synthesis of the PGA-SN38 conjugate [48]. Once purified, the amount of drugs loaded in the PGA-5FU-SN38 conjugates was measured by HPLC and UV-spectroscopy for 5-FU and SN-38, respectively.

Table 4. 23 Summary of the PGA-5-FU batches used for the PGA-5FU-SN38-(A-D) synthesis.

# Batch	PGA-5-FU source	Initial TDL (5-FU) %
#A	PGA-5-FU-A	4.05%
#B	PGA-5-FU-B	0.5%
#C	PGA-5-FU-A	4.05%
#D	PGA-5-FU-A	4.05%

As it was hypothesized in the synthesis of PGA-5FU-SN38 [49 #1] using the one-pot strategy, in all the products synthesized PGA-5FU-SN38-(**A,B,C,D**) (Table 4.24), the TDL of 5-FU suffered a decrease when the conjugation of SN-38 was performed. Accordingly, the achievement of a fixed TDL of 5-FU in the final PDC would not be related with the methodology followed (one-pot or multistep), but with the pH adjustment with DIEA when product SN38-Gly [47] was added to the reaction vessel.

As an example, the synthesis of the PGA-5FU-SN38-(**A**) conjugate is described. 75 mg of PGA-5-FU-**A** were dissolved in 10 mL of anhydrous DMF, then DIC (1.5 eq) was added and 5 min later HOBT (1.5 eq) was also added as a solid. After 10 min, product SN38-Gly [47] (83  $\mu$ g,  $1.8 \cdot 10^{-4}$  mmol) was added. The pH was controlled and adjusted with DIEA to pH=8. At time 24h, the same amount of DIC was added. The reaction was left to react during 36h at rt under agitation. After dialysis purification, the product was lyophilized and 140.1 mg of a white foamy solid were obtained. SN-38 TDL and FD were measured following the protocol detailed in section 3.5 by UV-spectroscopy and it was. TDL of 5-FU was confirmed also once SN-38 was conjugated by HPLC.



Table 4. 24 Summary of PGA-5FU-SN38 conjugates family (PGA-5FU-SN38-(A,B,C,D) synthesized following a two step process.

# Batch	Mass obtained (mg)	TDL (5-FU)% (mg/mg)	TDL (SN-38)% (mg/mg)	mM 5-FU	mM SN-38	Ratio SN-38:5-FU
#A	140.1	3.05%	0.025%	10	0.03	1:300
#B	179.4	0.26%	0.02%	0.34	0.02	1:40
#C	123.5	3.27%	5.15%	42.3	2.20	1:20
#D	260	2.55%	0.025%	10	0.03	1:300

As summarized in Table 4.24, the ratio of SN-38:5-FU obtained in the four syntheses was not reproducible. It was also observed a decrease of the 5-FU conjugated in the second step of the reaction, being the synthesis #D and #B the most affected, and causing an alteration of the desired ratio between both drugs. For this reason in the future it would be necessary a more precise optimization work seeking more specific pH conditions that allow to obtain more reproducible results.

#### 4.3.2.3.2 *In vitro* cytotoxicity of the PGA-5FU-SN38-(A,B,C,D) family

*In vitro* efficacy and synergy studies were carried out by personal of FVPR laboratory (CIBBIM Nanomedicine, VHIR) under the supervision of Dr. Ibane Abasolo.

The *in vitro* therapeutic activity of these four conjugates PGA-5FU-SN38-(A,B,C,D) was evaluated at the FVPR Laboratory (CIBBIM-Nanomedicine, VHIR).

The evaluation of the cytotoxicity of PGA-5FU-SN38-(A,B,C,D) conjugates was carried out in a different manner than the studies performed with PGA-5FU-SN38 [49 #1]. In this case, two different MTT experiments were performed with the difference of the fixed concentration tested with the aim of evaluating the cytotoxicity associated to each drug. Unlike in section 4.3.2.1.1 (*In vitro* cytotoxicity study of PGA-5FU-SN38 [49#1]), the maximum concentration tested was too low (1.4  $\mu$ M eq of 5-FU and 2  $\mu$ M eq of SN-38), and the 5-FU associated cytotoxicity could not be observed, in this experiments it was decided to duplicate the *in vitro* experiments. First it was studied in the two CRC cell lines the cytotoxicity of products PGA-5FU-SN38-(A,B,C,D) at a maximum concentration tested of 1  $\mu$ M eq of SN-38 with the aim of evaluate the SN-38 cytotoxicity associated, and secondly, a different experiment was performed fixing the maximum concentration of PGA-5FU-SN38-(A,B,C,D) to 330  $\mu$ M eq of 5-FU, with the aim of study the related 5-FU cytotoxicity. In both experiments it was also evaluated the cytotoxicity of PGA-5-FU-A.

Figure 4.87 represents the cytotoxicity curves of all products tested in HCT-116 and HT-29 cell lines when the maximum concentration tested was 1 $\mu$ M eq of SN-38. The IC<sub>50</sub> values are summarized in Table 4.25. As depicted, SN-38 showed a clear activity against both CRC cells, being slightly lower for the HCT-116 cells. PGA-5FU-SN38-(A,B,D) showed an IC<sub>50</sub> value one order of magnitude higher

than the free drug. Particularly, the most effective was PGA-5FU-SN38-D. On the other hand, PGA-5FU-SN38-C did not offer any cytotoxicity associated.

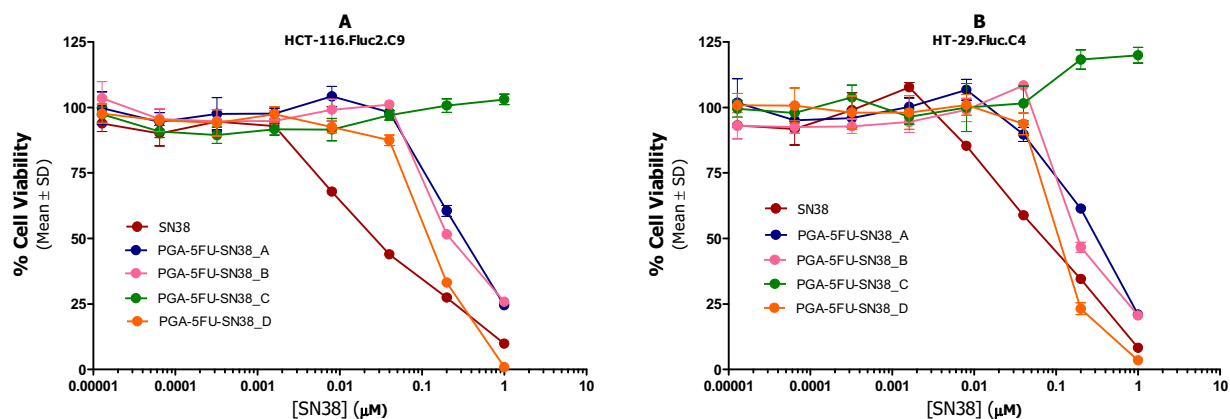


Figure 4. 87 Cytotoxicity of PGA-5FU-SN38 measured by MTT assay after 72 h of incubation fixing the maximum concentration tested to 1  $\mu$ M eq of SN-38. (A) HT-29.Fluc.C4 cells; (B) HCT-116.Fluc2.C9 cells.

Table 4. 25 SN-38  $IC_{50}$  ( $\mu$ M) values of PGA-5FU-SN38 conjugates (A-D). Results are expressed as Mean  $\pm$  SD.

	Compound	HCT-116. Fluc2.C9	HT-29. Fluc.C4
$IC_{50}$ ( $\mu$ M)	SN-38	0.031 $\pm$ 0.036	0.075 $\pm$ 0.045
	PGA-5-FU-A	-	-
	PGA-5FU-SN38-A	0.334 $\pm$ 0.027	0.304 $\pm$ 0.029
	PGA-5FU-SN38-B	0.285 $\pm$ 0.038	0.225 $\pm$ 0.221
	PGA-5FU-SN38-C	>1	>1
	PGA-5FU-SN38-D	0.128 $\pm$ 0.021	0.122 $\pm$ 0.224

Figure 4. 88 represents the cytotoxicity curves of all products tested in HCT-116 and HT-29 cell lines when the maximum concentration tested was 330  $\mu$ M eq of 5-FU. The  $IC_{50}$  values are summarized in Table 4.25. 5-FU as a single agent showed a clear activity and the PDC containing only 5-FU (PGA-5-FU-A) was most effective than those containing the combination of both drugs. Every PGA-5FU-SN38 of the family showed a different  $IC_{50}$  value. For PGA-5FU-SN38-A and PGA-5FU-SN38-D, the  $IC_{50}$  was one order of magnitude higher than the  $IC_{50}$  of the free drug 5-FU in both CRC cells, whereas for the PGA-5FU-SN38-B they were pretty similar. As it was observed in the experiment performed with a maximum concentration of 1  $\mu$ M eq of SN-38, the PGA-5FU-SN38-C did not show any cytotoxicity in both CRC cells.

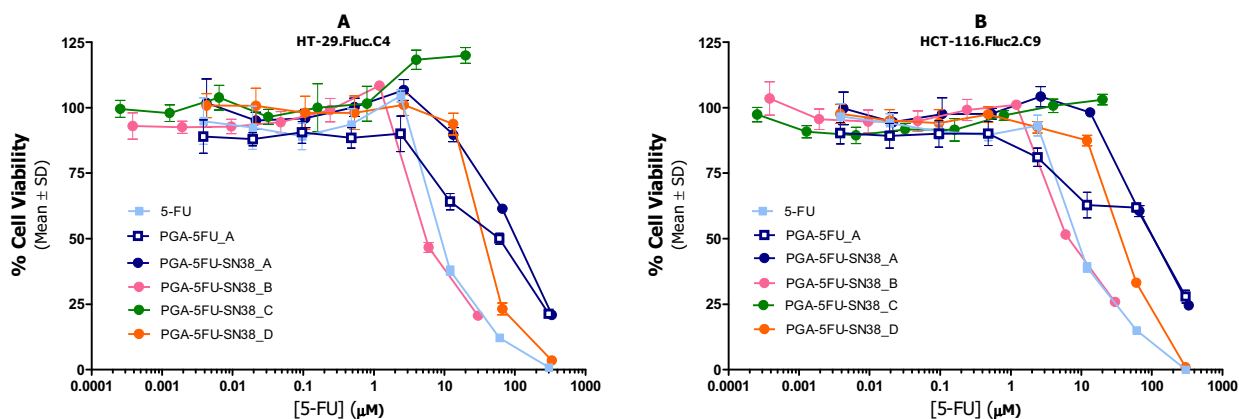


Figure 4. 88 Cytotoxicity of PGA-5FU-SN38 measured by MTT assay after 72 h of incubation fixing the maximum concentration tested to 330 $\mu$ M eq of 5-FU. (A) HT-29.Fluc.C4 cells; (B) HCT-116.Fluc2.C9 cells.

Table 4. 26 5-FU  $IC_{50}$  ( $\mu$ M) values obtained when evaluating the cytotoxicity of PGA-5FU-SN38 conjugates (A-D). Results are expressed as Mean  $\pm$  SD.

	Compound	HCT-116. Fluc2.C9	HT-29. Fluc.C4
$IC_{50}$ ( $\mu$ M)	5-FU	9.86 $\pm$ 0.032	10.94 $\pm$ 0.55
	PGA-5FU-A	70.08 $\pm$ 0.025	43.56 $\pm$ 0.035
	PGA-5FU-SN38-A	111.46 $\pm$ 0.027	101.30 $\pm$ 0.028
	PGA-5FU-SN38-B	8.55 $\pm$ 0.038	6.75 $\pm$ 0.04
	PGA-5FU-SN38-C	>20	>20
	PGA-5FU-SN38-D	38.55 $\pm$ 0.021	40.56 $\pm$ 0.022

#### 4.3.2.3.3 Study of the synergy of 5-FU and SN-38 in the PGA-5FU-SN38-(B,D) through the calculation of the combination index (CI)

The study of the synergy of both drugs was performed by personal of FVPR (CIBBIM-Nanomedicine, VHIR) under the supervision of Dr. Ibane Abasolo.

##### 4.3.2.3.3.1 Introduction to the CI calculation

By the calculation of the CI it is possible to quantitatively measure the dose-effect relationship of each drug alone and its combination and to determine whether or not a given drug combination as single agents or loaded in a polymeric chain would be traduced in a synergistic effect.

The synergy quantification of 5-FU and SN-38 loaded in a same polymeric carrier in products PGA-5FU-SN38-(B,D) (that showed the lowest IC<sub>50</sub> values) was carried out following the Chou-Talalay Method<sup>165</sup>. It was in 1983-1984 when Prof. Pal Talalay and Dr. Ting-Chao Chou introduced the scientific term Combination Index (CI) with the aim of quantify the drug interactions as a synergism, additive effect or antagonism. They found out the need to quantify the effect of combination of the drugs because a combined effect greater than each drug alone does not necessarily indicate synergism. This method is based on the multiple drug-effect equation of Chou-Talalay, which is originally derived for use in enzyme kinetic models and results in a quantitative calculation of the synergy in multidrug therapies.

Chou first defined the Unified Theory (Figure 4.89 (A)), which concluded in the Median-effect equation (MME). MME correlates the “Dose” and the “Effect” of a drug in the simplest possible form (Figure 4.89 (B)).

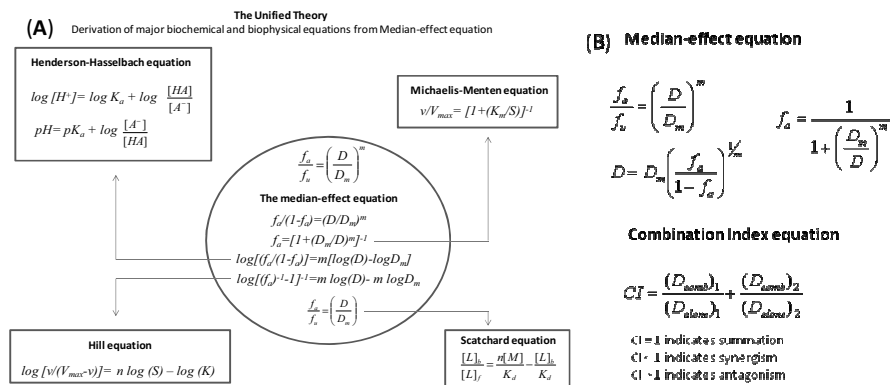


Figure 4. 89 A) Scheme of the unified theory to accomplish the median-effect equation. B) Median-effect equation and CI equation described by Chou-Talalay. D is the dose (or concentration) of a drug, fa is the fraction affected by D (i.e., percentage inhibition /100), fu refers to the fraction unaffected (fu=1-fa), Dm is the median-effect dose signifying the potency (i.e., IC50 or ED50, dose that inhibits the system under study by 50 %), and m is a coefficient signifying the shape of the dose-effect relationship.

According to CI equation, a CI value higher than 1 would mean antagonism, while a value near 0 represents synergism. When CI equals 1, there would be an additive effect. Further CI values interpretation is included in Table 4.27.

Table 4. 27 CI interpretation values according to Chou-Talalay<sup>165</sup>.

Range of CI	Effect	Graded symbols
<0.1	very strong synergism	+++++
0.1-0.3	strong synergism	++++
0.3-0.7	synergism	+++
0.7-0.85	moderate synergism	++
0.85-0.90	slight synergism	+
0.90-1.10	nearly additive	±
1.10-1.20	slight antagonism	-
1.20-1.45	moderate antagonism	--
1.45-3.3	antagonism	---
3.3-10	strong antagonism	----
>10	very strong antagonism	-----

CI quantification and synergy determination of products PGA-5FU-SN38-(B,D) was carried out with *Compusyn* software.

Data from cytotoxicity assays (4 to 7 values for each compound) was used to determine dose-effect curves for single and combination treatments. Further, combination index values were calculated in relation to effect-dose (ED) values 50, 75, 90 and 95. **ED** represents the drug/s dose at which the effect corresponds to the death of the 50, 75, 90 or 95% of the cells, being ED<sub>95</sub> the maximum effectivity of the treatment. The CI values were then interpreted according to Table 4.27 parameters, described by Chou-Talalay.

#### 4.3.2.3.3.2 CI calculation of PGA-5FU-SN38-B,D

PGA-5FU-SN38-(B,D) (1:40 and 1:300 (SN-38:5-FU)) were studied with 5-FU, SN-38 and its respective combinations as controls by MTT. In this case, 5-FU, SN-38 and combinations concentrations were adjusted to PGA-SN38-5FU levels. Cytotoxicity assays (Figure 4.90, Table 4.28 and Table 4.29) showed that there were no large differences between PGA-5FU-SN38 conjugates and their corresponding SN-38 and 5-FU combinations. Overall, free drugs presented better results than PDC, but it has to be considered that drug release from PDC might not have been totally accomplished. In addition, free drugs internalize by diffusion whereas the polymer-drug conjugates enters through the endocytic pathway, resulting in completely different molecular drug kinetics.

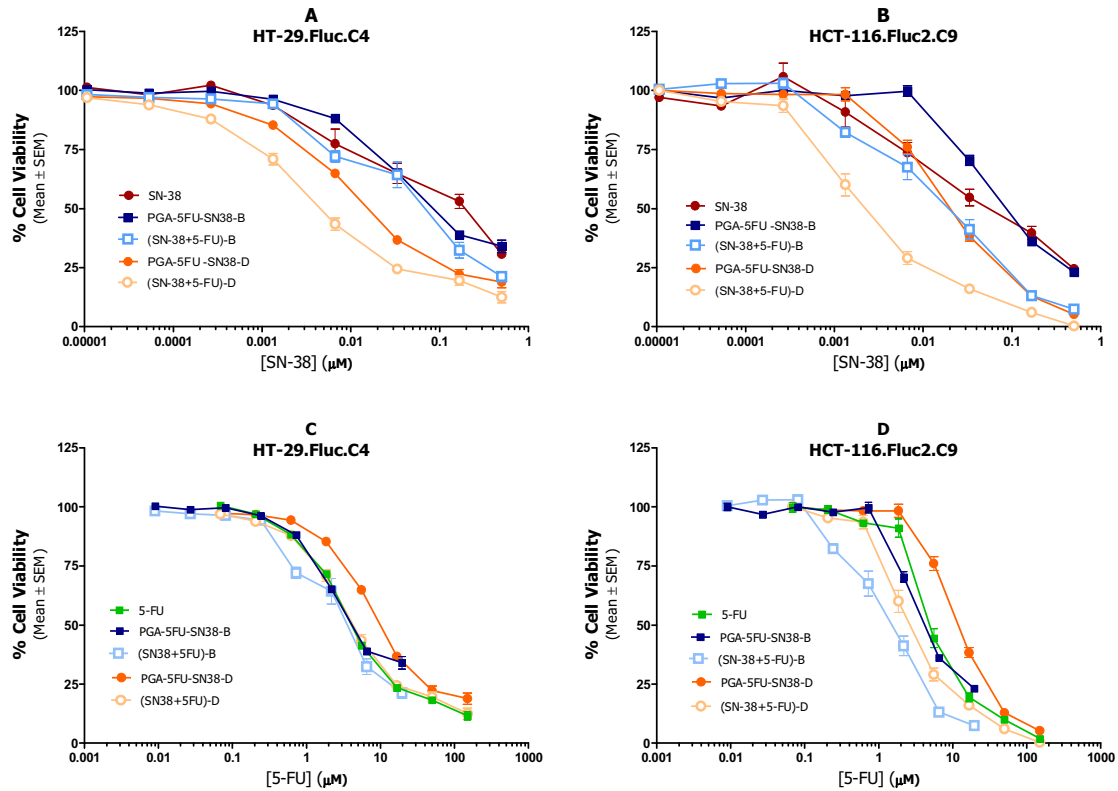


Figure 4. 90 Cytotoxicity of PGA-5FU-SN38 measured by MTT assay after 72 h of incubation fixing the maximum concentration tested to  $1\mu\text{M}$  eq of SN-38 (A and B) ((A) HT-29.Fluc.C4 cells; (B) HCT-116.Fluc2.C9 cells); and cytotoxicity of PGA-5FU-SN38 measured by MTT assay after 72 h of incubation fixing the maximum concentration tested to  $330\mu\text{M}$  eq of 5-FU (C and D) ((C) HT-29.Fluc.C4 cells; (D) HCT-116.Fluc2.C9 cells).

Table 4. 28  $\text{IC}_{50}$  ( $\mu\text{M}$ ) values obtained when evaluating the cytotoxicity of PGA-5FU-SN38 conjugates (B and D) when the maximum concentration tested was  $1\mu\text{M}$  eq of SN-38. Results are expressed as Mean  $\pm$  SEM.

	Compound	HCT-116. Fluc2.C9	HT-29. Fluc.C4
$\text{IC}_{50}$ ( $\mu\text{M}$ )	SN-38	$0.075 \pm 0.020$	$0.156 \pm 0.021$
	PGA-5FU-SN38-B	$0.098 \pm 0.021$	$0.127 \pm 0.043$
	(5-FU+SN38)-B*	$0.024 \pm 0.023$	$0.063 \pm 0.049$
	PGA-5FU-SN38-D	$0.022 \pm 0.025$	$0.029 \pm 0.032$
	(5-FU+SN38)-D*	$0.006 \pm 0.019$	$0.08 \pm 0.046$

\*Free drugs at the same ratio as in their corresponding PDC

Table 4. 29  $IC_{50}$  ( $\mu M$ ) values obtained when evaluating the cytotoxicity of PGA-5FU-SN38 conjugates (B and D) when the maximum concentration tested was 330  $\mu M$  eq of 5-FU. Results are expressed as Mean  $\pm$  SD.

	Compound	HCT-116. Fluc2.C9	HT-29. Fluc.C4
$IC_{50}$ ( $\mu M$ )	5-FU	6.10 $\pm$ 0.037	5.16 $\pm$ 0.019
	PGA-5FU-SN38-B	4.81 $\pm$ 0.041	6.02 $\pm$ 0.020
	(5-FU+SN38)-B*	1.619 $\pm$ 0.034	3.52 $\pm$ 0.016
	PGA-5FU-SN38-D	12.34 $\pm$ 0.027	12.38 $\pm$ 0.018
	(5-FU+SN38)-D*	4.750 $\pm$ 0.035	5.90 $\pm$ 0.014

\*Free drugs at the same ratio as in their corresponding PDC

Using data from several cytotoxicity assays (Tables 4.27 and 4.28), CI was calculated with *Compusyn* software in order to determine the grade of synergy of PGA-SN38-5FU-(B,D) products. This calculation was carried out by tanking as reference PGA-SN38 [48] and PGA-5FU-A (from previous studies), or SN-38 and 5-FU free drugs. This way it was possible to differentiate the effect of SN-38+5-FU conjugated to PGA, and the effect of PGA itself.

- Strong synergism was observed for both PGA-5FU-SN38-B,D conjugates, when PGA-SN38 [48] and PGA-5FU-A were used as reference drugs.

Thus, the conjugation of two drugs in the same vehicle produced higher synergic interactions of drugs than the administration of two single PDC carrying the same drugs separately.

Table 4. 30 CI values and graded symbols of PGA-5FU-SN38-B,D calculated with *Compusyn* software at ED50, 75, 90 and 95 using PGA-SN38 and PGA-5FU-A as reference drugs. + and - value meaning are detailed previously in Table 4.27.

Single-reference drugs	Cell line	Products	CI values			
			ED50	ED75	ED90	ED95
PGA-SN38 and PGA-5FU	HCT-116.Fluc2-C9	PGA-5FU-SN38-B (1:40)	2.624	0.689	0.181	0.073
			---	+++	++++	+++++
		PGA-5FU-SN38-D (1:300)	0.989	0.241	0.059	0.023
		$\pm$	++++	+++++	+++++	
	HT-29.Fluc-C4	PGA-5FU-SN38-B (1:40)	0.407	0.444	0.521	0.594
			+++	+++	+++	+++
PGA-5FU-SN38-D (1:300)		0.361	0.331	0.362	0.419	
	+++	+++	+++	+++		

- When the CI values were calculated using the single drugs as references, only in the HT-29 CRC cell line, that is less responsive to 5-FU treatment than HT-116 CRC cell line at the 1:40 ratio, showed a strong synergism. Probably, the rapid diffusion of single drugs versus the slower internalization of PDC might have an influence on the synergy results encountered.

Table 4. 311 CI values and graded symbols of PGA-5FU-SN38-B,D calculated with Compusyn software at ED50, 75, 90 and 95 using SN-38 and 5-FU as reference drugs. + and – value meaning are detailed previously in Table 4.27.

Single-reference drugs	Cell line	Products	CI values			
			ED50	ED75	ED90	ED95
SN-38 and 5-FU	HCT-116.Fluc2-C9	PGA-5FU-SN38-B (1:40)	2.943	1.585	1.148	1.052
			---	---	-	±
	HT-29.Fluc-C4	PGA-5FU-SN38-D (1:300)	2.546	2.114	1.987	1.964
			---	---	---	---
	HT-29.Fluc-C4	PGA-5FU-SN38-B (1:40)	1.724	1.023	0.824	0.762
			---	±	++	+++
HT-29.Fluc-C4	PGA-5FU-SN38-D (1:300)	2.733	2.819	3.102	3.346	
		---	---	---	---	

### 4.3.3 Conclusions

This study shows that the 20(S)-O-acylation of the SN-38 allows the conjugation of the SN-38 to a polymeric carrier of PGA with a molecular weight of 15 kDa through an ester bond, avoiding the conversion of the SN-38 in its active form (E-Ring) to the lactone hydrolyzed carboxylate form of SN-38 (inactive form) by opening of this ring. The obtained PGA-SN38 conjugate showed therapeutic activity *in vitro* in the HCT-116.Fluc2-C9 and HT-29.FlucC4 CRC cell lines studied.

The preliminary *in vitro* studies performed with the synthesized small family of PGA-5FU-SN38 conjugates through an ester bond showed an improvement of the cytotoxic activity in the HCT-116.Fluc2-C9 and HT-29.Fluc4 CRC cell lines of the conjugates carrying both agents in a ratio of SN-38/5-FU of 1:40 and 1:300 compared to the behavior observed with the combined drugs as single agents at the same ratio.

Finally, the mentioned compounds showed a strong synergism at high effective doses in both CRC cell lines studied measured through the calculation of the Combination Index with the Compusyn software using as references the single PDC carrying both drugs separately. This positive result confirmed that the conjugation of SN-38 and 5-FU in a single polymeric vehicle was translated into a better efficacy. In addition, the slower internalization of the nanoconjugates vs. the entrance of the single drugs by diffusion might explain the lower synergy detected when comparing the combined PDC vs. the single drugs in combination.





---

## 5. Discussion

---

This thesis provides a set of new PGA-drug conjugates designed to improve the current treatment of advanced colorectal cancer based, mainly, on the administration of 5-FU. The use of this type of nanomedicines offers good alternative for the treatment of CRC, by specifically delivering chemotherapeutics to malignant sites, while reducing their side effects.

The first nanoplatform studied (PGA-5-FU) consisted in the conjugation of 5-FU to the PGA polymeric backbone through an ester bond. This is a simple (single drug) nanoplatform, which advantage compared to the free drug should come from the (i) stabilization/protection of 5-FU in circulation; (ii) accumulation into tumors by the EPR effect (passive targeting); and (iii) reduction of systemic toxicity of 5-FU. The first two hypotheses have been fully confirmed in this work. The release of 5-FU from product PGA-5-FU in plasma is significantly low (below 6% after 30 min), probably because the conformational structure that the nanoconjugate adopts in solution protects the ester bond between the drug and the carrier from serum esterases. This has been also observed for other PGA polymer-drug conjugates that confirmed the sustained drug release when using ester bonds for linking other chemotherapeutic drugs such as PGA-PTX<sup>166</sup> and PGA-CPT<sup>167</sup>. The protection of 5-FU in circulation was also confirmed in the *in vivo* biodistribution experiments. In these assays, 5-FU remains in circulation 24 h post-administration; an especially long time considering that free 5-FU has a very short plasma half-life (10-20 min<sup>11</sup>). For this reason, the PGA-5-FU conjugate offers a very encouraging alternative to the administration of 5-FU as a single agent.

Regarding passive tumor targeting, *in vivo* FLI biodistribution experiments as well as HPLC analysis of tumor homogenates showed higher tumor-accumulation of PGA-5-FU (without any targeting moiety in its structure) in comparison to free 5-FU at 24 and 48 h post administration. Although tumor accumulation was anticipated, the clear and almost tumor-exclusive distribution of the PGA-5-FU conjugate after 24 and 48 h was highly unexpected. Based in our previous experience and similar studies published elsewhere<sup>168,169</sup>, nanoparticles administered intravenously accumulate in lungs, liver and spleen in a high extent, and in lower proportions into the tumor, due to the action of the RES and the almost unavoidable nanoparticles aggregation. It is worth mentioning that in the case of PGA-5-FU, drug accumulation in organs with RES is relatively low. Moreover, the presence of the polymer-drug conjugate in kidneys suggests that PGA-5-FU is excreted through this organ after its degradation.

Concerning the reduction of drug's systemic toxicity, it is also important to highlight that PGA-5-FU conjugate is a completely biodegradable polymer. During the last decades, the first-generation of nanomedicines were mainly based on non-biodegradable PEG and HPMA polymers<sup>34</sup>. One of them is the HPMA-5FU<sup>110</sup> conjugate, which reduces the toxicity associated to 5-FU anticancer treatment. Even though is true that molecular weight of PEG and HPMA polymers can be tailored to maximize the chance of renal elimination (< 40000 g/mol) and they are clinically well tolerated, these non-biodegradable polymers have the potential to accumulate intracellularly. Therefore, in contrast to

PGA-based PDC, PEG and HPMA polymers present the risk of “lysosomal storage disease” syndrome caused by a biopersistent polymer backbone. Taking into account the benefits from the use of biodegradable PGA polymers and the remarkable results found with the biodistribution of our PGA-5-FU conjugate, we believe that the use of a PGA-based system might become a promising great alternative to reduce the toxicity associated either with the use of 5-FU or with that of non-biodegradable systems carrying 5-FU.

In addition to the confirmation of the EPR effect, results also demonstrated that internalization of the PGA-5-FU system was through the endocytic pathway. This could partially explain the lower efficacy observed in the cytotoxic experiments performed in HCT-116.Fluc2-C9 and HT-29.FlucC4 CRC cell lines, in comparison to free 5-FU, because free 5-FU enters the cell by diffusion through the cellular membrane, that takes place faster than PGA-5-FU internalization by endocytosis. However, differences in the *in vitro* efficacy could also be due to the fact that not all 5-FU conjugated to the polymer might have been released from the PGA-system during the course of the experiment.

The use of a negatively charged PGA based drug delivery system loaded with a hydrophobic drug, such 5-FU, through covalent linkage could significantly reduce aggregability problems often seen in drug delivery systems. In this sense, results in the particle size measured by DLS showed that this system offers a nanometric size in the range of 100 nm, almost after 1 month from its synthesis. Although *in vitro* and *in vivo* experiments in this thesis have confirmed that the new nanoconjugate improves tumor accumulation and reduces 5-FU degradation while preventing drug metabolism in liver due to the polymer protection, unexpected results were observed in terms of degradation and consecutive aggregation of the nanoconjugate after a prolonged period of storage time (almost one year) at 4°C. This problem should be overcome by storing the nanoconjugate in a more protective atmosphere, under argon and if possible at -20°C, in order to ensure stability and avoid aggregation. These aggregability/storage problems also emphasize the need of performing all characterization and preclinical validation experiments with a unique batch of product. Indeed, in our hands, all the characterization of the PGA-5-FU conjugate was conducted using the same product. This fact later helped us to confirm that toxicities observed *in vivo* were due exclusively to the degradation of PGA-5-FU during the storage period, and not to the presence of potential contaminants as derived from the different synthetic processes.

The selection of the appropriate linkage between the drug and the carrier is a key issue to obtain a good candidate for the improvement of the therapeutic efficacy of a single drug treatment. In addition to this, the conformation adopted by the conjugate in solution is also a key aspect regarding the exposure of the selected linkage to the environment. Fortunately, in the PGA-5-FU conjugate, the combination of a polymeric carrier of PGA with a MW of 15 kDa together with, the conjugation of the drug through an ester bond and the use of an aliphatic linker, resulted in a very stable structure in terms of unspecific release of the drug during transport and internalization of the nanoconjugate into the cells. Nonetheless, because it suffered unexpected degradation after a large period of storage, new bonds should be studied in the future.

From a more technical point of view there are clear advantages of performing *in vivo* biodistribution assays using fluorescently labeled PGA-5-FU to monitor the product biodistribution *in vivo*. In addition, results reported here show the importance of using optical probes with fluorescence during the preclinical validation of the system to monitor cell internalization processes by confocal microscopy and flow cytometry, which showed us that the internalization was through the endocytic pathway. Therefore, the use of these techniques is a powerful tool for the biological evaluation of synthetic PDC behavior *in vitro* and *in vivo* in a preclinical stage.

Regarding to the enzyme-cleavable linkers studied in this thesis, we were able to synthesize and test two different peptide linkers, one for MMP-7 enzyme and a second one for MMP-9. The use of enzyme-cleavable linkers is a very promising alternative to achieve an active release of the drug in the target site. This strategy is widely used for theranostics applications using fluorescent probes<sup>141</sup>, and has been recently introduced also in drug delivery systems<sup>69</sup>. One of the most important examples is the GPLG linker that is cleaved by Cathepsin B. This linker present in the PK1 system that have reached clinical trials<sup>95</sup>. In our case, polymer-drug conjugates were only obtained with the MMP-7 sensitive linker, whose specificity was confirmed when the conjugate was incubated with the MMP-7 enzyme. However, the use of an MMP7-sensitive linker resulted in an exposure of the ester bond to the environment. In this case, cytotoxicity experiments showed that the polymeric carrier did not protect the linkage (although higher plasma stability was observed *in vitro*). Further, therapeutic efficacy of PGA-MMP7pept-5FU similar to the single drug, suggesting unexpected release was occurring. For this reason, selection of an adequate linkage to ensure high stability until the target site is of most importance to improve efficacy and decrease systemic toxicity. In this sense, the conjugation of the MMP-cleavable linker and the 5-FU through a carbamate bond resulted very much stable. Amide and hydrazone bonds are probably alternatives to overcome faster release of 5-FU in PGA-MMPpept-5FU systems because PGA-Daunorubicin<sup>170</sup> and PGA-Melphalan<sup>171</sup> conjugates using this bonds have shown already promising anticancer activity.

In addition to the conjugation of 5-FU to a PGA carrier with and without MMP-sensitive linkers, this thesis showed the versatility offered by the PGA polymeric platform. A new PDC carrying 5-FU and SN-38 in the same vehicle was achieved in a simple synthetic strategy (PGA-5FU-SN38) as a combination therapy approach. Although 5-FU is the mainstay of CRC cytotoxic treatment, the drug is commonly administered in combination with other drugs. In this sense, the PGA-5FU-SN38 is a combined nanoplatform, which advantages compared to the administration of free drugs in combination should come from the co-delivery of both drugs at the malignant site simultaneously. Thus, it is reasonable to expect that this polymer-based multi-drug conjugate will be able to deliver drugs to a predetermined ratio and therefore diminish the administration regimens enhancing patient compliance. Different studies based on these similar nanoplatforms are ongoing being the HPMA-AGM-Dox<sup>93</sup> and PGA-DOX-PTX<sup>172</sup> the most relevant examples. To our best knowledge, the PGA-5FU-SN38 system developed herein is the first nanoplatform combining 5-FU and SN-38<sup>174</sup>.

In this thesis, the 20(S)-O-acylation of the SN-38 allowed the conjugation of the SN-38 hydrophobic agent to a polymeric carrier of PGA with a molecular weight of 15 kDa through an ester bond. This avoids the conversion of the SN-38 in its active form (E-Ring) to the lactone hydrolyzed carboxylate

form of SN-38 (inactive form) by opening of the ring and resulting in a water soluble product. The PGA-SN38 conjugate showed therapeutic activity *in vitro* in the HCT-116, Fluc2-C9 and HT-29, Fluc4 CRC cell lines studied. Thus, this work positively confirmed the possibility to administer SN-38 which is more potent than Irinotecan, and overcome solubility problems of SN-38 due to its hydrophobic nature. Similar results have been obtained with PGA-CPT<sup>166</sup> conjugates, where CPT is conjugated through the hydroxyl group to polyglutamate. However, compared to CPT, direct release of SN-38 might render a better efficacy because the SN38 is the most active CPT analogue and offers a better PK/PD profile<sup>174</sup>.

In the preliminary studies carried out with the PGA-5FU-SN38 conjugates family exploring different ratios of drugs, data confirmed that the ester bond used for the conjugation of both drugs remained stable in cell culture media (cytotoxicity profiles showed lower cytotoxicity than single drugs). Nonetheless, since a very extensive study is needed to determine the best combination of drugs (loading, bonds, linkers,...), and also study different types of bonds. In addition, overall 3D conformation needs to be carefully addressed, because the exposure of the bond might depend on the TDL of each drug, and for this reason the study of every single PDC is required.

Furthermore, the new combined PDC PGA-5FU-SN38 showed very promising results in terms of synergy between both bioactive agents in comparison to the single PDC carrying both drugs separately, probably because the internalization and co-delivery of both drugs simultaneously at the site of action. Thus, this thesis has provided a new class of combined PDC that offers better therapeutic activity than combination of two platforms with single drugs. In addition, in the *in vitro* experiments performed in the HT-29 CRC cell line, that has higher resistance to 5-FU treatment, a better therapeutic profile of the conjugate PGA-5FU-SN38 was observed in comparison to the free drugs. For all these reasons, the PGA-5FU-SN38 conjugate provided here seems a very interesting alternative for the treatment of patients with advanced CRC in which, chemotherapy resistance often occurs.

In conclusion, this thesis has provided a set of PDC, exploring different type of linkages, drugs and combinations, to be considered in further studies as a starting point for the development of new drug delivery systems based on PGA.

---

## 6. General Conclusions

---

Different PDC based on polyglutamic acid and 5-FU with a molecular weight of 15 kDa have been synthesized and characterized showing therapeutic activity *in vitro* in the HCT-116.Fluc2-C9 and HT-29.FlucC4 CRC cell lines. 5-FU bioactive agent has been conjugated to PGA using ester cleavable linkages (PGA-5-FU) or MMP-sensitive peptide linkers (PGA-MMPpept-5FU), as well as in combination with the active metabolite of Irinotecan (CPT-11), the SN-38 (PGA-5FU-SN38), showing in all cases good yields and reproducible synthetic strategies, thus confirming the versatility of the PGA-biodegradable systems.

Cellular uptake experiments performed with PGA-5-FU conjugate labeled with carboxyfluorescein fluorescent probe and their colocalization with lysosomal makers indicated that the internalization of the PDC was through the endocytic pathway, as expected for this type of macromolecules. *In vivo* biodistribution experiments of PGA-5-FU conjugate labeled with an AlexaFluor dye confirmed that the polymer accumulated into subcutaneous CRC tumors. These assays as well as 5-FU tissue quantifications confirmed also that the product was excreted mainly through the kidneys.

Regarding the PDC carrying a peptidyl linker sensitive to MMPs, the nature and length of the peptide sequence has a relevant importance in the therapeutic activity of the conjugate when MMP are overexpressed, because the amino acid sequence is fully associated with the final conformation of the PDC. MMP-9 sensitive peptide was used for the evaluation of the carbamate bond between the peptide linker and the drug and it was confirmed, through cytotoxic experiments, that this type of bond was too stable *in vitro*, resulting as an undesirable linkage for their use in polymeric nanoconjugates designed to release drugs gradually. In the PGA-MMP7pept-5FU study it was confirmed that the conjugation of the MMP7-sensitive peptide AHX-RPLALWRS-AHX through an ester bond to the PGA carrier with a Mw of 15 kDa lead a PDC that adopted a conformation in solution that resulted very accessible for the MMP-7 enzyme. In addition to the cleavage of the sensitive peptide, the hydrolysis of the ester bond was produced faster than expected. For this reason, a different linkage than the ester one between the drug and the linker should be explored to control the faster release of the drug.

Finally, in the PGA-5FU-SN38 conjugate study confirmed that the 20(S)-O-acylation of the SN-38 allowed the conjugation of the SN-38 to a polymeric carrier of PGA with a molecular weight of 15 kDa through an ester bond, avoiding the conversion of the SN-38 in its active form (E-Ring) to the lactone hydrolyzed carboxylate form of SN-38 (inactive form) by opening of this ring. Synergism studies performed with the family of PGA-5FU-SN38 conjugates carrying different ratios of 5-FU and SN-38, showed strong synergy measured through the calculation of the Combination Index, at high effective doses in HCT-116.Fluc2-C9 and HT-29.FlucC4 CRC cell lines, using as references the single PDC carrying both drugs separately.



---

## 7. RESUMEN

---

### *“Diseño, síntesis y evaluación biológica de nuevos conjugados polímero-droga basados en ácido poliglutámico y 5-fluorouracilo para el tratamiento de cáncer colorectal avanzado”*

---

#### 7.1 Introducción

El índice de incidencia del cáncer colorectal (CCR) es ligeramente mayor en los hombres que en las mujeres de todo el mundo. En concreto, es el tercer cáncer más frecuente en los hombres (después del cáncer de próstata y de pulmón) y el segundo más común en mujeres (después del cáncer de mama)<sup>1</sup>. La cirugía es el tratamiento de primera línea para el cáncer colorectal. En muchos casos sólo como una terapia adyuvante, después de la cirugía, los pacientes de CRC son tratados por medio de la quimioterapia. Varios fármacos han sido estudiados durante las últimas décadas para el tratamiento de cáncer colorectal metastásico, pero desde el 1960 el agente 5-fluorouracilo (5-FU) sigue siendo el tratamiento sistémico esencial para este tipo de cáncer. Sin embargo, la supervivencia global y superación de la enfermedad de los pacientes tratados con el agente quimioterapéutico 5-FU como primera línea de tratamiento es sólo del 10-15%<sup>11</sup>. Con el objetivo de mejorar esta problemática, varias estrategias han sido estudiadas para aumentar la actividad anticancerígena del 5-FU con el fin de obtener un mayor índice terapéutico y una mayor prevención de la degradación de la droga. En este sentido, gracias al desarrollo de pro-fármacos de 5-FU y la administración de 5-FU en combinación con otros agentes (Irinotecan u Oxaliplatino, entre otros) se han obtenido resultados positivos. Así, se ha conseguido una mejora en la eficacia terapéutica del 5-FU, pero por otro lado, la administración conjunta de más de un fármaco produce un incremento en los efectos secundarios. Por lo tanto, con el fin de mejorar el tratamiento actual, se requieren fórmulas que permitan la administración de combinaciones de fármacos para mejorar la esperanza y calidad de vida de los pacientes, reduciendo los efectos secundarios.

En las dos últimas décadas más de 40 nanomedicinas han sido aprobadas como nuevos fármacos y hay muchos más en investigación en la actualidad<sup>34</sup>. Debido a su escala nanométrica, los nanomedicamentos pueden pasar a través de varias barreras biológicas y generar su efecto en las células de manera más eficiente, por lo que se les considera una alternativa al diseño de fármacos. Los nanomedicamentos se definen como un sistema nanométrico complejo, compuesto al menos por 2 componentes, siendo uno de ellos el agente bioactivo.



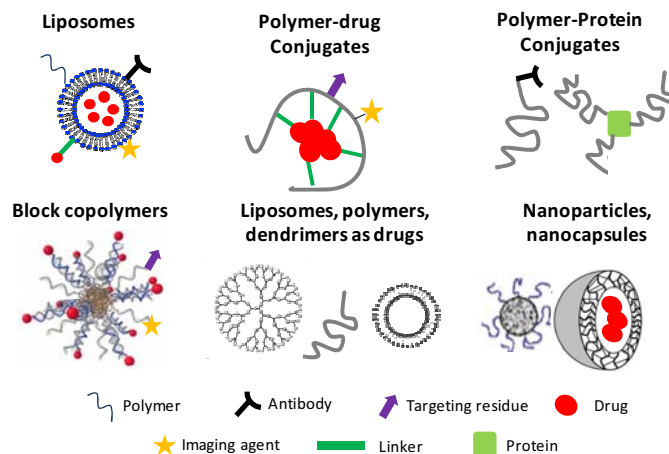


Figura 1. Esquema de las principales nanomedicinas (Adaptado de Duncan et al<sup>34</sup>).

Entre las distintas subclases de nanomedicinas, hemos centrado nuestra investigación en los Polímeros Terapéuticos (PT). Éstos son definidos como nuevas entidades químicas y a diferencia de los sistemas convencionales de administración de fármacos, en los que los fármacos son internalizados o solubilizados en la estructura del complejo, en los PT existe una unión covalente entre el vehículo y la droga (5-100 nm)<sup>39</sup>. Así pues, los PT son un enfoque positivo para controlar y mejorar la administración de fármacos. Por un lado, se caracterizan por proteger la droga y mejorar su biodistribución reduciendo la toxicidad, pero a su vez, impiden la degradación del fármaco y mejoran la absorción celular. Una de las características más importantes de los PT como nuevas nanomedicinas es la reducción de los efectos adversos de los fármacos debido al efecto EPR (*Enhanced Permeability and Retention Effect*, efecto de aumento de la permeabilidad y retención). Este efecto se produce por la alteración de la vasculatura en el tumor y de los defectos existentes en el sistema de drenaje linfático. Así, se produce una acumulación selectiva de las macromoléculas en el tumor, al contrario que los fármacos de bajo peso molecular donde la biodistribución no distingue entre el tumor y otros tejidos secundarios. Este fenómeno es también conocido como direccionamiento pasivo (*passive targeting*), ya que las nanomedicinas llegan a las células tumorales sin tener moléculas directoras, así como ocurre en el direccionamiento activo (*active targeting*). La acumulación preferencial en los tejidos tumorales permite, a su vez, el uso de dosis sustancialmente más bajas de fármacos y la minimización de los efectos secundarios.

En esta tesis se ha estudiado el diseño de nuevos conjugados polímero-droga (*Polymer Drug Conjugates*, PDC). Los PDC están compuestos por una estructura tripartita: la cadena principal del polímero (vehículo), el enlazador y el fármaco.

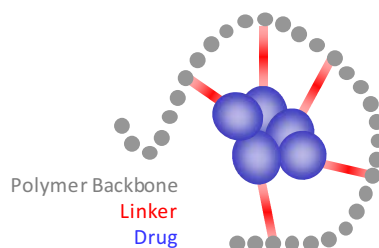


Figura 2. Esquema general de los conjugados polímero-droga.

En concreto, el trabajo se ha estructurado en tres apartados diferentes en los que se han diseñado y sintetizado diferentes PDC. Dado que los polímeros biodegradables se han convertido en los vehículos más apropiados para el diseño de sistemas de administración de fármacos para el tratamiento de enfermedades que requieren la administración parenteral crónica, o al menos repetida, en este proyecto se ha escogido como portador el polímero biodegradable ácido poli-L-glutámico (PGA) para el diseño de nuevos PDC vehiculizadores del 5-FU.

A parte de la conjugación de 5-FU a una cadena de PGA, se ha estudiado también un conjugado con una liberación selectiva de 5-FU sensible a metaloproteinasas de la matriz extracelular (*Matrix Metalloproteinases*, MMP) que se encuentran sobreexpresadas en tumores, esperando una liberación selectiva de la droga en ambientes ricos en MMP. Por lo tanto, con los PDC sensibles a MMPs, lo que se espera es combinar el efecto EPR con las ventajas adicionales de una liberación selectiva de 5-FU. Por último, se ha estudiado un diseño basado en la terapia combinada para la administración conjunta de 5-FU y SN-38 cargados en una misma cadena de PGA.

Durante todo el proceso el trabajo se ha realizado en colaboración entre la Unidad de Química Combinatoria en el Parque Científico de Barcelona (UQC-PCB), el Area de Validación Funcional y Ensayos Preclínicos (FVPR) y el Grupo *Drug Delivery and Targeting* del CIBBIM-Nanomedicina en el Instituto de Investigación del Hospital de la Vall d'Hebrón (VHIR).

## 7.2 Objetivos

Como se ha comentado, el objetivo principal de esta tesis es el diseño y desarrollo de nuevos conjugados polímero-droga basados en el portador polimérico biodegradable PGA para mejorar el tratamiento del cáncer colorectal avanzado basado en 5-FU. Dado que la estructura general está separada en 3 apartados principales (PGA-5-FU, PGA-MMPpept-5FU y PGA-5FU-SN38), se detallan a continuación los objetivos concretos para cada sección:

- **Nanoconjugado PGA-5-FU**

Síntesis, caracterización y validación *in vitro* e *in vivo* de un conjugado de PGA y 5-FU unidos mediante un enlace éster para conseguir una baja liberación del fármaco durante el transporte y una mejora de la biodistribución y actividad terapéutica de la macromolécula PGA-5-FU en modelos murinos.

- Síntesis y caracterización físico-química del conjugado PGA-5-FU mediante un enlace éster: tamaño, carga de fármaco y estabilidad en diferentes medios.
- Síntesis y caracterización del conjugado PGA-5-FU marcado con dos sondas fluorescentes para evaluar la biodistribución *in vivo* y la internalización celular (PGA-5FU-AF750 y PGA-5FU-CF).

- Evaluación de la citotoxicidad *in vitro* e internalización celular en líneas celulares de CRC del PGA-5-FU.
  - Evaluación de la biodistribución y la acumulación de PGA-5FU-AF750 en el tumor y la eficacia *in vivo* en modelos murinos.
- **Nanoconjugado PGA-MMPpept-5FU**

Síntesis, caracterización y validación *in vitro* de un conjugado de PGA y 5-FU sensible a MMPs sobreexpresadas en tumores. Para conseguir este objetivo se estudió la liberación con dos péptidos distintos sensibles a MMP-7 y MMP-9.

    - Estudio de la naturaleza de la unión entre el 5-FU y los péptidos sensibles a MMP-7 y MMP-9 en términos de estabilidad en distintos medios y frente a las enzimas MMP-7 y MMP-9 mediante dos tipos de enlace químico: éster y carbamato.
    - Diseño, síntesis y caracterización físico-química (tamaño, carga y estabilidad en distintos medios) de un nuevo conjugado sensible a MMP-7 basado en PGA y 5-FU (PGA-MMP7pept-5FU).
    - Evaluación de la citotoxicidad *in vitro* en líneas celulares de CRC con y sin sobreexpresión de MMP-7 de PGA-MMP7pept-5FU.
  - **Nanoconjugado PGA-5FU-SN38**

Síntesis, caracterización, validación *in vitro* y estudio de la sinergia de una familia de nanoconjugados de PGA con 5-FU y SN-38 conjugados a distintas proporciones (PGA-5FU-SN38).

    - Síntesis, caracterización físico-química (tamaño, carga y estabilidad en distintos medios) y evaluación de la citotoxicidad *in vitro* en líneas celulares de CRC de un conjugado de PGA y SN-38 unidos mediante un enlace éster (PGA-SN38).
    - Síntesis de una pequeña librería de conjugados de PGA-5FU-SN38 con distintas proporciones de SN-38:5-FU para la posterior evaluación *in vitro* en células de CCR y determinación del índice de combinación (CI) para el estudio del efecto sinérgico entre fármacos.

## 7.3 Resultados y discusión

### 7.3.1 Conjugado polimérico PGA-5-FU

Antes de la conjugación de 5-FU a los grupos carboxílicos de la cadena lateral del PGA fue necesario sintetizar un derivado de 5-FU. En concreto, en la posición N1 del 5-FU fue introducida una

molécula de ácido adípico mediante una unión éster, resultando la molécula 5-FU-adípico. En segundo lugar, una diamina fue conjugada con el grupo carboxílico de la molécula de 5-FU-adípico con el objetivo de tener un grupo amino libre en el derivado de 5-FU para reaccionar un siguiente paso con los grupos carboxílicos de la cadena lateral de PGA a través de un enlace amida.

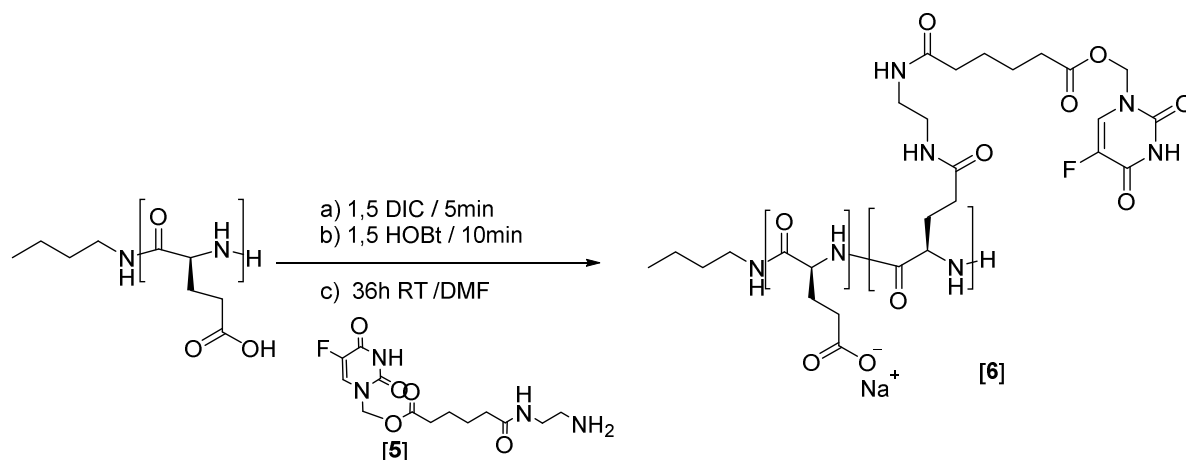


Figura 3. Esquema de Síntesis de PGA-5-FU. Condiciones: a) DIC (1.5 eq) 5 min; b) HOBT (1.5 eq), 10 min; c) 5-FUadipic-diamine (1 eq), 36 h (24 h DIC (1.5 eq)), RT.

Se realizaron diversas síntesis de PGA-5-FU (Tabla 1) para poner a punto la metodología sintética y además generar una cantidad suficiente de producto considerado como un único lote (después de mezclar algunos de los lotes individuales).

Tabla 1 Resumen de las distintas síntesis de PGA-5-FU realizadas.

# Lote	TDL % mg/mg	mg	Rdto. %	# Lote	TDL % mg/mg	mg	Rdto. %	# Lote	TDL % mg/mg	mg	Rdto. %
#1	1.6	28.5	27%	#7	9.06	40.5	37%	#13	1.92	153.8	20%
#2	7.63	22.5	27%	#8	12.82	246.9	28%	#14	6.27	509.2	42%
#3	10.2	32	22%	#9	9.18	250	35%	#15	5.68	808.9	58%
#4	3.29	168	25%	#10	10.2	1203	61%	#16	8.70	586.2	68%
#5	7.23	102.1	40%	#11	9.51	245	55%	Pool*	7.66	4175	-
#6	11.89	103.6	48%	#12	5.04	175	66%				

\* Pool corresponde al lote final considerados como un único producto donde se mezclaron los lotes # 8-16.

Así pues, la caracterización final y todos los ensayos de citotoxicidad y estabilidad *in vitro* y los experimentos de biodistribución e inhibición del tumor *in vivo* se realizaron con el mismo lote. Para cada síntesis, la cantidad de droga conjugada a la cadena polimérica (*Total Drug Loading*, TDL) se cuantificó mediante HPLC-UV, así como la droga atrapada en la estructura polimérica sin enlaces químicos (*Free Drug*, FD).

El producto PGA-5-FU [6] fue totalmente caracterizado y mostró un tamaño de partícula de 89.23 nm y una polidispersidad de 0.267 en agua (DLS).

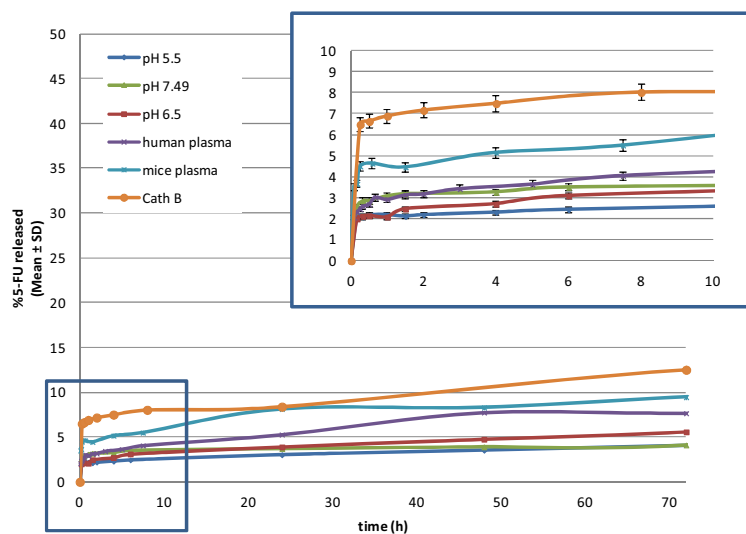


Figura 4. Curvas de degradación del conjugado PGA-5-FU incubado en distintos medios. El rectángulo azul corresponde a un área de ampliación de las primeras 10 horas de cada experimento.

Los estudios de estabilidad y liberación inespecífica de 5-FU en distintos medios (plasma humano y de ratón, PBS a diferentes pHs (5.5, 6.5 y 7.4) y Catepsina B) mostraron una alta estabilidad del enlace éster al detectar una liberación muy baja en plasma a lo largo del tiempo. Además, apenas se observó una liberación dependiente del pH, así como una degradación por acción de la enzima lisosomal Catepsina B del conjugado sostenida en el tiempo.

A lo largo de esta tesis se han utilizado dos líneas celulares de CCR distintas para llevar a cabo los experimentos de eficacia e internalización *in vitro*: HT-29.Fluc.C4 y HCT-116.FlucC2.C9. A las dos se les introdujo el gen *Firefly Luciferase* (Fluc) con el fin de permitir su monitorización *in vivo* por medio de imagen de bioluminiscencia.

La evaluación de la citotoxicidad de los diferentes lotes de PGA-5-FU se realizó mediante el método MTT. En todos los casos, la  $IC_{50}$  obtenida para el 5-FU era inferior a la correspondiente para el conjugado polimérico PGA-5-FU-pool [6]. Sin embargo, se confirmó la eficacia terapéutica de los compuestos sintetizados ya que los valores de  $IC_{50}$  tenían el mismo orden de magnitud que el fármaco solo ( $IC_{50}$  de 5-FU,  $4.88 \pm 0.01 \mu M$  en HCT-116 y  $14.21 \pm 0.05 \mu M$  en HT-29 vs.  $IC_{50}$  de PGA-5-FU-pool [6],  $33.38 \pm 0.01 \mu M$  en HCT-116 y  $82.25 \pm 0.02 \mu M$  en HT-29). Cabe destacar que tanto para el agente 5-FU como para el conjugado polimérico, la citotoxicidad siempre fue mayor en la línea celular HCT-116 que en la HT-29. Así pues, la línea celular HCT-116 mostró mayor sensibilidad al tratamiento basado en 5-FU.

Con el fin de poder visualizar mediante microscopía confocal la colocalización lisosomal del compuesto PGA-5-FU y confirmar su internalización, se marcó en una primera etapa el producto [6] con 6-carboxifluoreceína (PGA-5FU-CF [8]). Se realizaron los experimentos de internalización en las dos líneas celulares anteriormente mencionadas y se tomaron imágenes de microscopía confocal después de 30 minutos de incubación y al día siguiente (Figura 5). En ambos casos se observó colocalización lisosomal, de modo que se confirmó la internalización del producto PGA-5FU-CF por endocitosis.

Por otro lado, se procedió a cuantificar la internalización mediante citometría de flujo también en ambas líneas celulares, y los resultados mostraron una mayor cantidad de PGA-5FU-CF internalizado en las células HCT-116 que en las HT-29 además de internalizar más rápidamente en la primera línea celular.

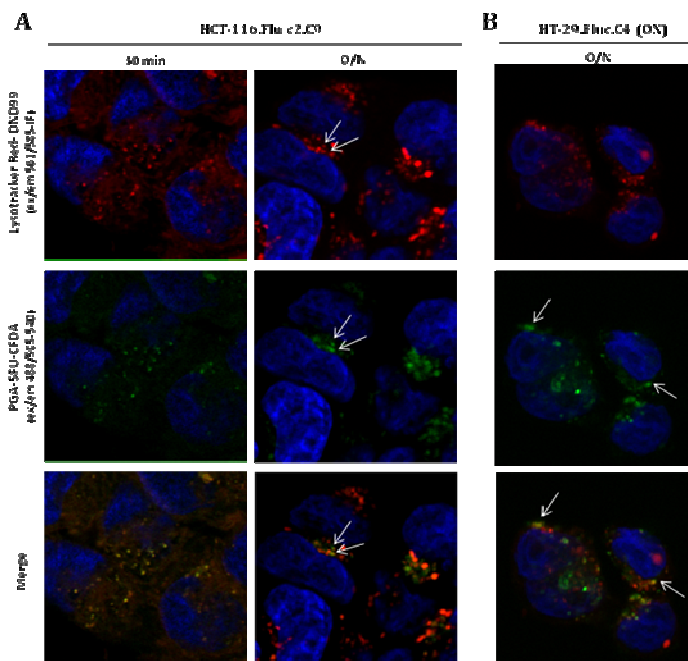


Figura 5 Imágenes de microscopía confocal *in vitro*: (A) células HCT-116.Fluc2.C9 a 100 mM eq de 5-FU después de 30 minutos y la incubación durante la noche (B) células HT-29.Fluc.C4 a 100 mM eq de 5-FU después de la incubación durante la noche. Se empleó LysoTracker-Red como marcador lisosomal (en rojo, primera línea) y el conjugado de polímero-fármaco se marcó con CF (en verde, segunda línea). La colocalización se ve en amarillo (tercera línea).

Con el fin de evaluar la acumulación tumoral y la biodistribución del conjugado PGA-5FU *in vivo* mediante imágenes de fluorescencia, fue necesario marcar el producto con el fluoróforo AF750 (PGA-5FU-AF750 [7]). Se realizaron dos síntesis distintas: PGA-5FU-AF750-1 y PGA-5FU-AF750-2. Cada producto fue utilizado para un experimento distinto. La diferencia de los ensayos yacía en la naturaleza de tumores crecidos de células inyectadas por vía subcutánea en el flanco trasero derecho: HCT-116.Fluc2-C9 y HT-29.Fluc-C4, respectivamente. En ambos casos se evaluó la acumulación en los tumores y la biodistribución del producto PGA-5FU-AF750 *in vivo* y *ex vivo* a partir de imágenes de fluorescencia con un equipo IVIS Spectrum®. Además, se cuantificaron con mayor precisión los niveles de acumulación a partir de una cuantificación de 5-FU por HPLC en los tejidos y plasma, mediante una metodología de homogenización y análisis puesta a punto para tal fin. Cabe destacar que en el experimento realizado con tumores crecidos de células HCT-116.Fluc2-C9 (PGA-5FU-AF750-1) se inyectó una dosis de 50 mg eq de 5-FU/kg, mientras que en el segundo experimento (HT-29.Fluc-C4, PGA-5FU-AF750-2) ésta resultó tóxica y el experimento se realizó con la mitad de la dosis (25 mg eq 5-FU/kg). La muerte del animal se produjo por un colapso pulmonar, motivo por el cual se sospechó que el producto PGA-5FU-AF750-2 a una dosis de 50 mg eq 5-FU/kg, podía haber agregado. Es conocido que las partículas de mayor tamaño pueden quedar atrapadas en capilares pulmonares después de la inyección por vía intravenosa. Desafortunadamente no se pudo medir el tamaño de partícula de la solución inyectada ya que la técnica DLS no permite analizar muestras que emitan señal de fluorescencia.

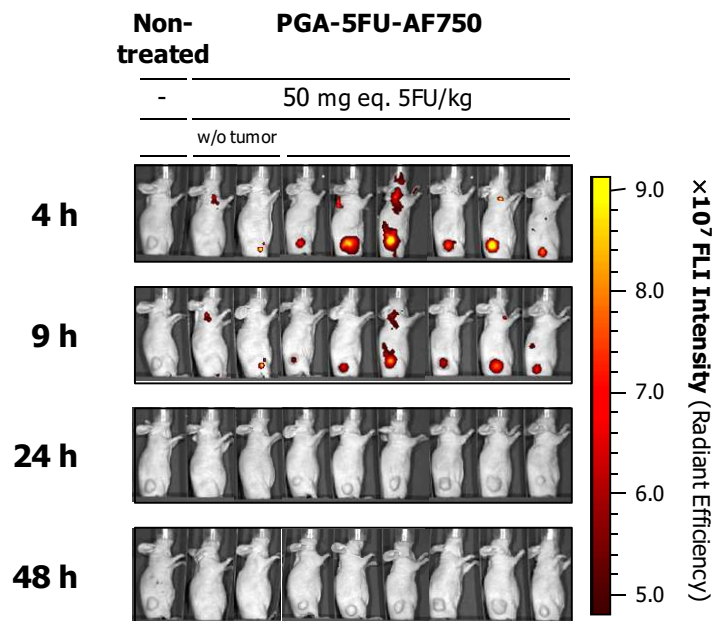


Figura 6 Imágenes FLI *in vivo* de ratones portadores de tumores crecidos de células HCT-116.Fluc2-C9.

Las imágenes de fluorescencia *in vivo* (FLI) mostraron una acumulación en el tumor (HCT-116.Fluc2-C9 (Figura 6)) en animales, siendo máxima 4 horas después de la administración y disminuyendo hasta las primeras 24 horas. Debido a la administración de una dosis reducida en la biodistribución realizada con animales portadores de tumores crecidos de células HT-29.Fluc-C4, la cantidad de fluoróforo quedó también reducida y no pudieron obtenerse buenas imágenes de FLI *in vivo*.

Las imágenes de fluorescencia tomadas *ex vivo* mostraron que el producto PGA-5FU-AF750 se encontraba en el riñón 4 h después de la administración y seguía presente hasta las primeras 48 h (excreción vía renal) en ambos experimentos. Por el contrario, sólo en el segundo experimento (HT-29.Fluc-C4) se observó mediante esta técnica, acumulación de producto en el hígado. Se recogieron tejidos (tumor, riñón, hígado y pulmón) y plasma de los animales inyectados con 5-FU o PGA-5FU-AF750 y se cuantificó la cantidad de 5-FU por HPLC después de su homogenización. Los resultados correlacionaron las medidas de FLI y proporcionaron información más detallada de la biodistribución del producto entre los tejidos analizados. El 5-FU se detectó en casi todos los tejidos y el plasma analizados para los animales inyectados con 5-FU y los inyectados con el conjugado polimérico marcado con AF750 (Figura 7) y se confirmó la excreción del nanoconjugado por vía renal y hepática. Además, en ambos experimentos se observó un aumento del tiempo de circulación del nanoconjugado respecto a la droga libre en plasma, confirmando así la estabilidad estudiada *in vitro* anteriormente.

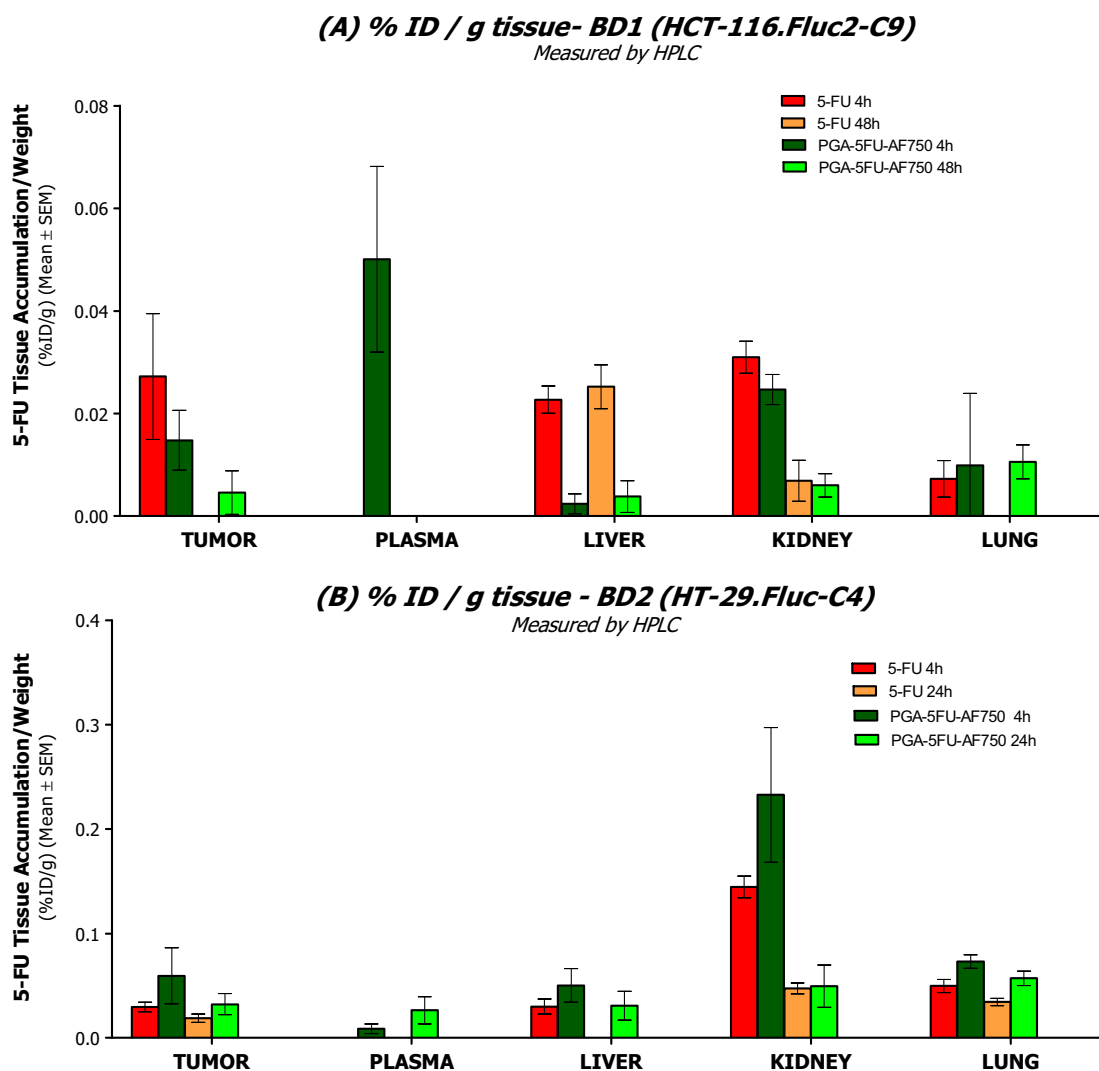


Figura 7. Representación de los niveles de 5-FU detectados en tejidos y plasma de animales inyectados con 5-FU o PGA-5FU-AF750, medido a 4 h y 24/48 h después de la administración en ratones portadores de tumores crecidos con células HCT-116.Fluc2-C9 (A) o HT-29.Fluc-C4 (B) inyectadas por vía subcutánea.

Posteriormente, se realizó un estudio de inhibición del crecimiento tumoral realizado en ratones portadores de tumores crecidos de células HCT-116.Fluc2-C9 inyectadas por vía subcutánea en el flanco trasero derecho. Cabe destacar que al igual que en el experimento de biodistribución realizado con animales portadores de tumores crecidos de células HT-29.Fluc-C4 la dosis de PGA-5-FU 50 mg eq 5-FU/kg resultó tóxica y se redujo a la mitad para la continuación del experimento. Desafortunadamente, *a posteriori* se confirmó que el producto se había deteriorado durante su almacenaje durante la espera a ser inyectado en los animales, confirmando la necesidad de guardarlo en atmósfera inerte para evitar agregaciones. Se prosiguió con el experimento de estudio de inhibición tumoral en ratones a una dosis de 30 mg eq 5-FU/kg y no se observó eficacia para el producto PGA-5-FU [6] en comparación con los animales control (inyectados con PBS). Sólo se observó una ligera eficacia (T/C=72%) para el grupo de animales tratados con 5-FU a una dosis de 30 mg eq 5-FU/kg. Esto confirmó también que la dosis administrada debido a los problemas de toxicidad estaba por debajo de la dosis eficaz para la droga libre.



### 7.3.2 Conjugado polimérico PGA-MMPpept-5FU

Como se ha mencionado, varias MMP se encuentran sobreexpresadas en estadios avanzados de CCR. En concreto, las encimas MMP-7 y MMP-9 fueron seleccionadas como diana para lograr una liberación controlada de fármacos de 5-FU en los tumores con el uso de péptidos sensibles a MMPs. Así pues, dos secuencias peptídicas sensibles a MMP-9 y MMP-7 se sintetizaron en fase sólida: GPVGLIG y AHX-RPLALWRS-AHX, respectivamente. Además, se sintetizaron los correspondientes péptidos alternados como un control negativo (GIVGPLG y AHX-RSWLPLRA-AHX, respectivamente). Posteriormente, se confirmó la selectividad respecto a MMP-7 y MMP-9 al incubar los péptidos con las enzimas.

En esta sección, si bien es cierto que se esperaba que existiera una liberación selectiva a MMP para el nanoconjugado PGA-MMPpept-5FU, decidimos explorar diferentes uniones (éster y carbamato) en la unidad 5-FU-péptido, para evaluar también la liberación del fármaco asociada a la hidrólisis de este enlace.

Para el estudio de la unión carbamato, se utilizó la secuencia sensible a MMP-9 (GPVGLIG) en la primera etapa del proyecto para la creación de la metodología sintética para conseguir este enlace. Se estudiaron varias estrategias y finalmente se obtuvo el producto 5-FU-Ala-COOH [26] (conjugando una  $\beta$ -alanina en la posición N1 de 5-FU a través de un enlace carbamato) para la posterior unión con el N-terminal del péptido mediante un enlace amida.

Se confirmó por HPLC-MS que el producto 5-FU-Ala-MMP9pept [26] es un sustrato para la enzima MMP-9 después de incubar el producto en presencia de la enzima, mientras que el producto 5-FU-ScramMMP9 no resultó sensible a MMP-9.

Para la evaluación de la idoneidad del enlace carbamato se realizó un ensayo de MTT *in vitro*. Si bien es cierto que se esperaba un comportamiento distinto una vez esta unidad droga-linker se conjugara con el polímero, se quiso estudiar si el enlace se hidrolizaba en las condiciones del ensayo celular. Sorprendentemente, no se observó citotoxicidad destacada para el producto 5-FU-Ala-MMP9pept a las concentraciones ensayadas (máximo testado: 200  $\mu$ M eq de 5-FU). Se observó que al aumentar la concentración de producto de 5-FU-Ala-MMP9pept la viabilidad celular disminuía. Sin embargo, la concentración máxima probada no era suficiente para lograr una toxicidad significativa, en comparación con el fármaco solo.

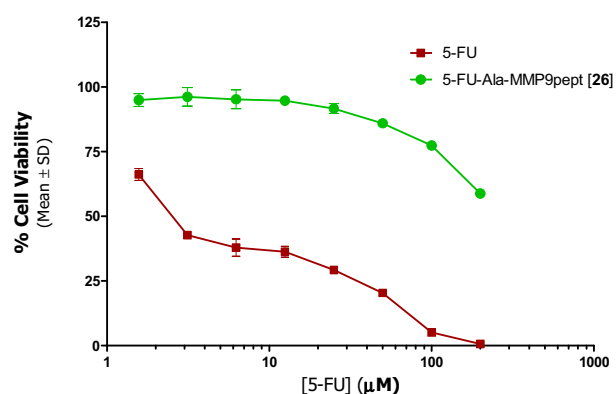


Figure 1. Curva de citotoxicidad del producto 5-FU-Ala-MMP9pept y 5-FU en la línea celular HCT-116. *Fluc2-C9*.  $IC_{50}$  (5-FU):  $3.36 \pm 0.039 \mu$ M,  $IC_{50}$  (product [26]):  $323.3 \pm 0.031 \mu$ M.

Desafortunadamente, se confirmó que la estabilidad del enlace carbamato era demasiado alta, lo que limitó en gran medida la actividad de 5-FU-Ala-MMP9pept [26] como compuesto citotóxico. Por lo tanto, decidimos evaluar el enlace éster para la síntesis del conjugado de PGA-MMPpept-5FU, teniendo en cuenta los buenos resultados obtenidos para el producto PGA-5-FU [6].

Se decidió sintetizar el nanoconjugado con el péptido sensible a MMP-7 unido a 5-FU a través de un enlace éster. La razón de esta decisión fue la mayor sobreexpresión de MMP-7 que MMP-9 en los tejidos de CCR. Además de la sobreexpresión de la encima MMP-9 en los tumores no se debe a las células tumorales únicamente, sino al comportamiento inflamatorio del tumor. Por lo tanto, decidimos trabajar principalmente con la enzima MMP-7, que sí está sobreexpresada por las células tumorales. La síntesis se realizó en un proceso de varias etapas utilizando el producto 5-FU-adipic [2] como producto de partida para obtener la molécula 5-FU-adipic-MMP7pept. Se incorporó una dimanina en el extremo C-terminal para la posterior conjugación a los grupos carboxílicos de la cadena de PGA. Se sintetizó también el conjugado de PGA-MMP7scram-5FU [38] como control negativo, con la secuencia alternada AHX-RSWLPLRA-AHX.

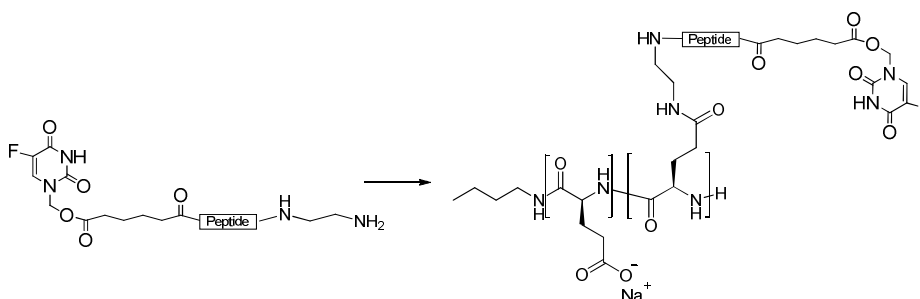


Figura 8 Esquema de síntesis de PGA-MMP-5-FU. Condiciones: a) DIC (1.5 eq) de 5 minutos; b) HOBt (1.5 eq), 10 min; c) 5-FUadipic-MMP-diamina (1 eq), 36 h (24 h DIC (1.5 eq)), RT.

El conjugado de PGA-MMP7pept-5FU [37] sintetizado mostró un tamaño de partícula de 208.2 nm y una polidispersidad de 0.566 en H<sub>2</sub>O medida mediante DLS. Los estudios de degradación mostraron una alta estabilidad en plasma y baja liberación dependiente del pH, pero al incubar el producto PGA-MMP7pept-5FU con MMP-7 se observó una alta liberación de la unidad 5-FU-RPLA (50%) durante las primeras 2 h. La enzima MMP-7 escinde el péptido inicial en las secuencias RPLA y LALWRS. Por lo tanto, se confirmó que la conformación que el conjugado polimérico PGA-MMP7pept-5FU [37] adopta en solución deja la cadena peptídica muy accesible para la enzima, permitiendo así su hidrólisis, incluso cuando se conjuga con el polímero macromolecular. Por otro lado, se confirmó que el producto liberado sería un 5-FU unido a un tetrapéptido (5-FU-RPLA).

Se realizó la evaluación de la citotoxicidad de producto de PGA-MMP7pept-5FU [37] mediante ensayos de MTT en las líneas celulares HCT-116 y HT-29 células con o sin sobreexpresión de MMP-7 (Figura 9).

Desafortunadamente, no se observaron diferencias significativas entre los dos tratamientos, con y sin sobreexpresión de MMP-7. Ninguno de los compuestos ensayados mostró el típico comportamiento esperado para los conjugados poliméricos, que normalmente tiene una  $IC_{50}$  ligeramente más alta que el fármaco libre debido al proceso de internalización y liberación posterior de la droga. Después del estudio de incubación del producto de PGA-MMP7pept-5FU [37] con MMP-7 se observó que el producto liberado cuando había sobreexpresión de MMP-7 era el 5-FU unido al tetrapéptido AHX-RPLA. Posteriormente al ensayo de MTT, se confirmó una hidrólisis rápida del enlace éster de la unidad 5-FU-RPLA liberando 5-FU libre. Esto se confirmó también al ver que no existían diferencias significativas entre los experimentos de incubación de PGA-MMP7pept-5FU y PGA-MMP7scram-5FU, ya que no se detectó una liberación dependiente de MMP7.

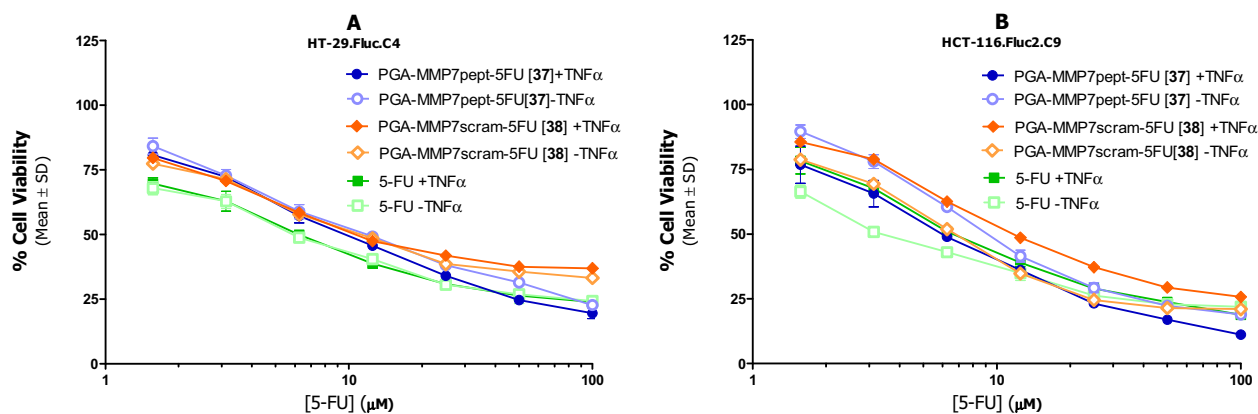


Figura 9. Gráficos de viabilidad celular de 5-FU y los productos de PGA-MMP7pept-5FU y PGA-MMP7scram-5FU obtenidos por el ensayo de MTT en las líneas celulares HT-29 (A) y HCT-116 (B) con y sin sobreexpresión de MMP-7.  $IC_{50}$  HCT-116 ( $\mu M$ ): 7.88 (5-FU+TNF $\alpha$ ), 4.08 (5-FU-TNF $\alpha$ ), 6.42 (PGA-MMP7-5FU+TNF $\alpha$ ), 10.77 (PGA-MMP7-5FU-TNF $\alpha$ ), 14.37(PGA-MMP7scram-5FU +TNF $\alpha$ ), 7.36 (PGA-MMP7scram-5FU +TNF $\alpha$ );  $IC_{50}$  HT-29 ( $\mu M$ ): 6.8 (5-FU+TNF $\alpha$ ), 6.64 (5-FU-TNF $\alpha$ ), 10.47(PGA-MMP7pept-5FU+TNF $\alpha$ ), 13.15 (PGA-MMP7pept-5FU-TNF $\alpha$ ), 16.46(PGA-MMP7scram-5FU +TNF $\alpha$ ), 14.28 (PGA-MMP7scram-5FU +TNF $\alpha$ ).

### 7.3.3 Conjugado polimérico PGA-5FU-SN38

En este apartado se decidió iniciar un estudio preliminar sobre el diseño de los conjugados poliméricos para el tratamiento de CCR con terapia combinada. En concreto, se estudió la conjugación de 5-FU y SN-38 (el metabolito activo de Irinotecan (CPT-11)) en un mismo portador polimérico de PGA.

Al tratarse de una etapa muy inicial para el desarrollo de un conjugado PGA-5FU-SN38 con una carga óptima de cada droga y una cinética de liberación de los dos fármacos ajustada, decidimos explorar inicialmente el enlace éster entre el fármaco y el vehículo de PGA para las dos drogas.

Entre todos los análogos de la CPT publicados en la literatura, se debe poner especial énfasis en los llamados: derivados 20-(S)-CPT-O-acilado. Dentro de todos los derivados de CPT descritos, los derivados 20-(S)-CPT-O-acilado tiene una mejor toxicidad asociada. El grupo hidroxilo de la posición

20(S) tiene una alta participación en el aumento de velocidad de hidrólisis de la lactona a la forma carboxilada (Figura 10). Por esta razón, la acilación del grupo hidroxilo para estabilizar el anillo de lactona es beneficiosa para bloquear su participación en la hidrólisis mediante la inhibición de la conversión hacia la forma carboxilada, lo que sugiere un beneficio terapéutico. Por lo tanto, decidimos utilizar en nuestro PDC con SN-38 esta estrategia para evitar el equilibrio lactona-carboxilato en favor de la forma carboxilada que es menos activa. En concreto, la O-acilación se realizó con una glicina. Por lo tanto, la conjugación del derivado de SN-38 a los grupos carboxílicos de la cadena de PGA se pudo realizar también a través de un enlace amida.

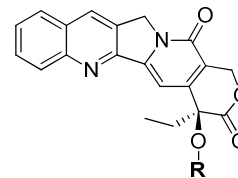


Figura 10 Estructura química de los derivados 20-(S)-CPT-O-acilado.

Con el fin de evaluar la ruta de síntesis para la conjugación del SN-38 a una cadena de PGA se realizó una primera síntesis de PGA-SN38 [48].

Se evaluó por espectroscopía la carga de SN-38 en el conjugado final (TDL), así como la droga libre atrapada sin unión química (FD) y se cuantificó el TDL en un 10% y el FD <0.1%. El conjugado de PGA-SN38 sintetizado [48] mostró un tamaño de partícula de 79.63 nm y una polidispersidad de 0.195 en PBS a pH 7.4 medido por DLS.

En los ensayos de estabilidad en distintos medios (plasma, pHs y Catepsina B), del mismo modo que el conjugado PGA-5-FU [6], el conjugado PGA-SN38 [48] mostró una liberación muy baja en relación al pH, una alta estabilidad en plasma y mostró degradación por la catepsina B *in vitro*.

Se realizaron ensayos de eficacia terapéutica *in vitro* mediante el ensayo de MTT, y se observó un comportamiento típico para los conjugados poliméricos, siendo más activa la droga sola pero mostrando actividad a las concentraciones testadas en las dos líneas celulares, siendo más resistente al SN-38 la línea HT-29. ( $IC_{50}$  de SN-38  $0.013 \pm 0.05 \mu\text{M}$  en HCT-116 y  $0.09 \pm 0.04 \mu\text{M}$  en HT-29;  $IC_{50}$  de PGA-SN38  $0.05 \pm 0.04 \mu\text{M}$  en HCT-116 y  $0.26 \pm 0.03 \mu\text{M}$  en HT-29).

Una vez que se confirmó que el producto de SN38-Gly [47] se podía conjugar al vehículo de PGA, una pequeña familia de conjugados de PGA-5FU-SN38 fue sintetizada con el objetivo de evaluar el posible efecto sinérgico de los productos sintetizados con diferentes cargas de 5-FU y SN-38. Se estudió la citotoxicidad *in vitro* con la combinación de los fármacos individuales en diferentes proporciones. Finalmente, se vio que una proporción de 1:240 (SN-38:5-FU) mostraba una actividad sinérgica de los fármacos solos. Es por ello que se intentó conseguir que los conjugados de PGA-5FU-SN38 [49] tuviesen esta relación de carga entre los dos fármacos.

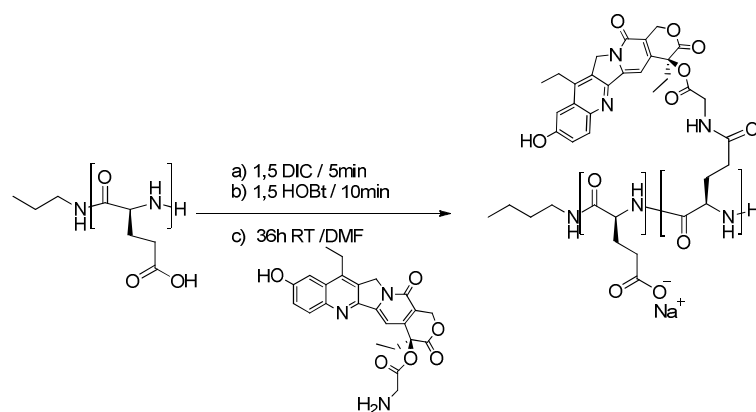


Figura 11 Esquema de síntesis de PGA-SN38. Condiciones: a) DIC (1.5 eq) de 5 min; b) HOBt (1.5 eq), 10 min; c) SN-38-Gly (1 eq), 36 h (24 h DIC (1.5 eq)), RT.

En la Tabla 2 se resumen los diferentes PGA-5FU-SN38 sintetizados. Los experimentos de MTT se realizaron también en las dos líneas celulares HT-29 y HCT-116 pero al contrario de los experimentos llevados a cabo antes, en este caso se duplicaron los experimentos para poder ver el efecto de los dos fármacos fijando la concentración máxima a 330  $\mu\text{M}$  eq de 5-FU y 1  $\mu\text{M}$  eq de SN-38, respectivamente. Además, también se estudiaron las combinaciones de los fármacos individuales en las mismas proporciones que en cada PDC.

Tabla 2. Resumen de los diferentes conjugados de PGA-5FU-SN38 [49] sintetizados.

# Lote	mg obtenidos	TDL (5-FU)% (mg/mg)	TDL(SN-38) % (mg/mg)	mM 5-FU	mM SN-38	Ratio SN-38:5-FU
#A	140.1	3.05%	0.025%	10	0.03	1:300
#B	179.4	0.26%	0.02%	0.34	0.02	1:40
#C	123.5	3.27%	5.15%	42.3	2.20	1:20
#D	260	2.55%	0.025%	10	0.03	1:300

Posteriormente se evaluó en Índice de Combinación (*Combinatory Index*, CI) para los conjugados #B y #D ya que fueron los que presentaban mayor actividad terapéutica *in vitro*, con el objetivo de evaluar la sinergia entre los dos fármacos unidos a una misma cadena de PGA, a partir del método de Chou-Talalay<sup>165</sup>. Se observó que la conjugación de SN-38 y 5-FU a proporciones 1:40 y 1:300, respectivamente, presentaba un efecto sinérgico fuerte al comparar estas mismas proporciones con conjugados simples (únicamente cargados con 5-FU o SN-38) o las drogas libres. Este resultado positivo se observó en las dos líneas celulares testadas. A partir de estos datos se pudo confirmar que la conjugación de las dos drogas en un mismo vehículo presentó mayor eficacia posiblemente debido a que ambas drogas se liberan simultáneamente en el mismo sitio. Además, cabe destacar que la fuerte sinergia se observó también en la línea celular HT-29, la cual a lo largo del proyecto ha

demostrado ser más resistente al tratamiento de 5-FU. Se sabe que los focos metastáticos pueden aparecer debido a la resistencia al tratamiento, por este motivo, consideramos que el tratamiento basado en terapia combinada de 5-FU y SN-38 utilizando un único vehículo, sería una gran alternativa para el tratamiento de pacientes con cáncer colorectal en estado avanzado.

## 7.4 Conclusiones

- En relación al primer nanoconjugado estudiado, **PGA-5-FU**, en esta tesis se ha demostrado que la conjugación de 5-FU a un portador polimérico de PGA de peso molecular 15 kDa mediante un enlace éster y un espaciador (ácido adípico) muestra actividad terapéutica *in vitro* en las dos líneas de CRC estudiadas (HCT-116 y HT-29).

Además, los ensayos de internalización celular realizados con el nanoconjugado marcado con una sonda fluorescente, demostraron la internalización del conjugado de PGA-5-FU por vía endocítica, que resultó ser más rápida en la línea celular HCT-116 que no en la HT-29, internalizando además mayor cantidad de compuesto. En los ensayos de biodistribución *in vivo* realizados en modelos murinos de CRC con animales portadores de tumores crecidos de células HCT-116 o HT-29 inyectadas por vía subcutánea, se pudo confirmar una mayor acumulación de PGA-5-FU a tiempos largos en tumor en comparación con los niveles de 5-FU detectados en animales inyectados con la droga libre. Se demostró también que el producto se excretó preferencialmente por vía renal, aunque también se eliminó en menor cantidad por vía hepática. Además se confirmó también que la conjugación de 5-FU a un polímero de PGA mediante la estrategia de síntesis utilizada, permitía aumentar el tiempo de vida media en plasma que es del orden de minutos para el 5-FU, al detectarlo hasta 24 h después de la inyección.

Finalmente, se detectó un problema de estabilidad del compuesto PGA-5-FU a las condiciones de almacenamiento utilizadas, que produjo un problema de degradación y posterior agregación del producto que resultó ser tóxico para los animales.

- Los resultados obtenidos en el apartado de estudio de nanoconjugados de PGA sensible a MMP (**PGA-MMPpept-5FU**) confirmaron que es de relevante importancia el tipo de enlace entre el péptido sintetizado sensible a MMP-7 o MMP-9 y el agente 5-FU. Se confirmó mediante la evaluación citotóxica de la unidad péptido-droga (con el péptido sensible a MMP-9), que la unión carbamato resultaba ser demasiado estable *in vitro*, ofreciendo un comportamiento opuesto al enlace éster, siendo así no aconsejable su uso en nanoconjugados poliméricos diseñados para una liberación progresiva de la droga.

En este apartado se confirmó mediante ensayos de actividad terapéutica con HCT-116.Fluc2-C9 y HT-29.Fluc4 que sobreexpresaban MMP-7 que la conformación que adopta el nanoconjugado PGA-MMP7-5FU, sintetizado a partir de la conjugación de la unidad péptido droga (con unión éster) a la cadena polimérica de PGA de peso molecular 15 kDa,

en solución deja las cadenas peptídicas muy accesibles al exterior del compuesto. Así pues, la ruptura del péptido se produjo a mayor velocidad de lo esperado a diferencia de lo observado *in vitro* en ensayos de actividad terapéutica con las células HCT-116.Fluc2-C9 y HT-29.FlucC4 sin sobreexpresión de MMP-7 así como en los estudios de incubación en los distintos medios por separado.

Al analizar los resultados observados para un nanoconjugado control sintetizado con una secuencia alternada no sensible a MMP-7 se concluyó que el enlace éster para este tipo de nanoconjugado con los péptidos AHX-RPLALWRS-AHX o AHX-RSWLPLRA-AHX no era una buena opción, ya que quedaba demasiado expuesto. Es por este motivo por el que se sugiere el estudio de distintos tipos de enlace entre péptido y droga para mejorar la selectividad del conjugado de PGA-MMP7pept-5FU, así como la evaluación del uso de polímeros de mayor peso molecular.

- Finalmente, en el estudio basado en la terapia combinada con el nanoconjugado **PGA-5FU-SN38** y se observó que mediante la O-acilación del SN-38 en la posición 20(S) se conseguía conjugar la droga a un portador polimérico de PGA de peso molecular 15 kDa mediante un enlace éster. Se confirmó así que el SN-38 permanecía en su forma activa evitando la hidrólisis de la lactona (SN-38 inactivo, anillo abierto) ya que el conjugado resultante PGA-SN38 mostró actividad terapéutica *in vitro* en las dos líneas de CRC estudiadas (HCT-116 y HT-29). Posteriormente, en los estudios preliminares *in vitro* realizados con una pequeña familia de conjugados sintetizados para conseguir una terapia combinada de 5-FU y SN-38 cargados con distintas proporciones de fármacos, sintetizados a través de un enlace éster (PGA-5FU-SN38), se observó actividad citotóxica en las líneas celulares mencionadas de ambos agentes en una relación de SN-38:5-FU de 1:40 y 1:300 en comparación con el comportamiento observado con los fármacos combinados como agentes individuales en la misma proporción. Además se confirmó un efecto sinérgico fuerte entre 5-FU y SN-38 en estos conjugados combinados a partir del cálculo del Índice de Combinación, demostrando los beneficios de unir los dos fármacos en un mismo vehículo y asegurar una liberación conjunta y simultánea de ambos.

# References

---

- <sup>1</sup> Ferlay, J.; Steliarova-Foucher, E.; Loutet-Tienlent, J.; Rosso, S.; Coebergh, J.W.W.; Comber, H.; Forman, D.; Bray, F., Cancer incidence and mortality patterns in Europe: Estimates for 40 countries in 2012. *European Journal of Cancer*, 2013, 49, 1374-1403.
- <sup>2</sup> Siegel, R.; Naishadham, D.; Jemal, A., Cancer statistics 2013. *Cancer Journal for Clinicians*, 2013, 63, 11-30.
- <sup>3</sup> Michor, F.; Iwasa, Y.; Lengauer, C.; Nowak, M.A., Dynamics of Colorectal Cancer. *Seminars in Cancer Biology*, 2005, 15, 6, 484-493.
- <sup>4</sup> Winslow, T., National Cancer Institute 2005, [www.nci.org](http://www.nci.org)
- <sup>5</sup> Brenner, H.; Kloor, M.; Pox, C.P., Colorectal Cancer. *The Lancet*, 2014, 383, 1490-1502.
- <sup>6</sup> Bacolod, M.; Barany, F., Molecular profiling of colon tumors: the search for clinically relevant biomarkers of progression, prognosis, therapeutics, and predisposition. *Annals of Surgical Oncology*, 2011, 18, 3694-3700.
- <sup>7</sup> Davies, J.; Miller, R.; Coleman, N., Colorectal cancer screening: prospects for molecular stool analysis. *Nature Reviews Cancer*, 2005, 5, 199-209.
- <sup>8</sup> Wagenaar-Miller, R.; Gorden, L.; Matryasian, L., Matrix Metalloproteinases in colorectal cancer: Is it worth talking about? *Cancer and Metastasis Reviews*, 2004, 23, 119-135.
- <sup>9</sup> Wolpin, B.; Mayer, R., Systemic treatment of colorectal cancer. *Gastroenterology*, 2008, 134(5), 1296-1310.
- <sup>10</sup> Rutman, R.J.; Cantarow, A.; Paschkis, K.E., Studies in 2-Acetylaminofluorene Carcinogenesis: III. The Utilization of Uracil-2-C<sup>14</sup> by Preneoplastic Rat Liver and Rat Hepatoma. *Cancer Research*, 1954, 14, 119.
- <sup>11</sup> Longley, D.; Harkin, P.; Johnston, P.G., 5-Fluorouracil: mechanisms of action and clinical strategies. *Nature Reviews Cancer*, 2003, 3, 330-339.
- <sup>12</sup> Marsoni, S.; Negri, M., Efficacy of adjuvant fluorouracil and folinic acid in colorectal cancer. *The Lancet*, 1995, 345, 939-944.
- <sup>13</sup> Johnston, P.G.; Kaye, R., Capecitabine: a novel agent for the treatment of solid tumors. *Anticancer Drugs*, 2001, 12, 639-646.
- <sup>14</sup> Scripture, C.; Figg, W., Drug interactions in cancer therapy. *Nature Reviews*, 2006, 6, 546-556.
- <sup>15</sup> Leyland-Jones, B.; O'Dwyer, R.J., Biochemical modulation: application of laboratory models to clinic. *Cancer treatment Reports*, 1986, 70, 219-229.
- <sup>16</sup> Meta-analysis of randomized trials testing the biochemical modulation of fluorouracil by MTX in metastatic colorectal cancer. Advanced Colorectal Cancer Meta-Analysis Project. *Journal of Clinical Oncology*, 1994, 12, 960-969.
- <sup>17</sup> Rothenberg, M., Irinotecan (CPT-11): Recent developments and future directions-colorectal cancer and beyond. *The Oncology*, 2001, 6, 66-80.
- <sup>18</sup> Senter, P.D.; Beam, K.S.; Micain, B.; Wahl, A., Identification of CPT-11, a clinically approved anticancer drug. *Bioconjugation Chemistry*, 2001, 12, 1074-1080.
- <sup>19</sup> Treeiney-Molsen, M.; Kanz, M.F., Intestinal tract injury by drugs: Importance of metabolite delivery by yellow bile road. *Pharmacology and Therapeutics*, 2006, 112, 659-667.
- <sup>20</sup> Horikawa, M.; Kato, Y.; Sugiyama, Y., Reduced gastrointestinal toxicity following inhibition of the biliary excretion of irinotecan and its metabolites by probenidol in rats. *Pharmaceutical Research*, 2002, 19 (13), 1345-1353.



- 
- <sup>21</sup> Kawato, Y.; Aonuma, M.; Hirota, Y., Intracellular roles of SN-38, a metabolite of the camptothecin derivative CPT-11, in the antitumor effect of CPT-11. *Cancer Research*, 1991, 51, 4187-4191.
- <sup>22</sup> Hartmann, J.T.; Lipp, H.P., Camptothecin and podophyllotoxin derivatives: inhibitors of topoisomerase I and II mechanisms of action, pharmacokinetics and toxicity profile. *Drug Safety*, 2006, 29, 209-230.
- <sup>23</sup> Pastorino, F.; Loi, M.; Sapra, P., Tumor regression and curability of preclinical neuroblastoma models by PEGylated SN-38 (EZN-2208), a novel Topoisomerase I inhibitor. *Clinical Cancer research*, 2010, 16, 4809-4821.
- <sup>24</sup> Alcindor, T.; Beauger, N., Oxaliplatin: a review in the era of molecularly targeted therapy. *Current Oncology*, 2011, 18, 18-25.
- <sup>25</sup> Park, J.; Lee, S.; Kim, J.; Park, K.; Kim, K.; Kwon, I., Polymeric Nanomedicine for cancer therapy. *Progress in Polymer Science*, 2008, 33, 113-137.
- <sup>26</sup> Ferrarotto, R.; Hoff, P., Antiangiogenic drugs for colorectal cancer: exploring new possibilities. *Clinical Colorectal Cancer*, 2013, 1-7.
- <sup>27</sup> Canevari, S.; Raspagliesi, F.; Lorusso, D., Bevacizumab treatment and quality of life in advanced ovarian cancer. *Future Oncology*, 2013, 9, 7, 951-954.
- <sup>28</sup> Sotelo, MJ.; Garcia-Paredes, B.; Aguado, C.; Satre, J.; Díaz-Rubio, E., Role of cetuximab in first-line treatment of metastatic colorectal cancer. *World Journal of Gastroenterology*, 2014, 15, 4208-4219.
- <sup>29</sup> Dievtvorst, M.; Eskens, L., Current and novel treatment options for metastatic colorectal cancer: emphasis on Aflibercept. *Biology Therapeutics*, 2013, 3, 25-33.
- <sup>30</sup> Mitchel, E., Targeted therapy for metastatic colorectal cancer: Role of Aflibercept. *Clinical Colorectal Cancer*, 2013, 73-85.
- <sup>31</sup> Douillard, J.; Cunningham, D.; Roth, A.; Navarro, M.; James, R.; Karasek, P.; Jandik, P.; Iveson, T.; Carmichael, J.; Alaki, M.; Gruia, G.; Awad, L.; Rougier, P., Irinotecan combined with fluorouracil compared with fluorouracil alone as first-line treatment for metastatic colorectal cancer: a multicentre randomized trial. *The Lancet*, 2000, 355, 1041-1047.
- <sup>32</sup> Saltz, L.; Cox, J.; Blanke, C.; Roen, L.; Fehrenbacher, L.; Moore, M.; Maroun, J.; Locker, P.; Pirotta, N.; Elfering, G.; Miller, L., Irinotecan plus fluorouracil and leucovorin for metastatic colorectal cancer. *The New England Journal of Medicine*, 2000, 343(13), 905-914.
- <sup>33</sup> Cidón, E., The challenge of metastatic colorectal cancer. *Clinical Medical insights: Oncology*, 2010, 4, 55-60.
- <sup>34</sup> Duncan, R.; Gaspar, R., Nanomedicine(s) under Microscope. *Molecular Pharmacology*, 2011, 8 (6), 2101-41.
- <sup>35</sup> Duncan, R., Polymer therapeutics as Nanomedicines: new perspectives. *Current opinion in Biotechnology*, 2011, 22, 492-501.
- <sup>36</sup> *European Science Foundation's Forward Look Nanomedicine: an EMRC Consensus opinion*, 2005; <http://www.esf.org>.
- <sup>37</sup> Duncan, R.; Vicent, MJ., Polymer therapeutics-prospects for 21<sup>st</sup> century: The end of the beginning. *Advanced Drug Delivery Reviews*, 2013, 65, 60-70.
- <sup>38</sup> Duncan, R.; Connors, T.A.; Maeda, H., Drug targeting in cancer therapy: the magic bullet, what next? *Journal of Drug Targeting*, 1996, 3 (5), 317-319.
- <sup>39</sup> Duncan, R., The dawning era of polymer therapeutics. *Nature Reviews*, 2003, 2, 347-360.
- <sup>40</sup> Duncan R., Polymer Conjugates as anticancer Nanomedicines. *Nature Reviews Cancer*, 2006, 6, 688-701.
- <sup>41</sup> Vasey, PA.; Kaye, SB.; Morrison, R.; Twelves, C.; Wilson, P.; Duncan, R.; Thomosn, AH.; Murray, LS.; Hilitch TE.; Murray, T.; Burtles, S.; Fraier, D.; Frigerio, E.; Cassidy, J., Phase I clinical and pharmacokinetic study of PK1 [N[N-(2-hydroxypropyl)methacrylamide copolymer doxorubicin]: first member of a new class of

---

chemotherapeutic agents-drug-polymer conjugates. Cancer Research Campaign Phase I/II Committee. *Clinical Cancer Research*, 1999, 5, 1, 83-94.

<sup>42</sup> Kavanov, A.; Batrakova, E.; Alakhov, V., Pluronic block copolymers for overcoming drug resistance in cancer. *Advanced Drug Delivery Reviews*, 2002, 54, 759-779.

<sup>43</sup> Vasir, J.; Labhsetwar, V., Polymeric nanoparticle for gene delivery. *Expert Opinion Drug Delivery*, 2006, 3, 325-344.

<sup>44</sup> Vicent, MJ.; Duncan, R., Polymer conjugates: nanosized medicines for treating cancer. *Trends in Biotechnology*, 2006, 24 (1), 39-47.

<sup>45</sup> Shy, Y.; Xu, T., Peptide-Polymer Conjugates: From fundamental Science to Application. *Annual Reviews of Physical Chemistry*, 2013, 64, 631-657.

<sup>46</sup> Sanchís, J.; Canal, F.; Lucas, R.; Vicent, MJ., Polymer-drug conjugates for novel molecular targets. *Future Medicine* 2010, 5 (6), 915-935.

<sup>47</sup> Peer, D.; Karp, J.; Hong, S.; Farokhzad, O.; Margalit, R.; Langer, R., Nanocarriers as an emerging platform for cancer therapy. *Nature Nanotechnology*, 2007, 2, 751-760.

<sup>48</sup> Rejmanova, P., Stability in plasma and serum of lysosomally degradable oligopeptide sequences in N-(2-hydroxypropyl) methacrylamide copolymers. *Biomaterials*, 1985, 6, 45-48.

<sup>49</sup> Brocchini, S.; Duncan R., Pendant drugs, release from polymers. In *Encyclopedia of Controlled Drug Delivery*, Mathiowitz, Ed. Wiley Interscience: New York, 1999; pp 786-816.

<sup>50</sup> Markovsky, E.; Baabur-Cohen, H.; Eldar-Boock, A.; Omer, L.; Tiram, G.; Ferber, S.; Ofek, P.; Polyak, D.; Scompatin, A.; Satchi-Fainaro, R., Administration, distribution, metabolism and elimination of polymer therapeutics. *Journal of Controlled Release*, 2012, 161, 446-460.

<sup>51</sup> Chau, Y.; Frederick, E.; Langer, R., Synthesis and Characterization of Dextran-Peptide-Methotrexate conjugates for tumor targeting via mediation by matrix metalloproteinase II and matrix metalloproteinase IX. *Bioconjugate Chemistry*, 2004, 15, 931-941.

<sup>52</sup> Stern, L.; Perry, R.; Ofek, P.; Many, A.; Shabat, D.; Satchi-Fainaro R., A novel antitumor prodrug platform designed to be cleaved by endoprotease legumain. *Bioconjugation Chemistry*, 2009, 20, 500-510.

<sup>53</sup> Duncan, R.; Richardson, S.C., Endocytosis and Intracellular trafficking as gateways for Nanomedicine delivery: Opportunities and Challenges in preparation. *Molecular Pharmacology*, 2012, 9, 2380-2402.

<sup>54</sup> Hardwike, J.; Moseley, R.; Stephens, P.; Harding, K.; Duncan, R.; Thomas, D., Bioresponsive dextrin-rhEGF conjugates: *in vitro* evaluation in models relevant to its proposed use as a treatment for chronic wounds. *Molecular Pharmaceutics*, 2010, 7 (3), 699-707.

<sup>55</sup> Singer, J.; Shaffer, S.; Baker, B.; Bernareggi, A.; Stromatt, S.; Nienstedt, D.; Besman, M., Paclitaxel polyglumex (XYTOAX; CT-2103): an intracellularly targeted taxane. *Anti-Cancer Drugs*, 2006, 16, 1-12.

<sup>56</sup> Vicent, MJ.; Pérez-Payá, E., Poly-L-glutamic acid aided inhibitors of apoptotic protease activating factor 1 (Apaf-1): An Antiapoptotic polymeric Nanomedicine. *Journal of Medicinal Chemistry*, 2006, 49, 13, 3763-3765.

<sup>57</sup> Li, C., Poly(L-glutamic acid)-anticancer drug conjugates. *Advanced drug Delivery Reviews*, 2002, 54, 695-713.

<sup>58</sup> Duncan, R., Polymer Therapeutics: Top 10 selling pharmaceuticals: What next? *Journal of Controlled release*, 2014, 1-10.

<sup>59</sup> Duncan R.; Sat-Klopsch, Y.; Sausville, E., Validation of tumor models for the use on anticancer Nanomedicine evaluation: the EPR effect and Cathepsin-B mediated drug release rate. *Cancer Chemotherapy and Pharmacology*, 2013, 72, 417-427.

- 
- <sup>60</sup> Bhat, R.; de Vries, P.; Tulinsky, J.; Bellamy, G.; Baker, B.; Singer, J.W.; Klein, P., Synthesis and *in vivo* antitumor activity of Poly(L-glutamic acid) conjugates of 20(S)-Camptothecin. *Journal of Medical Chemistry*, 2003, 46, 190-193.
- <sup>61</sup> Zunino, F.; Prateisi, G.; Micheloni, A., Poly(carboxylic acid) polymers as carriers for anthracyclines. *Journal of Controlled Release*, 1989, 10, 65-73.
- <sup>62</sup> Mochizuki, E.; Inaki, Y.; Takemoto, K., Synthesis of poly-L-glutamates containing 5-substitued uracil moieties. *Nucleic Acids Research Symposium*, 1985, 16, 121-124.
- <sup>63</sup> Roos, C.F.; Matsumoto, S.; Takarura, Y.; Hashida M.; Sezaki, H., Physicochemical and antitumor characteristics of some polyamino acid prodrugs of mitomycin C. *International Journal of Pharmacology*, 1984, 22, 75-87.
- <sup>64</sup> Duncan, R.; Vicent, M.J.; Greco, F.; Nicholson, R., Polymer-drug conjugates: toward a novel approach for the treatment of endocrine-related cancer. *Endocrine-related Cancer*, 2005, 1, 189-199.
- <sup>65</sup> Maeda, H.; Wu, J.; Sawa, T.; Matsumura, Y.; Hori, K., Tumor vascular permeability and the EPR effect in macromolecular therapeutics: a review. *Journal of Controlled Release*, 2000, 65, 271-284.
- <sup>66</sup> Matsumura, H.; Maeda, H., A new concept for macromolecular therapeutics in cancer chemotherapy: Mechanism of tumorotropic accumulation of proteins and the antitumor agent SMANCS. *Cancer Research*, 1986, 46, 6387-6392.
- <sup>67</sup> Peer, D.; Jeffrey, M, Karp, M.; Seungpyo, H.; Farokhzad, R.; Langer, R., Nanocarriers as an emerging platform for cancer therapy. *Nature Nanotechnology* 2007, 2, 751 - 760
- <sup>68</sup> Fang, J.; Nakamura, H.; Maeda, H., The EPR effect: Unique features of tumor blood vessels for drug delivery, factors involved, and limitations and argumentation of the effect. *Advanced Drug Delivery Reviews*, 2011, 63, 136-151.
- <sup>69</sup> Markovsky, E.; Baabur-Cohen, H.; Eldar-Boock, A.; Omer, L.; Tiram, G.; Ferber, S.; Ofek, P.; Polyak, D.; Scompatin, A.; Satchi-Fainaro, R., Administration, distribution, metabolism and elimination of polymer therapeutics. *Journal of Controlled Release*, 2012, 161, 446-460.
- <sup>70</sup> Hidalgo, M.; Eckhardt, G.S., Development of Matrix Metalloproteinase Inhibitors in Cancer Therapy. *Journal of National Cancer Institute*, 2001, 93, 3, 178-193.
- <sup>71</sup> Liotta, LA.; Tryggvason, K.; Garbisa, S.; Hart, I.; Foltz, CM.; Shafie, S., Metastatic potential correlates with enzymatic degradation of basement membrane collagen. *Nature*, 1980, 284, 67-68.
- <sup>72</sup> Leema, M., Curran, S., Murray, G.; New Insights into the roles of matrix metalloproteinases in colorectal cancer development and progression. *Journal of Pathology*, 2003, 201, 528-524.
- <sup>73</sup> Zucker, S.; Vacirca, J., Role of matrix metalloproteinases (MMPs) in colorectal cancer. *Cancer and Metastasis Reviews*, 2004, 23, 101-117.
- <sup>74</sup> Wagenaar-Miller, R.; Gorden, L.; Matrysián, L., Matrix Metalloproteinases in colorectal cancer: Is it worth talking about? *Cancer and Metastasis Reviews*, 2004, 23, 119-135.
- <sup>75</sup> Vihnen, P.; Kähäri, V., Matrix metalloproteinases in cancer: prognostic markers and therapeutic targets. *International Journal of Cancer*, 2002, 99, 157-166.
- <sup>76</sup> Vartak, D.G., Gemeinhart, R.; Matrix metalloproteases: Underutilized targets for drug delivery. *Journal of Drug Targeting*, 2007, 15, 1-20.
- <sup>77</sup> Wilson, C.L.; Heppner, K.; Labosky, P.; Hogan, B.L.M.; Matrisian, L., Intestinal tumorigenesis is suppressed in mice lacking the metalloproteinase matrylisin. *Proceedings of National Academy of Sciences*, 1997, 94, 1402-1407.
- <sup>78</sup> Said, A.; Raufman, J.; Xie, G., The role of matrix metalloproteinases in colorectal cancer. *Cancers*, 2014, 6, 366-375.

- 
- <sup>79</sup> Maradni, A.; Khoshnevisan, A.; Mousavi, SH.; Emamirazavi, SH.; Noruzijavidan, A., Role of matrix metalloproteinases (MMPs) and MMP inhibitors on intracranial aneurisms: a review article. *Medical Journal of the Islamic Republic of Iran*, 2013, 27, 4, 249-254.
- <sup>80</sup> Messerli, F.; TIMPs, MMPs and cardiovascular disease. *European Heart Journal*, 2004, 25, 1475-1476.
- <sup>81</sup> Zucker, S.; Cao, J., Selective matrix metalloproteinase (MMP) inhibitors in cancer therapy: Ready for prime time? *Cancer Biology Therapeutics*, 2009, 24, 8, 2371-2373.
- <sup>82</sup> Gong, Y.; Chippada-Venkata, U.; Oh, W., Roles of matrix metalloproteinases and their natural inhibitors in prostate cancer progression. *Cancers*, 2014, 6, 1298-1327.
- <sup>83</sup> Bodiga, V.; Eda, S.; Chavali, S.; Bodiga, S., *In vitro* biological evaluation of glyburide as potential inhibitor of collagenases. *International Journal of Biological Macromolecules*, 2014, 187-192.
- <sup>84</sup> Bremer, C.; Tung, C., Weissleder, R.; *In vivo* molecular target assessment of matrix metalloproteinase inhibition. *Nature Medicine*, 2001, 7, 743-748.
- <sup>85</sup> Chopra, A.; Cy5.5-Conjugated matrix metalloproteinase cleavable peptide nanoprobe. *Molecular Imaging and Contrast Agent Database*.
- <sup>86</sup> de Duve, C.; de Barse, T.; Poole, B.; Trouet, A.; Tulkens, P.; Van Hoof, F., Commentary, Lysosmotropic agents. *Biochemical Pharmacology*, 1974, 23 (18), 2495-2531.
- <sup>87</sup> Haag, R.; Kratz, F., Polymer Therapeutics: Concepts and Applications. *Angewandte Chemie*, 2006, 45, 1198-1215-
- <sup>88</sup> Greco, F.; Vicent, M.J., Combination therapy: opportunities and challenges for polymer-drug conjugates as anticancer Nanomedicines. *Advanced Drug Delivery Reviews*, 2009, 61, 1203-1213.
- <sup>89</sup> Verschraegen, C.F.; Skubitz, K.; Daud, A.; Kudelka, A.; Rabinowitz, I.; Allievi, C.; Eisenfeld, A.; Singer, J.; Oldham, F., A phase I and pharmacokinetic study of paclitaxel polyglumex and cisplatin in patients with advanced solid tumors. *Cancer Chemotherapy and Pharmacology*, 2009, 63, 903-910.
- <sup>90</sup> Dipetrillo, T.; Milas, L.; Evans, D., Paclitaxel Polyglumex (PPX-xyotax) and concurrent radiation for esophageal and gastric cancer- a phase I study. *Journal of Clinical Oncology*, 2006, 29, 376-379.
- <sup>91</sup> Hongrapipat, J.; Kopečková, P.; Liu, J.; Prakongpan, S.; Kopeček, J., Combination chemotherapy and photodynamic therapy with fab' fragment targeted HPMA copolymer conjugates in human ovarian carcinoma cells. *Molecular Pharmacology*, 2008, 5, 696-709.
- <sup>92</sup> Fang, J.; Sawa, T.; Akaike, T.; Greish, T.; Maeda, H., Enhancement of chemotherapeutic response of tumor cells by a heme oxygenase inhibitor, pegylated zinc protoporphyrin. *International Journal of Cancer*, 2004, 19, 1-8.
- <sup>93</sup> Vicent, M.J.; Greco, F.; Nicholson, R.; Paul, A.; Griffiths, P.; Duncan, R., Polymer Therapeutics designed for a combination therapy of hormone-dependent cancer. *Angewandte Chemie International Edition*, 2005, 44, 4061-4066.
- <sup>94</sup> Santucci, L.; Mencarelli, S.; Renga, B.; Ceccobelli, D.; Pasut, G.; Veronese, F.; Distrutti, E.; Fiorucci, M.D., Cardiac safety and anti-tumoral activity of a new nitric oxide derivative of pegylated epirubicin in mice. *Anticancer Drugs*, 2007, 18, 1081-1091.
- <sup>95</sup> Satchi, R.; Connors, T.A.; Duncan, R., PDEPT: polymer-directed enzyme prodrug therapy I. HPMA copolymer–cathepsin B and PK1 as a model combination, *British Journal of Cancer*, 2001, 85, 1070-1076.
- <sup>96</sup> Satchi-Fainaro, R.; Hailu, H.; Davies, J.W.; Summerford, C.; Duncan, R., PDEPT: Polymer-directed enzyme prodrug therapy. 2. HPMA copolymer–beta-lactamase and HPMA copolymer–C–Dox as a model combination. *Bioconjugate Chemistry*, 2003, 14 (4), 797-804.
- <sup>97</sup> Sanchís, J.; Canal, F.; Lucas, R.; Vicent, MJ., Polymer-drug conjugates for novel molecular targets. *Nanomedicine*, 2010, 5, 6, 915-935.

- 
- <sup>98</sup> Zhang, S., Poly (L-glutamic acid)-Paclitaxel Conjugates for cancer treatment. *Biomedical Science, Engineering and Technology*, 2012.
- <sup>99</sup> ElMeshad, A.; Mortazavi, S.; Mozafari, M., Formulation and characterization of nanoliposomal 5-fluorouracil for cancer nanotherapy. *Journal of Liposome Research*, 2014, 24, 1-9.
- <sup>100</sup> Thomas, A.; Kapanen, A.; Hare, J.; Ramsay, E.; Edwards, K.; Karlsson, G.; Bally, M., Development of a liposomal nanoparticle formulation of 5-Fluorouracil for parenteral administration: Formulation design, pharmacokinetics and efficacy. *Journal of Controlled Release*, 2011, 150, 212–219.
- <sup>101</sup> Paharia, A.; Yadav, K.; Rai, G.; Jain, S.; Pancholi, S.; Agrawal, G., Eudragit-coated Pectin Microspheres of 5-Fluorouracil for Colon Targeting, *AAPS PharmSciTech* 2007, 8, 1-8.
- <sup>102</sup> Mishra, R.; Ramasamy, K.; Ahmad, N.; Eshak, Z.; Majeed, A., pH dependent poly[2-methacryloyloxyethyl]trimethylammonium chloride-co-methacrylic acid]hydrogels for enhanced targeted delivery of 5-fluorouracil in colon cancer cells. *Journal of Materials Science*, 2014, 1-14.
- <sup>103</sup> Wang, Q.; Liu, Q.; Liu, L.; Feng, J.; Li, J.; Guo, Z.; Mei, Q., Synthesis and evaluation of the 5-fluorouracil-pectin conjugate targeted at the colon. *Medicinal Chemistry Research*, 2007, 16, 370-379.
- <sup>104</sup> Cheng, M.; Gao, X.; Wang, Y.; Chen, H.; He, B.; Xu, H.; Li, Y.; Han, Y.; Zhang, Z., Synthesis of Glycyrrhetic Acid-Modified Chitosan 5-Fluorouracil Nanoparticles and Its Inhibition of Liver Cancer Characteristics *in vitro* and *in Vivo*. *Marine Drugs*, 2013, 11, 3517-3536.
- <sup>105</sup> Ke, W.; Zhao, Y.; Huang, R.; Jiang, C.; Pei, Y., Enhanced oral bioavailability of doxorubicin in a dendrimer drug delivery system. *Journal of Pharmaceutical Sciences*, 2008, 97, 2208-2216.
- <sup>106</sup> Greenfield, R.; Kaneko, T.; Daves, A.; Edson, M.; Fitzgerald, K.; Olech, Grattan, G.; Spitanly, G.; Braslawsky, G., Evaluation *in vitro* of Adriamycin Immunoconjugates Synthesized Using an Acid-sensitive Hydrazone Linker. *Cancer Research*, 1990, 50, 6600-6607.
- <sup>107</sup> Ramaswamy, C.; Sakthivel, T.; Wilderspin, A.; Florence, A., Dendriplexes and their characterisation. *International Journal of Pharmaceutics*, 2008, 254, 17-21.
- <sup>108</sup> Mei, M.; Ren, Y.; Yuan, X.; Li, F.; Jiang, L.; Kang, C.; Yao, Z., Suppression of breast cancer cells *in vitro* by polyamidoamine-dendrimer-mediated 5-fluorouracil chemotherapy combined with antisense micro-RNA 21 gene therapy. *Journal of Applied Polymer Science*, 2009, 114, 3760–3766.
- <sup>109</sup> Laquintana, V.; Denora, N.; Lopalco, A.; Lopodota, A.; Cutrignelli, A.; Lasorsa, F.; Agostino, F.; Franco, M., Translocator Protein Ligand–PLGA Conjugated Nanoparticles for 5-Fluorouracil Delivery to Glioma Cancer Cells. *Molecular Pharmaceutics*, 2014, 11, 3, 859-871.
- <sup>110</sup> Yuan, F.; Qin, X.; Zhou, D.; Xiang, Q.; Wang, M.; Zhang, Z.; Huang, Y., *In vitro* cytotoxicity, *in vivo* biodistribution and antitumor activity of HPMA copolymer–5-fluorouracil conjugates. *European Journal of Pharmaceutics and Biopharmaceutics*, 2008, 70, 770-776.
- <sup>111</sup> Simón, L. Nanoconjugados como transportadores de fármacos anticancerígenos: Dendrímeros basados en PEG y Polimersomas del copolímero PMPC-PDPA. *Universitat de Barcelona*, 2011.
- <sup>112</sup> Ying-Qian, L.; Yang, H.; Tian, X., Design, Synthesis and Biological Evaluation of Novel Etoposide Analogues as cytotoxic agents. *Chinese Journal of Chemistry*, 2006, 6, 785-790.
- <sup>113</sup> Howard-Sparks, M.; Abeer, M.; Al-Ghananeem, A.; Pearson, P., Crooks, A., Evaluation of O3 $\alpha$ -, O21-Di-(N1-methyloxycarbonyl-2, 4-dioxo-5-fluoropyrimidinyl)17 $\alpha$ -hydroxy-5 $\beta$ -pregnan-20-one as a novel potential antiangiogenic codrug. *Journal of Enzyme Inhibition and Medicinal Chemistry*, 2005, 20, 417-428.
- <sup>114</sup> Frieden, M.; Giraud, M.; Reese, C.; Song, Q., Synthesis of 1-[*cis*-3-(hydroxymethyl)cyclobutyl]-uracil, -thymine and -cytosine. *Journal of Chemical Society, Perkin Transactions*, 1. 1998, 17, 2827-2832.
- <sup>115</sup> Ozaki, S., Synthesis and antitumor activity of 5-fluorouracil derivatives. *Nucleosides and Nucleotides*, 1897, 6, 249-256.

- 
- <sup>116</sup> Zhuo, R.; Du, B.; Rong, Z., *In vitro* release of 5-Fluorouracil with cyclic core dendritic polymer. *Journal of Controlled Release*, 1999, 57, 3, 249-257.
- <sup>117</sup> Kametani, T.; Kigasawa, K.; Hijragi, M.; Wakisaka, K.; Haga, S.; Nagamatsu, Y.; Sugi, H.; Fukawa, K.; Irino, O., Studies on the syntheses of heterocyclic compounds. 845. Studies on the synthesis of chemotherapeutics. 10. Synthesis and antitumor activity of N-acyl- and N-(alkoxycarbonyl)-5-fluorouracil derivatives. *Journal of Medicinal Chemistry*, 1980, 23, 1324-1329.
- <sup>118</sup> Chen, SW.; Xiang, R.; Liu, J.; Tian, X.; Synthesis and biological evaluation of novel conjugates of podophyllotoxin and 5-FU as antineoplastic agents. *Bioorganic and Medicinal Chemistry*, 2009, 17, 8, 3111-3117.
- <sup>119</sup> Wang, Q.; Liu, X.; Feng, J.; Li, Y.; Guo, Z.; Mei, O., Synthesis and evaluation of the 5-fluorouracil-pectin conjugate targeted at the colon. *Medicinal Chemistry Research*, 2007, 16, 370-379.
- <sup>120</sup> Howard-Sparks, M.; Al-Ghananeem, A.; Pearson, A.; Crooks, P., Evaluation of O3 $\alpha$ -, O21-Di-(N1-methyloxycarbonyl-2, 4-dioxo-5-fluoropyrimidinyl)17 $\alpha$ -hydroxy-5 $\beta$ -pregnan-20-one as a novel potential antiangiogenic codrug. *Journal of Enzyme Inhibition and Medicinal Chemistry*, 2005, 20(5), 417-428
- <sup>121</sup> Qian, S.; Wu, J.; Li, J.; Wu, Y., Synthesis and Characterization of New Liver Targeting 5-Fluorouracil-Cholic Acid Conjugates. *Archiv der Pharmazie*, 2009, 342, 9, 513-520.
- <sup>122</sup> Taylor, E.; Sloan, K., 1-Alkylcarbonyloxymethyl prodrugs of 5-fluorouracil (5-FU): Synthesis, physicochemical properties, and topical delivery of 5-FU. *Journal of Pharmaceutical Sciences*, 1985, 87, 1, 15-20.
- <sup>123</sup> Buur, A.; Bundgaard, H.; Falch, H., Prodrugs of 5-fluorouracil. IV. Hydrolysis kinetics, bioactivation and physicochemical properties of various N-acyloxymethyl derivatives of 5-fluorouracil. *International Journal of Pharmaceutics*, 1985, 24, 1, 43-60.
- <sup>124</sup> William, J.; Roberts, L.; Kenneth, B., Synthesis of 3-alkylcarbonyloxymethyl derivatives of 5-fluorouracil. *Journal of Heterocyclic Chemistry*, 2002, 39, 5, 905-910.
- <sup>125</sup> Fante, C.; Eldar-Boock, A.; Satchi-Fainaro, R.; Osborn, M.; Greco, F., Synthesis and Biological Evaluation of a Polyglutamic Acid-Dopamine Conjugate: A New Antiangiogenic Agent. *Journal of Medicinal Chemistry*, 2011, 54, 5255-5259.
- <sup>126</sup> Vicent, MJ.; Pérez-Payá, E., Poly-L-glutamic acid (PGA) Aided Inhibitors of Apoptotic Protease Activating Factor 1 (Apaf-1): An Antiapoptotic Polymeric Nanomedicine. *Journal of Medicinal Chemistry*, 2006, 49, 3763-3765
- <sup>127</sup> Rejmanova, P., Stability in plasma and serum of lysosomally degradable oligopeptide sequences in N-(2-hydroxypropyl) methacrylamide copolymers. *Biomaterials*, 1985, 6, 45-48.
- <sup>128</sup> Bajaj, I.; Singhal, R., Poly (glutamic acid) – An emerging biopolymer of commercial interest. *Biosource Technology*, 2011, 102, 5551-5561.
- <sup>129</sup> De Duve, C.; De Barsy, T.; Poole, B.; Trouet, A.; Tulkens, P.; Van Hoof, F., Lysosmotropic agents. *Biochemical Pharmacology*, 1974, 3, 2495-2531.
- <sup>130</sup> Van Kuilenburg, A.; Lenthe, H.; Maring, J.; Van Gennip, A., Determination of 5-Fluorouracil in plasma with HPLC-tandem mass spectrometry. *Nucleosides, Nucleotides and Nucleic Acids*, 2006, 25, 1257-1260.
- <sup>131</sup> Sabatini, L.; Barbieri, A.; Tosi, M.; Saverio Violante, F., A new high-performance liquid chromatographic/electrospray ionization tandem mass spectrometric method for the simultaneous determination of cyclophosphamide, methotrexate and 5-fluorouracil as markers of surface contamination for occupational exposure monitoring. *Journal of Mass Spectrometry*. 2005, 40, 669-674.
- <sup>132</sup> Jiang, H.; Zeng, J.; Zheng, N.; Kandoussi, H.; Peng, Q.; Valentine, J.; Lange, R.; Arnold, M., A convenient strategy for quantitative determination of drug concentrations in tissue homogenates using liquid

---

chromatography/Tandem mass spectrometry assay for plasma samples. *Analytical Chemistry*, 2011, 83, 6237-6244.

<sup>133</sup> Carli, D.; Honorat, M.; Cohen, S.; Megherbi, M.; Vignal, B.; Dumontet, C.; Payen, L.; Guitton, J., Simultaneous quantification of 5-FU, 5-FUrd, 5-FdUrd, 5-FdUMP, dUMP and TMP in cultured cell models by LC-MS/MS. *Journal of Chromatography B*, 2009, 877, 2937-2944.

<sup>134</sup> Wang, N.; Wang, T.; Maoling, W.; Hao, A.; Li, T., Using ultrafiltration to facilitate simultaneous quantification of 5-Fluorouracil in mouse plasma and tissues by HPLC. *Journal of Liquid Chromatography and Related Technologies*, 2011, 34, 2033-2047.

<sup>135</sup> Déporte-Féty, R.; Picot, M.; Amiand, M.; Moreau, A.; Campion, A.; Lanoe, D.; Renée, N.; Milano, G., High-performance liquid chromatographic assay with ultraviolet detection for quantification of dihydrofluorouracil in human lymphocytes: application to measurement of dihydropyrimidine dehydrogenase activity. *Journal of Chromatography B*, 2001, 762, 203-209.

<sup>136</sup> Casale, F.; Canaparo, R.; Muntoni, E.; Serpe, L.; Zara, G.; Della Pepa, C.; Berno, E.; Costa, M.; Eandi, M., Simultaneous HPLC determination of 5-fluorouracil and its metabolites in plasma of cancer patients. *Biomedical Chromatography*, 2002, 16, 446-452.

<sup>137</sup> Gamoun, S.; Saguem, S., Extraction sur phase solide et analyses par HPLC du 5-FU plasmatique. *Comptes Rendues Chimie*, 2005, 1688-1693.

<sup>138</sup> Oasis sample extraction products Brochure: Sensitivity in its purest form. <http://www.waters.com/webassets/cms/library/docs/720001692en.pdf>

<sup>139</sup> Turk, B.; Huang, L.; Piro, E.; Cantley, L., Determination of protease cleavage site motifs using mixture-based oriented peptide libraries. *Nature Biotechnology*, 2001, 19, 661-667.

<sup>140</sup> Lim, S.; Jeong, Y.; Moon, K.; Ryu, H.; Yong, J.; Jin, S.; Jung, T.; Kim, I.; Kang, S.; Jung, S., Anticancer activity of PEGylated matrix metalloproteinase cleavable peptide-conjugate adriamycin against malignant glioma cells. *International Journal of Pharmaceutics*, 2010, 387, 209-214.

<sup>141</sup> McIntyre, J.; Fingleton, B.; Wells, K.; Piston, D.; Lynch, C.; Gautam, S.; Matrisian, M., Development of a novel fluorogenic proteolytic beacon for *in vivo* detection and imaging of tumor-associated matrix metalloproteinase-7 activity. *Journal of Biochemistry*, 2004, 377, 617-628.

<sup>142</sup> Leung, K., Cy5.5-Aminohexanoic acid-RPLALWRS-aminohexanoic acid-C-G4-PAMAM-PEG-AF750. *Molecular Imaging and Contrast Database*.

<sup>143</sup> Welch, A.R.; Browner, C.; Gehring, M.; Kan, M.; Vanwart, H., Purification of human matrilysin produced in *Escherichia coli* and characterization using a new optimized fluorogenic peptide substrate. *Archives of Biochemistry and Biophysics*, 1995, 324, 59-64.

<sup>144</sup> Hu, X.; Liu, S.; Huang, Y.; Chen, X.; Jing, X., Biodegradable block copolymer-doxorubicin conjugates via different linkages: preparation, characterization, and *in vitro* evaluation. *Biomacromolecules*, 2010, 11, 2094-2102.

<sup>145</sup> Vaccaro, H.; Zhao, Z.; Clader, J.W.; Song, L.; Terracina, G.; Zhang, L.; Pissarnitski, D.A., Solution-phase parallel synthesis of carbamates as  $\gamma$ -secretase inhibitors. *Journal of Combinatorial Chemistry*, 2008, 10, 56-62.

<sup>146</sup> Pothukanuri, S.; Winssinger, N., A Highly efficient azide-based protecting group for amines and alcohols. *Organic Letters*, 2007, 9, 2223-2225.

<sup>147</sup> Theodoroi, v., Skobridis, K., Tzakos, A.G., Ragoussis, V.; A simple method for the alkaline hydrolysis of esters. *Tetrahedron Letters*, 2007, 48, 8230-8233.

<sup>148</sup> Lee, S.; Chao, Y.; Kim, H.; park, K.; Park, S.; Ha, S.; Kim, W., Inhibitory effects of the ethanol extract of thorns on human colon cancer HCT116 cells. *Oncology Reports*, 2009, 22, 1505-1512

- 
- <sup>149</sup> Bhat, R.M.; de Vries, P.; Tulinsky, J.; Bellamy, G.; Baker, B.; Singer, J.W.; Klein, P.; Synthesis and *in vivo* antitumor activity of Poly(L-glutamic acid) conjugates of 20(S)-Camptothecin. *Journal of Medical Chemistry*, 2003, 46, 190-193.
- <sup>150</sup> Zhao, H., EZN-2208 (PEG-SN38), A 40 kDa Polyethylene Glycol (PEG) Conjugate, As an anticancer agent: Review of Preclinical and clinical data. *Current Bioactive Compounds*, 2011, 7, 3-7.
- <sup>151</sup> Patnaik, A.; Papadopoulos, K.; Tolcher, A.; Beeram, M.; Urien, S.; Schaaf, L.J.; Tahiri, S.; Bekaii-Saab, T.; Lokiec, F.; Reza, K.; Buchbinder, A., Phase I dose-escalation study of EZN-2208 (PEG-SN38), a novel conjugate of poly(ethylene) glycol and SN-38, administered weekly in patients with advanced cancer. *Cancer Chemotherapy Pharmacology*, 2013, 71, 1499-1506.
- <sup>152</sup> Zhang, J.A.; Tong, X.; Manjeet, P.; Ma, L.; Sydney, U.; Shahid, A.; Imran, A., Development and characterization of a novel liposome-based formulation of SN-38. *International Journal of Pharmacology*, 2004, 270, 93-107.
- <sup>153</sup> Gu, Q.; Xing, J.; Huang, M.; He, C.; Chen, J., SN-38 loaded polymeric micelles to enhance cancer therapy. *Nanotechnology*, 2012, 23, 1-10.
- <sup>154</sup> Deborah, S.; Nirmalkumar, V.; Peter, W.; Hamidreza, G., G3.5 PAMAM dendrimers enhance transepithelial transport of SN-38 while minimizing gastrointestinal toxicity. *Journal of Controlled Release*, 2011, 150, 318-325.
- <sup>155</sup> Williams, C.; Thang, S.; Hantke, T.; Vogel, U.; Seeberger, P.; Tsanaktisidis, J.; Lepenies, B., RAFT-Derived Polymer-Drug conjugates: HPMA-7-ethyl-10-hydroxycamptothecin (SN38) conjugates. *ChemMedChem*, 2012, 7, 281- 291.
- <sup>156</sup> Yuquin, Y.; Xiolan, S.; Yongmei, X.; Yuxi, W.; Tairan, K.; Lantu, G.; Chen, Y.; Jinliang, Y., Synthesis, characterization and antitumor evaluation of the albumin-Sn38 conjugate. *Anticancer Drugs*, 2013, 24, 270-277.
- <sup>157</sup> Meyer-Losic, F.; Nicolazzi, C.; Quinonero, J.; Ribes, F.; Michel, M.; Boukaissi, M.; Chéné, A.; Tranchant, I.; Arranz, V.; Ravel, D.; Kearsley, J., DTS-108, A novel prodrug of SN-38: *in vivo* efficacy and toxicokinetic studies. *Clinical Cancer Research*, 2008, 14, 2145-2154.
- <sup>158</sup> Sharkey, R., Govindan, S., Cardillo, T., Goldenberg, D.; Epratuzumab-SN38: A new antibody-drug conjugate for the therapy of hematologic malignancies. *Molecular Cancer Therapeutics*, 2012, 11, 224-234.
- <sup>159</sup> Burke, T.G.; Mi, Z., Ethyl substitution at the 7 position extends the half-life of hydroxycamptothecin in the presence of human serum albumin. *Journal of Medical Chemistry*, 1993, 36, 2580-2582.
- <sup>160</sup> Muggia, F., Twenty years later. Review of clinical trials with camptothecin sodium (NSC-10080). In *Camptothecins: New Anticancer Agents*; Potmesil, M., Pinedo, H., Eds.; CRC Press: Boca Raton, FL, 1995; pp 43-50.
- <sup>161</sup> Giovanella, B.C.; Hunz, H.; Kozielski, A.; Stehlin, J.; Silber, R.; Potmesil, M., Complete growth inhibition of human cancer xenografts in nude mice by treatment with 20-(S)-Camptothecin. *Cancer Research*, 1991, 51, 3052-3055.
- <sup>162</sup> Hertzberg, R.; Caranfa, M.; Holden, K.; Jakas, D.; Gallagher, G.; Mattern, M.; Mong, S.; Bartus, J.; Johnson, R.; Kinsbury, W., Modification of the hydroxyl lactone ring of camptothecin: inhibition of mammalian topoisomerase I and biological activity. *Journal of Medical Chemistry*, 1989, 32, 715-720.
- <sup>163</sup> Zhao, H.; Rubio, B.; Sapra, P.; Reddy, P.; Sai, P.; Martinez, A.; Gao, Y.; Lozanguiez, Y.; Longley, C.; Greenberger, L.; Horal, I., Novel prodrugs of SN-38 using multiarm poly(ethylene glycol) linkers. *Bioconjugate Chemistry*, 2008, 19, 849-859.
- <sup>164</sup> Sanna, N.; Chillemi, G.; Gontrani, L.; Grandi, A.; Mancini, G.; Castelli, S.; Zagotto, G.; Zazza, C.; Barone, V.; Desideri, A., UV-Vis Spectra of the Anticancer Camptothecin Family Drugs in Aqueous Solution: Specific Spectroscopic Signatures Unraveled by a Combined Computational and Experimental. *The Journal of Physical Chemistry B*, 2009, 113, 5369-5375.



- 
- <sup>165</sup> Chou, TC., Drug combination studies and their synergy quantification using the Chou-Talalay method. *Cancer Research*, 2010, 70, 440-446.
- <sup>166</sup> Li, C.; Yu, D.; Newman, R.; Cabral, F.; Stephens, L.; Hunter, N.; Milas, L.; Wallace, S., Complete regression of well-established tumors using novel water-soluble poly(L-glutamic acid)–paclitaxel conjugates. *Cancer Research*, 1998, 58, 2404 – 2409.
- <sup>167</sup> Zou, Y.; Wu, Q.; Tansey, W.; Chow, D.; Hung, M.; Charnsangavej, C.; Wallace, S.; Li, C., Effectiveness of water soluble poly(L-glutamic acid)–camptothecin conjugate against resistant human lung cancer xenografted in nude mice. *International Journal of Oncology*, 2001, 18, 331–336.
- <sup>168</sup> Botella, P.; Abasolo, I.; Fernandez, Y.; Muniesa, C.; Miranda, S.; Quesada, M.; Ruiz, J.; Schwartz, S. Jr.; Corma, A., Surface-modified silica nanoparticles for tumor-targeted delivery of camptothecin and its biological evaluation. *Journal of Controlled Release*, 2011, 156, 2, 246-257.
- <sup>169</sup> Schädlich, A.; Caysa, H.; Mueller, T.; Tenambergen, F.; Rose, C.; Göpferich, A.; Kuntsche, J.; Mäder, K., Tumor accumulation of NIR fluorescent PEG-PLA nanoparticles: impact of particle size and human xenograft tumor model. *ACS Nano*, 2011, 22, 5, 8710-8720.
- <sup>170</sup> Hurwitz, E.; Wilchek, M.; Pitha, J., Soluble macromolecules as carriers for daunorubicin. *The Journal of Applied Biochemistry*, 1980, 2, 25-35.
- <sup>171</sup> Moromoto, Y.; Sugibayashi, K.; Sugihara, S.; Hosoya, K.-I.; Nozake, S.; Ogawa, Y., Antitumor agent poly(amino acid) conjugates as a drug carrier in chemotherapy. *Journal Pharmacobio-Dyn*, 1984, 688-698.
- <sup>172</sup> Markovskiy, E.; Baabur-Cohen, H.; Satchi-Fainaro, R., Anticancer polymeric nanomedicine bearing synergistic drug combination is superior to a mixture of individually-conjugated drugs. *Journal of Controlled Release*, 2014, 184, 145–157.
- <sup>173</sup> Clapper, M.L.; Hensley, HH.; Chang, W.; Devarajan, K.; Nguyen, M.; Cooper, H., Detection of colorectal adenomas using a bioactivable probe specific for matrix metalloprotenase activity. *Neoplasia*, 2011, 13, 685-691.
- <sup>174</sup> Bala, V.; Rao, S.; Boyd, B.; Prestidge, C., Prodrug and nanomedicine approaches for the delivery of the camptothecin analogue SN38. *Journal of Controlled Release*, 2013, 172, 48-61.